UNIWERSYTET JANA KOCHANOWSKIEGO W KIELCACH
COLLEGIUM MEDICUM

mgr Bartosz Skóra

Rozprawa doktorska stanowiąca cykl publikacji pt.

Ocena wykorzystania enkapsulacji liposomalnej oraz nabłonkowego czynnika wzrostu w ukierunkowaniu toksyczności nanocząstek srebra przeciwko komórkom nowotworowym z nadekspresją receptora nabłonkowego czynnika wzrostu

Rozprawa doktorska
napisana pod kierunkiem
dr hab. n. med.
Konrada Szychowskiego

Praca przyjęta pod względem
merytorycznym i formalnym
w formie papierowej i elektronicznej

……
/data i podpis promotora/

Kielce 2023

W tym miejscu chciałbym serdecznie podziękować mojemu Promotorowi
Panu ***dr hab. Konradowi Szychowskiemu, prof. WSIiZ***
za ogromną cierpliwość, bezcenne wskazówki,
poświęcony mi czas, zaufanie oraz wsparcie i ciągłą motywację do działania,
podczas pisania niniejszej rozprawy doktorskiej.

Spis treści

1. Wykaz stosowanych skrótów

Skrót	Termin angielskojęzyczny	Termin polskojęzyczny
ABC transporter	*ATP-binding cassette transporter*	transporter ABC wiążący ATP
AgNPs	*silver nanoparticles*	nanocząstki srebra
ATM	*ataxia telangiectasia kinase*	kinaza ataksji-teleagiegtazji
AP2M1	*adaptor-related protein complex 2 mu 1 subunit*	kompleks 2, podjednostka 1 białka adaptorowego
AuNPs	*gold nanoparticles*	nanocząstki złota
CAT	*catalase*	katalaza
CAV1	*caveolin 1*	kaweolina 1
CLTC	*clathrin heavy chain*	łańcuch ciężki klatryny
DENs	*dendrimer encapsulated nanoparticles*	nanocząstki pułapkowane w dendrymerach
DLS	*dynamic light scattering*	dynamiczne rozpraszanie światła
DMPC	*1,2-dimyristoylo-sn-glycero-3-fosfocholine*	1,2-dimirystylo-sn-glicero-3-fosfocholina
DPPC	*1,2-dipalmitoilo-sn-glicero-3-fosfocholine*	1,2-dipalmitylo-sn-glicero-3-fosfocholina
EGF	*epidermal growth factor*	nabłonkowy czynnik wzrostu
EGFR	*epidermal growth factor receptor*	receptor nabłonkowego czynnika wzrostu
HUVECs	*human umbilical vein endothelial cells*	ludzkie komórki śródbłonka żyły pępowinowej
mAb	*monoclonal antibodies*	przeciwciała monoklonalne
MDR	*multidrug resistance*	oporność wielolekowa
NPs	*nanoparticles*	nanocząstki
NSCLC	*non-small cell lung cancer*	niedrobnokomórkowy rak płuca
PAMAM	*poly(amidoamine) dendrimers*	dendrymery poliamidoaminowe
PEG	*polyethylene glycol*	glikol polietylenowy
ppm	*parts per million*	liczba cząstek na milion
ROS	*reactive oxygen species*	reaktywne formy tlenu
SH3GLB1	*SH3 domain containing GRB2 like endophilin B1*	domena SH3 związana z endofiliną B1 GRB2-podobną
siRNA	*small interfering ribonucleic acid*	mały interferujący kwas rybonukleinowy

SOD	*superoxide dismutase*	dysmutaza ponadtlenkowa
TEM	*transmission electron microscope*	mikroskop elektronowy, transmisyjny
UV-Vis	*ultraviolet–visible spectroscopy*	spektroskopia w zakresie światła ultrafioletowego i widzialnego

2. Analiza bibliometryczna publikacji wchodzących w skład cyklu stanowiących rozprawę doktorską

Kielce, dn. 23.05.2022 r.

Analiza bibliometryczna publikacji autorstwa **mgra inż. Bartosza Skóry***

I. Oryginalne pełnotekstowe prace naukowe (bez streszczeń zjazdowych i konferencyjnych, prac w suplementach czasopism, listów do redakcji oraz udziału autora wymienionego w dodatku (appendix) jako uczestnika badań wieloośrodkowych, recenzji):

A. W czasopismach z Impact Factor:

Rok	Tytuł czasopisma	Liczba prac	IF	Punkty MEiN
2022	Biomedicine and Pharmacotherapy	1	6.530	100
2022	Toxicology and Applied Pharmacology	1	4.219	140
2020	European Journal of Pharmaceutics and Biopharmaceutics	1	5.571	100
Łącznie:		3	16.320	340

B. W czasopismach bez Impact Factor:

Opisy przypadków:

A. W czasopismach z Impact Factor: 0

B. W czasopismach bez Impact Factor: 0

Prace przeglądowe:

A. W czasopismach z Impact Factor: 0

B. W czasopismach bez Impact Factor: 0

II. Publikacje w suplementach czasopism:

III. Publikacje książkowe (autorstwo lub współautorstwo):

A. W języku obcym: liczba: 0

B. W języku polskim: liczba: 0

IV. Rozdziały w wydawnictwach zwartych:

A. W języku obcym: liczba: 0

B. W języku polskim: liczba: 0

V. Redaktor naczelny czasopisma o zasięgu:

A. Międzynarodowym: liczba: 0

B. Krajowym: liczba: 0

VI. Redaktor naczelny wieloautorskiej publikacji książkowej:

*Na podstawie zweryfikowanej listy publikacji dostarczonej przez Autora.

A. W języku obcym:	liczba: 0
B. W języku polskim:	liczba: 0

Informacje dodatkowe:

VII. Liczba streszczeń:	0
VIII. Prace popularno-naukowe i inne:	0
IX. Liczba publikacji z udziałem autora w badaniach wieloośrodkowych:	0

Łączna liczba publikacji:	**3**
Łączna punktacja Impact Factor:	16.320
Łączna punktacja MEiN:	340

Liczba cytowań (Web of Science Core Collection):

sumaryczna liczba cytowań:	6
liczba cytowań bez autocytowań:	6
indeks Hirscha:	1

DYREKTOR
Biblioteki Uniwersyteckiej
w Kielcach
mgr Andrzej Antoniak

Podpis osoby zatwierdzającej

3. Publikacje wchodzące w skład cyklu prac

European Journal of Pharmaceutics and Biopharmaceutics 154 (2020) 153–165

Contents lists available at ScienceDirect

European Journal of Pharmaceutics and Biopharmaceutics

journal homepage: www.elsevier.com/locate/ejpb

A concise review of metallic nanoparticles encapsulation methods and their potential use in anticancer therapy and medicine

Bartosz Skóra*, Konrad A. Szychowski, Jan Gmiński

Department of Lifestyle Disorders and Regenerative Medicine, University of Information Technology and Management in Rzeszow, Sucharskiego 2, 35-225 Rzeszow, Poland

ARTICLE INFO

Keywords:
Nanoparticle
Dendrimer
Liposomes
Metallic nanoparticles
Encapsulation methods
NPs

ABSTRACT

Interest in the use of metallic nanoparticles (NPs) in medicine is constantly increasing. The key challenge to the introduction of NPs into anticancer treatment is to limit the contact of their surface with healthy cells and to enable specific targeting of certain tissues, for example, cancerous cells. These aspects have raised a question whether the recent methods of drug delivery allow restricting the contact of NPs with healthy and/or nontarget cells. NPs can be restricted by encapsulation, which involves entrapping them into organic layers. This review is the first to present the different approaches for the encapsulation of metallic NPs, using liposomes, dendrimers, and proteins. The types and methods of entrapping are shown in an accessible way, enriched with graphics, and the pros and cons of these methods are disputable. Furthermore, the potential uses of NP complexes in medicine are described.

1. Introduction

The use of nanoparticles (NPs) in the anticancer therapy is currently gaining interest in the medical field due to their unique physical and chemical properties. NPs are structures with a size ranging from 1 to 100 nm. Nanotechnology is a branch of biomedical science that deals with the production of NPs and optimization of their production process [1]. It is considered that the nanotechnology era started in 1857 when Michael Faraday discovered a method to obtain a colloidal gold solution containing gold NPs (AuNPs) [2], and the next discoveries in the field of nanotechnology were achieved in the following two centuries. Therefore, the current literature is rich in subject-matter knowledge to facilitate the production of metallic (Au, Ag, Pt) and nonmetallic NPs (e.g. carbon nanotubes (CNTs) or poly lactic-co-glycolic acid (PLGA)) [3]. Basically, three groups of methods are used for the production of NPs, namely chemical, physical, and "green synthesis" which is based on microorganisms. However, all of these groups has their own disadvantages and limitations [4].

Due to the interesting properties of NPs, the last decade saw hundreds of studies about their potential use in many fields, including pharmacy, diagnostics, and medicine. The main area of the medical field in which NPs are utilized is anticancer therapy. Given the resistance of cancer cells to many lipophilic drugs, resulting in a decrease in the effectiveness in chemotherapy and phenotypic changes, which may cause drug resistance in cancer cells, it is necessary to change the current attitude to cancer treatment. Various reports highlighted that magnetic nanoparticles applied *in vitro* together with adriamycin and tetrandrine to the chronic myelogenous leukemia cell line, characterized by drug resistance (K562/A02), were able to reverse they multidrug resistance [5]. Furthermore, due to their shape and size, AgNPs are refractory to the efflux from cancer cells; therefore, their cytotoxicity is high in many cell types [6]. Moreover, the induction of apoptosis, which is considered as the most desirable way of cancer elimination from the organism, can be fast initiated by the highly reactive surface of some metallic NPs due to the ROS generation ability [7,8]. The literature presents plenty of studies confirming the anticancer effect of various NPs on different cells (e.g. AgNPs on breast cancer (MDA-MB-231) cells [9], CeO_2NPs on lung cancer (A549) cells [10], and AuNPs on

Abbreviations: AgNPs, silver nanoparticles; AuNCs, gold nanocages; AuNPs, gold nanoparticles; BSA, bovine serum albumin; $CaFe_2O_4$NPs, calcium iron oxide nanoparticles; CeO_2NPs, cerium oxide nanoparticles; CNTs, carbon nanotubes; CuNPs, copper nanoparticles; DENs, dendrimer-encapsulated nanoparticles; DMPC, 1,2-dimyristoyl-sn-glycero-3-phosphocholine; DPPC, 1,2-dipalmitoyl-sn-glycero-3-phosphocholine; DSPC, 1,2-distearoyl-sn-glycero-3-phosphocholine; EI, ethanol injection; FDA, Food and Drug Administration; Fe_3O_4NPs, iron oxide nanoparticles; $NaBH_4$, sodium borohydride; NPs, nanoparticles; PAMAM, polyamidoamine; PdNPs, palladium nanoparticles; PEG, polyethylene glycol; PLGA, poly (lactic-co-glycolic acid); PtNPs, platinum nanoparticles; RhNPs, rhodium nanoparticles; ROS, reactive oxygen species; RPE, reverse-phase evaporation; SiO_2NPs, silicon dioxide nanoparticles; TFHE, thin-film hydration with extrusion; TNFα, tumor necrosis factor alpha; ZnNPs, zinc nanoparticles; β-gal, β-galactosidase

* Corresponding author.
E-mail address: bskora@wsiz.rzeszow.pl (B. Skóra).

https://doi.org/10.1016/j.ejpb.2020.07.002
Received 10 February 2020; Received in revised form 29 May 2020; Accepted 2 July 2020
Available online 16 July 2020
0939-6411/

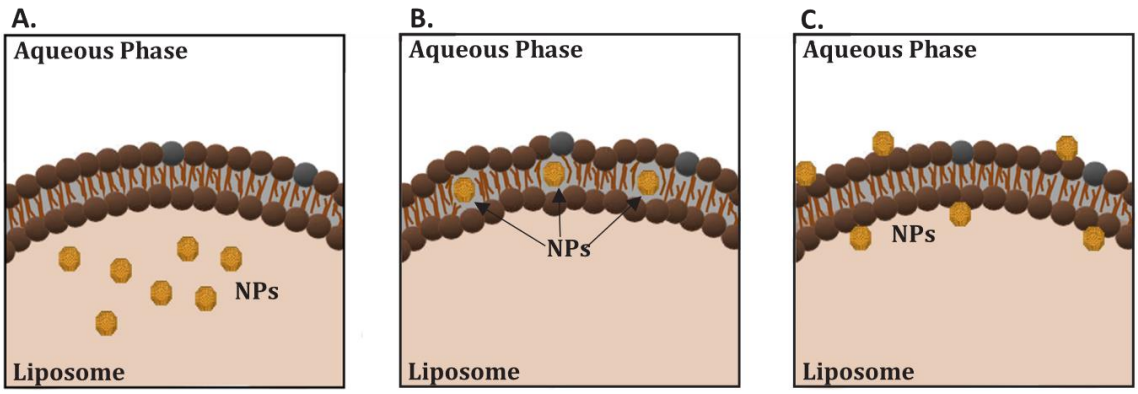

Fig. 1. Types of encapsulation of nanoparticles (NPs) by liposomes: (A) total encapsulation (NPs inside storage compartment); (B) bilayer entrapping (NPs between phospholipid layers); and (C) partial encapsulation (NPs bonded to hydrophilic phospholipid group inside/outside).

colorectal adenocarcinoma (HT-29) cells [11], where the cytotoxicity reached 60, 80 and 70%, respectively in a dose dependent manner). Unfortunately, the mechanisms of action of NPs on cancerous cells are not fully understood. It is believed that NPs induce oxidative stress which causes the peroxidation of lipids, resulting in increasing permeability of the cell membrane, and in consequence, cell lysis or apoptosis [12-14]. All the effects mentioned above are desirable in anticancer therapy, as they cause cancer cell damage; however, the low-selective action of metallic NPs is still a great barrier to use them as a simple way to induce cancer cell lysis.

The low-selective activity of NPs could be deleterious to normal cells. This negative effect has been observed for many widely used NPs including AgNPs, SiO_2NPs, and ZnNPs, which are able to inhibit cell proliferation or activate proteins involved in antioxidant protection, thereby inducing apoptosis or cytoskeleton regulation in normal cells such as human keratinocytes (HaCaT) or human aortic endothelial cells (HAECs) [15-19]. Based on the research results, two potential delivery routes of NPs are restricted—transdermal and intravenous—due to the observation that direct contact with the surface of NPs may lead to the destruction of healthy tissues [20,21].

The cytotoxicity of NPs to healthy cells can be possibly reduced by using different encapsulation methods [22,23]. These methods are based on coating the surface of NPs with certain substances such as phospholipids, dendrimers, and proteins which can restrict the NPs and prevent the direct contact of their surface with healthy cells that are not targeted in the therapy. The encapsulation process is dependent on the material and size of NPs. Therefore, nearly every group of NPs requires an individualized and optimized method of encapsulation. However, many drugs entrapped into liposomes, such as Doxil, Myocet, and others, are used clinically in modern medicine [24]; therefore, the encapsulation factors seem to be valuable agents in the NP restriction contact and, in consequence, the delivery of the nanostructures into specific tissue localization without damage to untargeted structures.

This paper presents a concise review of the available literature on the different methods of encapsulation of NPs, which can enable harmless delivery of these structures without damaging healthy cells. Further, the application of encapsulation methods in targeted drug delivery to cancer cells is discussed and the process of encapsulated NP uptake and release is described.

2. Encapsulation in liposomes

One of the methods to restrict the contact of NPs with healthy cells is to entrap them into liposomes. The basic component of liposome is phospholipid, which contains a lipid and a phosphoric acid group [25]. Phospholipids show amphiphilic properties due to the presence of both, hydrophilic (soluble in water) and hydrophobic group (soluble in lipids). This is the basis for the creation of lipid bilayer and therefore enables the liposomes to maintain a spherical shape which is their specific feature [26]. Phospholipids, which are used most commonly in liposome production, are choline derivates, including 1,2-dimyristoyl-sn-glycero-3-phosphocholine (DMPC), 1,2-dipalmitoyl-sn-glycero-3-phosphocholine (DPPC), and 1,2-distearoyl-sn-glycero-3-phosphocholine (DSPC) [27,28]. Inside the liposome structure, there is an empty space, called storage compartment, which is used as a capsule to incorporate certain substances, both lipophilic and hydrophilic, like NPs [29-31].

Liposomal bilayers also contain some additional molecules such as sterols [32]. The most commonly occurring representative of sterols is cholesterol which is naturally incorporated into the cell membrane [33]. The basic function of cholesterol in liposomes is to stabilize their structure [34]. Some reports show a correlation between the amount of cholesterol in the liposome membrane and the release of the substance entrapped in a liposome [35]. The optimal ratio of lipids and cholesterol in the liposome membrane is estimated at 2:1 [35]. The main limitation restricting the use of liposomes is their chemical and physical stability. It is reported that chemical degradation of liposomes occurs by two types of reactions: hydrolysis of ester-linked fatty acid with glycerol and peroxidation of the unsaturated fatty acid chain [36]. Both these may directly cause liposome damage. On the other hand, physical degradation of liposomes is associated with changes in temperature, osmotic pressure, or pH during their storage or while enclosing [37].

It is worth mentioning that liposomes are characterized by a lower phase transition temperature (Tc) than the melting temperature (Tm) which could facilitate the release of the drug from their storage compartment [38].

Research reports show that liposomes are frequently used in drug delivery [39,40]. Therefore, NPs could be successfully delivered using this structure. Additionally, the Food and Drug Administration (FDA) approved liposomes for the delivery of anticancer drugs to organisms, for example, doxorubicin encapsulated in PEGylated liposomes, which extend the doxorubicin circulation time in the organism and control its release due to the transmembrane ammonium sulfate gradient [41].

According to the literature, NPs could be encapsulated in liposomes in three ways: total, bilayer, and partial. These are described in detail as follows (Fig. 1).

2.1. Nanoparticles totally covered with phospholipids

The total encapsulation of NPs is based on the incorporation of these nanostructures inside the storage compartment located in the liposomes [42,43]. The liposome–NP complex so formed is called lipo-NPs. Depending on the encapsulation method, the storage compartment can consist of solid NPs (without aqueous suspension) or an aqueous solution of NPs entrapped by phospholipids (Fig. 1B) [44,45]. The totally coated NPs could be obtained by three methods: reverse-phase

evaporation (RPE), thin-film hydration with extrusion (TFHE), and ethanol injection (EI).

RPE approach is based on the amphiphilic properties of phospholipids, resulting from the presence of a hydrophobic part which is soluble in organic solvents and a hydrophilic part which is soluble in water [46]. In the first step of RPE, lipids previously dissolved in chloroform/toluene are added into a round-bottomed flask. The vessel is then placed into an ultrasonic bath at 0 °C. During the sonification of the phospholipid solution, the aqueous colloid of NPs is added, which results in the formation of two immiscible phases: (1) an organic phase containing lipids and (2) an aqueous phase containing suspended NPs [47]. The following step involves the evaporation of the organic solvent (chloroform at 65 °C or toluene at 111 °C) under reduced pressure. After evaporation, a viscous gel is formed at the bottom of the flask. The obtained gel is vigorously agitated to facilitate the total encapsulation of NPs within liposomes [46]. Studies have shown that the RPE approach was successfully used for entrapping AuNPs, which was proved in many studies [48-51], and AgNPs [52,53]. However, the aforementioned Lipo-AuNPs and Lipo-AgNPs produced with the RPE method were not tested on mammalian cells, even *in vitro*. However, the antibacterial properties of silver complexes were examined, indicating well-evidenced antibacterial properties. Nonetheless, the potential use of Lipo-AuNPs and Lipo-AgNPs in mammalian cells has not been investigated, hence, their usefulness in anticancer therapy is still unknown and needs to be evaluated.

TFHE involves the dissolution of phospholipids in an organic phase. The obtained lipid solution is added to a round-bottomed flask, similar to the RPE approach [54]. Subsequently, chloroform/toluene is evaporated under reduced pressure at a certain temperature (specific for the organic solvent). Evaporation leads to the removal of the nonpolar phase and formation of a thin lipid film at the flask walls. The obtained layer is then suspended in an aqueous NP colloid. Hydration enables the total enclosure of NPs into liposomes. However, the obtained complexes are heterogenous, and their sizes may differ [55]. Therefore, polycarbonate membrane extrusion is carried out to obtain homogenous lipo-NP complexes [56]. This process leads to the formation of small, homogenous lipo-NP complexes. TFHE approach is generally thought of as a method for obtaining smaller lipo-NP complexes compared to RPE but requires the utilization of polycarbonate membranes and hence involves higher procedure cost. Studies have reported the total encapsulation of Fe_3O_4NPs [54,57], which were tested as imaging agents to visualize the gastrointestinal and spleen tracks that can be further used in cancer diagnostics. As suggested by Gupta and Wells, minor modifications of the liposome-Fe_3O_4NPs surface with PEG significantly extend the half-life of complexes, which increases their usefulness in anticancer spleen and intestinal cancer diagnostics [56]. Moreover, AuNPs were also obtained using the TFHE method. The authors highlighted that the liposomes are one of the most appropriate encapsulation factors due to their potential use in biological field and drug delivery [58]. The anticancer properties of Lipo-AuNPs were investigated by Liang et al., who synthesized gold nanocages (AuNCs) encapsulated in liposome [59]. Subsequently, mice were treated with these complexes, after which the immune response against tumor and metastasis was increased [59]. A similar effect was observed using the lipo-AuNPs-doxorubicin in tumor-bearing mice, providing tumor suppression after near-infrared light cotreatment [60]. In turn, the THFE method was also applied to obtain Lipo-AgNPs, which showed a higher cytotoxicity effect on acute monocytic leukemia (THP1) in comparison to uncoated NPs [61]. Therefore, the anticancer application of encapsulated NPs, especially Au and AgNPs, seems to be reasonable; however the potential of the other lipo-NPs types, synthesized with the TFHE method, needs to be further evaluated due to the lack of information about their influence on even *in vitro* models.

EI is based on the dissolution of phospholipids in ethanol [62]. At the same time, the aqueous NP colloid is vigorously mixed using a magnetic stirrer. The resulting solution of lipids is subsequently injected into the rotating aqueous phase. As a result, a water-in-oil emulsion is obtained. The last step involves the evaporation of the organic phase at a specific temperature under reduced pressure. The EI approach results in the total encapsulation NPs in the phospholipid bilayer [63]. Studies have shown that this method was used to obtain lipo-$CaFe_2O_4$NPs, which were tested on two breast cell lines. The obtained results did not show any significant effect on cell viability, alone and enclosed with two new thienopyridine anticancer drugs, which allows using them as lipocarriers in anticancer therapy due to their ability to generate local heat, after laser exposure [62]. In the near future, the lipo-$CaFe_2O_4$NPs targeted by specific antibodies or proteins can be used as a new accurate drug delivery system of anticancer drugs. The EI method was also used as a way to produce lipo-CuNPs; however, their anticancer properties have not been evaluated yet [64]. In one study, a modification of the EI method was attempted, in which the solid lipo-NP complexes (without aqueous phase) were incorporated into the storage compartment [62]. This alternative approach requires the phospholipids to be suspended in methanol and the addition of a small amount of chloroform to the NP colloid [65]. Additionally, after the evaporation of the organic phase, another solution of methanol was injected. This EI method with minor changes was successfully used to produce CuNPs [66] and solid magnetic NPs entrapped in liposomes (without an aqueous phase), which were subsequently tested on a cell membrane model, resulting in uptake of lipo-$MnFe_2O_4$NPs [65,67]. The cited works were the first to prove that magnetoliposomes are able to fuse with cell membrane and, in the future, they may be used as drug-contained vehicles, whose trajectory can be controlled with a magnet due to the properties of $MnFe_2O_4$NPs. However, the Rodrigues et al. experiments were performed only in laboratory conditions; therefore, to evaluate the full mechanism and its potential in anticancer therapy, more tests should be conducted [65].

Summarizing, total liposome encapsulation of NPs can be applied to achieve selective drug delivery into targeted tissues [68]. Disruption of the liposomal bilayer could be controlled by some physical factors, such as light [69], temperature [68,70], ultrasound [71], or UV light [72]. This allows a safer liposomal delivery of NPs (e.g. using laser point light), which ensures that the healthy untargeted tissues are not damaged [48]. However, the total encapsulation method, which is most frequently reported in the literature, requires to be optimized [54,57,58,62]. The limitation on the size of NPs (maximum 2–3 nm) that could be incorporated into liposomes needs to be overcome, and the size of liposomes should be controllable to enhance the level of encapsulation [73].

As mentioned above, the liposome encapsulation of metallic NPs has to be improved and their anticancer properties need to be determined more comprehensively due to the lack of information about the influence of encapsulated NPs on cancer cells *in vivo*; however, some steps have been made in *in vitro* conditions. Additionally, the studies have shown that tumors are characterized by rapid growth of endothelial cells and a decreased number of pericytes as well as the presence of leaky sites in vasculatures, called pores, the size of which ranges from 100 to 300–400 nm [74]. These properties allow passive targeting of liposome-encapsulated NPs due to their small sizes which may fit into the leaky pores. A study reported the specific delivery of liposomal PtNP complexes to several types of cancers, for example, non-small-cell lung cancer (NCI-H322), pancreatic cancer (EPP85-181P), head cancer (Hep-3), neck cancer (Hep-2), and breast cancer (HER2), where the induction of apoptosis in all the tested cell lines was proved, allowing prediction of their promising features [75]. What is more, the liposome-encapsulated PtNPs are the main ingredient of a drug called Lipoplatin [76]. So far, this drug has been successfully tested in three phases (Phase I, II, and III) of clinical trials [77]. It is worth mentioning that AuNPs entrapped in liposomes are also tested for use in anticancer therapy; for example, AuNPs conjugated with porphyrin were found to significantly inhibit the growth of several tumors, including nasopharyngeal carcinoma (C666-1), hepatocellular carcinoma (Huh7), colon

cancer (Colo 205), neuroblastoma (Lan-1), and melanoma (SBcl2) [78]. Moreover, the liposome-entrapped AuNPs with porphyrin were tested *in vivo* on mouse neuroblastoma, resulting in reduction of tumor mass at an 80 μg dose without loss in the survival rate [79]. However, the increase in the dose to 100 μg caused the death of 67% of tested animals. This example shows clearly that many steps have to be made before liposome-encapsulated nanoparticles can be incorporated into anticancer therapy, and many analyses need to be performed to determine the benefits of lipo-NPs complexes in cancer treatment. However, many of the abovementioned reports have proved that liposomal encapsulation of metallic NPs can be a new approach in modern anticancer treatment.

2.2. Nanoparticles embedded between phospholipid layers

This type of entrapment is based on incorporating the metallic NPs between phospholipid layers which are involved in the formation of phospholipid bilayer [80]. Thus, NPs will not be present in the storage compartment within the liposomes [81]. The available literature reports that bilayer encapsulation of NPs can be achieved using only one method known as modified thin-film hydration [31]. The basis of this approach is analogical as described above but with minor changes. The organic phase (containing lipids dissolved in chloroform/toluene) and the aqueous solution of NPs are added into a flask concomitantly. Subsequently, the organic solvent is evaporated at a specific temperature under reduced pressure. In the next step, the mixture of lipids and NPs is suspended in water. As a result, lipo-NP complexes are formed, with the NPs located between the layers of phospholipids. This approach has been successfully used for the production of AuNPs [82], AgNPs [83], and magnetite (Fe_3O_4) [84] entrapped between the phospholipid layers. In contrast to the previous type of encapsulation which can be accomplished using three methods, bilayer entrapping could be carried out using only the method presented above [82]. Naturally, this type of encapsulation has limitations, including the size of NPs which could be entrapped. To achieve accessibility between the layers, the maximum size of NPs that could be incorporated should not be more than 5 nm [48]. A potential application of bilayer-encapsulated NPs is in anticancer therapy [85,86]. Reports indicate that the nanostructures most often entrapped using this approach are magnetic NPs (magnetoliposomes) [87,88]. These structures can be used in the delivery of anticancer drugs, whose targeting can be controlled with a magnet to supply lipo-NPs-drug complexes in tumor tissue [89] or to destroy the liposomal bilayer in a controlled manner [90] to allow the release of active substances near the cancer cells. Van Ballegooie et al. higlighted that succesful synthesis of magnetic NPs entrapped in the phoshpholipid bilayer created a new field in bioengenerging, which focused on creation of external devices for control of liposome bilayer disruption and, in consequence, drug release [90]. The use of magnetoliposomes in the breast cancer treatment has been proved as well [87,91]. Di Corato showed that the magnetic NPs encapsulated into the lipid bilayer served as a promising vector to induce the generation of reactive oxygen species (ROS) in breast cancer cells with the use of laser light, but as described above magnetic NPs were used to direct the liposomes near tumor cells and stimulate hyperthermia [87]. In consequence, the mass of tumor tissue was significantly decreased. Magnetoliposomes are also used as drug vectors in anticancer therapy. Yoshida et al. demonstrated a method for synthesis of magnetoliposomes containing docetaxel placed into the storage compartment [92]. The obtained complexes had double action: first, the delivery of docetaxel to the tumor region and next the release of the drug by heat generation, which caused damage to the cancer cells [92]. Furthermore, different studies have highlighted that the NPs conjugated with arsenic trioxide (in hepatocarcinoma—SMMC-7721 cell line) [93], doxorubicin (in breast adenocarcinoma—MCF-7 cell line) [94], and oxaliplatin or gemcitabine (MCF-7 cell line) [95] also damaged the cancer cells by activating apoptotic pathway.

Summarizing, the presence of metallic NPs (especially magnetic NPs) between the phospholipids layers of liposome is a very promising step in creation of a controled drug delivery system, due to the many factors that can be involved in the bilayer disruption, e.g. external radiation, ultrasounds, or magnetic field. However, external devices need to be invented to control the dustribution process precisely, which may create some limitations and increase the costs of the potential procedure.

2.3. Partial encapsulation of nanoparticles

According to the available literature, the third type of encapsulation of NPs - partial encapsulation (Fig. 1C), is the rarest, as this approach was reported in only one study [48]. In this approach, the NPs are entrapped only partially, showing a propensity to bond with the hydrophilic phospholipid part inside and outside the liposomes. The knowledge of this type of encapsulation is vestigial, and it is not clear how the lipo-NP complexes formed using this approach can be used in drug delivery [48].

2.4. Potential mechanism of lipo-NPs uptake and release in cell

As mentioned above, the liposomal encapsulation of NPs is used to restrict the contact of the highly reactive NP surface with untargeted cells. There are no reports explaining in detail the process of the uptake of lipo-NPs complexes, but the mechanism of liposome penetration per se is well described [96]. Since the entire NP surface is covered by the phospholipid bilayer, it is reasonable to suppose that lipo-NP structures will be uptaken by the cell in the same way.

Çağdaş et al. highlighted that liposomes (untargeted) are taken by the cell following the endocytosis pathway, early and late endosomes are subsequently created and, according to the lysosome-dependent degradation of liposome, the substance (in this case NPs) can be released from the compartment and act actively on cell organelles [97]. The same description of liposome uptake was presented by Yameen et al., who concluded that structures with a size of ca. 120 nm are uptaken via clathrin-mediated endocytosis, and the liposome content can be released by lysosomal enzymes [98]. The enzymatic degradation of the liposome bilayer results in drug deencapsulation. Subsequently, the “free” substance can further influence certain organella such as mitochondria, Golgi apparatus, and others [99]. However, the encapsulation process does not guarantee the targeting of the liposome into certain cell types; therefore, the surface ligand conjugation strategy is gaining more attention. The methods of protein and antibody targeting is well-described as being based on the use of mainly 1,2-distearoyl-sn-glycero-3-phosphoethanolamine-N-[succinimidyl(polyethylene glycol)] (NHS-PEG-DSPE) or 1,2-distearoyl-sn-glycero-3-phosphoethanolamine-N-[maleimide(polyethylene glycol)] (DSPE-PEG-Mal) as anchors [100,101]. The current trend in liposome-drug complexes is strictly related to overexpression of surface receptors in many cancer cells, e.g. epidermal growth factor receptor (EGFR) or folate receptor (FR), using natural or synthetic ligands [102,103]. In both cases, the targeting of drug liposome carriers was successfully achieved, resulting in higher toxicity in cancer than in normal cells. The effects of the presence of NPs inside the cell, namely oxidative stress generation, lipid permeabilization, and DNA damage, are also well described [104-106]. However, these processes are strictly correlated with the size, type, and charge; therefore, nearly each new type of NPs should be evaluated on *in vitro* and *in vivo* models to obtain reliable knowledge about the influence of lipo-NPs on the cell.

Summarizing, despite of the lack of reports on liposome-entrapped NPs, it can be predicted that these complexes will be uptaken via the endocytosis pathway. Subsequently, the release of NPs occurs due to the presence of lysosomal enzymes and, in consequence, the NP toxicity effect can be revealed inside the cell, causing mainly oxidative stress generation.

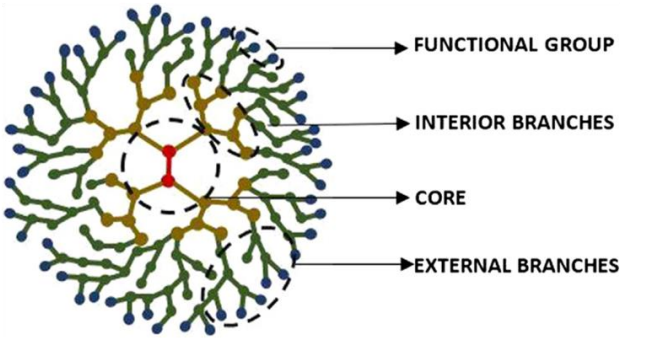

Fig. 2. Schematic of polyamidoamine (PAMAM) dendrimer structure. The specific parts are highlighted by colors: red—core/center of dendrimer; yellow—interior branches; green—external branches; and blue—peripheral functional group. (For interpretation of the references to colour in this figure legend, the reader is referred to the web version of this article.)

3. Dendrimer-encapsulated nanoparticles

Dendrimer encapsulation is used to constrain the biological and physical properties of NPs. Dendrimers are a well-defined group of organic polymers characterized by a symmetric and well-ordered structure, including core, internal, and external branches, and peripheral functional groups (Fig. 2) [107-109]. The main feature of dendrimers is the presence of empty spaces between branches, called internal cavities or internal voids. These spaces are used to carry some drugs [110], dyes [111], or NPs [112]. Additionally, dendrimers demonstrate a high reactivity, and it was proved that the substances placed into the cavities of dendrimers show higher activity in comparison to their unentrapped equivalent [113]. This phenomenon is called the dendritic effect [114].

Dendrimers are produced, mainly, by two types of methods: convergent (Frechet type [115]) and divergent (Tomalia type [116]). In the convergent method, the branches are produced first and then linked to the core. By contrast, in the divergent method, the core is produced first and then the branches are bonded [117,118].

Dendrimer-based delivery systems are considered as potential drug vectors in many fields, including anticancer therapy [119]; hence the interest of nanotechnology to facilitate entrapping NPs into dendrimers and create a new group of complexes called dendrimer-encapsulated nanoparticles (DENs) [120]. It is proved that the synthesis of nanostructures using dendrimers offers more benefits [121]. In addition, the size of NPs can be controlled allowing the formation of small-sized NPs. Furthermore, dendrimers can stabilize the NP colloid by preventing the agglomeration and increasing the solubility of NPs [122,123].

Polyamidoamine (PAMAM) dendrimers are used most frequently to entrap NPs due to their well-defined three-dimensional structure (important for the stabilization of NPs) [122]. Moreover, the PAMAM dendrimers are commercially available since 1992 [124]. The literature data show that the PAMAM structures are divided into generations based on the number of repeating branch points from the core to the periphery [122,125,126], starting from G0 + n where n means the number of branch points. In the case of the higher-generation dendrimers, the diameter and the number of cavities are higher, approximately linearly [127]. This feature enables altering the sizes of DENs according to their destination (e.g. cell or protein) [128]. The nomenclature also refers to the type of NPs and the number of materials encapsulated in DENs as shown in Table 1 [122].

Dendrimers are also frequently used to entrap NPs due to the following unique properties: (1) hosted NPs will not be able to contact each other, and thus, encapsulation prevents their agglomeration; (2) entrapped NPs are restricted primarily by the steric effect, and hence, a large part of the NP surface is active; (3) the dendrimer branches limit the NPs from contacting with large molecules, and thus determine selective mechanism, allowing only small substances to contact with entrapped NPs; and (4) the terminal groups can be tailored to direct DENs into certain tissues [134,135].

Table 1
Brief summary of the nomenclature of polyamidoamine (PAMAM) dendrimers, where n is the number of generations (1, 2, …), R is the type of terminal peripheral group (–NH_2, –OH), A and B are the metal ions used in the encapsulation, m is the oxidative state of A/B, and × and y are the stoichiometric amounts of A and B, respectively, used in the synthesis.

NOMENCLATURE	TYPE OF DENs	EXAMPLE	REF.
$\mathbf{G_n}$-R	general type name	G4-OH	[129]
$\mathbf{G_n}$-R($\mathbf{A^{m+}}$)$_x$	metal-ion precursor	G6-OH(Cu^{2+})$_{55}$	[130]
$\mathbf{G_n}$-R($\mathbf{A_x}$)	monometallic	G6-OH(Pd_{55})	[131]
$\mathbf{G_n}$-R($\mathbf{A_x}$, $\mathbf{B_y}$)	bimetallic	G4-NH_2($Pd_{27,5}$,$Au_{27,5}$)	[132]
$\mathbf{G_n}$-R($\mathbf{A_x@B_y}$)	core@shell bimetallic	G6-OH(Au_{147}@Pt_{147})	[133]

It is worth mentioning that the lower size of NPs guarantee their transmembrane passage into the cell structures to induce a higher cytotoxic effect [136]. Moreover, the use of dendrimers during the synthesis of NPs allows obtaining nanostructures of sizes between 1 and 5 nm, which is barely impossible, using classical methods of production. Furthermore, the produced NPs are characterized by homogeneous sizes.

Reports have shown that NPs are enclosed in dendrimers in four ways: incorporated in the center of a metallic core, bound to branches, incorporated into dendrimer cavities, and linked with terminal groups (not described in this paper because NPs are bound outside and cannot be included in the encapsulation method) [119,122].

3.1. Metallic core DENs

Metallic core DENs is a type of entrapped NPs in which the nanometal first forms the core of the dendrimer and then the branches are anchored (Fig. 3A) [136]. This approach enables restricting contact with the surface of NPs which can be cytotoxic to healthy tissue [137,138]. The production of metallic core DENs is not well described in the literature [139,140]. Generally, this type of DENs is produced using two approaches: reduction of intradendrimer metallic ions and assembly of branches to NPs.

Reduction of intradendrimer metallic ions is the frequently used method to obtain dendrimers with NPs in the center [141]. The approach is based on loading metallic ions into dendrimers which act as a precursor to obtain a desirable core. The following step is the reduction of metallic ions by vigorous stirring with sodium borohydride ($NaBH_4$). This leads to the accumulation of NPs into the dendrimer core. It is reported that the repetition of these two steps (loading and reduction) causes an increase in the amount of NPs inside the core. The method has been successfully applied to obtain AuNPs, which were subsequently tested on a cervix adenocarcinoma cell line (HeLa) after treatment with $\lambda = 532$ nm laser light for 15 min., resulting in a significant decrease in cell viability [136,142]. However, the influence of the tested compounds was characterized only with one method, i.e. Calcein-AM and propidium iodide staining; therefore it is difficult to predict how the AuNPs DENs influence this type of cells. Additionally, the PdNPs were also entrapped in dendrimers with the method of reduction of intradendrimer metallic ions; similarly to the abovementioned AuNPs DENs, they were tested on a HeLa cell line [143,144]. The obtained results showed a decrease in cell metabolism activity, following the increasing concentration of PdNPs DENs. In this case, the morphology of the treated cells was evaluated, which revealed holes in the cell membranes. As concluded by the authors, it is reasonable to assume that this type of encapsulation in both types of DENs increases the cytotoxicity of NPs (dendritic effect). On the other hand, the CuNPs DENs [145] were also entrapped using the same method; however, the cited report is only limited to the synthesis and physical characterization

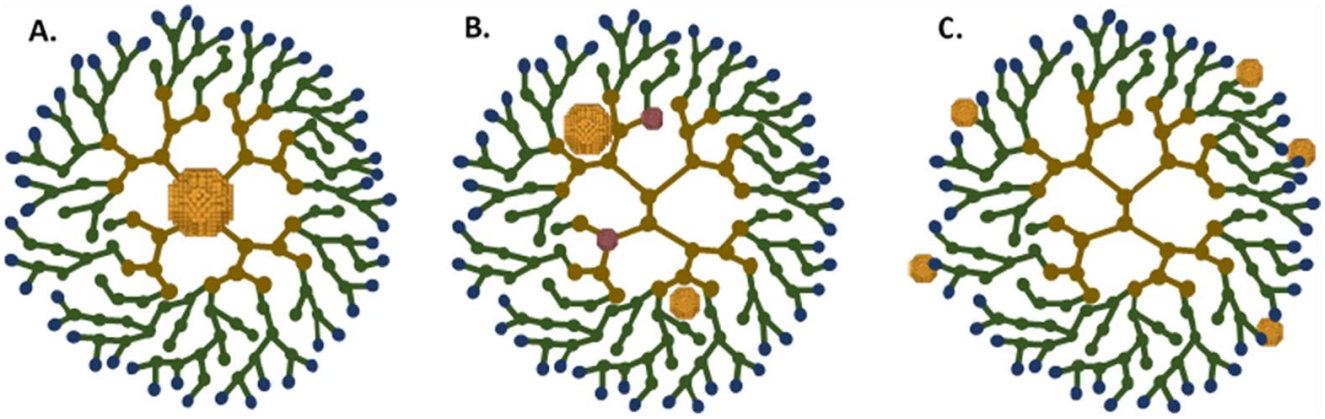

Fig. 3. Types of encapsulation of nanoparticles (NPs) by dendrimers: (A) metallic core (NPs are in the middle, branches are bonded to NPs surface); (B) branches/voids (NPs are entrapped in empty spaces between interior branches or bonded to them); and (C) terminally attached (NPs are bonded to the peripheral group).

fields, and it is difficult to predict the biological potential of these structures.

The second method involves bonding the dendrimer branches to NPs. Therefore, the first step is the production of NPs using a specific method dedicated to a particular group of NPs. The assimilation of branches requires covering the surface of NPs with amine groups. This is done through a reaction with a 3-aminopropyl compound [146] that initiates the bonding process. Subsequently, a reaction with acrylic methylate is performed, which results in branching and an increase in the diameter of DENs. The approach has been used to obtain Pd/core DENs [147] and Fe_3O_4/core DENs [146,148]. However, the obtained structures were not tested on biological models but their physical and chemical properties were evaluated. On the other hand, it is well known that AuNPs per se show low toxicity to cancer cells [149] but using them as a metal core of a dendrimer can in turn facilitate the utilization of NPs in anticancer therapy indirectly. The AuNPs DENs were used to deliver these nanoparticles near tumor tissues in photothermal therapy, which results in increasing the temperature locally and in consequence, causing cancer cell damage [136,150]. Au-core DENs are characterized by the ability to bind hydrophobic drugs into their structures [151]. Furthermore, this property enables the use of lipophilic substances without changing their structures. The presence of AuNPs core in dendrimers allows incorporating drugs through the formation of non-covalent bonds, which is beneficial for drug release anticancer therapy [152]. Moreover, there are reports showing that DENs with magnetic NPs can be used as a nucleic acid delivery system for cells [153]. This is due to the small sizes of magnetic DENs which enable transmembrane transport and DNA protection against endo- and exonucleases [154,155].

3.2. Branch-embedded DENs

Branch-embedded DENs are a type of dendrimer-encapsulated NPs which are formed by incorporating the nanostructures into the empty cavities of dendrimers or bonding them directly to branches [156]. Thus, the NPs are not present in the core of dendrimer. This approach restricts the surface contact of NPs with other structures but to a lesser extent in comparison to metallic core DENs; if a substance is small enough to pass through the branches of DENs, it can interact with the NP surface [157]. This type of dendrimer encapsulation is well defined and described in many studies [158-160]. Several approaches and their modifications are used in the production of branch-embedded DENs, but the most frequent ones are direct reduction and interdendrimer displacement reaction [136,161].

Direct reduction is analogical to the reduction of intradendrimer metallic ions described above in which $NaBH_4$ ions act as reducer [123]. However, the loading and reduction processes are not repeated in direct reduction. The synthesis reaction is performed only once, and the number of NPs entrapped is regulated by the number of substrates added to the reaction mixture. Therefore, the synthesis is based on two, unrepeated reactions: loading of metallic ions in the form of salts or acids inside dendrimers by mixing with PAMAM and reduction of the ions by $NaBH_4$. The NPs are formed and incorporated into cavities between the branches or bonded to the branches. This method has been used for obtaining AuNPs, CuNPs, PtNPs, PdNPs, and RhNPs [122,123,162], but these complexes were not tested on even *in vitro* models. Therefore, it is unreliable to predict their potential influence on cells, let alone the whole organism. It can only be predicted that, according to the dendritic effect, the cytotoxicity of these complexes will be higher than that of unentrapped NPs. However, their biological effects should be evaluated. At this point, it is worth mentioned that silver ions cannot be used in this reaction because of their weak complexation [163].

Interdendrimer displacement reaction is suitable for silver ions [123,130]. Basically, the reaction involves two steps. The first step is the formation of branched DENs by the method described above (direct reduction), with another metal placed inside. Subsequently, the target metal ions interact with the encapsulated NPs. Terminally, the NPs are oxidized and the target ions are reduced to NPs, and thus, the ion displacement is performed [164]. In the obtained DENs, the NPs are incorporated between the branches (interbranch incorporation). As mentioned above, this approach has been used to produce DENs with silver NPs.

Dendrimer branch entrapment is frequently used to limit the surface contact of NPs with other structures, but the properties of metals are not entirely covered by this technique. Therefore, branch-embedded DENs were examined as a potential label capable of transmembrane passage in mouse embryo fibroblast cells (NIH 3T3) [165]. It was proved that dendrimers were not cytotoxic to the cells [166]. In the near future, DENs branches enable to high specific marking of terminal dendrimers groups and directing the complexes to cancer cells, terminally detection [167]. The use of NPs entrapped in dendrimers can begin a new era in cancer diagnostics allowing treatment to be provided at an early stage [168].

AuNPs entrapped in dendrimer branches were successfully used in specific visualization of human epithelial carcinoma cells (KB cell line) [168]. Folic acid was bonded to Au-DENs for directing the complexes specific to KB cells [169]. The folate receptors in the cells were increased significantly, and AuDENs were internalized into lysosomes [168]. Moreover, folic acid was also successfully used to target cancer cells in various organs including ovary (SK-OV-6), kidney (SK-RC-2), uterus (MES-SA), testis (NCCIT), and colon (SW620) [170-173]. Overall, targeting of terminal DENs group can be used for specific imaging of cancer cells with the help of molecules such as folic acid or

fluorescein isothiocyanate and improving the diagnostic process in anticancer therapy.

In conclusion, it is worth mentioning that no dendrimer-NP complex has been tested in *in vivo* conditions; however, some *in vitro* evaluations have been made e.g. AuNPs- or PdNPs-DENs. It is difficult to predict their influence on the whole organism. The above-cited reports show that, following the dendrimer encapsulation, it is possible to modulate or prolong the cytotoxicity level in certain tissues in comparison to "unbound" NPs characterized by high reactivity of the surface. At this point, it is worth emphasizing that the terminal groups of dendrimers (Figs. 2 and 3) can be used as a docking site in which certain ligands may be attached and therefore the targeting of NP toxicity could be more precise. Duncan et al. claimed the biocompatibility and toxicity of dendrimers. They described that PAMAM dendrimers conjugated with cisplatin resulted in increasing toxicity against B16F10 tumor in C16 mice, compared to "free" drug, without changes in animal mortality [128]. Similarly, Chen et al. described that injection of 1.3 g/kg dose of PEG dendrimer hybrids in healthy mice did not cause any side effects such as pathological changes in organs [174]. Summarizing, the dendrimer-encapsulated NPs seem to be promising nanostructure carriers, which enhance the cytotoxicity and circulation time of these structures; however, more studies need to be performed both *in vitro* and *in vivo* to evaluate their properties in anticancer therapy.

3.3. DENs uptake and release mechanism in the cell

As mentioned above, PAMAM dendrimers are most often used as an encapsulation factor to entrap NPs into their structures. Their properties and influence on the tested cells were discussed earlier. However, the potential mode of the uptake and release of DENs (core and branch-embedded) were not described. Therefore, in this chapter, their present significance in this field of science will be considered. At this point, it is worth mentioning that, similarly to lipo-NPs complexes, the DENs have not been examined in terms of uptake and release. However, the probable mechanism of DEN internalization can be analogical to that of dendrimers per se.

The PAMAM dendrimers used to encapsulate metallic NPs are a diverse group of structures; basically, due to their generation, additional groups, and charge, the uptake mechanism of dendrimers is different for each group. However, some regularities can be highlighted. According to available literature, the mechanism of dendrimer uptake into the cell may involve endocytosis and passive diffusion, depending of their chemical structure [175]. Neutral and cationic charged dendrimers are uptaken via non-clathrin and non-caveolin endocytosis [176], in which early and late endosomes are created and the dendrimer is internalized by lysosomal enzyme degradation [177]. However, the anionic dendrimers tend to be uptaken via caveolin-mediated or clathrin-mediated endocytosis, which was presented by Kitchens et al. in human epithelial colorectal adenocarcinoma cells (CACO-2) [178]. On the other hand, Maher et al. [179] showed that low-generation dendrimers can pass through the cell membrane in the passive diffusion pathway [179]. More interestingly, the way of uptake of dendrimers into the cell determines their influence on the cell, i.e. structures that can be taken by passive diffusion do not show a tendency to induce ROS generation, in contrast to structures that are taken via the endocytosis pathway [175]. Furthermore, amine-terminated dendrimers were able to interact with cholesterol in the cell membrane during endocytosis, resulting in reduced uptake of these dendrimers by the cell [180]. As mentioned above, the release of dendrimers is based on lysosomal enzyme interaction during endocytosis, resulting in pH changes and increasing cytotoxicity. It was also proved that, after deencapsulation of PAMAM dendrimers, the mitochondrial membrane potential was changed, causing apoptosis [181].

To sum up, the uptake and release of DENs in the cell are still unknown and need to be evaluated to understand fully the mechanism of the action of DENs in biological systems. However, some steps have been made and the toxicity potential of certain DENs has been proved. Therefore, it is reasonable to assume that this type of encapsulation can potentially be used as an encapsulation factor of NPs with anticancer application.

4. Protein encapsulation

Apart from dendrimers and liposomes, NPs can be encapsulated in proteins. This method of encapsulation is considered as the most sophisticated [182], and there is no one universal approach considered appropriate for protein encapsulation. According to the literature reports, it is difficult to clearly point out how certain types of NPs are entrapped by proteins [183]. This is due to the differences in the surface properties of metal NPs and proteins [184]. Therefore, only the most common and universal approaches of protein encapsulation are described below.

Protein encapsulation is determined by a few factors, including the size and shape of NPs and encapsulation efficiency, which is strictly related to the concentration of NPs and proteins in the reaction mixture, the volume of the aqueous phase, and the presence of surfactant during entrapment process [185]. In this type of encapsulation, NPs are used as either a drug (entering cells) (Fig. 4A) and or a vector (which carries the proteins through the cell membrane) (Fig. 4B) [186-189].

NPs exhibit specific properties (Fig. 4A) related to their surface, such as high reactivity [190], the capability of inducing hyperthermia [191], interactions with electromagnetic field [192], and initiation of oxidative stress [12,193]. However, when introduced as such, NPs can firstly damage healthy tissues and secondly undergo agglomeration, which will result in a decrease or loss of their surface activity [194-196]. Therefore, the main purpose of protein encapsulation is to limit

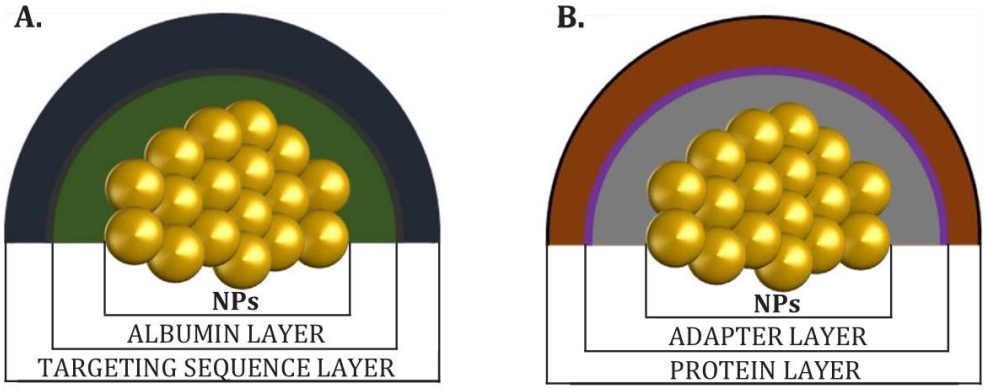

Fig. 4. Two strategies of encapsulation of nanoparticles (NPs) in proteins: (A) NPs as a drug (surface of NPs is covered by albumin, and then the targeting sequence is bonded); and (B) NPs as a vector (surface of NPs is bonded with a chemical adapter, and then the target proteins are attached).

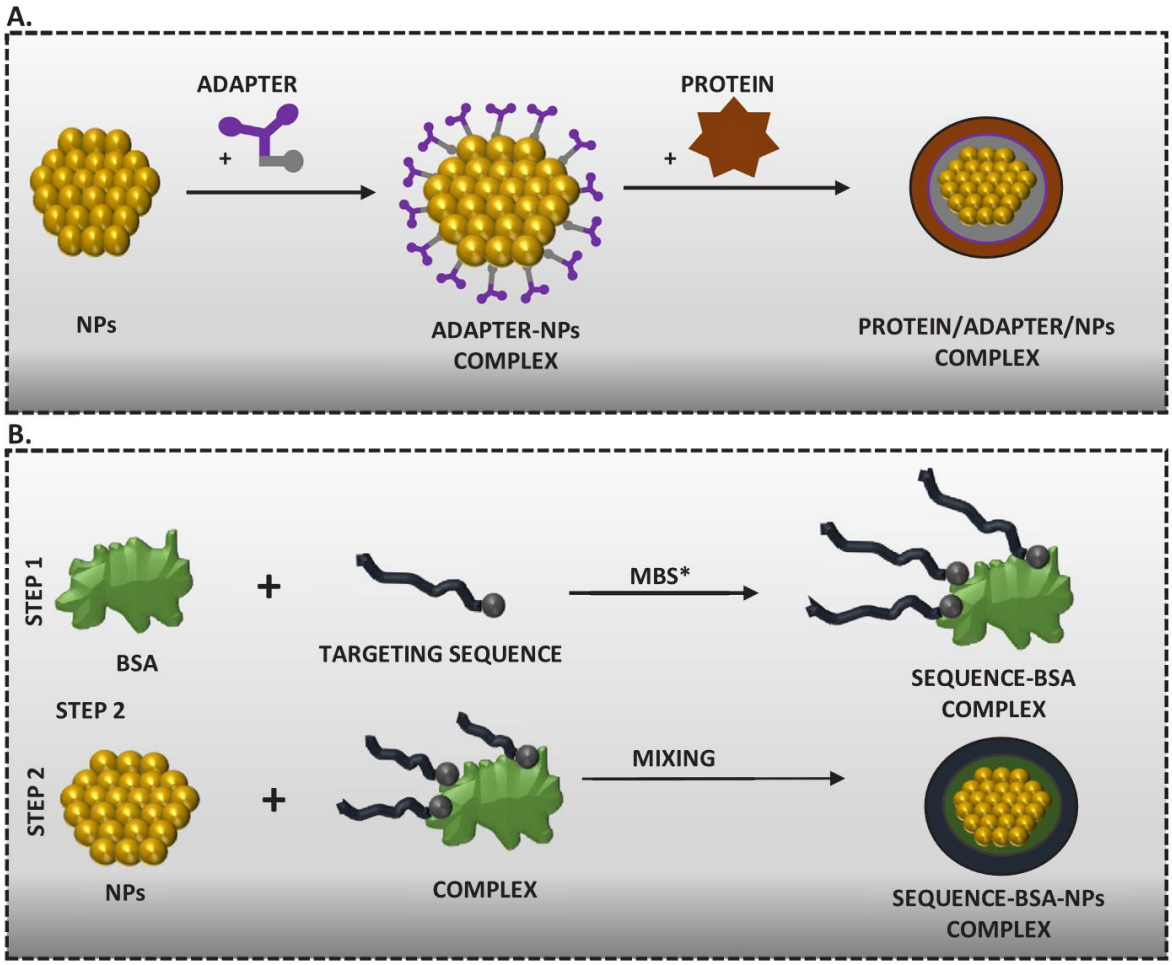

Fig. 5. The basic reactions involved in the protein encapsulation of nanoparticles (NPs), representing two approaches: (A) NPs as a vector and (B) NPs as a drug. *MBS—3-maleimidobenzoic acid N-hydroxysuccinimide ester.

the contact of the exterior of NPs with healthy cells and improve their distribution.

This approach involves enclosing NPs in a protein monolayer, usually albumins (Fig. 5B). The formed complex is called protein-layered NPs. Bovine serum albumin (BSA) is used as the source of albumin in the reaction mixture, and it is first conjugated with the targeting protein sequence. This is achieved by mixing BSA, 3-maleimidobenzoic acid N-hydroxysuccinimide ester (MBS), and the targeting sequence, which results in the formation of sequence–BSA complex. The following step is the encapsulation of NPs by the complex. This process is achieved by mixing NPs and the sequence–BSA complex. The protein-layered complex formed is suspended in an aqueous phase [182,197,198]. The transmembrane passage and entry into specific cell structures are mediated by the conjugated targeting sequences. The method was successfully used to target AuNPs to the interior of human liver carcinoma (HepG2) cells, HeLa cells, and NIH 3T3 cells [188,189]. The BSA–sequence approach is perceived as the method for targeting AuNPs to tumor cells, inducing local hyperthermia, and finally initiating damage of cancer cells [199]. Protein encapsulation was also performed in silver NPs using BSA [200]. Hence, in the near future, protein-encapsulated NPs can be used against bacterial infection caused by a specific type of pathogen, while ensuring the protection of the natural bacterial flora in the human gut.

In the second approach, NPs are used as a vector for specific proteins (Fig. 4B) [182]. This is possible due to their small size and ability of transmembrane passage [201]. Localizing proteins on the surface of NPs enables their entry into cells without being damaged by cell membrane [202]. This approach is most frequently accomplished by conjugation using an adapter specific to the NP surface (Fig. 5A) [182]. The aim of the conjugation process is to bind certain proteins to NPs without contact with their surface. Reports have shown that the most commonly used adapters are asparagine [203] and polyethylene glycol (PEG) [204] due to their affinity to proteins. Following conjugation, an adapter–NPs complex is formed. Subsequently, the obtained complex is connected to a targeting protein, creating protein–adapter–NPs complex. This approach of protein encapsulation enables increasing the activity and efficiency of proteins (by cumulation) and facilitates their distribution in the organism [182]. NP vectors were successfully used in studies on diabetes. For instance, AuNPs were coated by insulin using asparagine and then applied to rats suffering from diabetes. The results showed that the level of glucose in rats was significantly lowered compared to the control group [203]. Studies have also shown that NPs were coated by β-galactosidase (β-gal)[205].

AuNPs coated with PEG and bonded to tumor necrosis factor-α (TNFα) were examined against mice mammary carcinoma *in vivo* [206]. The cytokine was delivered to mice by injection followed by the induction of hyperthermia. TNFα acted as a targeting protein sequence which directed AuNPs to cancer cells (SCK) in the body of mice [207]. Results showed that the tumor sizes were decreased significantly, and the nearby normal tissues were not injured [206]. Another research indicated that transferrin bonded to PEG-coated AuNPs was used to accumulate NPs in mouse cancer cells (Neuro2A cells) [208]. The obtained results clearly showed that the amount of NPs in tumor cells was significantly higher, compared to the uncoated NPs [204].

Protein encapsulation has also been carried out using many other methods such as trimethylamine-N-oxidation, separation, or caging by archaeon [209-211] depending on the surface type of proteins and NPs. Generally, all the undescribed methods can be classified into two approaches as mentioned above. Protein encapsulation is a way to target drugs to certain tissues and to achieve co-transport of drugs such as proteins and nucleic acids. In the future, protein encapsulation can be used as an elementary mechanism to modulate or regulate cell conditions. Research reports confirm that there is a need to further develop this encapsulation method, mainly by unifying the different approaches in groups [212]. Literature data support that protein encapsulation is used in many studies [213], and in the near future, this type of encapsulation may become a standard.

5. Future perspectives

Although encapsulation using liposomes, dendrimers, and proteins is known more than a decade, the best approach of NP entrapment remains to be identified. Coating NPs with organic substances enables restricting the surface of NPs from contacting healthy tissues which can be toxic due to their high surface reactivity. It is reasonable to consider encapsulation as a method to direct NPs as a drug to specific cells by bonding targeting sequences to a protein layer or exchanging the terminal functional group in dendrimers. The small size of NPs (1–100 nm) is promising, especially for their use as a drug or protein vector. It was proved that the NP–drug template can readily pass through the cell membrane without damaging it. As mentioned above, the most defined methods of encapsulation of NPs are entrapment in dendrimers and phospholipid coating. Furthermore, the described methods are carried out using different approaches and their modifications to obtain specific NP-encapsulated molecules. On the other hand, protein encapsulation is still developing. The different features of proteins determined by their structure and interactions with the surface of NPs make it difficult to find a versatile method of encapsulation. However, the protein encapsulation approach is the most promising because the targeting sequences can be bonded with proteins. In conclusion, the encapsulation methods can allow incorporating NPs as therapeutic agents in anticancer therapy in the near future.

Acknowledgments

This work was supported by statutory funds from the University of Information Technology and Management in Rzeszow, Poland (DS 503-07-01-21).

Declaration of Competing Interest

The authors declare that they have no conflict of interest.

References:

[1] E. Abbasi, M. Milani, S. Fekri Aval, M. Kouhi, A. Akbarzadeh, H. Tayefi Nasrabadi, P. Nikasa, S.W. Joo, Y. Hanifehpour, K. Nejati-Koshki, M. Samiei, Silver nanoparticles: Synthesis methods, bio-applications and properties, Crit. Rev. Microbiol. 42 (2016) 173–180, https://doi.org/10.3109/1040841X.2014.912200.

[2] P.P. Edwards, J.M. Thomas, Gold in a metallic divided state–from Faraday to present-day nanoscience, Angew. Chem. Int. Ed. Engl. 46 (2007) 5480–5486, https://doi.org/10.1002/anie.200700428.

[3] S. Hasan, A review on nanoparticles: their synthesis and types, Res. J. Recent Sci. ISSN. 2277 (2015) 2502.

[4] A.V. Rane, K. Kanny, V.K. Abitha, S. Thomas, Methods for Synthesis of Nanoparticles and Fabrication of Nanocomposites, in, Synth. Inorg. Nanomater. (2018), https://doi.org/10.1016/b978-0-08-101975-7.00005-1.

[5] B. Chen, Reversal of multidrug resistance by magnetic Fe3O4 nanoparticle copolymerizating daunorubicin and 5-bromotetrandrine in xenograft nude-mice, Int. J. Nanomed. (2009) 73, https://doi.org/10.2147/IJN.S5093.

[6] W. Fan, B. Yung, P. Huang, X. Chen, Nanotechnology for Multimodal Synergistic Cancer Therapy, Chem. Rev. (2017), https://doi.org/10.1021/acs.chemrev.7b00258.

[7] B. Plackal Adimuriyil George, N. Kumar, H. Abrahamse, S.S. Ray, Apoptotic efficacy of multifaceted biosynthesized silver nanoparticles on human adenocarcinoma cells, Sci. Rep. (2018). doi:10.1038/s41598-018-32480-5.

[8] A.A. Dayem, M.K. Hossain, S. Bin Lee, K. Kim, S.K. Saha, G.M. Yang, H.Y. Choi, S.G. Cho, The role of reactive oxygen species (ROS) in the biological activities of metallic nanoparticles, Int. J. Mol. Sci. (2017), https://doi.org/10.3390/ijms18010120.

[9] S. Gurunathan, J.W. Han, V. Eppakayala, M. Jeyaraj, J.H. Kim, Cytotoxicity of biologically synthesized silver nanoparticles in MDA-MB-231 human breast cancer cells, Biomed. Res. Int. 2013 (2013) 535796, , https://doi.org/10.1155/2013/535796.

[10] I.S. Kim, M. Baek, S.J. Choi, Comparative cytotoxicity of Al2O3, CeO2, TiO2 and ZnO nanoparticles to human lung cells, J. Nanosci. Nanotechnol. 10 (2010) 3453–3458, https://doi.org/10.1166/jnn.2010.2340.

[11] R.F. Huang, Y.J. Wei, B.S. Inbaraj, B.H. Chen, Inhibition of colon cancer cell growth by nanoemulsion carrying gold nanoparticles and lycopene, Int. J. Nanomed. 10 (2015) 2823–2846, https://doi.org/10.2147/IJN.S79107.

[12] A. Manke, L. Wang, Y. Rojanasakul, Mechanisms of nanoparticle-induced oxidative stress and toxicity, Biomed. Res. Int. 2013 (2013) 942916, , https://doi.org/10.1155/2013/942916.

[13] C. Carlson, S.M. Hussain, A.M. Schrand, L.K. Braydich-Stolle, K.L. Hess, R.L. Jones, J.J. Schlager, Unique cellular interaction of silver nanoparticles: size-dependent generation of reactive oxygen species, J. Phys. Chem. B. 112 (2008) 13608–13619, https://doi.org/10.1021/jp712087m.

[14] C. Lopez-Chaves, J. Soto-Alvaredo, M. Montes-Bayon, J. Bettmer, J. Llopis, C. Sanchez-Gonzalez, Gold nanoparticles: Distribution, bioaccumulation and toxicity. In vitro and in vivo studies, Nanomedicine. 14 (2018) 1–12, https://doi.org/10.1016/j.nano.2017.08.011.

[15] G. Ge, H. Wu, F. Xiong, Y. Zhang, Z. Guo, Z. Bian, J. Xu, C. Gu, N. Gu, X. Chen, D. Yang, The cytotoxicity evaluation of magnetic iron oxide nanoparticles on human aortic endothelial cells, Nanoscale Res. Lett. (2013), https://doi.org/10.1186/1556-276X-8-215.

[16] A.M. Holmes, J. Lim, H. Studier, M.S. Roberts, Varying the morphology of silver nanoparticles results in differential toxicity against micro-organisms, HaCaT keratinocytes and affects skin deposition, Nanotoxicology. (2016), https://doi.org/10.1080/17435390.2016.1236993.

[17] H. Liang, C. Jin, Y. Tang, F. Wang, C. Ma, Y. Yang, Cytotoxicity of silica nanoparticles on HaCaT cells, J. Appl. Toxicol. (2014), https://doi.org/10.1002/jat.2953.

[18] M. Wang, Q. Yang, J. Long, Y. Ding, X. Zou, G. Liao, Y. Cao, A comparative study of toxicity of TiO 2, ZnO, and Ag nanoparticles to human aortic smooth-muscle cells, Int. J. Nanomed. (2018), https://doi.org/10.2147/IJN.S188175.

[19] V.R. Lopes, V. Loitto, J.N. Audinot, N. Bayat, A.C. Gutleb, S. Cristobal, Dose-dependent autophagic effect of titanium dioxide nanoparticles in human HaCaT cells at non-cytotoxic levels, J. Nanobiotechnol. (2016), https://doi.org/10.1186/s12951-016-0174-0.

[20] R. Duffin, L. Tran, D. Brown, V. Stone, K. Donaldson, Proinflammogenic effects of low-toxicity and metal nanoparticles in vivo and in vitro: Highlighting the role of particle surface area and surface reactivity, Inhal. Toxicol. (2007), https://doi.org/10.1080/08958370701479323.

[21] A. Sukhanova, S. Bozrova, P. Sokolov, M. Berestovoy, A. Karaulov, I. Nabiev, Dependence of Nanoparticle Toxicity on Their Physical and Chemical Properties, Nanoscale Res. Lett. (2018), https://doi.org/10.1186/s11671-018-2457-x.

[22] P.R. Leroueil, S.A. Berry, K. Duthie, G. Han, V.M. Rotello, D.Q. McNerny, J.R. Baker, B.G. Orr, M.M.B. Holl, Wide varieties of cationic nanoparticles induce defects in supported lipid bilayers, Nano Lett. (2008), https://doi.org/10.1021/nl0722929.

[23] F. Wang, J. Liu, Liposome supported metal oxide nanoparticles: interaction mechanism, light controlled content release, and intracellular delivery, Small. (2014), https://doi.org/10.1002/smll.201400850.

[24] U. Bulbake, S. Doppalapudi, N. Kommineni, W. Khan, Liposomal formulations in clinical use: an updated review, Pharmaceutics. 9 (2017) 12, https://doi.org/10.3390/pharmaceutics9020012.

[25] O. Mertins, P.H. Schneider, A.R. Pohlmann, N.P. da Silveira, Interaction between phospholipids bilayer and chitosan in liposomes investigated by 31P NMR spectroscopy, Colloids Surf. B Biointerfaces. 75 (2010) 294–299, https://doi.org/10.1016/j.colsurfb.2009.08.048.

[26] A.S. Abu Lila, T. Ishida, Liposomal Delivery Systems: Design Optimization and Current Applications, Biol. Pharm. Bull. 40 (2017) 1–10, https://doi.org/10.1248/bpb.b16-00624.

[27] A. Wagner, M. Platzgummer, G. Kreismayr, H. Quendler, G. Stiegler, B. Ferko, G. Vecera, K. Vorauer-Uhl, H. Katinger, GMP production of liposomes–a new industrial approach, J. Liposome Res. 16 (2006) 311–319, https://doi.org/10.1080/08982100600851086.

[28] D. Carugo, E. Bottaro, J. Owen, E. Stride, C. Nastruzzi, Liposome production by microfluidics: potential and limiting factors, Sci. Rep. 6 (2016) 25876, https://doi.org/10.1038/srep25876.

[29] N. Lozano, W.T. Al-Jamal, A. Taruttis, N. Beziere, N.C. Burton, J. Van Den Bossche, M. Mazza, E. Herzog, V. Ntziachristos, K. Kostarelos, Liposome-gold nanorod hybrids for high-resolution visualization deep in tissues, J. Am. Chem. Soc. (2012), https://doi.org/10.1021/ja304499q.

[30] Š. Koudelka, J. Turánek, Liposomal paclitaxel formulations, J. Control. Release. (2012), https://doi.org/10.1016/j.jconrel.2012.09.006.

[31] Y. Chen, A. Bose, G.D. Bothun, Controlled release from bilayer-decorated magnetoliposomes via electromagnetic heating, ACS Nano. (2010), https://doi.org/10.1021/nn100274v.

[32] M.C. Woodle, D.D. Lasic, Sterically stabilized liposomes, BBA - Rev. Biomembr.

(1992), https://doi.org/10.1016/0304-4157(92)90038-C.
[33] L. Xu, T.A. Davis, N.A. Porter, Rate constants for peroxidation of polyunsaturated fatty acids and sterols in solution and in liposomes, J. Am. Chem. Soc. (2009), https://doi.org/10.1021/ja9029076.
[34] R.A. Demel, B. De Kruyff, The function of sterols in membranes, BBA - Rev. Biomembr. (1976), https://doi.org/10.1016/0304-4157(76)90008-3.
[35] M.L. Briuglia, C. Rotella, A. McFarlane, D.A. Lamprou, Influence of cholesterol on liposome stability and on in vitro drug release, Drug Deliv. Transl. Res. (2015), https://doi.org/10.1007/s13346-015-0220-8.
[36] T. Khan, P. Gurav, PhytoNanotechnology: Enhancing delivery of plant based anticancer drugs, Front. Pharmacol. (2018), https://doi.org/10.3389/fphar.2017.01002.
[37] G. Cevc, Phospholipids Handbook, 2018. doi:10.1201/9780203743577.
[38] Y. Panahi, M. Farshbaf, M. Mohammadhosseini, M. Mirahadi, R. Khalilov, S. Saghfi, A. Akbarzadeh, Recent advances on liposomal nanoparticles: synthesis, characterization and biomedical applications, Artif. Cells Nanomed. Biotechnol. 45 (2017) 788–799, https://doi.org/10.1080/21691401.2017.1282496.
[39] L. Juillerat-Jeanneret, The targeted delivery of cancer drugs across the blood-brain barrier: chemical modifications of drugs or drug-nanoparticles? Drug Discov. Today. (2008), https://doi.org/10.1016/j.drudis.2008.09.005.
[40] E.E.L. Swan, M.J. Mescher, W.F. Sewell, S.L. Tao, J.T. Borenstein, Inner ear drug delivery for auditory applications, Adv. Drug Deliv. Rev. (2008), https://doi.org/10.1016/j.addr.2008.08.001.
[41] Y.C. Barenholz, Doxil®—the first FDA-approved nano-drug: lessons learned, J. Control. Release. 160 (2012) 117–134.
[42] G. Beaune, C. Ménager, V. Cabuil, Location of magnetic and fluorescent nanoparticles encapsulated inside giant liposomes, J. Phys. Chem. B. (2008), https://doi.org/10.1021/jp711811u.
[43] J.P. Fortin-Ripoche, M.S. Martina, F. Gazeau, C. Ménager, C. Wilhelm, J.C. Bacri, S. Lesieur, O. Clément, Magnetic targeting of magnetoliposomes to solid tumors with MR imaging monitoring in mice: Feasibility, Radiology. (2006), https://doi.org/10.1148/radiol.2392042110.
[44] B. Steitz, J. Salaklang, A. Finka, C. O'Neil, H. Hofmann, A. Petri-Fink, Fixed bed reactor for solid-phase surface derivatization of superparamagnetic nanoparticles, Bioconjug. Chem. (2007), https://doi.org/10.1021/bc070100v.
[45] C.J. Meledandri, T. Ninjbadgar, D.F. Brougham, Size-controlled magnetoliposomes with tunable magnetic resonance relaxation enhancements, J. Mater. Chem. (2011), https://doi.org/10.1039/c0jm01061h.
[46] F. Maestrelli, M.L. González-Rodríguez, A.M. Rabasco, P. Mura, Effect of preparation technique on the properties of liposomes encapsulating ketoprofen-cyclodextrin complexes aimed for transdermal delivery, Int. J. Pharm. (2006), https://doi.org/10.1016/j.ijpharm.2005.12.047.
[47] L. Wang, M.P. Pileni, Encapsulation of Zwitterionic Au Nanocrystals into Liposomes by Reverse Phase Evaporation Method: Influence of the Surface Charge, Langmuir. (2016), https://doi.org/10.1021/acs.langmuir.6b01132.
[48] L. Paasonen, T. Laaksonen, C. Johans, M. Yliperttula, K. Kontturi, A. Urtti, Gold nanoparticles enable selective light-induced contents release from liposomes, J. Control. Release. (2007), https://doi.org/10.1016/j.jconrel.2007.06.009.
[49] G.A. Dichello, T. Fukuda, T. Maekawa, R.L.D. Whitby, S.V. Mikhalovsky, M. Alavijeh, A.S. Pannala, D.K. Sarker, Preparation of liposomes containing small gold nanoparticles using electrostatic interactions, Eur. J. Pharm. Sci. (2017), https://doi.org/10.1016/j.ejps.2017.05.001.
[50] Z. Al-Ahmady, N. Lozano, K.C. Mei, W.T. Al-Jamal, K. Kostarelos, Engineering thermosensitive liposome-nanoparticle hybrids loaded with doxorubicin for heat-triggered drug release, Int. J. Pharm. (2016), https://doi.org/10.1016/j.ijpharm.2016.09.009.
[51] V. Živanovic, J. Kneipp, Nano-bio interactions as characterized by SERS: The interaction of liposomes with gold nanostructures is highly dependent on lipid composition and charge, in: 2019. doi:10.1117/12.2508584.
[52] K.A.M. Eid, H.M.E. Azzazy, Sustained broad-spectrum antibacterial effects of nanoliposomes loaded with silver nanoparticles, Nanomedicine. (2014), https://doi.org/10.2217/nnm.13.89.
[53] T. Chen, X. Wang, M.H. Alizadeh, B.M. Reinhard, Monitoring transient nanoparticle interactions with liposome-confined plasmonic transducers, Microsyst. Nanoeng. 3 (2017) 16086, https://doi.org/10.1038/micronano.2016.86.
[54] S. Petralito, R. Spera, A. Memoli, G. D'Inzeo, M. Liberti, F. Apollonio, Preparation and characterization of lipid vesicles entrapping iron oxide nanoparticles, Asia-Pacific J. Chem. Eng. (2012), https://doi.org/10.1002/apj.1653.
[55] G. Piel, M. Piette, V. Barillaro, D. Castagne, B. Evrard, L. Delattre, Study of the relationship between lipid binding properties of cyclodextrins and their effect on the integrity of liposomes, Int. J. Pharm. (2007), https://doi.org/10.1016/j.ijpharm.2007.01.015.
[56] A.K. Gupta, S. Wells, Surface-Modified Superparamagnetic Nanoparticles for Drug Delivery: Preparation, Characterization, and Cytotoxicity Studies, IEEE Trans. Nanobiosci. (2004), https://doi.org/10.1109/TNB.2003.820277.
[57] J. Giri, S. Guha Thakurta, J. Bellare, A. Kumar Nigam, D. Bahadur, Preparation and characterization of phospholipid stabilized uniform sized magnetite nanoparticles, J. Magn. Magn. Mater. (2005), https://doi.org/10.1016/j.jmmm.2005.01.044.
[58] S. Gudlur, C. Sandén, P. Matoušková, C. Fasciani, D. Aili, Liposomes as nanoreactors for the photochemical synthesis of gold nanoparticles, J. Colloid Interface Sci. (2015), https://doi.org/10.1016/j.jcis.2015.06.033.
[59] R. Liang, J. Xie, J. Li, K. Wang, L. Liu, Y. Gao, M. Hussain, G. Shen, J. Zhu, J. Tao, Liposomes-coated gold nanocages with antigens and adjuvants targeted delivery to dendritic cells for enhancing antitumor immune response, Biomaterials. 149 (2017) 41–50, https://doi.org/10.1016/j.biomaterials.2017.09.029.
[60] S. Xing, X. Zhang, L. Luo, W. Cao, L. Li, Y. He, J. An, D. Gao, Doxorubicin/gold nanoparticles coated with liposomes for chemo-photothermal synergetic antitumor therapy, Nanotechnology. 29 (2018) 405101, , https://doi.org/10.1088/1361-6528/aad358.
[61] A. Yusuf, A. Brophy, B. Gorey, A. Casey, Liposomal encapsulation of silver nanoparticles enhances cytotoxicity and causes induction of reactive oxygen species-independent apoptosis, J. Appl. Toxicol. 38 (2018) 616–627, https://doi.org/10.1002/jat.3566.
[62] D.S.M. Pereira, B.D. Cardoso, A.R.O. Rodrigues, C.O. Amorim, V.S. Amaral, B.G. Almeida, M.-J.R.P. Queiroz, O. Martinho, F. Baltazar, R.C. Calhelha, et al., Magnetoliposomes Containing Calcium Ferrite Nanoparticles for Applications in Breast Cancer Therapy, Pharmaceutics 11 (2019) 477.
[63] S. Shaker, A. Gardouh, M. Ghorab, Factors affecting liposomes particle size prepared by ethanol injection method, Res. Pharm. Sci. (2017), https://doi.org/10.4103/1735-5362.213979.
[64] P. Hervella, E. Parra, D. Needham, Encapsulation and retention of chelated-copper inside hydrophobic nanoparticles: Liquid cored nanoparticles show better retention than a solid core formulation, Eur. J. Pharm. Biopharm. (2016), https://doi.org/10.1016/j.ejpb.2016.02.015.
[65] A.R.O. Rodrigues, J.M.F. Ramos, I.T. Gomes, B.G. Almeida, J.P. Araújo, M.J.R.P. Queiroz, P.J.G. Coutinho, E.M.S. Castanheira, Magnetoliposomes based on manganese ferrite nanoparticles as nanocarriers for antitumor drugs, RSC Adv. (2016), https://doi.org/10.1039/c5ra27058h.
[66] L. Zhou, L. Yang, C. Yang, Y. Liu, Q. Chen, W. Pan, Q. Cai, L. Luo, L. Liu, S. Jiang, H. He, Y. Zhang, T. Yin, X. Tang, Membrane Loaded Copper Oleate PEGylated Liposome Combined with Disulfiram for Improving Synergistic Antitumor Effect In Vivo, Pharm. Res. 35 (2018) 147, https://doi.org/10.1007/s11095-018-2414-5.
[67] A.R.O. Rodrigues, I.T. Gomes, B.G. Almeida, J.P. Araújo, E.M.S. Castanheira, P.J.G. Coutinho, Magnetic liposomes based on nickel ferrite nanoparticles for biomedical applications, Phys. Chem. Chem. Phys. (2015), https://doi.org/10.1039/c5cp01894c.
[68] D. Needham, M.W. Dewhirst, The development and testing of a new temperature-sensitive drug delivery system for the treatment of solid tumors, Adv. Drug Deliv. Rev. (2001), https://doi.org/10.1016/S0169-409X(01)00233-2.
[69] S. Ebrahim, G.A. Peyman, P.J. Lee, Applications of liposomes in ophthalmology, Surv. Ophthalmol. (2005), https://doi.org/10.1016/j.survophthal.2004.12.006.
[70] L.H. Lindner, M.E. Eichhorn, H. Eibl, N. Teichert, M. Schmitt-Sody, R.D. Issels, M. Dellian, Novel Temperature-Sensitive Liposomes with Prolonged Circulation Time, Clin. Cancer Res. (2004), https://doi.org/10.1158/1078-0432.CCR-03-0035.
[71] S.L. Huang, R.C. MacDonald, Acoustically active liposomes for drug encapsulation and ultrasound-triggered release, Biochim. Biophys. Acta - Biomembr. (2004), https://doi.org/10.1016/j.bbamem.2004.07.003.
[72] A. Mueller, B. Bondurant, D.F. O'Brien, Visible-light-stimulated destabilization of PEG-liposomes, Macromolecules. (2000), https://doi.org/10.1021/ma000055l.
[73] K.B. Ghaghanda, M. Ravoori, D. Sabapathy, J. Bankson, V. Kundra, A. Annapraganda, New dual mode gadolinium nanoparticle contrast agent for magnetic resonance imaging, PLoS One. (2009), https://doi.org/10.1371/journal.pone.0007628.
[74] C.N. Lok, T. Zou, J.J. Zhang, I.W.S. Lin, C.M. Che, Controlled-release systems for metal-based nanomedicine: Encapsulated/self-assembled nanoparticles of anticancer gold(III)/platinum(II) complexes and antimicrobial silver nanoparticles, Adv. Mater. (2014), https://doi.org/10.1002/adma.201305617.
[75] T. Boulikas, A. Pantos, E. Bellis, P. Christofis, Designing platinum compounds in cancer: structures and mechanisms, Cancer Ther (2007).
[76] G.P. Stathopoulos, T. Boulikas, Lipoplatin Formulation Review Article, J. Drug Deliv. (2012), https://doi.org/10.1155/2012/581363.
[77] M. Fantini, L. Gianni, C. Santelmo, F. Drudi, C. Castellani, A. Affatato, M. Nicolini, A. Ravaioli, Lipoplatin Treatment in Lung and Breast Cancer, Chemother. Res. Pract. (2011), https://doi.org/10.1155/2011/125192.
[78] P. Lee, K.K.Y. Wong, Lipophilic-Formulated Gold Porphyrin Nanoparticles for Chemotherapy, in: Cell. Subcell. Nanotechnol., Springer, 2013: pp. 93–98.
[79] P. Lee, Y. Zhu, J.J. Yan, R.W.Y. Sun, W. Hao, X. Liu, C.M. Che, K.K.Y. Wong, The cytotoxic effects of lipidic formulated gold porphyrin nanoparticles for the treatment of neuroblastoma, Nanotechnol. Sci. Appl. (2010), https://doi.org/10.2147/nsa.s8224.
[80] C. Contini, M. Schneemilch, S. Gaisford, N. Quirke, Nanoparticle–membrane interactions, J. Exp. Nanosci. (2018), https://doi.org/10.1080/17458080.2017.1413253.
[81] M. Daniel, J. Řezníčková, M. Handl, A. Iglič, V. Kralj-Iglič, Clustering and separation of hydrophobic nanoparticles in lipid bilayer explained by membrane mechanics, Sci. Rep. (2018), https://doi.org/10.1038/s41598-018-28965-y.
[82] S.H. Park, S.G. Oh, J.Y. Mun, S.S. Han, Loading of gold nanoparticles inside the DPPC bilayers of liposome and their effects on membrane fluidities, Colloids Surf. B Biointerfaces. (2006), https://doi.org/10.1016/j.colsurfb.2006.01.006.
[83] G.D. Bothun, Hydrophobic silver nanoparticles trapped in lipid bilayers: Size distribution, bilayer phase behavior, and optical properties, J. Nanobiotechnol. (2008), https://doi.org/10.1186/1477-3155-6-13.
[84] C. Bonnaud, C.A. Monnier, D. Demurtas, C. Jud, D. Vanhecke, X. Montet, R. Hovius, M. Lattuada, B. Rothen-Rutishauser, A. Petri-Fink, Insertion of nanoparticle clusters into vesicle bilayers, ACS Nano. (2014), https://doi.org/10.1021/nn406349z.
[85] T. Kubo, T. Sugita, S. Shimose, Y. Nitta, Y. Ikuta, T. Murakami, Targeted delivery of anticancer drugs with intravenously administered magnetic liposomes in osteosarcoma-bearing hamsters, Int. J. Oncol. (2000), https://doi.org/10.3892/ijo.17.2.309.

[86] X. Yue, Z. Dai, Liposomal nanotechnology for cancer theranostics, Curr. Med. Chem. 25 (2018) 1397–1408.
[87] R. Di Corato, G. Béalle, J. Kolosnjaj-Tabi, A. Espinosa, O. Clément, A.K.A. Silva, C. Ménager, C. Wilhelm, Combining magnetic hyperthermia and photodynamic therapy for tumor ablation with photoresponsive magnetic liposomes, ACS Nano. (2015), https://doi.org/10.1021/nn506949t.
[88] C.A. Monnier, D. Burnand, B. Rothen-Rutishauser, M. Lattuada, A. Petri-Fink, Magnetoliposomes: Opportunities and challenges, Eur. J. Nanomed. (2014), https://doi.org/10.1515/ejnm-2014-0042.
[89] M.S. Martina, C. Wilhelm, S. Lesieur, The effect of magnetic targeting on the uptake of magnetic-fluid-loaded liposomes by human prostatic adenocarcinoma cells, Biomaterials. (2008), https://doi.org/10.1016/j.biomaterials.2008.07.011.
[90] C. Van Ballegooie, A. Man, M. Win, D.T. Yapp, Spatially specific liposomal cancer therapy triggered by clinical external sources of energy, Pharmaceutics. (2019), https://doi.org/10.3390/pharmaceutics11030125.
[91] H. Nobuto, T. Sugita, T. Kubo, S. Shimose, Y. Yasunaga, T. Murakami, M. Ochi, Evaluation of systemic chemotherapy with magnetic liposomal doxorubicin and a dipole external electromagnet, Int. J. Cancer. (2004), https://doi.org/10.1002/ijc.20035.
[92] M. Yoshida, M. Sato, Y. Yamamoto, T. Maehara, T. Naohara, H. Aono, H. Sugishita, K. Sato, Y. Watanabe, Tumor local chemohyperthermia using docetaxel-embedded magnetoliposomes: Interaction of chemotherapy and hyperthermia, J. Gastroenterol. Hepatol. (2012), https://doi.org/10.1111/j.1440-1746.2011.06972.x.
[93] Y. Du, D. Zhang, H. Liu, R. Lai, Thermochemotherapy effect of nanosized As2O3/Fe3O4complex on experimental mouse tumors and its influence on the expression of CD44v6, VEGF-C and MMP-9, BMC Biotechnol. (2009), https://doi.org/10.1186/1472-6750-9-84.
[94] P. Pradhan, J. Giri, F. Rieken, C. Koch, O. Mykhaylyk, M. Döblinger, R. Banerjee, D. Bahadur, C. Plank, Targeted temperature sensitive magnetic liposomes for thermo-chemotherapy, J. Control. Release. (2010), https://doi.org/10.1016/j.jconrel.2009.10.002.
[95] H. Ye, J. Tong, J. Liu, W. Lin, C. Zhang, K. Chen, J. Zhao, W. Zhu, Combination of gemcitabine-containing magnetoliposome and oxaliplatin-containing magnetoliposome in breast cancer treatment: A possible mechanism with potential for clinical application, Oncotarget. (2016), https://doi.org/10.18632/oncotarget.9671.
[96] M. Pinzon-Daza, I. Campia, J. Kopecka, R. Garzon, D. Ghigo, C. Rigant, Nanoparticle- and Liposome-carried Drugs: New Strategies for Active Targeting and Drug Delivery Across Blood-brain Barrier, Curr. Drug Metab. (2013), https://doi.org/10.2174/1389200211314060001.
[97] M. Çağdaş, A.D. Sezer, S. Bucak, Liposomes as Potential Drug Carrier Systems for Drug Delivery, in: Appl. Nanotechnol. Drug Deliv., 2014. doi:10.5772/58459.
[98] B. Yameen, W. Il Choi, C. Vilos, A. Swami, J. Shi, O.C. Farokhzad, Insight into nanoparticle cellular uptake and intracellular targeting, J. Control. Release. (2014), https://doi.org/10.1016/j.jconrel.2014.06.038.
[99] G. Sahay, D.Y. Alakhova, A.V. Kabanov, Endocytosis of nanomedicines, J. Control. Release. (2010), https://doi.org/10.1016/j.jconrel.2010.01.036.
[100] J. Che, C. Okeke, Z.-B. Hu, J. Xu, DSPE-PEG: A Distinctive Component in Drug Delivery System, Curr. Pharm. Des. (2015), https://doi.org/10.2174/1381612821666150115144003.
[101] X. Fu, Y. Lu, J. Guo, H. Liu, A. Deng, C. Kuang, X. Xie, K237-modified thermosensitive liposome enhanced the delivery efficiency and cytotoxicity of paclitaxel in vitro, J. Liposome Res. (2019), https://doi.org/10.1080/08982104.2018.1458863.
[102] A. Tomas, C.E. Futter, E.R. Eden, EGF receptor trafficking: Consequences for signaling and cancer, Trends Cell Biol. (2014), https://doi.org/10.1016/j.tcb.2013.11.002.
[103] P.P. Deshpande, S. Biswas, V.P. Torchilin, Current trends in the use of liposomes for tumor targeting, Nanomedicine. (2013), https://doi.org/10.2217/nnm.13.118.
[104] E. Barcińska, J. Wierzbicka, A. Zauszkiewicz-Pawlak, D. Jacewicz, A. Dabrowska, I. Inkielewicz-Stepniak, Role of Oxidative and Nitro-Oxidative Damage in Silver Nanoparticles Cytotoxic Effect against Human Pancreatic Ductal Adenocarcinoma Cells, Oxid. Med. Cell. Longev. (2018), https://doi.org/10.1155/2018/8251961.
[105] W. Jiang, B.Y.S. Kim, J.T. Rutka, W.C.W. Chan, Nanoparticle-mediated cellular response is size-dependent, Nat. Nanotechnol. (2008), https://doi.org/10.1038/nnano.2008.30.
[106] M. Ahamed, M. Karns, M. Goodson, J. Rowe, S.M. Hussain, J.J. Schlager, Y. Hong, DNA damage response to different surface chemistry of silver nanoparticles in mammalian cells, Toxicol. Appl. Pharmacol. (2008), https://doi.org/10.1016/j.taap.2008.09.015.
[107] K. Jain, P. Kesharwani, U. Gupta, N.K. Jain, Dendrimer toxicity: Let's meet the challenge, Int. J. Pharm. (2010), https://doi.org/10.1016/j.ijpharm.2010.04.027.
[108] I. Brigger, C. Dubernet, P. Couvreur, Nanoparticles in cancer therapy and diagnosis, Adv. Drug Deliv. Rev. (2012), https://doi.org/10.1016/j.addr.2012.09.006.
[109] D.J. Bharali, M. Khalil, M. Gurbuz, T.M. Simone, S.A. Mousa, Nanoparticles and cancer therapy: A concise review with emphasis on dendrimers, Int. J. Nanomed. (2009).
[110] K. Madaan, S. Kumar, N. Poonia, V. Lather, D. Pandita, Dendrimers in drug delivery and targeting: Drug-dendrimer interactions and toxicity issues, J. Pharm. Bioallied Sci. (2014), https://doi.org/10.4103/0975-7406.130965.
[111] P.E. Froehling, Dendrimers and dyes - A review, Dye. Pigment. (2001), https://doi.org/10.1016/S0143-7208(00)00099-1.
[112] R.W.J. Scott, O.M. Wilson, R.M. Crooks, Synthesis, characterization, and applications of dendrimer-encapsulated nanoparticles, J. Phys. Chem. B. (2005), https://doi.org/10.1021/jp0469665.
[113] E.R. Gillies, J.M.J. Fréchet, Dendrimers and dendritic polymers in drug delivery, Drug Discov. Today. (2005), https://doi.org/10.1016/S1359-6446(04)03276-3.
[114] L. Ropartz, R.E. Morris, D.F. Foster, D.J. Cole-Hamilton, Increased selectivity in hydroformylation reactions using dendrimer based catalysts; a positive dendrimer effect, Chem. Commun. (2001), https://doi.org/10.1039/b009574p.
[115] C.J. Hawker, J.M.J. Fréchet, Preparation of Polymers with Controlled Molecular Architecture. A New Convergent Approach to Dendritic Macromolecules, J. Am. Chem. Soc. (1990), https://doi.org/10.1021/ja00177a027.
[116] D.A. Tomalia, J.M.J. Fréchet, Discovery of dendrimers and dendritic polymers: A brief historical perspective, J. Polym. Sci. Part A Polym. Chem. (2002), https://doi.org/10.1002/pola.10301.
[117] P.J. Gittins, L.J. Twyman, Dendrimers and supramolecular chemistry, Supramol. Chem. (2003), https://doi.org/10.1080/1061027031000073199.
[118] J.M.J. Fréchet, D.A. Tomalia, eds., Dendrimers and Other Dendritic Polymers, John Wiley & Sons, Ltd, Chichester, UK, 2001. doi:10.1002/0470845821.
[119] J. Singh, K. Jain, N.K. Mehra, N.K. Jain, Dendrimers in anticancer drug delivery: mechanism of interaction of drug and dendrimers, Artif. Cells, Nanomedicine Biotechnol. (2016), https://doi.org/10.3109/21691401.2015.1129625.
[120] Y. Niu, R.M. Crooks, Dendrimer-encapsulated metal nanoparticles and their applications to catalysis, Comptes Rendus Chim. (2003), https://doi.org/10.1016/j.crci.2003.08.001.
[121] F. Gröhn, B.J. Bauer, Y.A. Akpalu, C.L. Jackson, E.J. Amis, Dendrimer templates for the formation of gold nanoclusters, Macromolecules. (2000), https://doi.org/10.1021/ma000149v.
[122] V.S. Myers, M.G. Weir, E.V. Carino, D.F. Yancey, S. Pande, R.M. Crooks, Dendrimer-encapsulated nanoparticles: New synthetic and characterization methods and catalytic applications, Chem. Sci. (2011), https://doi.org/10.1039/c1sc00256b.
[123] R.M. Crooks, M. Zhao, L. Sun, V. Chechik, L.K. Yeung, Dendrimer-encapsulated metal nanoparticles: Synthesis, characterization, and applications to catalysis, Acc. Chem. Res. (2001), https://doi.org/10.1021/ar000110a.
[124] R. Esfand, D.A. Tomalia, Poly(amidoamine) (PAMAM) dendrimers: From biomimicry to drug delivery and biomedical applications, Drug Discov. Today. (2001), https://doi.org/10.1016/S1359-6446(01)01757-3.
[125] M.J. Cho, D.H. Choi, P.A. Sullivan, A.J.P. Akelaitis, L.R. Dalton, Recent progress in second-order nonlinear optical polymers and dendrimers, Prog. Polym. Sci. (2008), https://doi.org/10.1016/j.progpolymsci.2008.07.007.
[126] D. Astruc, E. Boisselier, C. Ornelas, Dendrimers designed for functions: From physical, photophysical, and supramolecular properties to applications in sensing, catalysis, molecular electronics, photonics, and nanomedicine, Chem. Rev. (2010), https://doi.org/10.1021/cr900327d.
[127] X. Li, M. Zamponi, K. Hong, L. Porcar, C.Y. Shew, T. Jenkins, E. Liu, G.S. Smith, K.W. Herwig, Y. Liu, W.R. Chen, PH Responsiveness of polyelectrolyte dendrimers: A dynamical perspective, Soft Matter. (2011), https://doi.org/10.1039/c0sm00671h.
[128] P. Kesharwani, K. Jain, N.K. Jain, Dendrimer as nanocarrier for drug delivery, Prog. Polym. Sci. (2014), https://doi.org/10.1016/j.progpolymsci.2013.07.005.
[129] R. Jevprasesphant, J. Penny, R. Jalal, D. Attwood, N.B. McKeown, A. D'Emanuele, The influence of surface modification on the cytotoxicity of PAMAM dendrimers, Int. J. Pharm. (2003), https://doi.org/10.1016/S0378-5173(02)00623-3.
[130] M. Zhao, R.M. Crooks, Intradendrimer exchange of metal nanoparticles, Chem. Mater. (1999), https://doi.org/10.1021/cm990435p.
[131] D. Glasner, A.I. Frenkel, Geometrical characteristics of regular polyhedra: Application to EXAFS studies of nanoclusters, AIP Conf. Proc. (2007), https://doi.org/10.1063/1.2644651.
[132] R.W.J. Scott, C. Sivadinarayana, O.M. Wilson, Z. Yan, D.W. Goodman, R.M. Crooks, Titania-supported PdAu bimetallic catalysts prepared from dendrimer-encapsulated nanoparticle precursors, J. Am. Chem. Soc. (2005), https://doi.org/10.1021/ja044446h.
[133] D.F. Yancey, E.V. Carino, R.M. Crooks, Electrochemical synthesis and electrocatalytic properties of Au@Pt dendrimer-encapsulated nanoparticles, J. Am. Chem. Soc. (2010), https://doi.org/10.1021/ja104677z.
[134] D.A. Tomalia, Birth of a new macromolecular architecture: Dendrimers as quantized building blocks for nanoscale synthetic polymer chemistry, Prog. Polym. Sci. (2005), https://doi.org/10.1016/j.progpolymsci.2005.01.007.
[135] C.C. Lee, J.A. MacKay, J.M.J. Fréchet, F.C. Szoka, Designing dendrimers for biological applications, Nat. Biotechnol. (2005), https://doi.org/10.1038/nbt1171.
[136] Y. Umeda, C. Kojima, A. Harada, H. Horinaka, K. Kono, PEG-attached PAMAM dendrimers encapsulating gold nanoparticles: Growing gold nanoparticles in the dendrimers for improvement of their photothermal properties, Bioconjug. Chem. (2010), https://doi.org/10.1021/bc1001399.
[137] C.B. Anders, J.E. Eixenberger, N.A. Franco, R.J. Hermann, K.D. Rainey, J.J. Chess, A. Punnoose, D.G. Wingett, ZnO nanoparticle preparation route influences surface reactivity, dissolution and cytotoxicity, Environ. Sci. Nano. (2018), https://doi.org/10.1039/c7en00888k.
[138] S. Runa, M. Hussey, C.K. Payne, Nanoparticle-Cell Interactions: Relevance for Public Health, J. Phys. Chem. B. (2018), https://doi.org/10.1021/acs.jpcb.7b08650.
[139] M.T. McMahon, J.W.M. Bulte, Two decades of dendrimers as versatile MRI agents: a tale with and without metals, Wiley Interdiscip. Rev. Nanomed. Nanobiotechnol. (2018), https://doi.org/10.1002/wnan.1496.
[140] A.B. Witte, A.N. Leistra, P.T. Wong, S. Bharathi, K. Refior, P. Smith, O. Kaso, K. Sinniah, S.K. Choi, Atomic force microscopy probing of receptor-nanoparticle interactions for riboflavin receptor targeted gold-dendrimer nanocomposites, J. Phys. Chem. B. (2014), https://doi.org/10.1021/jp412053w.

[141] K.R. Gopidas, J.K. Whitesell, M.A. Fox, Metal-Core-Organic Shell Dendrimers as Unimolecular Micelles, J. Am. Chem. Soc. (2003), https://doi.org/10.1021/ja036626h.
[142] H. Wu, Z. Liu, X. Wang, B. Zhao, J. Zhang, C. Li, Preparation of hollow capsule-stabilized gold nanoparticles through the encapsulation of the dendrimer, J. Colloid Interface Sci. (2006), https://doi.org/10.1016/j.jcis.2006.06.019.
[143] H. Xiao, R. Wang, L. Dong, Y. Cui, S. Chen, H. Sun, G. Ma, D. Gao, L. Wang, Biocompatible Dendrimer-Encapsulated Palladium Nanoparticles for Oxidation of Morin, ACS Omega. (2019), https://doi.org/10.1021/acsomega.9b02606.
[144] M. Koprowski, R.M. Sebastián, V. Maraval, M. Zablocka, V. Cadierno, B. Donnadieu, A. Igau, A.M. Caminade, J.P. Majoral, Iminophosphine palladium complexes in catalytic stille coupling reactions: From monomers to dendrimers, Organometallics. (2002), https://doi.org/10.1021/om011076m.
[145] K. Esumi, Dendrimers for Nanoparticle Synthesis and Dispersion Stabilization, in: 2003. doi:10.1007/3-540-36412-9_2.
[146] A. Pourjavadi, S.H. Hosseini, S.T. Hosseini, S.A. Aghayeemeibody, Magnetic nanoparticles coated by acidic functionalized poly(amidoamine) dendrimer: Effective acidic organocatalyst, Catal. Commun. (2012), https://doi.org/10.1016/j.catcom.2012.08.018.
[147] F. Ramírez-Crescencio, A.E. Enciso, M. Hasan, V.C.P. Da Costa, O. Annunziata, R. Redón, J.L. Coffer, E.E. Simanek, Thermoregulated coacervation, metal-encapsulation and nanoparticle synthesis in novel triazine dendrimers, Molecules. (2016), https://doi.org/10.3390/molecules21050599.
[148] S. Aliannejadi, A. hesam Hassani, H. Ahmad panahi, S.M. Borghei, Synthesis of Fe3O4 Nanoparticles Modified with Hyper Branched Dendrimers to Remove Anthracene from Contaminated Water, J. Ilam Univ. Med. Sci. (2020). doi:10.29252/sjimu.27.6.1.
[149] Y. Pan, A. Leifert, D. Ruau, S. Neuss, J. Bornemann, G. Schmid, W. Brandau, U. Simon, W. Jahnen-Dechent, Gold nanoparticles of diameter 1.4 nm trigger necrosis by oxidative stress and mitochondrial damage, Small. (2009), https://doi.org/10.1002/smll.200900466.
[150] P.K. Jain, I.H. ElSayed, M.A. El-Sayed, Au nanoparticles target cancer, Nano Today. (2007), https://doi.org/10.1016/S1748-0132(07)70016-6.
[151] D. Ma, H. Bin Zhang, Y.Y. Chen, J.T. Lin, L.M. Zhang, New cyclodextrin derivative containing poly(L-lysine) dendrons for gene and drug co-delivery, J. Colloid Interface Sci. (2013). doi:10.1016/j.jcis.2013.05.017.
[152] V. Brunetti, L.M. Bouchet, M.C. Strumia, Nanoparticle-cored dendrimers: Functional hybrid nanocomposites as a new platform for drug delivery systems, Nanoscale. (2015), https://doi.org/10.1039/c4nr04438j.
[153] L.P. Mendes, J. Pan, V.P. Torchilin, Dendrimers as nanocarriers for nucleic acid and drug delivery in cancer therapy, Molecules. (2017), https://doi.org/10.3390/molecules22091401.
[154] W.M. Liu, Y.N. Xue, N. Peng, W.T. He, R.X. Zhuo, S.W. Huang, Dendrimer modified magnetic iron oxide nanoparticle/DNA/PEI ternary magnetoplexes: A novel strategy for magnetofection, J. Mater. Chem. (2011), https://doi.org/10.1039/c1jm11460c.
[155] B. Pan, D. Cui, Y. Sheng, C. Ozkan, F. Gao, R. He, Q. Li, P. Xu, T. Huang, Dendrimer-modified magnetic nanoparticles enhance efficiency of gene delivery system, Cancer Res. (2007), https://doi.org/10.1158/0008-5472.CAN-06-4762.
[156] R.M. Crooks, B.I. Lemon, L. Sun, L.K. Yeung, M. Zhao, Dendrimer-Encapsulated Metals and Semiconductors: Synthesis, Characterization, and Applications, in: 2001. doi:10.1007/3-540-44924-8_3.
[157] M. Nemanashi, R. Meijboom, Synthesis and characterization of Cu, Ag and Au dendrimer-encapsulated nanoparticles and their application in the reduction of 4-nitrophenol to 4-aminophenol, J. Colloid Interface Sci. (2013), https://doi.org/10.1016/j.jcis.2012.09.012.
[158] D. Astruc, F. Chardac, Dendritic catalysts and dendrimers in catalysis, Chem. Rev. (2001), https://doi.org/10.1021/cr010323t.
[159] C. Kojima, Y. Umeda, M. Ogawa, A. Harada, Y. Magata, K. Kono, X-ray computed tomography contrast agents prepared by seeded growth of gold nanoparticles in PEGylated dendrimer, Nanotechnology. (2010), https://doi.org/10.1088/0957-4484/21/24/245104.
[160] K. Yamamoto, T. Imaoka, M. Tanabe, T. Kambe, New Horizon of Nanoparticle and Cluster Catalysis with Dendrimers, Chem. Rev. (2019), https://doi.org/10.1021/acs.chemrev.9b00188.
[161] E. Vasile, A. Serafim, D. Petre, D. Giol, P. Dubruel, H. Iovu, I.C. Stancu, Direct synthesis and morphological characterization of gold-dendrimer nanocomposites prepared using PAMAM succinamic acid dendrimers: Preliminary study of the calcification potential, Sci. World J. (2014), https://doi.org/10.1155/2014/103462.
[162] M. Bernechea, E. De Jesus, C. Lopez-Mardomingo, P. Terreros, Dendrimer-encapsulated Pd nanoparticles versus palladium acetate as catalytic precursors in the stille reaction in water, Inorg. Chem. (2009), https://doi.org/10.1021/ic9002753.
[163] H. Müller, Optical Properties of Metal Clusters, Zeitschrift Für Phys. Chemie. (1996), https://doi.org/10.1524/zpch.1996.194.part_2.278.
[164] X. Yuan, S. Wen, M. Shen, X. Shi, Dendrimer-stabilized silver nanoparticles enable efficient colorimetric sensing of mercury ions in aqueous solution, Anal. Methods. (2013), https://doi.org/10.1039/c3ay41331d.
[165] J. Ruan, J. Shen, Z. Wang, J. Ji, H. Song, K. Wang, B. Liu, J. Li, D. Cui, Efficient preparation and labeling of human induced pluripotent stem cells by nanotechnology, Int. J. Nanomed. (2011), https://doi.org/10.2147/ijn.s16498.
[166] W. Lesniak, A.U. Blelinska, K. Sun, K.W. Janczak, X. Shi, J.R. Baker, L.P. Balogh, Silver/dendrimer nanocomposites as biomarkers: Fabrication, characterization, in vitro toxicity, and intracellular detection, Nano Lett. (2005), https://doi.org/10.1021/nl051077u.
[167] V. Márquez-Miranda, J.P. Peñaloza, I. Araya-Durán, R. Reyes, S. Vidaurre, V. Romero, J. Fuentes, F. Céric, L. Velásquez, F.D. González-Nilo, C. Otero, Effect of Terminal Groups of Dendrimers in the Complexation with Antisense Oligonucleotides and Cell Uptake, Nanoscale Res. Lett. (2016), https://doi.org/10.1186/s11671-016-1260-9.
[168] X. Shi, S. Wang, S. Meshinchi, M.E. Van Antwerp, X. Bi, I. Lee, J.R. Baker, Dendrimer-entrapped gold nanoparticles as a platform for cancer-cell targeting and imaging, Small. (2007), https://doi.org/10.1002/smll.200700054.
[169] X. Shi, S. Wang, H. Sun, J.R. Baker, Improved biocompatibility of surface functionalized dendrimer-entrapped gold nanoparticles, Soft Matter. (2007), https://doi.org/10.1039/b612972b.
[170] D. Pan, J.L. Turner, K.L. Wooley, Folic acid-conjugated nanostructured materials designed for cancer cell targeting, Chem. Commun. (2003), https://doi.org/10.1039/b307878g.
[171] P. Garin-Chesa, I. Campbell, P.E. Saigo, J.L. Lewis, L.J. Old, W.J. Rettig, Trophoblast and ovarian cancer antigen LK26: Sensitivity and specificity in immunopathology and molecular identification as a folate-binding protein, Am. J. Pathol. (1993).
[172] X. Shi, S.H. Wang, S.D. Swanson, S. Ge, Z. Cao, M.E. Van Antwerp, K.J. Landmark, J.R. Baker, Dendrimer-functionalized shell-crosslinked iron oxide nanoparticles for in-vivo magnetic resonance imaging of tumors, Adv. Mater. (2008), https://doi.org/10.1002/adma.200702770.
[173] S.S. Malhi, A. Budhiraja, S. Arora, K.R. Chaudhari, K. Nepali, R. Kumar, H. Sohi, R.S.R. Murthy, Intracellular delivery of redox cycler-doxorubicin to the mitochondria of cancer cell by folate receptor targeted mitocancerotropic liposomes, Int. J. Pharm. (2012), https://doi.org/10.1016/j.ijpharm.2012.04.030.
[174] Y. Cheng, L. Zhao, Y. Li, T. Xu, Design of biocompatible dendrimers for cancer diagnosis and therapy: current status and future perspectives, Chem. Soc. Rev. 40 (2011) 2673, https://doi.org/10.1039/c0cs00097c.
[175] L.J. Fox, R.M. Richardson, W.H. Briscoe, PAMAM dendrimer - cell membrane interactions, Adv. Colloid Interface Sci. 257 (2018) 1–18, https://doi.org/10.1016/j.cis.2018.06.005.
[176] O.P. Perumal, R. Inapagolla, S. Kannan, R.M. Kannan, The effect of surface functionality on cellular trafficking of dendrimers, Biomaterials. 29 (2008) 3469–3476, https://doi.org/10.1016/j.biomaterials.2008.04.038.
[177] C. Le Roy, J.L. Wrana, Clathrin- and non-clathrin-mediated endocytic regulation of cell signalling, Nat. Rev. Mol. Cell Biol. 6 (2005) 112–126, https://doi.org/10.1038/nrm1571.
[178] K.M. Kitchens, A.B. Foraker, R.B. Kolhatkar, P.W. Swaan, H. Ghandehari, Endocytosis and Interaction of Poly (Amidoamine) Dendrimers with Caco-2 Cells, Pharm. Res. 24 (2007) 2138–2145, https://doi.org/10.1007/s11095-007-9415-0.
[179] M.A. Maher, H.J. Byrne, Modification of the in vitro uptake mechanism and antioxidant levels in HaCaT cells and resultant changes to toxicity and oxidative stress of G4 and G6 poly(amidoamine) dendrimer nanoparticles, Anal. Bioanal. Chem. 408 (2016) 5295–5307, https://doi.org/10.1007/s00216-016-9623-8.
[180] M. Manunta, Gene delivery by dendrimers operates via a cholesterol dependent pathway, Nucleic Acids Res. 32 (2004) 2730–2739, https://doi.org/10.1093/nar/gkh595.
[181] T.P. Thomas, I. Majoros, A. Kotlyar, D. Mullen, M.M.B. Holl, J.R. Baker, Cationic poly(amidoamine) dendrimer induces lysosomal apoptotic pathway at therapeutically relevant concentrations, Biomacromolecules. 10 (2009) 3207–3214, https://doi.org/10.1021/bm900683r.
[182] S. Rana, A. Bajaj, R. Mout, V.M. Rotello, Monolayer coated gold nanoparticles for delivery applications, Adv. Drug Deliv. Rev. (2012), https://doi.org/10.1016/j.addr.2011.08.006.
[183] Y. Yang, P. Burkhard, Encapsulation of gold nanoparticles into self-assembling protein nanoparticles, J. Nanobiotechnol. (2012), https://doi.org/10.1186/1477-3155-10-42.
[184] C.D. Spicer, C. Jumeaux, B. Gupta, M.M. Stevens, Peptide and protein nanoparticle conjugates: Versatile platforms for biomedical applications, Chem. Soc. Rev. (2018), https://doi.org/10.1039/c7cs00877e.
[185] Y. Amini, S. Amel Jamehdar, K. Sadri, S. Zare, D. Musavi, M. Tafaghodi, Different methods to determine the encapsulation efficiency of protein in PLGA nanoparticles, Biomed. Mater. Eng. (2017), https://doi.org/10.3233/BME-171705.
[186] B.D. Chithrani, W.C.W. Chan, Elucidating the mechanism of cellular uptake and removal of protein-coated gold nanoparticles of different sizes and shapes, Nano Lett. (2007), https://doi.org/10.1021/nl070363y.
[187] W.T. Leach, D.T. Simpson, T.N. Val, Z. Yu, K.T. Lim, E.J. Park, R.O. Williams, K.P. Johnston, Encapsulation of protein nanoparticles into uniform-sized microspheres formed in a spinning oil film, AAPS PharmSciTech. (2005), https://doi.org/10.1208/pt060475.
[188] A.G. Tkachenko, H. Xie, Y. Liu, D. Coleman, J. Ryan, W.R. Glomm, M.K. Shipton, S. Franzen, D.L. Feldheim, Cellular trajectories of peptide-modified gold particle complexes: Comparison of nuclear localization signals and peptide transduction domains, Bioconjug. Chem. (2004), https://doi.org/10.1021/bc034189q.
[189] A.G. Tkachenko, H. Xie, D. Coleman, W. Glomm, J. Ryan, M.F. Anderson, S. Franzen, D.L. Feldheim, Multifunctional gold nanoparticle-peptide complexes for nuclear targeting, J. Am. Chem. Soc. (2003), https://doi.org/10.1021/ja0296935.
[190] N. Sanvicens, M.P. Marco, Multifunctional nanoparticles - properties and prospects for their use in human medicine, Trends Biotechnol. (2008), https://doi.org/10.1016/j.tibtech.2008.04.005.
[191] G.S. Terentyuk, G.N. Maslyakova, L.V. Suleymanova, N.G. Khlebtsov, B.N. Khlebtsov, G.G. Akchurin, I.L. Maksimova, V.V. Tuchin, Laser-induced tissue hyperthermia mediated by gold nanoparticles: toward cancer phototherapy, J. Biomed. Opt. (2009), https://doi.org/10.1117/1.3122371.
[192] C. Bárcena, A.K. Sra, J. Gao, Applications of magnetic nanoparticles in

biomedicine, in: Nanoscale Magn. Mater. Appl., 2009. doi:10.1007/978-0-387-85600-1_20.
[193] S. Kim, J.E. Choi, J. Choi, K.-H. Chung, K. Park, J. Yi, D.-Y. Ryu, Oxidative stress-dependent toxicity of silver nanoparticles in human hepatoma cells, Toxicol. Vitr. 23 (2009) 1076–1084.
[194] P. Bihari, M. Vippola, S. Schultes, M. Praetner, A.G. Khandoga, C.A. Reichel, C. Coester, T. Tuomi, M. Rehberg, F. Krombach, Optimized dispersion of nanoparticles for biological in vitro and in vivo studies, Part. Fibre Toxicol. (2008), https://doi.org/10.1186/1743-8977-5-14.
[195] P.K. Mishra, H. Mishra, A. Ekielski, S. Talegaonkar, B. Vaidya, Zinc oxide nanoparticles: a promising nanomaterial for biomedical applications, Drug Discov. Today. (2017), https://doi.org/10.1016/j.drudis.2017.08.006.
[196] R. Mittler, Oxidative stress, antioxidants and stress tolerance, Trends Plant Sci. (2002), https://doi.org/10.1016/S1360-1385(02)02312-9.
[197] R.F.S. Huang, Y.J. Wei, B.S. Inbaraj, B.H. Chen, Inhibition of colon cancer cell growth by nanoemulsion carrying gold nanoparticles and lycopene, Int. J. Nanomed. (2015), https://doi.org/10.2147/IJN.S79107.
[198] J.C.M. Espinosa, N.A.C. Ramírez, L.E.F. Oliva, T.C. Fraga, J.B. Alvarado, A.R. Pablo, R.E.N. Anita, Coating of gold nanoparticles for medical application: UV-VIS, AIP Conf. Proc. 1626 (2014) 147–150, https://doi.org/10.1063/1.4901380.
[199] Y. Huang, Y. Luo, W. Zheng, T. Chen, Rational design of cancer-targeted BSA protein nanoparticles as radiosensitizer to overcome cancer radioresistance, ACS Appl. Mater. Interfaces. (2014), https://doi.org/10.1021/am505246w.
[200] Z.P. Xu, Q.H. Zeng, G.Q. Lu, A.B. Yu, Inorganic nanoparticles as carriers for efficient cellular delivery, Chem. Eng. Sci. (2006), https://doi.org/10.1016/j.ces.2005.06.019.
[201] A.R. Gliga, S. Skoglund, I. Odnevall Wallinder, B. Fadeel, H.L. Karlsson, Size-dependent cytotoxicity of silver nanoparticles in human lung cells: The role of cellular uptake, agglomeration and Ag release, Part. Fibre Toxicol. (2014), https://doi.org/10.1186/1743-8977-11-11.
[202] R. de Lima, A.B. Seabra, N. Durán, Silver nanoparticles: A brief review of cytotoxicity and genotoxicity of chemically and biogenically synthesized nanoparticles, J. Appl. Toxicol. (2012), https://doi.org/10.1002/jat.2780.
[203] H.M. Joshi, D.R. Bhumkar, K. Joshi, V. Pokharkar, M. Sastry, Gold nanoparticles as carriers for efficient transmucosal insulin delivery, Langmuir. (2006), https://doi.org/10.1021/la051982u.
[204] C.H.J. Choi, C.A. Alabi, P. Webster, M.E. Davis, Mechanism of active targeting in solid tumors with transferrin-containing gold nanoparticles, Proc. Natl. Acad. Sci. U. S. A. (2010), https://doi.org/10.1073/pnas.0914140107.
[205] A. Verma, J.M. Simard, J.W.E. Worrall, V.M. Rotello, Tunable reactivation of nanoparticle-inhibited β-galactosidase by glutathione at intracellular concentrations, J. Am. Chem. Soc. (2004), https://doi.org/10.1021/ja046572r.
[206] R.K. Visaria, R.J. Griffin, B.W. Williams, E.S. Ebbini, G.F. Paciotti, C.W. Song, J.C. Bischof, Enhancement of tumor thermal therapy using gold nanoparticle-assisted tumor necrosis factor-α delivery, Mol. Cancer Ther. (2006), https://doi.org/10.1158/1535-7163.MCT-05-0381.
[207] K.A. Frankola, N.H. Greig, W. Luo, D. Tweedie, Targeting TNF-Alpha to Elucidate and Ameliorate Neuroinflammation in Neurodegenerative Diseases, CNS Neurol. Disord. - Drug Targets. (2011), https://doi.org/10.2174/187152711794653751.
[208] R. Goel, N. Shah, R. Visaria, G.F. Paciotti, J.C. Bischof, Biodistribution of TNF-α-coated gold nanoparticles in an in vivo model system, Nanomedicine. (2009), https://doi.org/10.2217/nnm.09.21.
[209] M.T. Klem, D. Willits, D.J. Solis, A.M. Belcher, M. Young, T. Douglas, Bio-inspired synthesis of protein-encapsulated CoPt nanoparticles, Adv. Funct. Mater. (2005), https://doi.org/10.1002/adfm.200400453.
[210] K.K.W. Wong, T. Douglas, S. Gider, D.D. Awschalom, S. Mann, Biomimetic Synthesis and Characterization of Magnetic Proteins (Magnetoferritin), Chem. Mater. (1998), https://doi.org/10.1021/cm970421o.
[211] R. Lévy, Peptide-capped gold nanoparticles: Towards artificial proteins, ChemBioChem. (2006), https://doi.org/10.1002/cbic.200600129.
[212] J.Y. Oh, H.S. Kim, L. Palanikumar, E.M. Go, B. Jana, S.A. Park, H.Y. Kim, K. Kim, J.K. Seo, S.K. Kwak, C. Kim, S. Kang, J.H. Ryu, Cloaking nanoparticles with protein corona shield for targeted drug delivery, Nat. Commun. (2018), https://doi.org/10.1038/s41467-018-06979-4.
[213] R. De Alteriis, R. Vecchione, C. Attanasio, M. De Gregorio, M. Porzio, E. Battista, P.A. Netti, A method to tune the shape of protein-encapsulated polymeric microspheres, Sci. Rep. (2015), https://doi.org/10.1038/srep12634.

Toxicology and Applied Pharmacology 443 (2022) 116009

Contents lists available at ScienceDirect

Toxicology and Applied Pharmacology

journal homepage: www.elsevier.com/locate/taap

Epidermal Growth Factor-labeled liposomes as a way to target the toxicity of silver nanoparticles into EGFR-overexpressing cancer cells *in vitro*

Bartosz Skóra [a,*], Tomasz Piechowiak [b], Konrad A. Szychowski [a]

[a] Department of Biotechnology and Cell Biology, Medical College, University of Information Technology and Management, St. Sucharskiego 2, 35-225 Rzeszow, Poland
[b] Department of Chemistry and Food Toxicology, Institute of Food Technology and Nutrition, University of Rzeszow, St. Cwiklinskiej 1A, 35-601 Rzeszow, Poland

ARTICLE INFO

Editor name: Lawrence Lash

Keywords:
Silver nanoparticles
Liposomes
Epidermal growth factor
EGFR
Oxidative stress
Anticancer treatment
Drug delivery system

ABSTRACT

Silver nanoparticles (AgNPs) are the most toxic nanostructures for both cancer and healthy cells. Thus, their usefulness in the anticancer therapy is limited. Interestingly, the epidermal growth factor receptor (EGFR) is overexpressed in many cancer cells, e.g. in lung and tongue cancers. Therefore, the aim of this study was to develop a way to direct the cytotoxic effect of AgNPs against cancer cells, saving healthy ones by entrapping these NPs inside liposomes labeled with the epidermal growth factor (EGF-LipoAgNPs) and directing these structures into EGFR-overexpressing cancer cells. The obtained results showed spherical structures with a 107.9 nm size and − 16.60 mV zeta-potential. The UV–Vis scan and TEM images did not show free AgNPs in the solution. The obtained complexes were able to decrease the metabolic activity in the A549 and SCC-15 cells more effectively than native AgNPs. Furthermore, the ROS production, lactate dehydrogenase release, and caspase-9 and -3 activity were significantly increased after the treatment with EGF-LipoAgNPs for 24 and 48 h. The expression of genes encoding catalase, superoxide dismutase, and p53 protein increased significantly, while the KI67 gene expression decreased, especially in the A549 and SCC-15 cells. Moreover, the KI67 protein expression was lower than in the cells treated with native AgNPs, while catalase activity was decreased significantly after the treatment with the obtained complexes. In turn, SOD activity increased more efficiently in the EGFR-overexpressing cancer cells. In all tested parameters, EGF-LipoAgNPs exerted a lower toxic effect on the BJ cells than native AgNPs. Summarizing, the created liposomal system reduces the toxicity of AgNPs against normal human fibroblasts and enhances the toxic and proapoptotic effect of these NPs, which may be caused by improvement of their uptake by EGFR-overexpressing cancer cells.

1. Introduction

Silver nanoparticles (AgNPs) are well-described antibacterial agents, which significantly decrease bacterial vitality and even cause eradication of the bacterial biofilm (Sánchez-López et al., 2020). Therefore, an increase in the use of AgNP-containing materials in medicine, e.g. as part of dressings to hard-to-heal-wounds, has been observed for the last decades (Morones et al., 2005). The impact of AgNPs is well tested in *in vitro* and *in vivo* models. Given the reports, the ability of AgNPs to induce oxidative stress and subsequently apoptosis even in nanomole concentrations has been repeatedly proved in the literature (Wiemann et al., 2017; George et al., 2018a; Skóra et al., 2021). The mechanism of the cytotoxic effect of AgNPs in cells is strictly correlated with their prooxidative properties. Due to their highly reactive surface, these NPs are able to cause permeabilization and subsequent leaking of the cell membrane and, in consequence, cell death as in human umbilical vein endothelial cells (HUVECs) described by Sun et al. (Sun et al., 2016). It has also been described that, after contact with cytoplasmic and mitochondrial enzymes, silver ions (Ag^{+}) can be released, which leads to insufficiency of the antioxidant systems due to induction of reactive oxygen species (ROS) in the cells and, in consequence, cell death (Govindaraju et al., 2015). These NPs are also a source of the

Abbreviations: AgNPs, silver nanoparticles; AuNPs, gold nanoparticles; CAT, catalase; CuNPs, copper nanoparticles; DMEM/F12, Dulbecco's Modified Eagle Medium/Nutrient Mixture F-12; DSPE-CF, 1,2-dioleoyl-sn-glycero-3-phosphoethanolamine-N-(carboxyfluorescein); FBS, fetal bovine serum; F-12 K, Ham's F-12 K (Kaighn's) Medium; H_2DCF-DA, 2′,7′-dichlorodihydrofluorescein diacetate; H_2O_2, hydrogen peroxide; EGF, epidermal growth factor; EGFR, epidermal growth factor receptor; MDR, multidrug-resistance; MEM, minimal essential medium; NPs, nanoparticles; SOD, superoxide dismutase.

* Corresponding author.
E-mail address: bskora@wsiz.edu.pl (B. Skóra).

https://doi.org/10.1016/j.taap.2022.116009
Received 10 September 2021; Received in revised form 24 March 2022; Accepted 30 March 2022
Available online 3 April 2022

dysfunction of mitochondria by causing depolarization of their membrane and, subsequently, activation of caspase-9 preceded by cytochrome c release (Sanpui et al., 2011). The ability of AgNPs to induce the intrinsic apoptotic pathway with the crucial role of caspase-9 has been well-described e.g. by Banerjee et al., who proved induction of apoptosis in breast cancer cells after treatment with 156 ppm of AgNPs (Banerjee et al., 2017). In turn, Zielinska et al. proved the ability of AgNPs to induce apoptosis in pancreatic cancer cells after treatment with 50 ppm (Zielinska et al., 2018).

Recent studies have also shown the ability of AgNPs to overcome multidrug-resistance (MDR) in cancer cells, which is defined as biochemical and cellular changes in these cells such as an increased apoptosis induction threshold or drug efflux from the cytoplasm (Kovács et al., 2016). This phenomenon is considered an emerging problem in the current anticancer treatment, requiring development of new more efficient drugs. However, Kovács et al. showed that AgNPs can inhibit proliferation of MDR cells with induction of ROS-dependent apoptosis (Kovács et al., 2016). Unfortunately, the cytotoxic effect after AgNP treatment is also observed in healthy cells such as human fibroblasts, microvascular endothelial cells, or mouse embryonic stem cells (Rajanahalli et al., 2015; Franková et al., 2016; Castiglioni, 2014). Therefore, the usefulness of AgNPs in the specific anticancer therapy is limited.

Over the last decade, encapsulation procedures have been developed to deliver metallic nanoparticles such as AgNPs, gold nanoparticles (AuNPs), or copper nanoparticles (CuNPs) in a safer and more effective way (reviewed in (Skóra et al., 2020)). The procedure is based on drug entrapment inside the liposome lumen or between the layers of the lipid bilayer (Skóra et al., 2020). This process allows improving the uptake of a certain substance by cells and, consequently, increasing its toxicity, facilitating the uptake of such complexes. It has been shown that doxorubicin encapsulated in liposomes is characterized by a higher toxic effect on breast cancer cells than cells treated with pure solutions of this drug (Elamir et al., 2021). The encapsulation procedure was also used to entrap metallic nanoparticles inside such as AgNPs, which were subsequently tested *in vitro* by Yusuf and Casey, who showed that by only encapsulation the cytotoxic effect of AgNPs can be increased by inducing ROS-dependent apoptosis (Yusuf and Casey, 2019). Unfortunately, the encapsulation procedure alone does not ensure targeting the cytotoxicity of AgNPs into certain cells. Therefore, labeling of the surface of the liposomes with certain ligands has been developed, which is mainly the target of a receptor involved in the endocytosis process, resulting in improvement in the uptake of such drug-containing liposomes (Chaudhury and Das, 2015; Aronson et al., 2021).

The Epidermal Growth Factor Receptor (EGFR) is a transmembrane protein, whose intracellular domain has the activity of kinases, playing a crucial role in many cellular processes such as proliferation, differentiation, gene regulation, and apoptosis (Rude Voldborg et al., 1997). It has been estimated that the number of EGFR in a normal cell reaches about 60,000 per cell (Singh et al., 2016). It has been also proved that many types of cancers overexpress this receptor, with head and neck, renal, and non-small lung cancers being the most intensive (Herbst and Shin, 2002). The natural ligands of this receptor are well defined and include e.g. the Epidermal Growth Factor (EGF), a protein which is characterized by 6 kDa mass (Singh et al., 2016). EGFR is also involved in the endocytosis process, which determines its usefulness in the improvement of the uptake of certain drugs, such as oxaliplatin, into xenograft colocarcinoma cell lines or siRNA as a treatment agent in ovarian cancers (Cao et al., 2019; Mangala et al., 2009). However, there are no data on EGFR targeting of the highly reactive surface of AgNPs into EGFR-overexpressing cancer cells.

Therefore, the aim of this study was to develop a way to direct the toxicity of AgNPs by entrapping them in liposomes labeled with the EGF protein into human lung carcinoma (A549) and human tongue squamous carcinoma (SCC-15) cell lines *in vitro* as models of EGFR-overexpressing cancer cells, in contrast to normal fibroblasts (BJ) - standard EGFR-expressing cells. The physicochemical characterization of the novel complexes such as their size, stability, and morphology was performed. Furthermore, the impact of such complexes on metabolic activity, intracellular ROS production, toxicity, apoptosis induction, antioxidant enzyme activity, and certain genes was determined. Moreover, the involvement of the EGF receptor in the uptake of such liposomes was tested by pretreatment of the cells with a pure solution of EGF. Lastly, the uptake of the studied compounds was evaluated using the fluorescence staining method.

2. Material and methods

2.1. Reagents

Trypsin, penicillin, streptomycin, resazurin, 2′, 7′ – dichlorodihydrofluorescein diacetate (H_2DCF-DA), cholesterol, ammonium metavanadate, perhydrol, epinephrine, sodium carbonate, sodium bicarbonate, caspase-3 (Ac-DEVD-pNA) and caspase-9 (Ac-LEHD-pNA) substrate, Tris base, methylene chloride, ethanol, L-glutamine, hydroxyethyl piperazineethanesulfonic acid (HEPES), sodium chloride, 3-[(3-Cholamidopropyl)dimethylammonio]-1-propanesulfonate hydrate (CHAPS), ethylenediaminetetraacetic acid (EDTA), glycerol, dithiothreitol (DTT), 2′-(4-Ethoxyphenyl)-5-(4-methyl-1-piperazinyl)-2,5′-bi-1H-benzimidazole trihydrochloride (Hoechst 33342), Rhodamine B, and 1,2-dioleoyl-sn-glycero-3-phosphoethanolamine-N-(carboxyfluorescein) (DSPE-CF) were purchased from Sigma-Aldrich (St. Louis, USA). 1,2-distearoyl-sn-glycero-3phosphatoethanoloamine (DSPC), N-hydroxysuccinimide-PEG$_{3400}$-DSPE (NHS-PEG$_{3400}$-DSPE), and DSPE-PEG$_{2000}$-Amine were purchased from Nanocs (Boston, USA). The human epidermal growth factor (EGF) protein was purchased from SinoBiological (Eschborn, Germany). Ham's F-12 K (Kaighn's) Medium (F12-K), Dulbecco's Modified Eagle Medium/Nutrient Mixture F-12 (DMEM/F12), and phosphate-buffer saline (PBS) were purchased from Corning (Tewksbury, MA, USA). The RIPA buffer, fetal bovine serum (FBS), Universal RNA Purification Kit and Fast Probe qPCR Master Mix (2x×), plus ROX Solution were obtained from EURx (Gdańsk, Poland). TaqMan probes corresponding to genes encoding *ACTB* (Hs01060665_g1), *EGFR* (Hs06634166_s1), *KI67* (Hs04260396_g1), *BP53* (Hs01034249_m1), *CAT* (Hs00156308_m1), and *SOD2* (Hs00167309_m1) were purchased from ThermoFisher (Grand Island, NY, USA). Spherical PVP-stabilized silver nanoparticles with a size of 5 nm were purchased from nanoComposix (San Diego, USA). The dialysis membranes (MWCO = 6000–8000 Da and MWCO = 10,000–12,000 Da) were purchased from Carl Roth (Karlsruhe, Germany).

2.2. Conjugation of EGF and NHS-PEG$_{3400}$-DSPE

The conjugation of EGF with NHS-PEG$_{3400}$-DSPE is based on the reaction between lysine residues in EGF and the NHS group. The method was applied according to Jung et al. with minor modifications (Jung et al., 2018). Briefly, the EGF protein and NHS-PEG$_{3400}$-DSPE were dissolved in PBS (pH = 7.4) and mixed together at a molar ratio of 1:2 (EGF: NHS-PEG$_{3400}$-DSPE). Subsequently, the mixture was shaken overnight at RT. After this time, the obtained solution was placed in a dialysis membrane (MWCO = 6000–8000) to remove unbound EGF. The dialysis procedure was performed for 24 h with continuous stirring and changing the PBS every 2 h. The obtained solution was subsequently used to label the liposomes with the EGF protein. The efficiency of the EGF and NHS-PEG$_{3400}$-DSPE conjugation was calculated as 68.05%, which was determined based on the Bradford method.

2.3. Liposome preparation

The liposomal encapsulation procedure was performed using thin-film hydration with the extrusion method according to Kullberg et al. and Yusuf and Casey with minor modifications (Yusuf and Casey, 2019; Kullberg et al., 2005). Briefly, DSPC, cholesterol, and DSPE-PEG$_{2000}$ at a molar ratio of 56:40:4, respectively, were dissolved in a methylene

chloride/ethanol mixture (volume ratio of 6:1). In the case of fluorescence liposomes, 10% of DSPC was replaced with DSPE-CE. The obtained solution was placed in a round-bottom flask, and the solvent was evaporated and dried at 55 °C with 300-mbar vacuum on a rotary evaporator (Heidolph, Schwabach, Germany). The obtained lipid film was solubilized using an AgNP solution (weight ratio of 1:100) – LipoAgNPs or an equal volume of PBS (LipoE) at 60 °C, sonicated for 20 min, and finally vortexed for 1 min. The obtained multilamellar vesicles (MLV) were subsequently extruded 11 times through a polycarbonate filter with 0.1 μm pore size above the transition temperature of lipids, using a mini-extruder according to the manufacturer manual (Avanti Polar Lipids, Alabama, USA). Subsequently, the obtained liposomes (LipoAgNPs and LipoE) were mixed with the EGF-NHS-PEG_{3400}-DSPE conjugate at a molar ratio of 1:30 and left for 4 h at 60 °C to incorporate the conjugate into the liposome bilayer. Finally, the unbound EGF-conjugate was removed by dialysis (MWCO = 10,000–12,000). After this, the efficiency of the EGF-NHS-PEG_{3400}-DSPE incorporation into the liposome layer was determined as 85.92%, based on the Bradford method. The obtained EGF-LipoAgNPs and EGF-LipoE liposomes were maintained in the modified atmosphere (under nitrogen) and used in further experiments. The mass/volume concentration (m/v) of each solution was determined as 12.5 mg/mL, using a laboratory evaporator (Radwag, Polska) and, subsequently, EGF-LipoAgNPs were normalized to the AgNP content using PBS as a solvent. Next, the concentration of empty liposomes (EGF-LipoE) was normalized to the EGF-LipoAgNP concentration to create comparable stocks, which were subsequently used in the further studies.

2.4. Physicochemical characterization

The AgNPs, EGF-LipoAgNPs, and EGF-LipoE were scanned at the 300–700 nm wavelength every 5 nm to determine the presence of unbound AgNPs in the liposome solution using a microplate reader (EPOCH BIOTEK, USA). The morphology and size of the tested compounds were analyzed using a transmission electron microscope (TEM) at the Laboratory of Electron Microscopy (Department of Cell Biology and Imaging, Institute of Zoology and Biomedical Research, Jagiellonian University, Krakow). Finally, the measurements of the size, polydisperse index (PdI), and stability (ζ-potential) were performed at the Laboratory of A.P.I. Instruments Industry (Warsaw, Poland).

2.5. Cell culture and treatment

Human lung carcinoma (A549, ATCC® CCL-185), human tongue squamous cell carcinoma (SCC-15, ATCC® CRL-1623), and human fibroblasts (BJ, ATCC® CRL-2522) were obtained from the American Type Culture Collection (ATCC, distributor: LGS Standard, Łomianki, Poland). The BJ cells were grown in the MEM medium with the 10% FBS and 2.5 mM solution of the L-glutamine, the A549 cells were cultured in F12-K medium with the 10% FBS and the SCC-15 cells were grown in the DMEM/F12 medium with 10% FBS supplemented with 400 ng/mL of hydrocortisone. Each medium used in this study were supplemented with 100 U/mL penicillin, 0.10 mg/mL streptomycin, and 250 ng/mL amphotericin B. The cells were cultured in the humidified atmosphere at 37 °C and 5% CO_2 until reaching confluence. Before the experiments, the cells were trypsinized and seeded on 6-, 12-, or 96-well plates (depending on the experiment) at the density of 9×10^4, 5×10^4, or 5×10^3 cells/well, respectively, and precultured for 24 h. After this time, the medium was removed and a fresh one containing increasing concentrations of AgNPs, EGF-LipoAgNPs (tested compound), or EGF-LipoE (negative control) was added for 6 h, 24 h, and 48 h (depending on the experiment), in contrast to the control group (medium with an equivalent volume of PBS).

In the second part of this study, the cells were pretreated with a 0.16 nM solution of pure EGF in the respective media for 30 min to saturate the receptor and determine the involvement of EGFR in the uptake of EGF-LipoAgNPs. Later, the cells were treated with the tested compounds for respective time intervals. A 0.003% concentration of hydrogen peroxide was used in each experiment as a positive control (data not shown).

2.6. Resazurin reduction assay

Resazurin is a non-fluorescent blue dye, which is nontoxic to cells and easily penetrates through the cell membrane. Thus, due to the activity of mitochondrial enzymes, resazurin is converted into fluorescent violet resorufin. The intensity of the fluorescence can be measured, thus the metabolic activity in certain cells can be determined. In this study, this method was used to evaluate the impact of AgNPs, EGF-LipoAgNPs, and EGF-LipoE on two EGFR-overexpressing cancer cell lines (A549, SCC-15), in contrast to normal fibroblasts (BJ). The method was performed as in Szychowski et al. (Szychowski et al., 2021). In the case of the EGF-pretreatment experiments, a 0.16 nM solution of EGF in respective media was added for 30 min before the tested compounds were added to the cells. After the 6 h, 24 h, and 48 h treatment, the fluorescence was measured with 530 nm excitation and 590 nm emission wavelengths using a microplate reader (FilterMax F5). The results were expressed as a percentage of the control.

2.7. Intracellular ROS production

The H_2DCF-DA probe is able to penetrate through the cell membrane passively into the cytoplasm, where certain enzymes catalyze the deacetylation reaction. The product is subsequently changed into fluorescent 2′, 7′-dichlorofluorescein after contact with ROS. In this study, this probe was chosen to determine the impact of the native AgNPs, EGF-LipoAgNPs, and EGF-LipoE complexes on the intracellular ROS production in the A549 and SCC-15 cell lines (as models of EGFR-overexpressing cancer cells), compared to the BJ cells. The procedure was performed as in Skóra et al. (Skóra et al., 2021). In the case of the EGF-pretreatment experiments, a 0.16 nM solution of EGF in respective media was added for 30 min before the tested compounds were added to the cells. After the 6 h, 24 h, or 48 h treatment, the fluorescence was measured at $\lambda = 485$ nm (excitation wavelength) and $\lambda = 535$ nm (emission wavelength) using a microplate reader (FilterMax F5). The results were expressed as a percentage of the control.

2.8. Lactate dehydrogenase assay

Lactate dehydrogenase (LDH) is an enzyme indicator of cell integrity. It naturally occurs inside the cell; however, due to the damage to the cell membrane, LDH is released into the medium. Therefore, the amount of released LDH was used to determine the toxic effect of the tested compounds on the BJ, A549, and SCC-15 cells. The assay was performed after the 6 h, 24 h, and 48 h treatment with the tested compounds, according to the producer's manual (Takara Bio). The results were expressed as a percentage of the control.

2.9. Caspase-3 and -9 activity assay

Apoptosis is considered the safest way to remove cancer cells from the organism. Given the ability of AgNPs to induce apoptosis, caspase-9 and caspase-3 activity was determined in this study. The method was performed as in Nicholson et al. with modifications presented by Szychowski et al. (Szychowski et al., 2015; Nicholson et al., 1995). The measurement was performed after the 6 h, 24 h, and 48 h of treatment of the cells with the tested compounds using a microplate reader (FiletrMax F5). The results were expressed as a percentage.

2.10. qPCR

The Real-Time quantitative Polymerase Chain Reaction (qPCR) is a

method for quantification of gene expression. In this study, the method was chosen to determine the impact of the tested compounds on EGFR gene expression, oxidative stress (*CAT, SOD*)-, proliferation (*Ki67*)-, and apoptosis (*BP53*)-related genes. The two-step qPCR was performed as in Szychowski et al. (Szychowski et al., 2020). The qPCR reaction mixture contained the cDNA template, the Fast Probe qPCR Master Mix (2×) (EURx), TaqMan probe, and primers corresponding to the gene encoding *EGFR*, *ACTB*, *KI67*, *BP53*, *CAT*, and *SOD2* (ThermoFisher). The reaction was performed as follows: 2 min at 50 °C and 10 min at 95 °C, followed by 40 cycles of 15 s at 95 °C and 1 min at 60 °C. During the exponential phase, the threshold value (C_t) was set and the ΔΔCt method was used for analysis of data normalized to the *ACTB* expression after the treatment of the cells with the tested compounds for 6 h and 24 h. To study the stability of the gene expression levels, three candidates of the reference genes (*ACTB*, *GAPDH*, *18S*) were selected and validated. To evaluate the reference gene expression, the RefFinder web-based comprehensive tool was used.

2.11. Expression of the KI67 protein

The KI67 protein is described as an indicator of cell proliferation. Therefore, the expression of this protein was used in this study to determine the impact of the tested compounds on the proliferation properties of BJ, A549, and SCC-15. The involvement of EGFR was also assessed by pretreating the cells with 0.16 nM of EGF for 30 min. The enzyme-linked immunosorbent assay (ELISA) was performed in cell lysates after the 24 h and 48 h treatment (alone or pretreatment) according to the producer's manual (Biorbyt). The total protein content was first measured using the Bradford method. The results were expressed as Ki67 protein expression in ng/mL, first normalized to the total protein content.

2.12. Activity of catalase and superoxide dismutase

Catalase (CAT) and superoxide dismutase (SOD) are the main enzymes involved in the antiradical defense system, preventing cells from oxidative stress. In this study, the activity of these two enzymes was measured to determine the impact of AgNPs, EGF-LipoAgNPs, and EGF-LipoE on the occurrence of oxidative stress in the tested cell lines. The method was performed as in Piechowiak et al. and Skóra et al., respectively (Skóra et al., 2021; Piechowiak et al., 2021). In the case of the EGF-pretreatment experiments, a 0.16 nM solution of EGF in respective media was added for 30 min before the tested compounds were added to the cells. The CAT and SOD activity was measured as in Piechowiak et al. and Skóra et al., respectively, after the 48 h treatment of the cells with the tested compounds (Skóra et al., 2021; Piechowiak et al., 2021). The results were expressed as a percentage of the control; earlier, the results were normalized to the total protein content using the Bradford method.

2.13. Confocal microscopy

In this study, confocal microscopy was used to confirm the uptake of EGF-LipoAgNPs (labeled with DSPE-CF) into the A549, SCC-15, and BJ cells. Briefly, the cells were seeded on a ϕ35 mm culture dish at the density of 1×10^5 cells per dish. After 24 h, the medium was removed and a fresh one containing 10 ng/mL of Fluo-EGF-LipoAgNPs was added for 12 h. After this, the medium was removed, and the cells were washed 3 times with warm PBS to remove outside complexes. Subsequently, serum-free medium containing 10 μM of Hoechst 33342 and 10 μM of Rhodamine B was added for 5 min. Finally, the uptake of EGF-LipoAgNPs was determined using confocal microscopy with a laser scanner module (ZEISS LSM700).

2.14. Statistical analysis

The data presented in this study are mean values with standard deviations (SD). The encapsulation procedure was performed in triplicate and subsequently each concentration was tested in 6 replicates; thus, the total number of the repetitions was 18 ($n = 18$). The obtained results were used in the statistical analysis performed using GraphPad Prism 8.0 Statistical Analysis Mode. The statistical difference between the control and certain concentrations of the tested compound was determined using one-way ANOVA with the post-hoc Tukey test at $^{***}p < 0.001$, $^{**}p < 0.01$, and $^{*}p < 0.5$. The statistical difference between certain groups was determined using the *t*-test at $\#p < 0.05$.

3. Results

3.1. Physicochemical characterization of the tested compounds

The UV–Vis scan of the AgNP solution showed a maximum peak at the 398-nm wavelength characteristic for AgNP solutions (Fig. 1A). The EGF-LipoAgNP and EGF-LipoE solutions did not show any peak at this wavelength (Fig. 1A). The measurement of the hydrodiameter showed the presence of structures with 107.9 nm and 116.8 nm size and PdI equal to 0.2047 and 0.1521, respectively, for EGF-LipoAgNPs and EGF-LipoE (Fig. 1D, G). The zeta-potential of the tested solutions was −20.16 mV, −16.69 mV, and − 1,72 mV for the AgNP, EGF-LipoAgNP, and EGF-LipoE solutions, respectively. The TEM images of the EGF-LipoAgNPs revealed the presence of spherical structures with a size ranging from 71.97 to 121.17 nm (Fig. 1E-F). Moreover, the presence of AgNPs at the center of the liposomes was noticed (Fig. 1E). In turn, the TEM images of EGF-LipoE showed spherical structures with a size in the range of 157.26–163.53 nm (Fig. 1H-I) (See Table 1.).

3.2. Metabolic activity

The well-described resazurin reduction metabolic activity assay was chosen in this study to determine the impact of EGF-LipoAgNPs on the BJ, A549, and SCC-15 cells. After the 6 h treatment with AgNPs, the BJ cells showed a significant decrease in the metabolic activity in each tested concentration (1–100 ng/mL), ranging from 16% to 28%, compared to the control (Fig. 2A). In turn, no significant changes were detected for EGF-LipoAgNPs and EGF-LipoE (Fig. 2A). In contrast, the A549 cells treated with AgNPs, EGF-LipoAgNPs, and EGF-LipoE did not show any changes in the metabolic activity (Fig. 2B). A similar effect was observed for the SCC-15 cells, which did not show any significant changes in the metabolic activity after the treatment with the tested compounds for 6 h (Fig. 2C).

After the 24 h treatment, the BJ cells were characterized by a significant up to 44% and 12% decrease in the metabolic activity after the treatment with AgNPs and EGF-LipoAgNPs at 100 ng/mL respectively, compared to the control (Fig. 2D). The A549 cells treated with AgNPs and EGF-LipoAgNPs for 24 h showed a significant decrease in the metabolic activity up to 12% at 50 ng/mL and 23% at 100 ng/mL, respectively (Fig. 2E). The EGF-LipoE-treated cells did not exert any significant effect on the A549 cells (Fig. 2E). After the 24 h treatment with AgNPs, the SCC-15 cells showed a significant decrease in the metabolic activity in the concentration range from 10 ng/mL to 100 ng/mL (Fig. 2F). The highest effect reaching 20% and 44% was observed for EGF-LipoAgNPs in the same concentration range (Fig. 2F). The cells treated with EGF-LipoE did not show any significant changes in the metabolic activity (Fig. 2F).

After the 48 h treatment with AgNPs, the BJ cells were characterized by a significant decrease in the metabolic activity in all tested concentrations (1–100 ng/mL), reaching 28% to 63%, compared to the control (Fig. 2G). In turn, a lower effect was observed in the cells treated with EGF-LipoAgNPs (Fig. 2G). The EGF-LipoE did not induce any changes in the BJ cells (Fig. 2G). In turn, the A549 cells treated with AgNPs showed a significant decrease in the metabolic activity at the 50 and 100 ng/mL concentrations, reaching 21% and 22%, respectively, compared to the control (Fig. 2H). EGF-LipoAgNPs caused a significant decrease in the

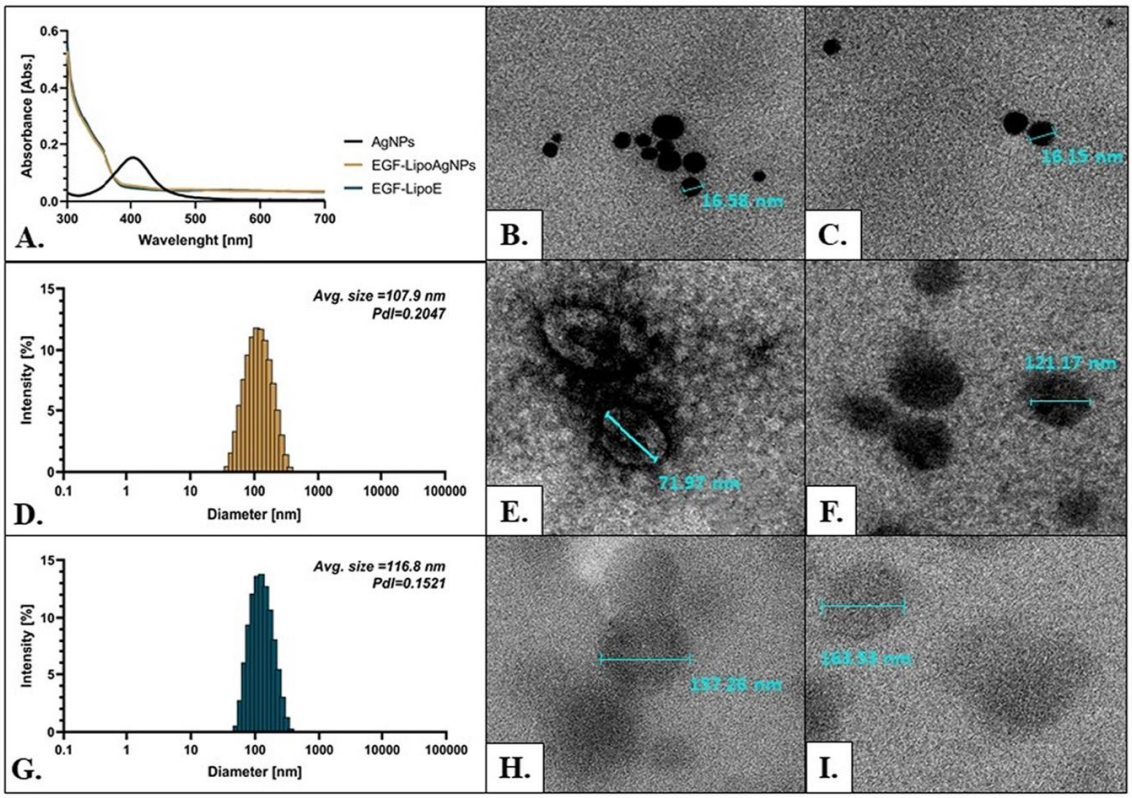

Fig. 1. Characterization of the tested compounds. UV–Vis scan of AgNPs, EGF-LipoAgNPs, and EGF-LipoE (A); TEM images of AgNPs (B-C), EGF-LipoAgNPs (E-F), and EGF-LipoE (H-I); DLS measurement of EGF-LipoAgNPs (D) and EGF-LipoE (G) with an average size and polydisperse index (PdI)

Table 1
Zeta potential [mV] and conductivity [ms/cm] of the AgNP, EGF-LipoAgNP, and EGF-LipoE solutions.

Sample	Zeta-potential	Conductivity
AgNPs	−20.16 ± 1.09 mV	0.032 ms/cm
EGF-LipoAgNPs	−16.69 ± 1.01 mV	0.304 ms/cm
EGF-LipoE	−1.72 ± 0.01 mV	3.102 ms/cm

metabolic activity in the range from 12% to 48%, respectively, for the concentrations of 1–100 ng/mL (Fig. 2H). After the 48 h treatment with AgNPs, the SCC-15 cells exhibited a significant 13% and 17% decrease in the metabolic activity at 50 ng/mL and 100 mg/mL, compared to the control (Fig. 2I). In contrast, the cells treated with EGF-LipoAgNPs showed a higher decrease in the metabolic activity at each tested concentration, up to 68% for 100 ng/mL, compared to the control (Fig. 2I).

3.3. Intracellular ROS production

The H_2DCF-DA probe was chosen in this study to determine the impact of the tested compounds on the ROS production level in the BJ, A549, and SCC-15 cells. After the 6 h treatment, AgNPs caused a significant increase (up to 32%) in the ROS production only in the BJ cells at the concentration range of 10–100 ng/mL, compared to the control (Fig. 3A). The A549 cells treated with 100 ng/mL AgNPs were characterized by a significantly increase (up to 29%) in ROS production at all tested concentrations, compared to the control (Fig. 3B). In turn, the cells treated with EGF-LipoAgNPs did not show any changes in the metabolic activity (Fig. 3B). In contrast, EGF-LipoE caused a decrease in the ROS production (Fig. 3B). In the SCC-15 cell line, an up to 45% increase in the ROS production was observed only in the EGF-LipoAgNPs-treated cells at 100 ng/mL, compared to the control (Fig. 3C).

The BJ cells treated with AgNPs and EGF-LipoAgNPs for 24 h were characterized by an increase in the ROS production level up to 33% and 17%, respectively, compared to the control (Fig. 3D). No effect was observed in the cells treated with the empty liposomes. The A549 cell line treated with AgNPs showed a significant increase (19%–53%) in the ROS production in all tested concentrations, compared to the control (Fig. 3E). However, EGF-LipoAgNPs exerted a significantly higher effect and increased the ROS production in the range from 29% to 86%, compared to the control (Fig. 3E). After the 24 h treatment with AgNPs, the SCC-15 cells showed an increase (up to 173% at 100 ng/mL) in the ROS production level in all tested concentrations (Fig. 3F). In turn, the same concentration of EGF-LipoAgNPs caused a decrease in the ROS production, reaching 31%, compared to the control (Fig. 3F).

After the 48 h contact with AgNPs, the BJ cells showed an increase in the ROS production in the range from 18% to 46% at the 1, 10, and 50 ng/mL concentrations, compared to the control. In turn, a significant decrease in the ROS production was observed at 100 ng/mL (Fig. 3G). The BJ cells treated with EGF-LipoAgNPs showed an increase in the ROS production level reaching 13% - 43% at 10–100 ng/mL, compared to the control (Fig. 3G). The A549 cells treated with AgNPs exhibited an increase in the ROS production in all tested concentrations, up to 93% (at 100 ng/mL), compared to the control (Fig. 3H). EGF-LipoAgNPs caused a significant increase in the ROS production up to 74%, compared to the control at 50 ng/mL, while a 31% decrease in the ROS production was observed at the 100 ng/mL concentration (Fig. 3H). In turn, the SCC-15 cells treated with AgNPs showed an increase in the ROS production level only at 100 ng/mL (Fig. 3I). In turn, increased ROS production in the EGF-LipoAgNPs-treated cells reaching 49% was observed only for the 1 ng/mL concentration, compared to the control (Fig. 3I).

3.4. Lactate dehydrogenase (LDH) release level

Lactate dehydrogenase (LDH) is a well-described indicator of cell membrane disruption or cell damage. Therefore, this parameter was

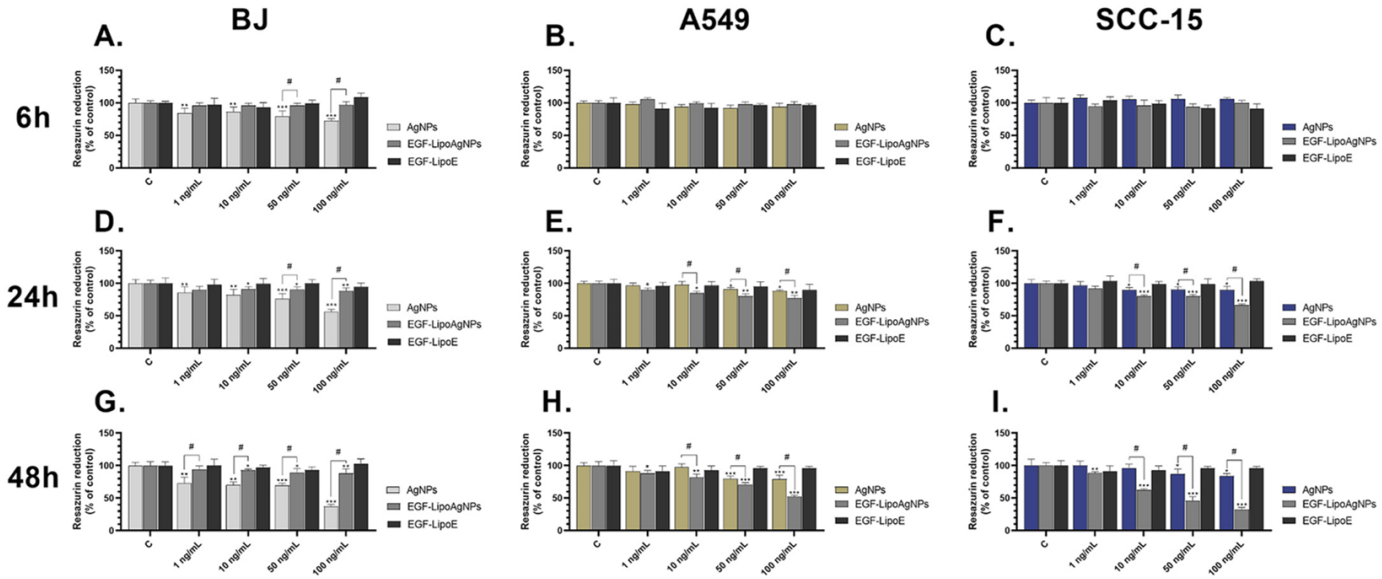

Fig. 2. Results of the metabolic activity. Resazurin reduction assay after the treatment of the BJ (A, D, G), A549 (B, E, H), and SCC-15 (C, F, I) cells with AgNPs, EGF-LipoAgNPs, and EGF-LipoE for 6 h (A-C), 24 h (D-F), and 48 h (G-I). The means ± SD (error bars) with *, **, *** are statistically different from the respective control at $p < 0.05$, $p < 0.01$, and $p < 0.001$, respectively (one-way ANOVA, Tukey test). # means statistically significant differences ($P < 0.05$) between certain groups (*t*-test). The control was regarded as 100%

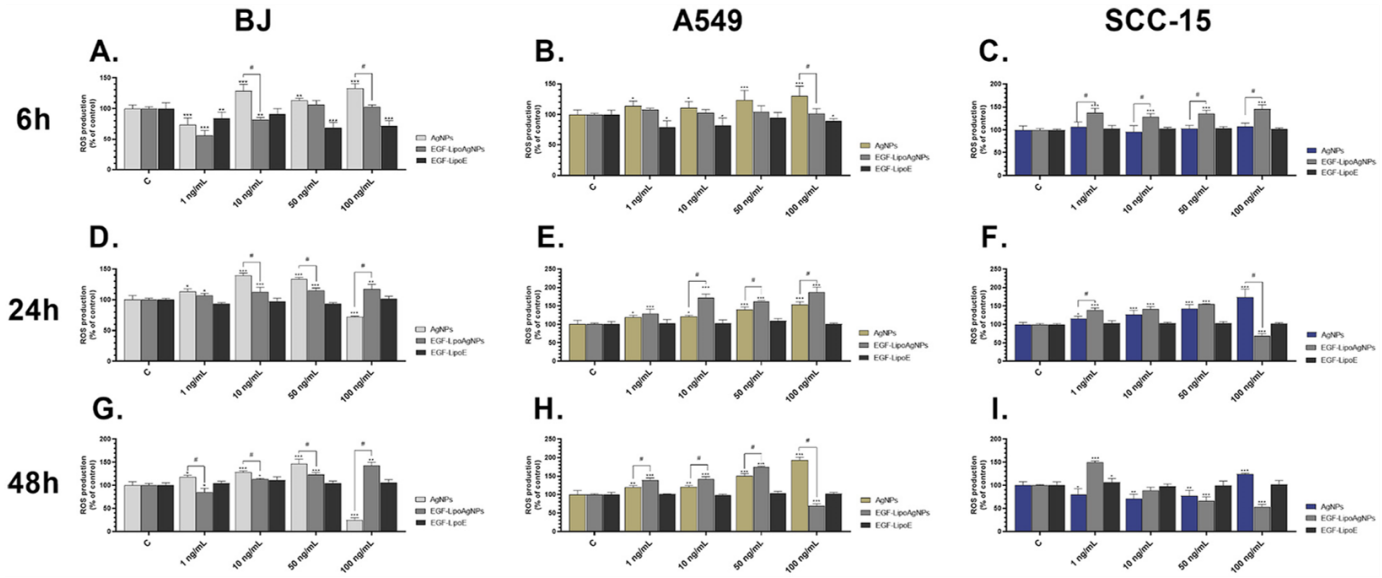

Fig. 3. ROS levels in the cells. Results of the H_2DCF-DA analysis after the treatment of the BJ (A, D, G), A549 (B, E, H), and SCC-15 (C, F, I) cells with AgNPs, EGF-LipoAgNPs, and EGF-LipoE for 6 h (A-C), 24 h (D-F), and 48 h (G-I). The means ± SD (error bars) with *, **, *** are statistically different from the respective control at $p < 0.05$, $p < 0.01$, and $p < 0.001$, respectively (one-way ANOVA, Tukey test). # means statistically significant differences ($P < 0.05$) between certain groups (t-test). The control was regarded as 100%

used in this study to determine the toxic effect of the tested compounds on the BJ, A549, and SCC-15 cells. After the 6 h treatment with AgNPs, the BJ cells showed a 26% decrease in the LDH release at 100 ng/mL, compared to the control (Fig. 4A). No changes were observed after the treatment of the cells with EGF-LipoAgNPs and EGF-LipoE (Fig. 4A). The A549 cells treated with AgNPs were characterized by an increase in LDH release in the range from 13.73% to 13.83% at the 50 ng/mL and 100 ng/mL concentrations, compared to the control (Fig. 4B). In contrast, the SCC-15 cells treated with AgNPs were characterized by a 14% increase in the LDH release only at the 100 ng/mL concentration (Fig. 4C).

After the 24 h treatment with AgNPs and EGF-LipoAgNPs, the BJ cells showed an up to 12% and 14% increase in the LDH release at 100 ng/mL, respectively, compared to the control (Fig. 4D). EGF-LipoE did not exert any significantly effect on the BJ cells after 24 h. The A549 cells treated with AgNPs for 24 h did not exhibit any changes in the LDH release (Fig. 4E). In contrast, the cells treated with EGF-LipoAgNPs showed a 12%–30% increase in the LDH release in all tested concentrations, compared to the control (Fig. 4E). AgNPs applied at the 50 ng/mL and 100 ng/mL concentrations caused a significant increase (18% and 15%, respectively) in the LDH release in the SCC-15 cells, compared to the control (Fig. 4F). In turn, a significantly stronger effect was noticed on the EGF-LipoAgNPs-treated cells at all tested concentrations, showing an 8%–41% increase in the LDH release, compared to the control (Fig. 4F).

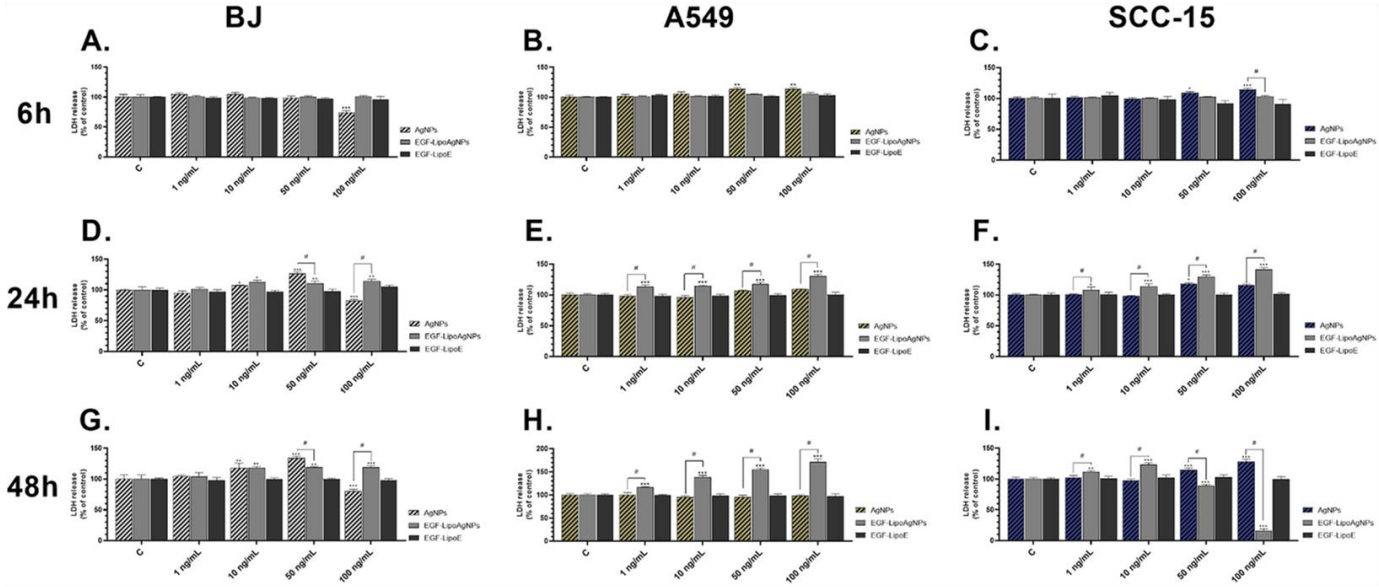

Fig. 4. Levels of the released LDH. Results of the LDH release from the BJ (A, D, G), A549 (B, E, H), and SCC-15 (C, F, I) cells after the treatment with AgNPs, EGF-LipoAgNPs, and EGF-LipoE. The means ± SD (error bars) with *, **, *** are statistically different from the respective control at $p < 0.05$, $p < 0.01$, and $p < 0.001$, respectively (one-way ANOVA, Tukey test). # means statistically significant differences ($P < 0.05$) between certain groups (t-test). The control was regarded as 100%

After the 48 h treatment with the AgNPs and EGF-LipoAgNPs, the BJ cells were characterized by an increase in the LDH release up to 34% and 18% at 100 ng/mL, compared to the control, (Fig. 4G). The A549 cells treated with AgNPs did not show any changes in the level of released LDH after the 48 h treatment, while EGF-LipoAgNPs caused a significant increase in this parameter (in the range of 17%–71%) in all tested concentrations, compared to the control (Fig. 4H). Interestingly, the SCC-15 cells treated with AgNPs exhibited a 14% and 28% increase in the LDH release only at the 50 ng/mL and 100 ng/mL concentrations, respectively, compared to the control (Fig. 4I). In turn, the 50 ng/mL and 100 ng/mL concentrations of EGF-LipoAgNPs caused a 12% and 84% decrease in the LDH release, compared to the control (Fig. 4I).

3.5. Caspase-9 activity

Caspase-9 is a well-known indicator of mitochondria-dependent apoptosis induction, which is strictly correlated with oxidative stress. Therefore, in this study, the caspase-9 activity was chosen to determine the involvement of ROS in apoptosis induction by the tested compounds. After the 6 h treatment with AgNPs, the BJ cells were characterized by an up to 23% increase in caspase-9 at 100 ng/mL, compared to the control (Fig. 5A). The A549 cells treated for 6 h with AgNPs showed a

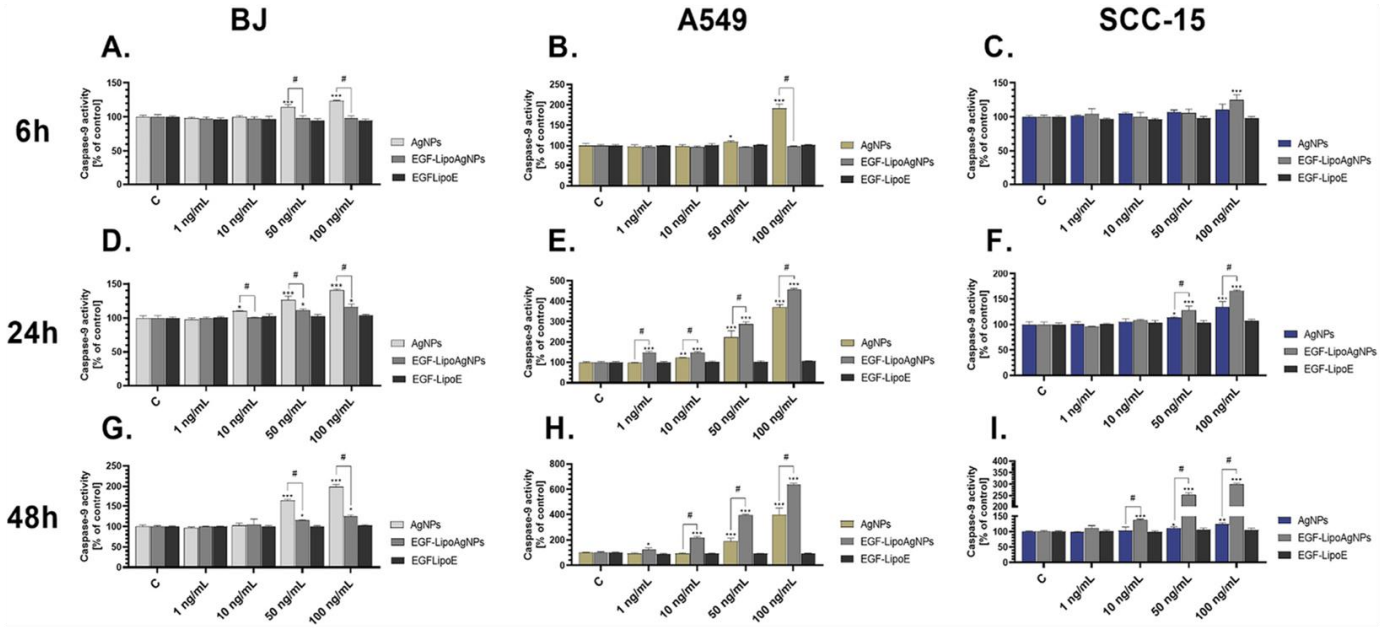

Fig. 5. Caspase-9 activity. Results of caspase-9 activity after the treatment of the BJ (A, D, G), A549 (B, E, H), and SCC-15 (C, F, I) cells with AgNPs, EGF-LipoAgNPs, and EGF-LipoE for 6 h (A-C), 24 h (D-F), and 48 h (G-I). The means ± SD (error bars) with *, **, *** are statistically different from the respective control at $p < 0.05$, $p < 0.01$, and $p < 0.001$, respectively (one-way ANOVA, Tukey test). # means statistically significant differences ($P < 0.05$) between certain groups (t-test). The control was regarded as 100%

significant increase in caspase-9 activity by 8% and 91% at the 50 ng/mL and 100 ng/mL concentrations, respectively, compared to the control (Fig. 5B). The SCC-15 cells treated with EGF-LipoAgNPs caused a 25% increase in caspase-9, compared to the control at 100 ng/mL (Fig. 5C).

The 24 h treatment of the BJ cells with AgNPs and EGF-LipoAgNPs caused an up to 40% and 15% increase in caspase-9 activity at 100 ng/mL, compared to the control (Fig. 5D). A stronger effect was noticed for the A549 cells after the treatment with AgNPs and EGF-LipoAgNPs, where an up to 270% and 357% increase in caspase-9 activity was shown at 100 ng/mL, respectively, compared to the control (Fig. 5E). In turn, AgNPs and EGF-LipoAgNPs caused an increase in caspase-9 activity by 34% and 65% at 100 ng/mL, respectively, compared to the control (Fig. 5F).

After the 48 h treatment of the BJ cells with AgNPs and EGF-LipoAgNPs, a 98% and 25% increase in caspase-9 activity at 100 ng/mL, respectively, was recorded compared to the control (Fig. 5G). The A549 cells treated with 100 ng/mL of the AgNP solutions caused an increase in caspase-9 activity by 297%, compared to the control, while EGF-LipoAgNPs were able to increase this parameter up to 539%, compared to the control (Fig. 5H). EGF-LipoE did not cause any changes in caspase-9 activity (Fig. 5H). After the 48 h treatment of the SCC-15 cells with AgNPs, an increase in caspase-9 activity was observed for the 50 and 100 ng/mL concentrations, which reached 10% and 25% of the control (Fig. 5I). In turn, a stronger effect was observed in the EGF-LipoAgNPs-treated cells, which showed a significant 37%, 154%, and 201% increase in this parameter, respectively, in the 10, 50, and 100 ng/mL concentrations, compared to the control (Fig. 5I).

3.6. Caspase-3 activity

Caspase-3 activity is considered an indicator of active apoptosis. Therefore, in this study, this parameter was chosen to determine the impact of the obtained complexes on the apoptosis process. The BJ cells treated with AgNPs, EGF-LipoAgNPs, and EGF-LipoE for 6 h did not show any changes in caspase-3 activity (Fig. 6A). The same effect was observed in the A549 and SCC-15 cells, which did not show any changes in this parameter (Fig. 6B-C).

Interestingly, in the BJ cells, an up to 46% and 26% increase in caspase-3 activity was observed after the 24 h treatment with AgNPs and EGF-LipoAgNPs, respectively, at 100 ng/mL (Fig. 6D). The A549 cells treated with AgNPs and the tested liposomes in the range from 50 ng/mL to 100 ng/mL showed a 57% and 104% increase in caspase-3 activity, compared to the control (Fig. 6E). After the 24 h treatment with AgNPs and EGF-LipoAgNPs, the SCC-15 cells exhibited enhanced caspase-3 activity up to 52% and 191% at 100 ng/mL, respectively, compared to the control (Fig. 6F).

After the 48 h treatment of the BJ cells with AgNPs and EGF-LipoAgNPs, an up to 91% and 27% increase in caspase-3 activity was observed at 100 ng/mL, respectively, compared to the control (Fig. 6G). The A549 cells showed opposite results. The A549 cell treatment with AgNPs and the tested liposomes for 48 h caused an increase in caspase-3 activity up to 96% and 175% at 50 and 100 ng/mL, respectively, compared to the control. AgNPs caused a 31% and 60% increase in caspase-3 activity in the SCC-15 cells after the 48 h treatment at the 50 ng/mL and 100 ng/mL concentrations, respectively, compared to the control (Fig. 6I). EGF-LipoAgNPs exerted a higher effect and caused a 79%, 162%, and 195% increase in caspase-3 activity at the 10, 50, and 100 ng/mL concentrations, compared to the control (Fig. 6I).

3.7. Pretreatment of cells with EGF

After the 24 h- and 48 h-treatment, the BJ cells pretreated with the EGF and later treated with the EGF-LipoAgNPs exhibited a significant different effect on the metabolic activity, which decreased by 23% and 7% after 24 h in the non-pretreated and pretreated cells, respectively, compared to the control (Fig. Fig. 7A). A similar effect was observed in the A549 line, where the cells pretreated with the EGF solutions and later treated with EGF-LipoAgNPs did not show any significant effect on metabolic activity in any time interval. Moreover, the results after 24 h and 48 h were statistically different from the control and showed a decrease in the metabolic activity by 23% and 4% after 24 h as well as a 48% decrease and a 3% increase after 48 h in the non-pretreated and pretreated cells, respectively (Fig. 7B). The same correlation was observed in the SCC-15 cells, which showed that the EGF-LipoAgNPs were able to decrease the metabolic activity up to 34% after the 24 h treatment and 68% after the 48 h treatment, compared to the control. In

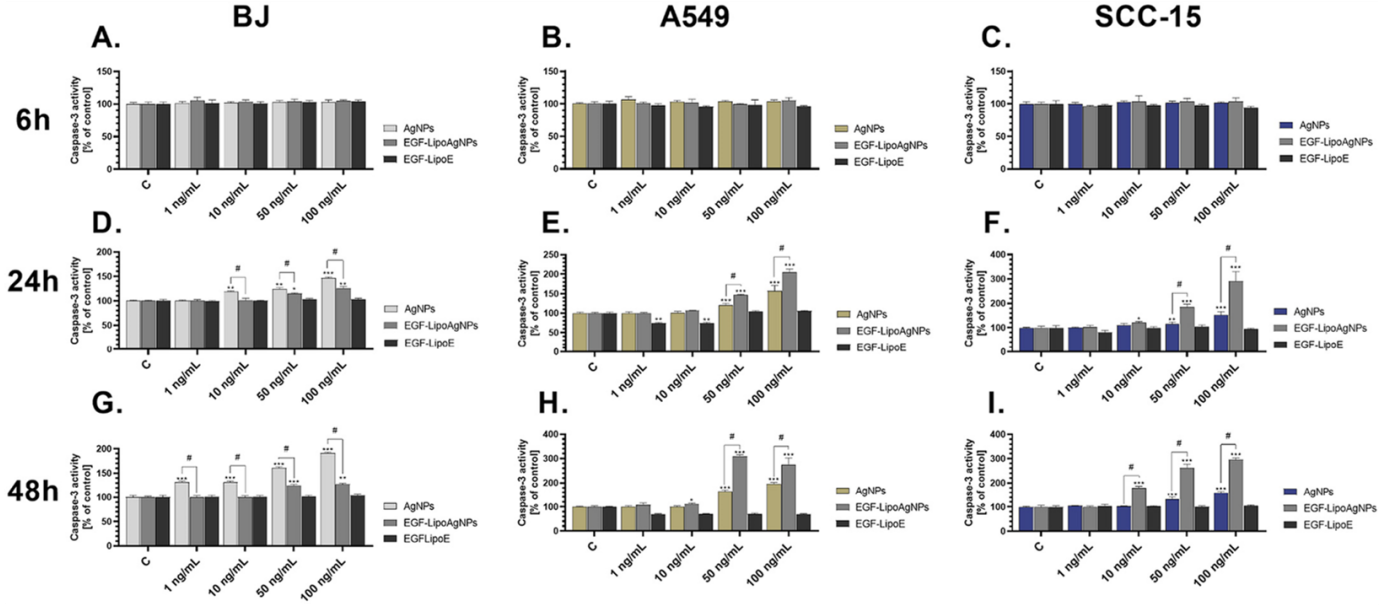

Fig. 6. Caspase-3 activity. Results of caspase-3 activity after the treatment of the BJ (A, D, G), A549 (B, E, H), and SCC-15 (C, F, I) cells with AgNPs, EGF-LipoAgNPs, and EGF-LipoE for 6 h (A-C), 24 h (D-F), and 48 h (G-I). The means ± SD (error bars) with *, **, *** are statistically different from the respective control at $p < 0.05$, $p < 0.01$, and $p < 0.001$, respectively (one-way ANOVA, Tukey test). # means statistically significant differences ($P < 0.05$) between certain groups (t-test). The control was regarded as 100%

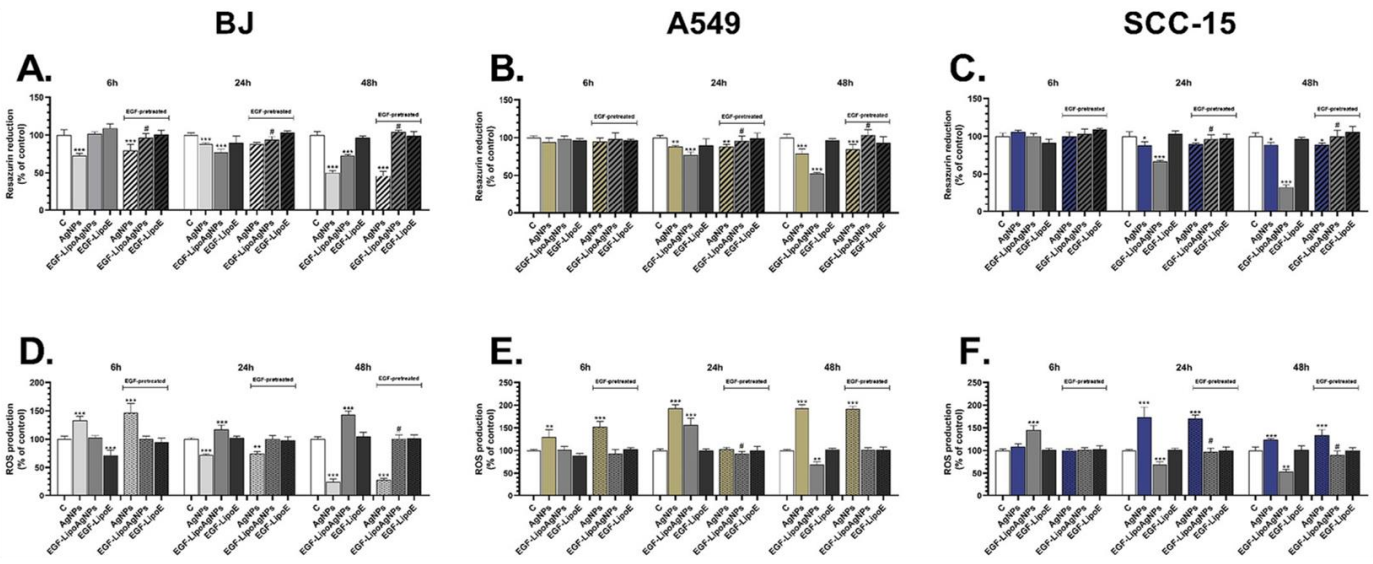

Fig. 7. Pretreatment of the cells with the EGF solution. Results of the resazurin reduction assay (A-C) and H_2DCF-DA analysis (D-F) after the treatment of the BJ (A, D), A549 (B, E), and SCC-15 (C, F) cells with the 10 ng/mL concentration of AgNPs, EGF-LipoAgNPs, and EGF-LipoE for 6 h, 24 h, and 48 h. The means ± SD (error bars) with *, **, *** are statistically different from the respective control at $p < 0.05$, $p < 0.01$, and $p < 0.001$, respectively (one-way ANOVA, Tukey test). # means statistically significant differences ($P < 0.05$) between certain groups (t-test). The control was regarded as 100%

turn, the EGF-pretreated cells did not exhibit any significant changes in the metabolic activity (Fig. 7C).

Similar dependences were observed in the ROS production results in all cell lines. The treatment with AgNPs was able to increase the ROS level in the non-pretreated and pretreated BJ cells (Fig. 7D). EGF-LipoAgNPs added to the EGF-pretreated BJ cells did not induce any significant changes in the ROS production, and statistically significant differences were observed compared with the non-pretreated cells in both time intervals (Fig. 7D). The A549 cells pretreated with EGF and later treated with EGF-LipoAgNPs showed a significantly different ROS production level than the non-treated ones, i.e. the parameter increased by 56% and decreased by 7% after 24 h, respectively, compared to the control; a 31% decrease and no changes, compared to the control, were noted in the non-pretreated and pretreated cells, respectively (Fig. 7E). In turn, the SCC-15 cells pretreated with EGF and later treated with the EGF-LipoAgNPs showed statistically significant differences in the ROS production already after 6 h, i.e. 45% and 1% of the control in the non-pretreated and pretreated cells, respectively (Fig. 7F). A similar effect was also visible after 24 h when a 31% and 3% decline in this parameter was observed, compared to the control, in the non-pretreated and pretreated cells, respectively (Fig. 7F). After the 48 h treatment, the ROS production was decreased by 47% and 10%, compared to the control, in the non-pretreated and pretreated cells, respectively (Fig. 7F).

3.8. Impact on oxidative stress-, proliferation-, and apoptosis-related genes

The qPCR method is commonly used to determine the activity of certain genes. Thus, this analysis was used in this study to determine the impact of the tested compounds on the oxidative stress (*CAT, SOD2)*-, proliferation (*KI67)*-, and apoptosis *(BP53)*-related genes.

The *CAT* gene expression was significant increased in the BJ and A549 cell lines after the 6 h treatment with AgNPs, reaching 132% and 174%, respectively (Fig. 8A). In contrast, the SCC-15 cells showed 30% lower expression of *CAT* than the control group (Fig. 8A). After the 24 h treatment, the expression of *CAT* in the BJ cells treated with AgNPs was 452% higher than in the control. In turn, the EGF-LipoAgNPs-treated cells were characterized by a 127% increase in the expression of this gene (Fig. 8B). Opposite results were observed in the A549 cells treated with EGF-LipoAgNPs, which showed 413% higher expression of *CAT*, compared to the control. In turn, AgNPs were able to increase the expression by 270%, compared to the control (Fig. 8B). The SCC-15 cells were characterized by 156% higher expression of the *CAT* gene after the treatment with AgNPs, while EGF-LipoAgNPs caused 273% higher expression of this gene (Fig. 8B).

The *SOD2* gene expression was decreased by 43%, 42%, and 40% in the BJ, A549, and SCC-15 cells after the 6 h treatment with AgNPs, compared to the control (Fig. 8C). No changes were detected in the BJ and A549 cells treated with EGF-LipoAgNPs, in contrast to the SCC-15 cells, which showed 176% higher expression of the *SOD2* gene (Fig. 8C). After the 24 h treatment, AgNPs caused 654%, 237%, and 149% higher expression of *SOD2* in the BJ, A549, and SCC-15 cells, respectively, compared to the control (Fig. 8D). The BJ cells treated with the tested liposomes showed 68% lower *SOD2* expression, compared to the control (Fig. 8C). However, the expression of *SOD2* in the A549 and SCC-15 cells treated with EGF-LipoAgNPs was increased by 764% and 243%, compared to the control (Fig. 8D).

The *KI67* gene expression in the BJ cells after the 6 h treatment with AgNPs was 27% and 48% higher in the groups of the AgNPs- and EGF-LipoAgNPs-treated cells, respectively, compared to the control (Fig. 10D). No changes were noted for the A549 cells, whereas the treatment of the SCC-15 cells with AgNPs reduced the *KI67* expression by 26%, compared to the control (Fig. 8D). After the 24 h treatment, the expression of the *KI67* gene was 72%, 39%, and 22% lower for the BJ, A549, and SCC-15 cells, respectively, compared to the control (Fig. 8E). The BJ cells treated with EGF-LipoAgNPs showed 18% lower expression of *KI67*, compared to the control (Fig. 8E). In contrast, the expression of this gene in the EGF-LipoAgNPs-treated A549 and SCC-15 cells was 61% and 79% lower than in the control, respectively (Fig. 8E).

The expression of the *BP53* gene was increased by 41% and 53%, in the BJ and A549 cell lines after the 6 h treatment with AgNPs, respectively, compared to the control (Fig. 8G), while a 18% decrease in the expression of this gene was observed in the SCC-15 cells, compared to the control (Fig. 8H). After the 24 h treatment, the BJ cells showed a 209% increase in the *BP53* gene expression, compared to the control, while EGF-LipoAgNPs did not exert any significantly effect on this gene (Fig. 8H). In turn, the A549 cells showed 126% higher expression of the *BP53* gene after the treatment with AgNPs and 210% higher expression in the EGF-LipoAgNPs treatment (Fig. 8H). The SCC-15 cells were characterized by 116% higher expression of the *BP53* gene, whereas the

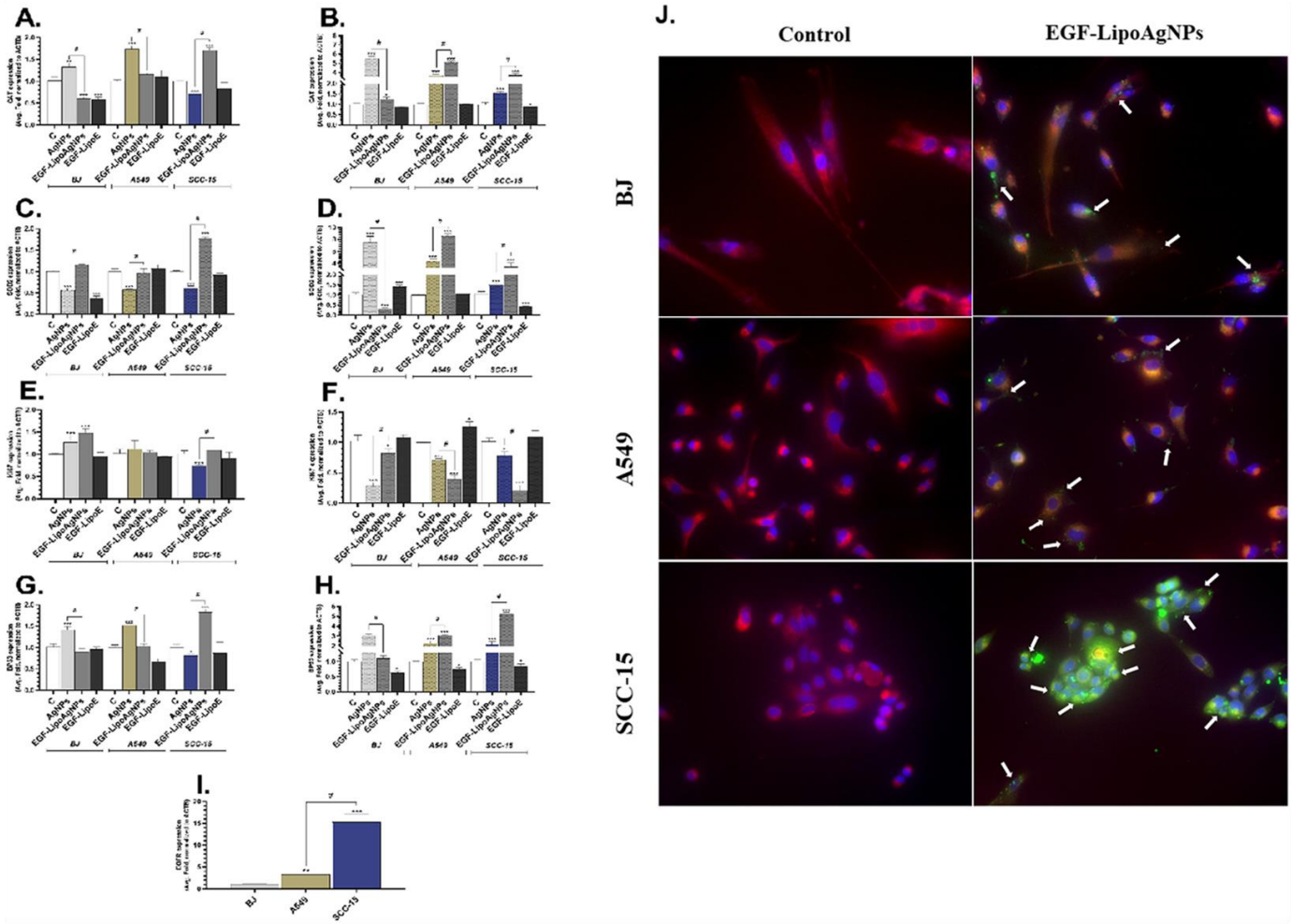

Fig. 8. qPCR analysis and the uptake of the obtained complexes. Expression of the *CAT* (A-B), *SOD* (C-D), *KI67* (E-F), *BP53* (G-H), and *EGFR* (I) genes after the treatment with the AgNPs, EGF-LipoAgNPs, and EGF-LipoE for 6 h (A C, E, G) and 24 h (B, D, F, H). Effect of Hoechst 33342 and Rhodamine B staining of the BJ, A549, and SCC-15 cells and the uptake of the fluorescent (DSPE-CF-labeled) variant of EGF-LipoAgNPs after the 12 h treatment (J). The means ± SD (error bars) with *, **, *** are statistically different from the respective control at $p < 0.05$, $p < 0.01$, and $p < 0.001$, respectively (one-way ANOVA, Tukey test). # means statistically significant differences ($P < 0.05$) between certain groups (t-test)

EGF-LipoAgNPs-treated cells showed 425% higher expression of this gene (Fig. 8H).

The BJ cells were characterized by the lowest expression of the *EGFR* gene, in contrast to the A549 cells, which showed 203% higher expression of this gene (Fig. 8I). Interestingly, the SCC-15 cells showed 1405% higher expression of the *EGFR* gene, compared to the healthy fibroblasts (Fig. 8I).

3.9. KI67 protein expression

The KI67 protein occurs naturally in the nucleus. It is involved in mitotic divisions and therefore is strictly correlated with the cell proliferation ability. For this reason, the expression of this protein was chosen in this study to determine the impact of the tested compounds on the BJ, A549, and SCC-15 cells. After the 24 h treatment, the BJ cells were characterized by a decrease in the level of KI67 expression after the treatment with AgNPs up to 1.23 ng/mL (control 6.36 ng/mL), while no significant changes were detected in the EGF-LipoAgNPs- and EGF-LipoE-treated cells (Fig. 8A). A similar tendency was noticed in the 48 h treatment; however, the EGF-LipoAgNPs-treated cells showed a significant decrease in the KI67 expression reaching 1.03 ng/mL (control 2.62 ng/mL) (Fig. 9A). Interestingly, the EGF-pretreated BJ cells did not show a decrease in the KI67 protein expression after the treatment with EGF-LipoAgNPs, compared to the control in both tested time intervals (Fig. 9D).

In turn, the A549 cells were characterized by a decrease in the KI67 expression after the treatment with AgNPs (by 6.08 ng/mL) and with EGF-LipoAgNPs (by 4.50 ng/mL) (control 7.84 ng/mL). The same tendency, i.e. a 7.41 ng/mL decrease in the KI67 expression in AgNPs-treated cells and a 3.86 ng/mL reduction in the EGF-LipoAgNPs-treated cells was noticed after the 48 h treatment (Fig. 9B). In the experiment, the EGF-pretreated cells did not show any changes after the treatment with EGF-LipoAgNPs, compared to the control (Fig. 8E). The SCC-15 cells treated with AgNPs exhibited a decline in the KI67 expression after the 24 h and 48 h treatments, reaching 7.58 ng/mL and 7.57 ng/mL, respectively. EGF-LipoAgNPs caused a higher reduction in the KI67 expression by 4.37 ng/mL and 3.68 ng/mL in the 24 h and 48 h treatments, respectively (Fig. 9C). In turn, the KI67 expression in the control cells was 9.78 ng/mL and 9.19 ng/mL in the 24 h and 48 h treatments, respectively (Fig. 9C). The SCC-15 cells pretreated with EGF and subsequently treated with EGF-LipoAgNPs did not exhibit significant changes in the KI67 expression in both time intervals (Fig. 9F).

3.10. Activity of CAT and SOD

CAT and SOD are two main enzymes playing a crucial role in the cell

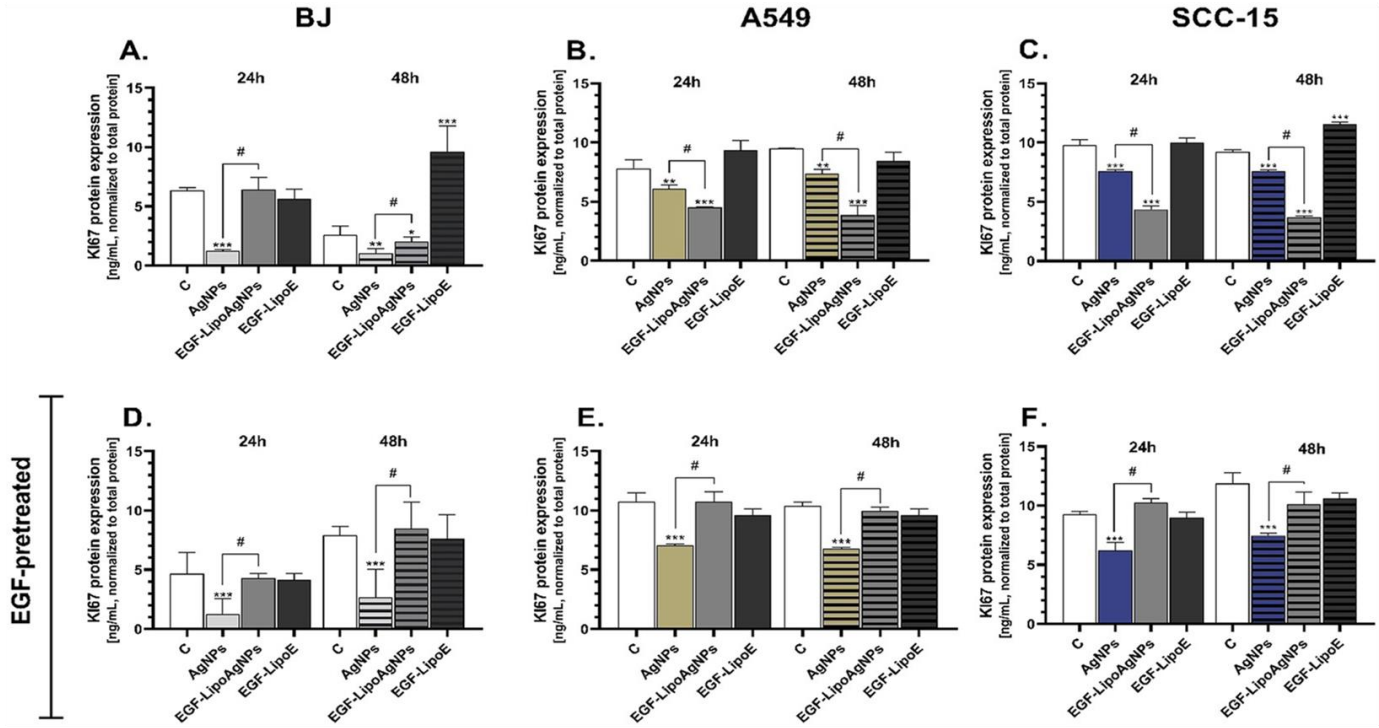

Fig. 9. KI67 protein expression. Results (normalized to total protein) of the KI67-specific ELISA Kit after treatment of the BJ (A, D), A549 (B, E), and SCC-15 (C, F) cells with the 10 ng/mL concentration of AgNPs, EGF-LipoAgNPs, and EGF-LipoE for 24 h and 48 h. The cells were pretreated with the 0.16 nM solution of EGF (D-F), and later the tested compounds were added for 24 h and 48 h. The means ± SD (error bars) with *, **, *** are statistically different from the respective control at $p < 0.05$, $p < 0.01$, and $p < 0.001$, respectively (one-way ANOVA, Tukey test). # means statistically significant differences ($P < 0.05$) between certain groups (t-test)

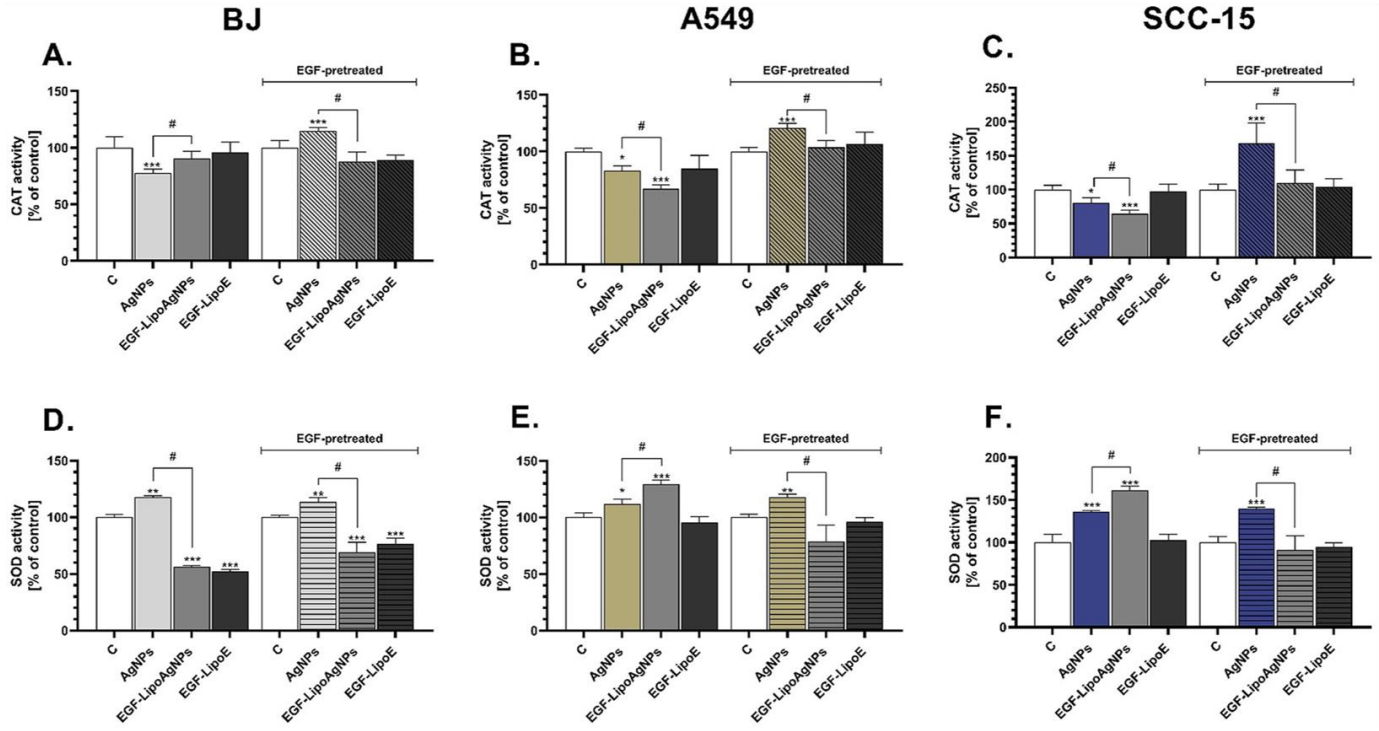

Fig. 10. Catalase and superoxide dismutase activity. Results of catalase (CAT) and superoxide dismutase (SOD) activity after the treatment of the BJ (A, D), A549 (B, E), and SCC-15 (C, F) cells with the 10 ng/mL solution of AgNPs, and their equivalent in EGF-LipoAgNPs and EGF-LipoE (normalized to total protein). The cells were pretreated with the 0.16 nM solution of EGF and later treated with the tested compounds. The means ± SD (error bars) with *, **, *** are statistically different from the respective control at $p < 0.05$, $p < 0.01$, and $p < 0.001$, respectively (one-way ANOVA, Tukey test). # means statistically significant differences ($P < 0.05$) between certain groups (t-test). The control was regarded as 100%

antioxidant system and regarded as indicators of oxidative stress in the cell. Therefore, the activity of these two enzymes was assessed in the study to determine the impact of the tested complexes on oxidative stress in the cell. The activity of CAT in the BJ cells treated with AgNPs decreased by 23%, compared to the control, and was statistically significantly different from that in the EGF-LipoAgNPs-treated cells, which did not show any effect of the EGF-pretreatment (Fig. 10A). In turn, no effect was observed in the case of EGF-LipoAgNPs (Fig. 10A). The A549 cell line treated with AgNPs exhibited a 17% decrease in CAT activity, compared to the control, while the EGF-LipoAgNPs-treated cells showed a 33%-decrease in the activity of this enzyme (Fig. 10B). The EGF-pretreated cells exposed to AgNPs and EGF-LipoAgNPs showed an increase in CAT activity or no changes in this parameter, respectively (Fig. 10B). The SCC-15 cells treated with AgNPs were characterized by a significant 20% decrease in CAT activity. However, EGF-LipoAgNPs induced a stronger decrease, which was 36%, compared to the control (Fig. 10C). The EGF-LipoE complexes did not influence CAT activity in any of the tested cell lines.

The SOD activity in the BJ cells treated with AgNPs was significantly higher than in the control group and reached 17%, compared to the control. In turn, EGF-LipoAgNPs and EGF-LipoE reduced this parameter by 44% and 48%, respectively (Fig. 10D). A similar effect was observed after the pretreatment of the cells with the EGF solution. In turn, the A549 cells exposed to AgNPs exhibited a significant 12% increase in SOD activity, while EGF-LipoAgNPs caused a 29% increase, compared to the control (Fig. 10E). The EGF-pretreated cells pretreated exposed to AgNPs showed an increase in SOD activity. In contrast, no changes were noticed in the EGF-LipoAgNPs- and EGF-LipoE-treated cells (Fig. 10E). The SCC-15 cells were characterized by a 36% and 61% increase in SOD activity in the AgNPs and EGF-LipoAgNPs treatments, respectively (Fig. 10F). The cell pretreatment with EGF and the treatment with EGF-LipoAgNPs and EGF-LipoE did not exert any effect (Fig. 10F).

4. Discussion

The interest in the encapsulation of metal nanoparticles has been increasing over the last few years. There are a few well-described methods of entrapment of such NPs, which were reviewed in our previous study (Skóra et al., 2020). The most promising tool to use AgNPs as potential therapeutic agents is the encapsulation inside the liposome. Liposomes have a similar structure to the cell membrane, facilitating the uptake. Additionally, the lipid character of these structures allows labeling using certain ligands (Eroğlu and İbrahim, 2020). In the present study, the encapsulation procedure for entrapment of AgNPs in the liposome bilayer and conjugation with EGF to target the toxicity of NPs was performed. Our experiments showed structures with the 107.9 nm and 116.8 nm size were formed in the case of EGF-LipoAgNPs (tested compound) and EGF-Lipo (empty liposomes – negative control), respectively. The TEM analysis revealed the presence of spherical structures with a visible lipid bilayer with a narrow size distribution. Additionally, the DLS measurement showed low PdI values of 0.2047 and 0.1521 for EGF-LipoAgNPs and EGF-LipoE, respectively. Our further UV–Vis scan studies showed no characteristic peak for AgNPs (~400 nm) in the case of EGF-LipoAgNPs, which is probably caused by covering the AgNPs surface by the lipids and changing the characteristic surface plasmon resonance (SPR) of these nanostructures. Similar data were shown by Episnoza et al., who described a decrease in the AgNPs peak at the 400 nm wavelength after encapsulation in liposomes (Espinoza et al., 2020). Therefore, based on these results, it is justified to assume the high efficiency of the THFE encapsulation. Yusuf and Casey have shown that the extrusion method is more efficient than e.g. the sonication method in acquisition of size homogenous complexes in the encapsulation procedure of such NPs (Yusuf and Casey, 2019). Similarly, according to the results reported by Guilleux et al., the extrusion technique yields liposomes with an approx. 150 nm diameter (Guilleux et al., 2018). In turn, Aid and Azzazy obtained homogenous liposomes using the sonication method; however, they had a diameter in the range from 240 nm to 450 nm (Eid and Azzazy, 2014). Our results show that the zeta potential of the obtained complexes was −16.69 mV and − 1.72 mV for EGF-LipoAgNPs and EGF-LipoE, respectively. As shown by Joseph and Singhvi, solutions of liposomes with zeta potential in the range from −30 mV to 30 mV are considered stable colloids (Joseph and Singhvi, 2019). Taking the above into account, we have proved that the AgNP encapsulation procedure can be done efficiently with the THFE method; subsequently, the EGF conjugation procedure can be also performed with high efficiency.

In the next stages of this study, the obtained EGF-LipoAgNP complexes used as the tested compound, EGF-LipoE as a negative control, and the AgNPs solution as a positive control were tested in *in vitro* conditions. The Epidermal Growth Factor Receptor (EGFR) is overexpressed in many cancer types e.g. head, neck, and lung tumors (Singh et al., 2016). Therefore, this structure seems to be valuable as a potential target to direct certain substances straight into cancer cells. Our preliminary experiments show that the EGFR gene expression in the analyzed A549 and SCC-15 cell lines was 203% and 1415% higher, respectively, compared to the normal human fibroblasts (BJ) cell line. These findings are in agreement with the data reported by Thomas and Weihua anf Daragmeh et al., who also showed the same EGFR gene expression in similar lung and tongue cancer cell lines (Thomas and Weihua, 2019; Daragmeh et al., 2016). Therefore, these two cell lines as representatives of EGFR-overexpressing cancer cells are good models to evaluate the properties of the obtained EGF-LipoAgNPs as a potential nano agent, enhancing the toxicity in cancer cells, compared to normal one (BJ).

Generally, the cytotoxic effect caused by AgNPs is nonspecific and results in decreasing decrease in the metabolic activity and induction of apoptosis in cancer and healthy cells (Sanpui et al., 2011). Nevertheless, the use of AgNPs as potential anticancer factors is postulated inter alia by Kovács et al., who have proved that these nanostructures alone or in co-treatment with chemotherapeutics are able to overcome multidrug-resistance (MDR) in cancers, which is an emerging problem in the present medicine (Kovács et al., 2016). Our results showed that, after the 6 h cell treatment, the toxicity of EGF-LipoAgNPs against normal fibroblasts (BJ cells) measured with the resazurin reduction and LDH release assays was lower compared to the AgNPs-treated cells. This relationship was stronger after 24 h and 48 h, as proved by the resazurin reduction and LDH release assays. Our experiments also showed higher toxicity of EGF-LipoAgNPs in the A549 and SCC-15 cells compared to the AgNPs-treated cells, especially at the 50 and 100 ng/mL concentrations. This effect was dose- and time-dependent in each tested cell line. Furthermore, the involvement of the EGFR-dependent uptake can be assumed, given the higher effect in the cancer cells than in the normal ones. A similar toxic effect of native AgNPs was reported in A549 cells by Sambale et al., who showed a 10 ppm (10 ng/mL) IC_{50} concentration of AgNPs for these cells, while healthy fibroblasts were more sensitive to the AgNP treatment (IC_{50} = 4 ppm) after 24 h (Sambale et al., 2015). Greulich et al. showed that healthy monocytes and T-cells were characterized by an approx. 50% decrease in the viability after treatment with 70 nm AgNPs (Greulich et al., 2012). In turn, our results showed that the SCC-15 cells required longer exposure to AgNPs to induce toxicity, as there were no changes after 6 h and only a slight decrease in the metabolic activity after the 24 h treatment with AgNPs. Our results are similar to those reported by Dziedzic et al., who showed a slight increase in the toxic effect after 24 h treatment with AgNPs in the tongue cancer cell line (SCC-25) (Dziedzic et al., 2016). None of the mentioned authors performed the AgNP encapsulation procedure; thus, it is difficult to compare these results with our findings. However, Yusuf et al. showed that entrapment of AgNPs into DPPC-based liposomes increased the toxicity of such complexes, compared to native AgNPs (Yusuf et al., 2018a). A similar tendency was shown in the A549 and SCC-15 cells. We showed a correlation between the EGFR-overexpressing status and the toxicity of EGF-LipoAgNPs. The experiments showed a weaker effect of

EGF-LipoAgNPs on the metabolic activity and LDH release level in the BJ cells and a stronger effect in the A549 and SCC-15 cells. A similar effect was observed in a xenograft colocarcinoma model, where cells were treated with EGF-conjugated oxaliplatin-containing liposomes, showing higher accumulation of such complexes in the tumor, compared to cells treated with unlabeled liposomes, which were accumulated in healthy spleen cells (Zalba et al., 2016). Our results also showed a significant decrease in the LDH release in the SCC-15 cells at the highest concentration of EGF-LipoAgNPs, which is correlated with the cytotoxic effect of such complexes. This is in agreement with the results obtained by Szychowski et al., who showed that a decrease in the level of LDH release may occur after treatment of cells with high toxic xenobiotics, resulting in release of high amounts of proteases, which can subsequently degrade LDH (Szychowski et al., 2017). However, as described by Han et al., the AgNPs with 35-nm size may affect the NADH, which is a substrate in the LDH release assay reaction, therefore we have performed subsequently more specific methods to fully elucidate the toxic effect of our complexes on tested cell lines (Han et al., 2011).

Based on literature reports, AgNPs are strong prooxidative factors with an ability to induce high ROS generation and, subsequently, induce apoptosis, which is considered the most promising way to remove cancer cells from the organism during anticancer therapy (Kang et al., 2012). The ROS level in the BJ cells was increased already after the 6 h treatment with AgNPs, which was intensified after 24 h and 48 h. This effect was not observed in the EGF-LipoAgNPs-treated cells. This corresponds with caspase-9 activity, which was increased after 6 h contact with AgNPs, and with caspase-3 activity. In turn, lower activity of caspases was observed in the EGF-LipoAgNPs-treated cells. Gurunathan et al. showed that the higher concentration of AgNPs in mouse fibroblasts where a higher ROS level was generated in consequence induced caspase-3 activity (Gurunathan et al., 2018). Similarly, our experiments showed that the ROS production increased in the A549 cells after the 6 h treatment with AgNPs, and this subsequently increased caspase-9 but not caspase-3 activity. This effect was weaker than in the A549 cells treated with EGF-LipoAgNPs. After the 24 h and 48 h treatments, the cells exhibited an increase in ROS production, caspase-9 activity, and caspase-3 activity in the variant with EGF-LipoAgNPs. The SCC-15 cells were characterized by higher ROS production in the EGF-LipoAgNPs treatment already after 6 h, and a similar effect was noted in caspase-9 and -3 activity in all time intervals. In turn, a lower effect was observed in the AgNPs-treated cells. Baharara et al. showed that AgNPs can induce caspase-9 activity through ROS production by changing the mitochondrial membrane potential (Baharara et al., 2015). This correlation agrees with our results, which show increased ROS production in all tested cell lines treated with AgNPs and a subsequent increase in caspase-9 activity. This effect was intensified in the A549 and SCC-15 cells, suggesting increased uptake of AgNPs entrapped in the liposomes by overexpressing EGFR in such cells. Moreover, higher ROS production and caspase-9 and -3 activity were observed in the SCC-15 cells than in the A549 cells, which was associated with the higher EGFR expression in the SCC-15 than A549 cells. In our experimental model, caspase-3 was activated by caspase-9 as a response to the prooxidative effect of AgNPs, which was described previously by Plackal Adimuriyil George (George et al., 2018b). Our results show that the EGF-LipoAgNPs induce apoptosis through a ROS-dependent pathway. To date, Yusuf et al. have discovered that AgNPs entrapped in liposomes are able to induce apoptosis via a caspase-7-dependent pathway, which is an alternative pathway to caspase-3 (Yusuf et al., 2018b). Moreover, Urbańska et al. have shown that AgNPs are able to increase the expression of active caspase-9 in glioblastoma multiforme cells (Urbańska et al., 2015). This shows that the effect may vary depending on the tested cell type and the size of the tested AgNPs.

In the second part of the study, we decided to determine whether the tested nanoliposomes act via an EGFR-dependent pathway by pretreatment of the cell lines with the 0.16 nM concentration of pure EGF. The concentration of EGF was chosen as in Peterson at el., who have found that the saturation of this receptor can be induced by 0.16 nM without causing a lethal effect (Peterson et al., 2014). In this part of the study, the 10 ng/mL concentration of native AgNPs, EGF-LipoAgNPs, and EGF-LipoE was chosen. In our experimental model, there were no significant changes in the metabolic activity and ROS production results between the EGF-pretreated cells later exposed to AgNPs and those treated with AgNPs only. However, in both cases, a significant decrease in the metabolic activity and ROS production results was observed, compared to the control. This indicated that native AgNPs were uptaken *via* the EGFR-independent pathway facilitated by the 5 nm size of AgNPs, which can passively go through the cell membrane. As reported by Wu et al., AgNPs with the same size were detected in the cytoplasm already after 0.5 h treatment (Wu et al., 2019). In contrast, the EGF-pretreated cells and later treated with EGF-LipoAgNPs did not show any significant changes in metabolic activity and ROS production. Similar results were shown by Zalba et al., who pretreated cells with Cetuximab, which is a monoclonal antibody against EGFR, and thus no effect was observed in the cells after the treatment with EGF-conjugated oxaliplatin-containing liposomes (Zalba et al., 2016). This shows that EGF-LipoAgNPs can act through the EGFR-dependent pathway, which is also visible in the other tested parameters. There was a correlation between the EGFR expression in the cells (BJ < A549 < SCC-15) and the toxic effect, resulting in a higher negative effect of such complexes in the SCC-15 than A549 cells and then in the BJ cells. This indicates better uptake of liposome-entrapped AgNPs by the cells than the uptake of the native complexes. To show the accumulation of the complexes fully, we labeled the liposomes with carboxyfluorescein. The results showed much higher uptake of EGF-LipoAgNPs resulting in increased green fluorescence.in the SCC-15 cells than in the other tested cell lines, Moreover, the A549 cells showed higher uptake of such complexes than healthy fibroblasts, which are characterized by the lowest EGFR expression. These results indicate that the toxicity of AgNPs can be successfully directed using the EGFR-dependent pathway. Yu et al. showed that AgNPs conjugated to the anti-EGFR antibody were able to be uptaken more efficiently, thus the inhibition of proliferation and induction of apoptosis was more efficient in nasopharyngeal carcinoma cells, which are characterized by overexpression of EGFR (Yu et al., 2017). Mamot et al. showed that conjugation of the anti-EGFR antibody with the surface of liposomes containing chemotherapeutics resulted in better uptake and enhanced effects of this drug, compared to carcinomas with lower EGFR expression (Mamot et al., 2006).

The last part of our study was focused on determination of the impact of these nanostructures on certain genes. The impact of the tested compounds on the activity of two oxidative stress-related genes, i.e. catalase (*CAT*) and superoxide dismutase (*SOD2*), was determined. According to literature reports, these two enzymes are involved in the enzymatic antioxidant cell defense system and can be used as indicators of the oxidative stress in the cells (Weydert and Cullen, 2010). Our experiments show that after the 6 h, the increased in the *CAT* and *SOD2* expression was shown only for BJ and A549 cells treated with the AgNPs, while this effect was not observed in the SCC-15 cells. This covers the results from metabolic activity, ROS and caspases activity, which showed higher resistance of such cell line to the AgNPs. Interestingly, only in the SCC-15 cell line some effect was observed in the *CAT* and *SOD2* genes after the 6 h treatment with the EGF-LipoAgNPs which is correlated to the increased expression of the EGFR and better uptaken. On the other hand, after the 24 h treatment of the BJ cells, which are characterized by the normal EGFR expression, the *CAT* and *SOD2* expression was higher in the cells treated with the AgNPs than EGF-LipoAgNPs. The increased in the *CAT* and *SOD2* expression after 24 h in the A549 and SCC-15 cells also corresponded with ROS level, showing the higher expression of these two genes in cells treated with the EGF-LipoAgNPs compared to the AgNPs – treated cells. According to the Patlevič et al. ROS can trigger the expression of the *CAT* and *SOD2* as an answer from the antioxidant system in the cell on stress factor (Patlevič et al., 2016). The SOD activity measured after the 48 h

treatment cover the results of the *SOD2* gene expression after 24 h, which is caused by the time needed to produce protein based one the gene. The SOD activity was higher in the A549 and SCC-15 cells after the treatment with the EGF-LipoAgNPs than AgNPs, while in the BJ cells the SOD activity was lower after the treatment with the EGF-LipoAgNPs than AgNPs. Our results are consistent with data presented by Barcińska et al. who showed on model of human pancreatic ductal adenocarcinoma cells prior size-dependent impact of AgNPs on SOD activity but also proved that the AgNPs can significant increasing in this enzyme expression (Barcińska et al., 2018). Moreover, Fang et al. showed that the AgNPs are able to increase in SOD activity in the red blood cells, up to 60%, compared to the control (Fang et al., 2019). Thus, we claim that by enclosing the AgNPs into EGF-labeled liposomes, the oxidative stress in the healthy cells can be mitigate, while the same procedure improves the effectiveness of the AgNPs uptaken in the cancer cells. The pretreatment of the cells with the EGF showed abolishing of the negative effect on the metabolic activity and ROS, proving the involvement of the EGF receptor in the uptake of these complexes. In turn, CAT activity was decreased by AgNPs after 48-h and was significantly lower in the A549 and SCC-15 cells treated with EGF-LipoAgNPs, compared to the cells treated with native AgNPs. The EGF pretreatment of the cells abolished such an effect in the cells treated with the tested compounds. AgNPs are able to induce high ROS levels and subsequently influence the antioxidant enzymatic system in the cell. Liu et al. showed that these NPs were able to form a complex with the CAT protein, changing its conformation and, consequently, reducing CAT activity, but this effect was not detected in the case of SOD activity (Liu et al., 2020). Therefore, we suppose that this phenomenon occurs in the tested cells, which is connected in some way with the better uptake of AgNPs in our liposomes than the native ones, which also suggests accumulation of AgNPs inside the cytoplasm and the handicap of the CAT activity.

The *KI67* gene expression, which is a marker of cell proliferation, was characterized by an increase in the BJ cells after the 6 h treatment, which is in contrast to the metabolic activity results. However, Braun et al. have demonstrated that modified AgNPs can trigger *KI67* gene expression in healthy neuron cells in response to high ROS production (Braun et al., 2013). A stronger decrease in the *KI67* expression was observed in the EGF-LipoAgNPs-treated A549 and SCC-15 cells, which confirms the assumptions of our work on targeting using EGFR. After 24 h, the toxicity measured by metabolic activity and LDH release was much higher in the lung and tongue cancer cells than in the BJ cells, similarly to the gene expression results. Wang et al. have shown that EGFR-targeted liposomes containing chemotherapeutic can be internalized 5- and 7-fold more efficiently in cervix adenocarcinoma and ovarian cancer cell lines than in fibroblasts (Wang et al., 2016). Therefore, our liposomes can be uptaken with higher efficiency and cause accumulation of high quantities of AgNPs in the cytoplasm, thus increasing their cytotoxic effect. The impact of these NPs on the *KI67* gene or protein is rarely reported in the literature. However, Swanner et al. showed that AgNPs did not exert an impact on KI67 protein expression significantly, but the authors did not determine the impact of this NPs on *KI67* gene expression, thus these results cannot be directly compared with each other (Swanner et al., 2019). However, Chairuangkitti et al. used the proliferating cell nuclear antigen (PCNA) as another proliferation indicator gene and showed that the treatment of cells with AgNPs decreased the expression of this protein (Chairuangkitti et al., 2013). These findings correspond to our results of the KI67 protein expression measured by ELISA. The 24 h treatment with EGF-LipoAgNPs caused a significant decrease in the expression of this protein in the A549 and SCC-15 cells. Moreover, this effect was stronger than in the AgNPs-treated cells and was enhanced over time, causing a stronger decrease in the KI67 protein level. As proved by our previous results, the accumulation of EGF-LipoAgNPs liposomes is strictly dependent on the EGF receptor status in the cells. Therefore, we believe that the stronger effect of such complexes on the proliferation protein is caused by the higher amount of AgNPs accumulated in the cytoplasm and their ability to induce oxidative stress more efficiently than native AgNPs. This corresponds to the conclusions formulated by Kang et al. and Avalos et al., who showed dose-dependent ROS generation by AgNPs in cells (Kang et al., 2012; Avalos et al., 2014). In contrast, the BJ cells treated with EGF-LipoAgNPs exhibited lower KI67 protein expression than the AgNPs-treated cells in both time intervals. The high toxic effect of AgNPs on healthy cells is well-described in the literature (Peng et al., 2012; Zhang et al., 2016; Liu et al., 2021), but our results show that the uptake of AgNPs entrapped in labeled liposomes is less efficient, resulting in lower toxicity. Interestingly, in all tested cell lines and time intervals, cells pretreated with EGF and later with the tested compounds did not show any significant changes in the KI67 protein expression, proving the uptake of such complexes through an EGFR-dependent pathway

It is well-described that AgNPs are able to induce apoptosis in both ROS-dependent and ROS-independent pathways (Yusuf et al., 2018b; Zhu et al., 2016). Our results showed that EGF-LipoAgNPs were able to decrease caspase-3 and -9 activity in healthy fibroblasts, compared to native AgNPs. More interestingly, the complexes enhanced the apoptotic effect of AgNPs in the EGFR-overexpressing cancer cells. Therefore, we have determined the expression of the *BP53* gene, which is considered an indicator of active apoptosis. Our results showed that, already after the 6 h treatment, AgNPs were able to increase the *BP53* gene expression significantly in the BJ and A549 cells. In this time interval, an increase in the expression of this gene was observed in the SCC-15 cells treated with EGF-LipoAgNPs. These findings coincided with the results of the metabolic activity and caspase activity, which were strictly connected with the EGFR number in the cells, as shown above. After the 24 h treatment, the *BP53* gene expression was still significantly different in the A549 and SCC-15 cells treated with EGF-LipoAgNPs, compared to the native AgNPs-treated cells. In turn, the BJ cells were characterized by higher *BP53* expression after the treatment with native AgNPs. These results are convergent with the conclusions shown by Satapathy et al., who have proved that AgNPs are able to induce apoptosis through the p53-dependent pathway (Satapathy et al., 2013). Moreover, Mytych et al. reported the ability of AgNPs to induce higher expression of the p53 protein in hippocampal neuronal cells both after 48 h and 144 h, showing a prolonged impact of AgNPs on the expression of this protein (Mytych et al., 2017). As reported by Yusuf et al., the induction of apoptosis by DPPC-based liposomes with AgNPs, independently from ROS, showed the ability of AgNPs to act through a DNA-damage pathway (Yusuf et al., 2018b). Our data show that AgNPs delivered to the cell by EGF-labeled liposomes are characterized by higher toxicity effect in the cancer cells than native AgNPs. However, more research in this field is needed to fully understand the exact mechanism of the uptake and impact on EGFR-overexpressing cancers *in vivo*. Especially in case of results obtained by Milane et al., who show that EGF-labeled polymer, containing lonidamine and paclitaxel (chemotherapeutic drugs) were accumulated in first stage in liver and kidney and then incorporated in tumor in *in vivo* mouse experiments, showing that such platforms may show some negative effect on healthy tissues (Milane et al., 2011).

5. Conclusions

This study is the first to show that AgNP toxicity can be directed with the encapsulation method and labeling with EGF. The physicochemical characterization proved that, with the use of the THFE method, size homogenous and stable liposomes can be obtained with a size of approx. 110 nm. Our results show that EGF-LipoAgNPs cause a lower toxic effect in healthy human fibroblasts, compared to the EGFR-overexpressing lung and cancer cells by increasing ROS production, causing oxidative stress, and in consequence induction of apoptosis by increasing caspase-9 and -3 activity. Moreover, our study revealed that AgNPs entrapped in liposomes and delivered to the cell through the EGF receptor exert a higher toxic effect in cancer cells than AgNPs, while a mitigating effect

of these NPs is observed in BJ cells. Finally, the inhibitory effect of EGF-LipoAgNPs on cell proliferation measured by the KI67 expression was proved

Funding

This work was supported by statutory funds from the University of the Information Technology and Management, Poland (DS: 503-07-01-27 and DS: 503-07-01-31)

Availability of data and material

The datasets generated during and/or analysed during the current study are available from the corresponding author on reasonable request

Code availability

Not applicable

Ethics approval

Not applicable

Consent to participate

Not applicable

Consent for publication

Not applicable

CRediT authorship contribution statement

Bartosz Skóra: Conceptualization, Data curation, Formal analysis, Funding acquisition, Investigation, Methodology, Visualization, Writing – original draft, Writing – review & editing. **Tomasz Piechowiak:** Investigation. **Konrad A. Szychowski:** Writing – original draft, Supervision.

Declaration of Competing Interest

The Authors declare no conflict of the interest

Acknowledgement

We want to thank Prof. Elżbieta Pyza and Dr. Olga Woźnicka (Laboratory of Electron Microscopy, Department of Cell Biology and Imaging, Institute of Zoology and Biomedical Research, Jagiellonian University, Krakow) for performing the TEM analyses of the obtained complexes

References

Aronson, M.R., Medina, S.H., Mitchell, M.J., 2021. Peptide functionalized liposomes for receptor targeted cancer therapy. APL Bioeng. 5 https://doi.org/10.1063/5.0029860.

Avalos, A., Haza, A.I., Mateo, D., Morales, P., 2014. Cytotoxicity and ROS production of manufactured silver nanoparticles of different sizes in hepatoma and leukemia cells. J. Appl. Toxicol. 34 https://doi.org/10.1002/jat.2957.

Baharara, J., Namvar, F., Ramezani, T., Mousavi, M., Mohamad, R., 2015. Silver nanoparticles biosynthesized using achillea biebersteinii flower extract: apoptosis induction in MCF-7 cells via caspase activation and regulation of Bax and Bcl-2 gene expression. Molecules. 20 https://doi.org/10.3390/molecules20022693.

Banerjee, P.P., Bandyopadhyay, A., Nagesh, H., Policegoudra, R., Bhattacharya, S., Karak, N., Chattopadhyay, A., 2017. *Mentha arvensis* (Linn.)-mediated green silver nanoparticles trigger caspase 9-dependent cell death in MCF7 and MDA-MB-231 cells. Breast Cancer Targets Ther. 9 https://doi.org/10.2147/BCTT.S130952.

Barcińska, E., Wierzbicka, J., Zauszkiewicz-Pawlak, A., Jacewicz, D., Dabrowska, A., Inkielewicz-Stepniak, I., 2018. Role of oxidative and nitro-oxidative damage in silver nanoparticles cytotoxic effect against human pancreatic ductal adenocarcinoma cells. Oxidative Med. Cell. Longev. https://doi.org/10.1155/2018/8251961.

Braun, N.J., Comfort, K.K., Schlager, J.J., Hussain, S.M., 2013. Partial recovery of silver nanoparticle-induced neural cytotoxicity through the application of a static magnetic field. Bionanoscience. 3 https://doi.org/10.1007/s12668-013-0109-2.

Cao, P., Xia, Y., He, W., Zhang, T., Hong, L., Zheng, P., Shen, X., Liang, G., Cui, R., Zou, P., 2019. Enhancement of oxaliplatin-induced colon cancer cell apoptosis by alantolactone, a natural product inducer of ROS. Int. J. Biol. Sci. 15 https://doi.org/10.7150/ijbs.35265.

Castiglioni, S., 2014. Short- and long-term effects of silver nanoparticles on human microvascular endothelial cells. World J. Biol. Chem. 5 https://doi.org/10.4331/wjbc.v5.i4.457.

Chairuangkitti, P., Lawanprasert, S., Roytrakul, S., Aueviriyavit, S., Phummiratch, D., Kulthong, K., Chanvorachote, P., Maniratanachote, R., 2013. Silver nanoparticles induce toxicity in A549 cells via ROS-dependent and ROS-independent pathways. Toxicol. in Vitro. https://doi.org/10.1016/j.tiv.2012.08.021.

Chaudhury, A., Das, S., 2015. Folate receptor targeted liposomes encapsulating anti-cancer drugs. Curr. Pharm. Biotechnol. 16 https://doi.org/10.2174/1389201016666150118135107.

Daragmeh, J., Barriah, W., Saad, B., Zaid, H., 2016. Analysis of PI3K pathway components in human cancers. Oncol. Lett. 11 https://doi.org/10.3892/ol.2016.4309.

Dziedzic, A., Kubina, R., Bułdak, R., Skonieczna, M., Cholewa, K., 2016. Silver nanoparticles exhibit the dose-dependent anti-proliferative effect against human squamous carcinoma cells attenuated in the presence of berberine. Molecules. 21 https://doi.org/10.3390/molecules21030365.

Eid, K.A.M., Azzazy, H.M.E., 2014. Sustained broad-spectrum antibacterial effects of nanoliposomes loaded with silver nanoparticles. Nanomedicine. https://doi.org/10.2217/nnm.13.89.

Elamir, A., Ajith, S., Al Sawaftah, N., Abuwatfa, W., Mukhopadhyay, D., Paul, V., Al-Sayah, M.H., Awad, N., Husseini, G.A., 2021. Ultrasound-triggered herceptin liposomes for breast cancer therapy. Sci. Rep. 11 https://doi.org/10.1038/s41598-021-86860-5.

Eroğlu, İ., İbrahim, M., 2020. Liposome–ligand conjugates: a review on the current state of art. J. Drug Target. 28 https://doi.org/10.1080/1061186X.2019.1648479.

Espinoza, J.T., Novak, R.S., Magalhães, C.G., Budel, J.M., Justus, B., Gonçalves, M.M., Boscardin, P.M.D., Farago, P.V., De Paula, J. de F.P., 2020. Preparation and characterization of liposomes loaded with silver nanoparticles obtained by green synthesis, Brazilian. J. Pharm. Sci. 56 https://doi.org/10.1590/s2175-97902020000118601.

Fang, W., Chi, Z., Li, W., Zhang, X., Zhang, Q., 2019. Comparative study on the toxic mechanisms of medical nanosilver and silver ions on the antioxidant system of erythrocytes: from the aspects of antioxidant enzyme activities and molecular interaction mechanisms. J. Nanobiotechnol. 17 https://doi.org/10.1186/s12951-019-0502-2.

Franková, J., Pivodová, V., Vágnerová, H., Juráňová, J., Ulrichová, J., 2016. Effects of silver nanoparticles on primary cell cultures of fibroblasts and keratinocytes in a wound-healing model. J. Appl. Biomater. Funct. Mater. https://doi.org/10.5301/jabfm.5000268.

George, B. Plackal Adimuriyil, Kumar, N., Abrahamse, H., Ray, S.S., 2018a. Apoptotic efficacy of multifaceted biosynthesized silver nanoparticles on human adenocarcinoma cells. Sci. Rep. 8 https://doi.org/10.1038/s41598-018-32480-5.

George, B. Plackal Adimuriyil, Kumar, N., Abrahamse, H., Ray, S.S., 2018b. Apoptotic efficacy of multifaceted biosynthesized silver nanoparticles on human adenocarcinoma cells. Sci. Rep. https://doi.org/10.1038/s41598-018-32480-5.

Govindaraju, K., Krishnamoorthy, K., Alsagaby, S.A., Singaravelu, G., Premanathan, M., 2015. Green synthesis of silver nanoparticles for selective toxicity towards cancer cells. IET Nanobiotechnol. https://doi.org/10.1049/iet-nbt.2015.0001.

Greulich, C., Braun, D., Peetsch, A., Diendorf, J., Siebers, B., Epple, M., Köller, M., 2012. The toxic effect of silver ions and silver nanoparticles towards bacteria and human cells occurs in the same concentration range. RSC Adv. 2 https://doi.org/10.1039/c2ra20684f.

Guilleux, C., Campbell, P.G.C., Fortin, C., 2018. Interactions between silver nanoparticles/silver ions and liposomes: evaluation of the potential passive diffusion of silver and effects of speciation. Arch. Environ. Contam. Toxicol. 75, 634–646. https://doi.org/10.1007/s00244-018-0562-6.

Gurunathan, S., Qasim, M., Park, C., Yoo, H., Choi, D., Song, H., Park, C., Kim, J.-H., Hong, K., 2018. Cytotoxicity and transcriptomic analysis of silver nanoparticles in mouse embryonic fibroblast cells. Int. J. Mol. Sci. 19 https://doi.org/10.3390/ijms19113618.

Han, X., Gelein, R., Corson, N., Wade-Mercer, P., Jiang, J., Biswas, P., Finkelstein, J.N., Elder, A., Oberdörster, G., 2011. Validation of an LDH assay for assessing nanoparticle toxicity. Toxicology. 287, 99–104. https://doi.org/10.1016/j.tox.2011.06.011.

Herbst, R.S., Shin, D.M., 2002. Monoclonal antibodies to target epidermal growth factor receptor-positive tumors a new paradigm for cancer therapy. Cancer. https://doi.org/10.1002/cncr.10372.

Joseph, E., Singhvi, G., 2019. Multifunctional nanocrystals for cancer therapy: a potential nanocarrier. In: Nanomater. Drug Deliv. Ther. Elsevier. https://doi.org/10.1016/B978-0-12-816505-8.00007-2.

Jung, K., Lee, J., Park, J., Kim, D., Moon, S., Cho, Y., Lee, K., 2018. Targeted therapy of triple negative MDA-MB-468 breast cancer with curcumin delivered by epidermal growth factor-conjugated phospholipid nanoparticles. Oncol. Lett. https://doi.org/10.3892/ol.2018.8471.

Kang, K.-A., Jung, H.-Y., Lim, J.-S., 2012. Cell death by polyvinylpyrrolidine-coated silver nanoparticles is mediated by ROS-dependent signaling. Biomol. Ther. 20 https://doi.org/10.4062/biomolther.2012.20.4.399.

Kovács, D., Szőke, K., Igaz, N., Spengler, G., Molnár, J., Tóth, T., Madarász, D., Rázga, Z., Kónya, Z., Boros, I.M., Kiricsi, M., 2016. Silver nanoparticles modulate ABC transporter activity and enhance chemotherapy in multidrug resistant cancer, Nanomedicine Nanotechnology. Biol. Med. 12 https://doi.org/10.1016/j.nano.2015.10.015.

Kullberg, E.B., Wei, Q., Capala, J., Giusti, V., Malmström, P.-U., Gedda, L., 2005. EGF-receptor targeted liposomes with boronated acridine: growth inhibition of cultured glioma cells after neutron irradiation. Int. J. Radiat. Biol. 81 https://doi.org/10.1080/09553000500332137.

Liu, W., Worms, I., Slaveykova, V.I., 2020. Interaction of silver nanoparticles with antioxidant enzymes. Environ. Sci. Nano. 7 https://doi.org/10.1039/C9EN01284B.

Liu, X., Shan, K., Shao, X., Shi, X., He, Y., Liu, Z., Jacob, J.A., Deng, L., 2021. Nanotoxic effects of silver nanoparticles on normal HEK-293 cells in comparison to cancerous HeLa cell line. Int. J. Nanomedicine 16. https://doi.org/10.2147/IJN.S289008.

Mamot, C., Ritschard, R., Küng, W., Park, J.W., Herrmann, R., Rochlitz, C.F., 2006. EGFR-targeted immunoliposomes derived from the monoclonal antibody EMD72000 mediate specific and efficient drug delivery to a variety of colorectal cancer cells. J. Drug Target. 14 https://doi.org/10.1080/10611860600691049.

Mangala, L.S., Han, H.D., Lopez-Berestein, G., Sood, A.K., 2009. Liposomal siRNA for Ovarian Cancer, in. https://doi.org/10.1007/978-1-60327-295-7_3.

Milane, L., Duan, Z., Amiji, M., 2011. Pharmacokinetics and biodistribution of lonidamine/paclitaxel loaded, EGFR-targeted nanoparticles in an orthotopic animal model of multi-drug resistant breast cancer, Nanomedicine Nanotechnology. Biol. Med. 7, 435–444. https://doi.org/10.1016/j.nano.2010.12.009.

Morones, J.R., Elechiguerra, J.L., Camacho, A., Holt, K., Kouri, J.B., Ramírez, J.T., Yacaman, M.J., 2005. The bactericidal effect of silver nanoparticles. Nanotechnology. 16, 2346–2353. https://doi.org/10.1088/0957-4484/16/10/059.

Mytych, J., Zebrowski, J., Lewinska, A., Wnuk, M., 2017. Prolonged effects of silver nanoparticles on p53/p21 pathway-mediated proliferation, DNA damage response, and methylation parameters in HT22 hippocampal neuronal cells. Mol. Neurobiol. 54 https://doi.org/10.1007/s12035-016-9688-6.

Nicholson, D.W., Ali, A., Thornberry, N.A., Vaillancourt, J.P., Ding, C.K., Gallant, M., Gareau, Y., Griffin, P.R., Labelle, M., Lazebnik, Y.A., Munday, N.A., Raju, S.M., Smulson, M.E., Yamin, T.-T., Yu, V.L., Miller, D.K., 1995. Identification and inhibition of the ICE/CED-3 protease necessary for mammalian apoptosis. Nature. 376 https://doi.org/10.1038/376037a0.

Patlevič, P., Vašková, J., Švorc, P., Vaško, L., Švorc, P., 2016. Reactive oxygen species and antioxidant defense in human gastrointestinal diseases. Integr. Med. Res. 5 https://doi.org/10.1016/j.imr.2016.07.004.

Peng, H., Zhang, X., Wei, Y., Liu, W., Li, S., Yu, G., Fu, X., Cao, T., Deng, X., 2012. Cytotoxicity of silver nanoparticles in human embryonic stem cell-derived fibroblasts and an L-929 cell line. J. Nanomater. 2012 https://doi.org/10.1155/2012/160145.

Peterson, J.L., Phelps, E.D., Doll, M.A., Schaal, S., Ceresa, B.P., 2014. The role of endogenous epidermal growth factor receptor ligands in mediating corneal epithelial homeostasis. Investig. Opthalmology Vis. Sci. 55 https://doi.org/10.1167/iovs.13-12943.

Piechowiak, T., Skóra, B., Grzelak-Błaszczyk, K., Sójka, M., 2021. Extraction of antioxidant compounds from blueberry fruit waste and evaluation of their in vitro biological activity in human keratinocytes (HaCaT). Food Anal. Methods 14 (11), 2317–2327. https://doi.org/10.1007/s12161-021-02056-7.

Rajanahalli, P., Stucke, C.J., Hong, Y., 2015. The effects of silver nanoparticles on mouse embryonic stem cell self-renewal and proliferation. Toxicol. Rep. 2 https://doi.org/10.1016/j.toxrep.2015.05.005.

Rude Voldborg, B., Damstrup, L., Spang-Thomsen, M., Skovgaard Poulsen, H., 1997. Epidermal growth factor receptor (EGFR) and EGFR mutations, function and possible role in clinical trials. Ann. Oncol. https://doi.org/10.1023/A:1008209720526.

Sambale, F., Wagner, S., Stahl, F., Khaydarov, R.R., Scheper, T., Bahnemann, D., 2015. Investigations of the toxic effect of silver nanoparticles on mammalian cell lines. J. Nanomater. 16, 6.

Sánchez-López, E., Gomes, D., Esteruelas, G., Bonilla, L., Lopez-Machado, A.L., Galindo, R., Cano, A., Espina, M., Ettcheto, M., Camins, A., Silva, A.M., Durazzo, A., Santini, A., Garcia, M.L., Souto, E.B., 2020. Metal-Based nanoparticles as antimicrobial agents: an overview. Nanomaterials. 10 https://doi.org/10.3390/nano10020292.

Sanpui, P., Chattopadhyay, A., Ghosh, S.S., 2011. Induction of apoptosis in cancer cells at low silver nanoparticle concentrations using chitosan nanocarrier. ACS Appl. Mater. Interfaces. https://doi.org/10.1021/am100840c.

Satapathy, S.R., Mohapatra, P., Preet, R., Das, D., Sarkar, B., Choudhuri, T., Wyatt, M.D., Kundu, C.N., 2013. Silver-based nanoparticles induce apoptosis in human colon cancer cells mediated through p53. Nanomedicine. 8 https://doi.org/10.2217/nnm.12.176.

Singh, B., Carpenter, G., Coffey, R.J., 2016. EGF receptor ligands: recent advances. F1000Research. https://doi.org/10.12688/f1000research.9025.1.

Skóra, B., Szychowski, K.A., Gmiński, J., 2020. A concise review of metallic nanoparticles encapsulation methods and their potential use in anticancer therapy and medicine. Eur. J. Pharm. Biopharm. https://doi.org/10.1016/j.ejpb.2020.07.002.

Skóra, B., Piechowiak, T., Szychowski, K.A., Gmiński, J., 2021. Entrapment of silver nanoparticles in L-α-phosphatidylcholine/cholesterol-based liposomes mitigates the oxidative stress in human keratinocyte (HaCaT) cells. Eur. J. Pharm. Biopharm. 166 https://doi.org/10.1016/j.ejpb.2021.06.006.

Sun, X., Shi, J., Zou, X., Wang, C., Yang, Y., Zhang, H., 2016. Silver nanoparticles interact with the cell membrane and increase endothelial permeability by promoting VE-cadherin internalization. J. Hazard. Mater. 317 https://doi.org/10.1016/j.jhazmat.2016.06.023.

Swanner, J., Fahrenholtz, C.D., Tenvooren, I., Bernish, B.W., Sears, J.J., Hooker, A., Furdui, C.M., Alli, E., Li, W., Donati, G.L., Cook, K.L., Vidi, P., Singh, R., 2019. Silver nanoparticles selectively treat triple-negative breast cancer cells without affecting non-malignant breast epithelial cells in vitro and in vivo. FASEB BioAdv. 1 https://doi.org/10.1096/fba.2019-00021.

Szychowski, K.A., Sitarz, A.M., Wojtowicz, A.K., 2015. Triclosan induces Fas receptor-dependent apoptosis in mouse neocortical neurons in vitro. Neuroscience. 284 https://doi.org/10.1016/j.neuroscience.2014.10.001.

Szychowski, K.A., Leja, M.L., Kaminskyy, D.V., Binduga, U.E., Pinyazhko, O.R., Lesyk, R. B., Gmiński, J., 2017. Study of novel anticancer 4-thiazolidinone derivatives. Chem. Biol. Interact. 262 https://doi.org/10.1016/j.cbi.2016.12.008.

Szychowski, K.A., Skóra, B., Kryshchyshyn-Dylevych, A., Kaminskyy, D., Rybczyńska-Tkaczyk, K., Lesyk, R., Gmiński, J., 2020. Induction of Cyp450 enzymes by 4-thiazolidinone-based derivatives in 3T3-L1 cells in vitro. Naunyn Schmiedeberg's Arch. Pharmacol. https://doi.org/10.1007/s00210-020-02025-7.

Szychowski, K.A., Skóra, B., Kryshchyshyn-Dylevych, A., Kaminskyy, D., Tobiasz, J., Lesyk, R.B., Gmiński, J., 2021. 4-Thiazolidinone-based derivatives do not affect differentiation of mouse embryo fibroblasts (3T3-L1 cell line) into adipocytes. Chem. Biol. Interact. 345 https://doi.org/10.1016/j.cbi.2021.109538.

Thomas, R., Weihua, Z., 2019. Rethink of EGFR in cancer with its kinase independent function on board. Front. Oncol. 9 https://doi.org/10.3389/fonc.2019.00800.

Urbańska, K., Pająk, B., Orzechowski, A., Sokołowska, J., Grodzik, M., Sawosz, E., Szmidt, M., Sysa, P., 2015. The effect of silver nanoparticles (AgNPs) on proliferation and apoptosis of in ovo cultured glioblastoma multiforme (GBM) cells. Nanoscale Res. Lett. 10 https://doi.org/10.1186/s11671-015-0823-5.

Wang, S., Hüttmann, G., Scholzen, T., Zhang, Z., Vogel, A., Hasan, T., Rahmanzadeh, R., 2016. A light-controlled switch after dual targeting of proliferating tumor cells via the membrane receptor EGFR and the nuclear protein Ki-67. Sci. Rep. 6 https://doi.org/10.1038/srep27032.

Weydert, C.J., Cullen, J.J., 2010. Measurement of superoxide dismutase, catalase and glutathione peroxidase in cultured cells and tissue. Nat. Protoc. 5 https://doi.org/10.1038/nprot.2009.197.

Wiemann, M., Vennemann, A., Blaske, F., Sperling, M., Karst, U., 2017. Silver nanoparticles in the lung: toxic effects and focal accumulation of silver in remote organs. Nanomaterials. 7 https://doi.org/10.3390/nano7120441.

Wu, M., Guo, H., Liu, L., Liu, Y., Xie, L., 2019. Size-dependent cellular uptake and localization profiles of silver nanoparticles. Int. J. Nanomedicine 14. https://doi.org/10.2147/IJN.S201107.

Yu, D., Zhang, Y., Lu, H., Zhao, D., 2017. Silver nanoparticles coupled to anti-EGFR antibodies sensitize nasopharyngeal carcinoma cells to irradiation. Mol. Med. Rep. 16 https://doi.org/10.3892/mmr.2017.7704.

Yusuf, A., Casey, A., 2019. Evaluation of silver nanoparticle encapsulation in DPPC-based liposome by different methods for enhanced cytotoxicity. Int. J. Polym. Mater. Polym. Biomater. https://doi.org/10.1080/00914037.2019.1626390.

Yusuf, A., Brophy, A., Gorey, B., Casey, A., 2018a. Liposomal encapsulation of silver nanoparticles enhances cytotoxicity and causes induction of reactive oxygen species-independent apoptosis. J. Appl. Toxicol. 38, 616–627. https://doi.org/10.1002/jat.3566.

Yusuf, A., Brophy, A., Gorey, B., Casey, A., 2018b. Liposomal encapsulation of silver nanoparticles enhances cytotoxicity and causes induction of reactive oxygen species-independent apoptosis. J. Appl. Toxicol. 38 https://doi.org/10.1002/jat.3566.

Zalba, S., Contreras, A.M., Merino, M., Navarro, I., de Ilarduya, C.T., Trocóniz, I.F., Koning, G., Garrido, M.J., 2016. EGF-liposomes promote efficient EGFR targeting in xenograft colocarcinoma model. Nanomedicine. 11 https://doi.org/10.2217/nnm.15.208.

Zhang, X.F., Shen, W., Gurunathan, S., 2016. Silver nanoparticle-mediated cellular responses in various cell lines: an in vitro model. Int. J. Mol. Sci. 17 https://doi.org/10.3390/ijms17101603.

Zhu, B., Li, Y., Lin, Z., Zhao, M., Xu, T., Wang, C., Deng, N., 2016. Silver nanoparticles induce HePG-2 cells apoptosis through ROS-mediated signaling pathways. Nanoscale Res. Lett. 11 https://doi.org/10.1186/s11671-016-1419-4.

Zielinska, E., Zauszkiewicz-Pawlak, A., Wojcik, M., Inkielewicz-Stepniak, I., 2018. Silver nanoparticles of different sizes induce a mixed type of programmed cell death in human pancreatic ductal adenocarcinoma. Oncotarget. 9 https://doi.org/10.18632/oncotarget.22563.

Biomedicine & Pharmacotherapy 150 (2022) 113085

Contents lists available at ScienceDirect

Biomedicine & Pharmacotherapy

journal homepage: www.elsevier.com/locate/biopha

Molecular mechanism of the uptake and toxicity of EGF-LipoAgNPs in EGFR-overexpressing cancer cells

Bartosz Skóra [*,1], Konrad A. Szychowski [2]

Department of Biotechnology and Cell Biology, Medical College, University of Information Technology and Management in Rzeszow, St. Sucharskiego 2, Rzeszow 35-225, Poland

ARTICLE INFO

Keywords:
Silver nanoparticles
Anticancer therapy
Endocytosis
EGFR
Liposomes

ABSTRACT

The surface of silver nanoparticles (AgNPs) is characterized by high reactivity resulting in prooxidative and cytotoxic properties. These effects are observed both in normal and in cancer cells, which overexpress the Epidermal Growth Factor Receptor (EGFR). In our previous paper, we have demonstrated that, with the use of liposomes labeled with the Epidermal Growth Factor (EGF), it is possible to direct the toxic effect of AgNPs in EGFR-overexpressing cells. Unfortunately, the mechanism of uptake and toxicity induction by such liposomes is still unknown. Therefore, the aim of this study was to determine the impact of EGF-LipoAgNPs on certain genes related to endocytosis and toxicity induction by such liposomes in human lung (A549) and tongue (SCC-15) cancer cells. The siRNA knock-out gene method was used in this study to determine the engagement of EGFR in this process. The confocal microscopy study revealed that the number of liposomes in the cytoplasm of the $A549^{EGFR-}$ and $SCC\text{-}15^{EGFR-}$ cells was lowered by 51.99×10^3 RFU and 138.50×10^3 RFU, respectively, proving the crucial role of EGFR in the liposome uptake. Moreover, the expression of the *SHH* and *ATM* genes was significantly increased, whereas the expression of the *NRF2* gene was decreased after the treatment with EGF-LipoAgNPs and native AgNPs. Furthermore, the expression of the *CLTC, AP2M1, CAV1*, and *SH3GLB1* genes indicated that the tested liposomes are uptaken via the clathrin-dependent pathway with engagement of the AP-2 complex and endophilin in this process. Summarizing, the created targeted delivery system of AgNPs causes an increase in the prooxidative and toxic effect of such NPs and has an impact on endocytosis regulatory genes, especially those related to the clathrin-mediated endocytosis.

1. Introduction

Liposomal encapsulation is a well-known vehicle to deliver certain substances into the cell [1,2]. There are several methods for entrapping certain substances inside liposomes, among which the most popular are thin film hydration with extrusion (THFE) and reverse phase evaporation (RPE) (reviewed in [3]). Due to their similarity to the cell membrane, liposomes facilitate increased uptake of such carriers by the cell. Moreover, the lipid character of these molecules increases the possibility of surface modifications e.g. by the 3-maleimidobenzoic acid N-hydroxysuccinimide ester (MBA) anchor [3,4]. As reported by Rennick et al. (2021), liposomes can be uptaken via the endocytosis-dependent pathway and internalized entirely by the cell or they can interact directly with the cell membrane, resulting in the leakage of the liposome content inside the cell cytoplasm [5]. The basic endocytosis pathways described by Sahay et al. are included into two

Abbreviations: AgNPs, silver nanoparticles; CTCF, corrected total cell fluorescence; DMEM/F12, Dulbecco's Modified Eagle Medium/Nutrient Mixture F-12; DSPC, 1,2-distearoyl-sn-glycero-3phosphatoethanolamine; DSPE-CF, 1,2-dioleoyl-sn-glycero-3-phosphoethanolamine-N-(carboxyfluorescein); EGF, epidermal growth factor; EGFR, epidermal growth factor receptor; EGF-LipoAgNPs, silver nanoparticles entrapped in the EGF-labeled liposomes; EGF-LipoE, PBS solution entrapped in the EGF-labeled liposomes; F12-K, Ham's F-12 K (Kaighn's) Medium; FBS, fetal bovine serum; Hoechst 33342, 2′-(4-Ethoxyphenyl)−5-(4-methyl-1-piperazinyl)−2,5′-bi-1H-benzimidazole trihydrochloride; MBA, 3-maleimidobenzoic acid N-hydroxysuccinimide ester; NHS-PEG3400-DSPE, N-hydroxysuccinimide-PEG3400-DSPE; ROS, reactive oxygen species; PBS, phosphate-buffer saline; RPE, reverse phase evaporation; THFE, thin film hydration with extrusion.

* Correspondence to: Department of Biotechnology and Cell Biology, Medical College, University of Information Technology and Management, St. Sucharskiego 2, Rzeszow 35-225, Poland.

E-mail address: bskora@wsiz.edu.pl (B. Skóra).

[1] 0000–0001-7833–9985

[2] 0000–0003-2207–1160

https://doi.org/10.1016/j.biopha.2022.113085

Received 13 April 2022; Received in revised form 30 April 2022; Accepted 4 May 2022

main groups: clathrin-dependent and clathrin-independent, with the caveolin-dependent pathway comprised in the latter group [6]. Many proteins or factors are engaged in the different endocytosis pathways, e.g. dynamin, AP-2 complex, endophilin, clathrin, and/or caveolin. They allow rearrangement of the cell membrane, subsequent formation of intracellular vehicles, and release of certain substances inside the cytoplasm [7]. It has been described that the uptake of liposomes is independent of their chemical nature. As shown by Kang et al. (2017), cationic, anionic, and neutral liposomes enter the cell actively via the endocytosis pathway in human glioblastoma cells (U87-MG) [8]. In turn, Takikawa et al. have proved that siRNA-entrapped liposomes are able to penetrate the cell through direct fusion with the cell membrane and via the endocytosis pathway [9].

The uptake of liposomes is strictly correlated with their size [10]. Andar et al. showed that non-liganded liposomes with a size range of 97.8–162 nm are uptaken only via clathrin-dependent endocytosis, while liposomes with a size of approx. 41 nm are uptaken through the caveolin-dependent pathway [11]. Another dependence was shown by Alshehri et al. (2018), who highlighted that large liposomes (200–300 nm) containing siRNA were uptaken via the clathrin-dependent pathway in the human lung cancer cells (A549), which was proved by pretreatment of such cells with concanavalin A – an inhibitor of the G-protein engaged in clathrin-dependent endocytosis [12]. This shows that, depending on their size, liposomes can be uptaken in different ways. Therefore, it is necessary to study the mechanism of this process in every newly invented molecule/liposome.

Silver nanoparticles (AgNPs) are characterized by high surface reactivity, which directly determines their high prooxidative and cytotoxic properties. It has been reported that AgNPs can interact with the cell structure, e.g. the cell membrane, antioxidant enzymes, and/or DNA, mainly due to the generation of reactive oxygen species (ROS) [13]. Interestingly, Yusuf and Casey (2019) showed that AgNPs enclosed inside liposomes enhanced the toxic effect of such nanostructures but also induced redox imbalance and apoptosis [14]. However, the cytotoxic effect of AgNPs is observed in both normal and cancer cells, which underlines the need to target their reactivity straight toward cancer cells to save healthy structures [15,16]. As reported in our previous study, the cytotoxic effect of AgNPs can be targeted with high efficiency, using the THFE method and subsequent labeling with the Epidermal Growth Factor (EGF). The obtained liposomes (EGF-LipoAgNPs) showed a much higher toxic effect on the tongue cancer cell line (SCC-15) and lung cancer cells (A549) (EGFR-overexpressing cells) than on normal fibroblasts (BJ), which are characterized by standard EGFR expression. Moreover, a lower toxic effect of AgNPs delivered as EGF-LipoAgNPs on BJ cells was proved, which is the first step towards overcoming the limitations in the use of such nanostructures in the anticancer treatment [17]. Higher antiproliferation properties of such carriers were shown in EGFR-overexpressing cancer cells by determining the level of the KI67 protein (well-described proliferation marker). Unfortunately, there are no reports on the exact mechanism of EGF-LipoAgNP uptake and toxicity induction in EGFR-overexpressing cancer cells.

Therefore, the aim of the present study was to determine the molecular mechanism of the *in vitro* action and uptake of AgNPs entrapped in EGF-labeled liposomes (EGF-LipoAgNPs) by human lung (A549) and tongue (SCC-15) cancer cells as representatives of EGFR-overexpressing cells. The engagement of certain genes in the endocytosis pathway and toxicity induction was assed using molecular methods (siRNA knock-out and Real-Time PCR). Additionally, the amount of liposomes uptaken by both cell types was determined using confocal microscopy.

2. Materials and method

2.1. Reagents

Silver nanoparticles (AgNPs), 2′-(4-Ethoxyphenyl)−5-(4-methyl-1-piperazinyl)−2,5′-bi-1H-benzimidazole trihydrochloride (Hoechst 33342), cholesterol, methylene chloride, ethanol, and 1,2-dioleoyl-sn-glycero-3-phosphoethanolamine-N-(carboxyfluorescein) (DSPE-CF) were purchased from Merck (St. Louis, USA). N-hydroxysuccinimide-PEG3400-DSPE (NHS-PEG3400-DSPE), 1,2-distearoyl-sn-glycero-3phosphatoethanolamine (DSPC), and DSPE-PEG2000-Amine were purchased from Nanocs (Boston, USA). The human Epidermal Growth Factor (EGF) was purchased from SinoBiological (Eschborn, Germany). Ham's F-12 K (Kaighn's) Medium (F12-K), Dulbecco's Modified Eagle Medium/Nutrient Mixture F-12 (DMEM/F12), and phosphate-buffer saline (PBS) were purchased from Corning (Tewksbury, MA, USA). Fetal bovine serum (FBS), Universal RNA Purification Kit, Fast Probe qPCR Master Mix (2x), and plus ROX Solution were obtained from EURx (Gdańsk, Poland). The High-Capacity cDNA Reverse Transcription Kit, TaqMan probes, and primers corresponding to the genes encoding *ACTB* (Hs01060665_g1), *EGFR* (Hs06634166_s1), *SHH* (Hs01037584_m1), *ATM* (Hs01037584_m1), *CAV1* (Hs01037584_m1), *CLTC* (Hs01037584_m1), *SH3GLB1* (Hs01037584_m1), *AP2M1* (Hs01037584_m1), and *NFE2L2* (Hs00765730_m1) were purchased from ThermoFisher (Grand Island, USA). EGFR siRNA (sc-29301), Random siRNA, and transfection reagent (sc-29528) were purchased from Santa-Cruz Biotechnology (Texas, USA).

2.2. Synthesis of experimental compounds

AgNPs enclosed in liposomes and labeled with EGF (EGF-LipoAgNPs – experimental compounds) and empty liposomes (EGF-LipoE – negative control), were synthesized as described by Skóra et al. [17]. 5-nm AgNPs were purchased from Econix Company to ensure low polydisperse index (PdI) and accurate stability. The fluorescence variant of the tested substances was synthesized as described in the previous work by adding DSPE-CF to the forming lipid film [17]. After synthesis, the obtained compounds were sterilized by filtration through a filter with a 0.22-μm pore diameter. The physicochemical properties of the obtained complexes such as size, PdI, ζ-potential and conductivity were described and presented in the previous study [17]. Subsequently, 10 ng/mL of the compounds were used in the study. Their concentration was chosen based on the results of the dose-response analysis presented in our previous work [17].

2.3. Cell culture

Human lung carcinoma (A549, ATCC® CCL-185) and human tongue squamous cell carcinoma (SCC-15, ATCC® CRL-1623) were purchased from the American Type Culture Collection (ATCC, distributor: LGS Standard, Łomianki, Poland). The A549 cells were maintained in the F-12 K medium with 10% of FBS, and the SCC-15 cells were cultured in DMEM/F12 with 10% of FBS and 400 ng/mL of hydrocortisone. All media used in this study were supplemented with 100 U/mL penicillin, 0.10 mg/mL streptomycin, and 250 ng/mL amphotericin B. The cells were maintained at 37 °C and 5% of CO_2 until they reached confluency. Before the experiment, the cells were seeded in a 12-well plate at the density of 9×10^4 cells/well (qPCR) or ⌀35 mm culture dish (microscope) at the density of 1×10^5 cells/well and precultured for 24 h.

2.4. siRNA EGFR gene knock-out procedure

The Epidermal Growth Factor Receptor (EGFR) siRNA was used in this study to reveal and prove the mechanism of the uptake of EGF-LipoAgNPs by EGFR-overexpressing cancer cells (SCC-15^{EGFR-} and A549^{EGFR-}). siRNA with a random sequence, which does not cause knock-out of any known gene (SCC-15^{EGFR+} and A549^{EGFR+}), served as the control of the transfection. The procedure was performed as described by Szychowski et al. [18]. Briefly, the SCC-15 and A549 cells were seeded on a 12-well plate or a culture dish as described above. Next, the cells were treated with the 50 nM solution of EGFR siRNA (targeted gene) or with random siRNA (control) for 7 h in a serum- and

antibiotic-free medium, containing INTERFERin siRNA transfection reagent. After the transfection, the medium was removed and replaced with fresh one containing serum and antibiotics. Next, the cells were cultured for 12 h. After this time, the cells were treated with fresh medium containing 10 ng/mL of AgNPs (positive control), EGF-LipoAgNPs (experimental liposomes), and EGF-LipoE (negative control) for 6 h and 24 h and subsequently used in the qPCR analysis. In the case of fluorescence microscopy, the transfected cells were treated with the fluorescence variant (labeled with DSPE-CF) of the EGF-LipoAgNPs for 12 h and then subjected to confocal microscopy analysis.

2.5. Confocal microscopy analysis

Confocal microscopy is based on fluorescence measurements characterized by high resolution. Therefore, this method was chosen to determine the uptake of Fluo-EGF-LipoAgNPs by the SCC-15 and A549 cells. Briefly, after 24 h of seeding the cells on a ⌀35 mm culture dish, the transfection procedure was performed as described above. Subsequently, the medium was removed and replaced with fresh one containing 10 ng/mL of fluorescence EGF-LipoAgNPs for 12 h. After this, the medium was removed and the cells were washed three times with warm PBS to remove residues of the tested compounds from the cell surface. Subsequently, fresh serum-free medium containing 10 μM of Hoechst 33342 was added to the cells and the mixture was incubated for 5 min at 37 °C with 5% CO_2. Next, the cells were visualized by confocal microscopy with a laser scanner module at the x630 magnification (ZEISS LSM700). The fluorescence of the internalized complexes was measured using ImageJ software and expressed as corrected total cell fluorescence (CTCF), using the following equation:

$$CTFC = Integrated\ \ density - (Area\ \ of\ \ selected\ \ cell \bullet\ \ Mean\ \ fluorescence\ \ of\ \ background\ \ readings)$$

At least 10 images were used in the calculations, in which at least fluorescence of 20 cells was measured.

2.6. qPCR of genes related to metabolism and caveolin- and clathrin-dependent endocytosis

The quantitative polymerase chain reaction (qPCR) was used to determine the impact of EGF-LipoAgNPs on the expression of the certain genes related to metabolism (*SHH, ATM*, and *NRF2*), caveolin-mediated endocytosis (*CAV1, SH3GLB1*), and clathrin-mediated endocytosis (*CLTC1*, *AP2M1*) in the A549 and SCC-15 cells (both $EGFR^-$ and $EGFR^+$). Moreover, the qPCR method was used to determine the effectiveness of the siRNA knock-out of the EGFR gene. The method was performed as in Szychowski et al. [19]. Briefly, after the transfection procedure, the cells were treated with 10 ng/mL of the tested compounds for 6 h and 24 h. After a certain time interval, the total mRNA was isolated using the GeneMATRIX Universal RNA Purification Kit (EURx). Subsequently, the reverse transcription reaction was performed using the High-Capacity cDNA Reverse Transcription Kit (ThermoFisher) according to the producer's manual. The obtained cDNA template was then used in the qPCR reaction mixture (the total reaction volume was always 20 μL) containing qPCR master mix (EURx), 1 μL of cDNA template, and TaqMan probes specific for *ACTB*, *EGFR*, *SHH, ATM, NRF2, CAV1, SH3GLB1, CLTC1* or *AP2M1*. The qPCR analysis in this study was carried out as follows: 2 min at 50 °C and 10 min at 95 °C, followed by 45 cycles of 15 s at 95 °C and 1 min at 60 °C. The threshold value (C_t) for each sample was calculated during the exponential phase, and $\Delta\Delta_{Ct}$ was used to determine the Average Fold (Avg. Fold) of expression of certain genes. *ACTB* was used as a reference gene.

2.7. Statistical analyses

All data presented in this study are mean values with ± standard deviations (SD). Each experiment was repeated at least 3 times and each compound treatment was tested 3 times, thus the total number of repetitions was 9 (n = 9). The obtained results were subsequently used in the statistical analysis performed using the GraphPad Prism 8.0 Statistical Analysis Mode. The statistical analysis of differences between the respective control cells and the treated cells was performed using one-way ANOVA with post-hoc Tukey's test at *** $p < 0.001$, ** $p < 0.01$, and * $p < 0.5$. The statistical analysis of differences between the Random siRNA-treated cells and the EGFR siRNA-treated cells was performed using the *t*-test and described as # $p < 0.05$. Moreover, the statistical differences between the AgNPs- and EGF-LipoAgNPs-treated cells were analyzed with the *t*-test and denoted as @ $p < 0.05$.

3. Results

3.1. Efficiency of the siRNA transfection

The siRNA transfection method is commonly used to knock-out certain genes temporarily. Therefore, this method was used in this study to determine the engagement of EGFR in the uptake of the EGF-LipoAgNPs liposomes. The *EGFR* gene expression was decreased by 59% in the $A549^{EGFR-}$ cells, compared to the Random siRNA-treated cells (Fig. 1). On the other hand, the $SCC\text{-}15^{EGFR-}$ cells were characterized by 40% lower expression of the EGFR gene, compared to the $SCC\text{-}15^{EGFR+}$ cells (Fig. 1).

3.2. Uptake of the liposomes by the cells

The confocal fluorescence microscopy and the corrected total cell fluorescence were used in this study to determine the EGFR-dependent uptake of the tested liposomes. The obtained results showed that the uptake of the liposomes by the $A549^{EGFR-}$ cells was reduced to 51.99×10^3 RFU (compared to the Random siRNA-treated cells) (Fig. 2A). In turn, the $SCC\text{-}15^{EGFR-}$ cells treated with the fluorescence liposomes showed 138.50×10^3 RFU lower liposome uptake, compared to the $SCC\text{-}15^{EGFR+}$ cells (Fig. 2A). No changes were observed in the nucleus morphology in any tested cell line (Fig. 2B).

3.3. Expression of the gene related to cell damage and cell stress

The *SHH* gene expression in the $EGFR^+$ and $EGFR^-$ A549 cells was increased by 120% and 115%, respectively, after the 6-h treatment with AgNPs, compared to the control (Fig. 3A). After 24 h, a 126% and 127% increase in the *SHH* expression was observed in the $EGFR^-$ and $EGFR^+$ cells treated with AgNPs, respectively, compared to the control (Fig. 3B). In turn, the random siRNA cells were characterized by a 284% increase in the *SHH* expression, compared to the control, but the EGFR siRNA

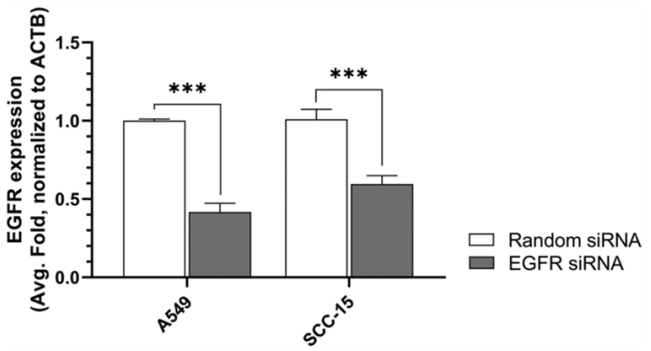

Fig. 1. Effectiveness of the siRNA knock-out. The *EGFR* expression after transfection of the A549 and SCC-15 cells with EGFR siRNA. The means ± standard deviations (SD) with *** are statistically different from the values for the Random siRNA-treated cells at $p < 0.001$.

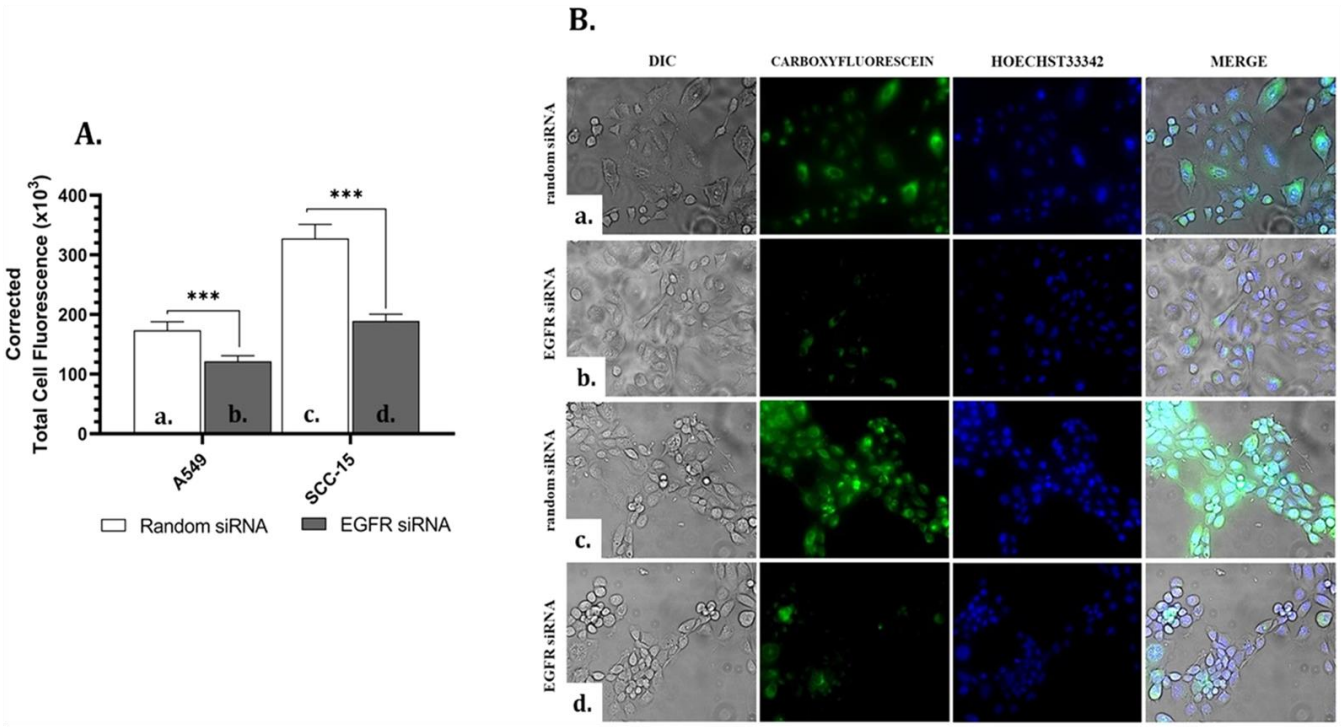

Fig. 2. Uptake of the fluorescence of EGF-LipoAgNPs. Corrected Total Cell Fluorescence of uptaken liposomes in the A549^{EGFR+}(a), A549^{EGFR-} (b), SCC-15^{EGFR+} (c) and SCC-15^{EGFR-} (d) cell lines after 12 h of treatment (A) and representative images of the liposomes uptaken by the cells (B). The representative images of certain cell groups are denoted as small letters (a, b, c, d). The mean RFU ± standard deviations (SD) with *** are statistically different from the values for the Random siRNA-treated cells at $p < 0.001$.

cells showed only a 134% increase in the expression of this gene (Fig. 3B). EGF-LipoE did not exert any significant effect on the A549 cells in any time interval (Fig. 3A-B).

The *ATM* gene expression after the 6-h treatment with AgNPs increased by 57% and 52% in the EGFR$^+$ and EGFR$^-$ cells, respectively, compared to the control (Fig. 3C). No changes were detected in the EGF-LipoAgNPs- and EGF-LipoE-treated cells in this time interval, compared to the control (Fig. 3C). After the 24 h-treatment, the EGFR$^+$ cells treated with AgNPs showed a 114.7% increase in the *ATM* mRNA expression, compared to the control. In turn, the EGFR$^-$ cells were characterized by a similar effect, i.e. a 107% increase in the expression of this gene, compared to the control (Fig. 3D). The EGFR$^+$ cells treated with EGF-LipoAgNPs showed a 140% increase in the *ATM* mRNA expression, compared to the control, whereas the EGFR siRNA cells were characterized by only a 26% increase in the expression of this gene, compared to the control (Fig. 3D).

The *NFR2* mRNA expression after the 6-h treatment with AgNPs was decreased in the EGFR$^+$ and EGFR$^-$ cells by 31% and 25%, respectively, compared to the control (Fig. 3E). No significant changes were noted in any cells treated with EGF-LipoAgNPs and EGF-LipoE in this time interval (Fig. 3E). An up to 34% and 36% decrease in the *NFR2* mRNA expression was also observed in the random siRNA and EGFR siRNA cells, respectively, after the 24-h treatment of the cells with AgNPs, compared to the control (Fig. 3F). A stronger 64% decrease in the expression of this gene was observed in the EGF-LipoAgNPs-treated EGFR$^+$ cells, compared to the control, in contrast to the EGFR$^-$ cells, which exhibited no significant changes in this parameter (Fig. 3F). No changes were detected in the EGF-LipoE-treated cells (Fig. 3F).

The *SHH* gene expression after the 6-h treatment of AgNPs in the SCC-15 cells was increased by 88% and 100% in the SCC-15^{EGFR+} and SCC-15^{EGFR-} cells, respectively, compared to the control (Fig. 4A). After the 24-h treatment with AgNPs, the cells were characterized by a 100% and 113% increase in the *SHH* gene expression in the EGFR$^+$ and EGFR$^-$ cells, respectively, compared to the control (Fig. 4B). In turn, the EGF-LipoAgNPs-treated cells showed a 543% and 169% increase in this mRNA expression in the random siRNA and EGFR siRNA cells, respectively, compared to the control (Fig. 4B).

No changes were detected in the *ATM* gene expression after the 6-h treatment of the SCC-15^{EGFR-} and SCC-15^{EGFR+} cells with EGF-LipoAgNPs and EGF-LipoE (Fig. 4C). On the other hand, AgNPs caused a significant increase in the *ATM* gene expression, i.e. by 60% and 67% in the Random siRNA and EGFR siRNA cells, respectively, compared to the control (Fig. 4C). The expression of the *ATM* gene after 24 h in the AgNPs-treated cells reached 187% and 192% of the control in the EGFR$^+$ and EGFR$^-$ cells, respectively (Fig. D). In turn, the *ATM* gene expression in the SCC-15^{EGFR+} cells treated with EGF-LipoAgNPs was increased by 296%, compared to the control, in contrast to the EGFR$^-$ cells, which were characterized by only an 88% increase in the mRNA expression, compared to the control (Fig. 4D).

The *NFR2* gene expression after the 6-h treatment with AgNPs in the SCC-15^{EGFR+} and SCC-15^{EGFR-} cells was increased by 31% and 25%, compared to the control (Fig. 4E). After 24 h, the expression of this mRNA in the AgNPs-treated cells was increased by 34% and 36% in the random siRNA and EGFR siRNA cells, respectively (Fig. 4F). However, EGF-LipoAgNPs caused a 64% decrease in the *NRF2* expression in the EGFR$^+$ cells, in contrast to the EGFR$^-$ cells, which did not show any significant changes in the mRNA expression, compared to control (Fig. 4F).

3.4. Expression of genes related to clathrin-dependent endocytosis

The *AP2M1* gene expression after the 6-h treatment with AgNPs caused a 43% and 50% decrease in the mRNA expression in the EGFR$^+$ and EGFR$^-$ A549 cells compared to the control, respectively (Fig. 5A). Additionally, the EGF-LipoAgNPs-treated EGFR$^+$ cells were characterized by a 91% increase in the expression of this gene, while the EGFR$^-$ cells did not show significant changes (Fig. 5A). A similar effect was observed in the EGFR$^+$ cells treated with EGF-LipoE, i.e. a 56% increase

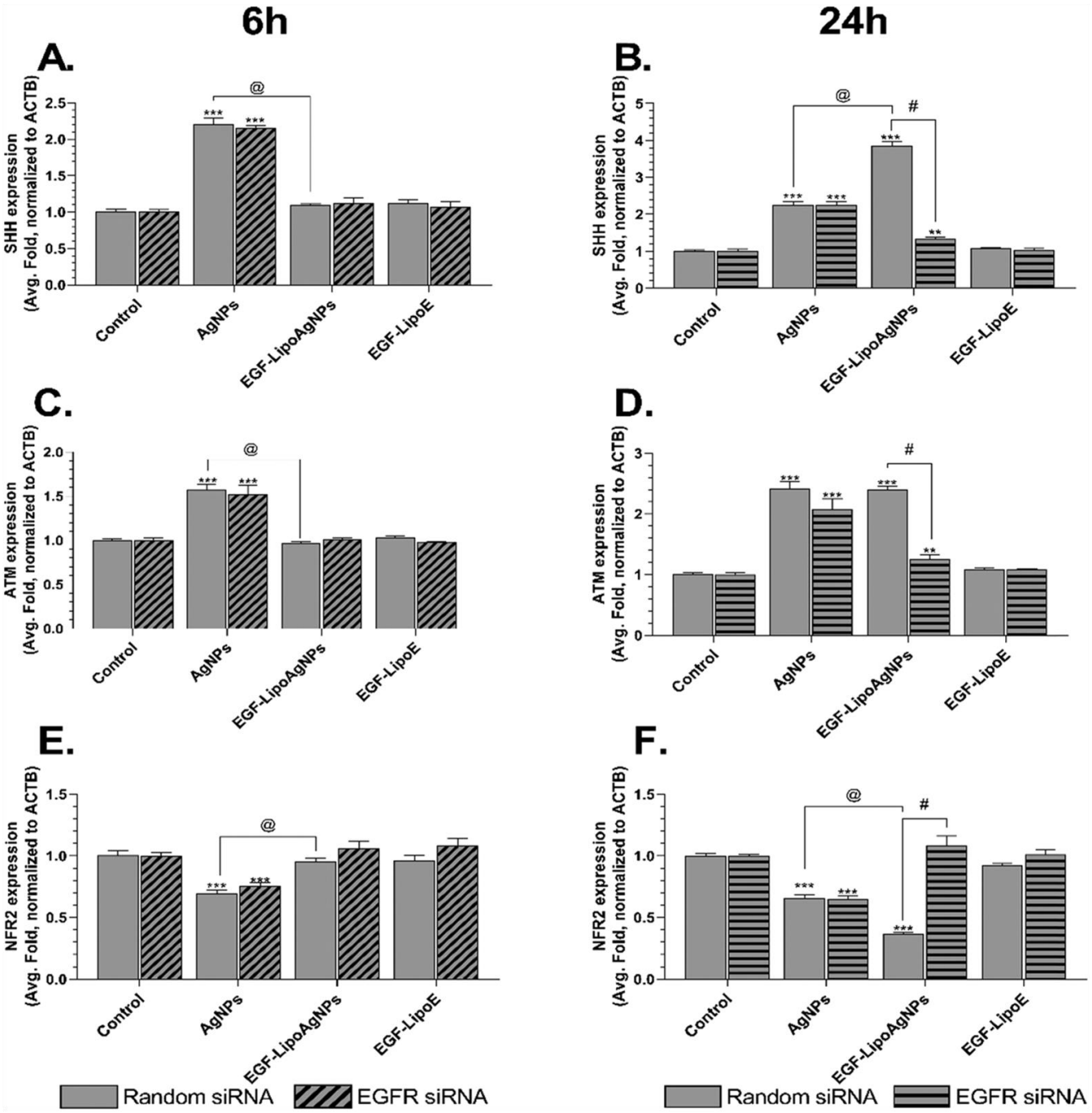

Fig. 3. Expression of *SHH* (A-B), *ATM* (C-D), and *NRF2* (E-F) in the A549 cells transfected with Random siRNA and EGFR siRNA after the 6-h and 24-h treatment with AgNPs, EGF-LipoAgNPs, and EGF-LipoE. The means ± SD (error bars) with ** and *** are statistically different from the respective control at $p < 0.01$ and $p < 0.001$, respectively (one-way ANOVA, Tukey's test). # and @ mean statistically significant differences ($p < 0.05$) between certain groups (*t*-test).

in the mRNA expression, compared to the control (Fig. 5A). After the 24-h treatment, the $EGFR^+$ and $EGFR^-$ cells treated with AgNPs were characterized by a 50% and 25% decrease in the *AP2M1* gene expression, respectively (Fig. 5B). In contrast, the $EGFR^+$ cells treated with EGF-LipoAgNPs showed a 387% increase in the mRNA expression, while a 22% decrease was noted in the $EGFR^-$ cells (Fig. 5B). Similarly, the $EGFR^+$ cells showed a 321% increase in the *AP2M1* gene expression, compared to the control, while the $EGFR^-$ cells exhibited a 30% decrease in the mRNA expression, compared to the control (Fig. 5B).

The 6-h treatment with AgNPs decreased the *CLTC* gene expression by 49% and 42% in the cells transfected with Random siRNA and EGFR siRNA, respectively, compared to control (Fig. 5C). In contrast, the liposomes were able to increase this mRNA expression by 74.5% in the $EGFR^+$ cells, compared to the control, while the $EGFR^-$ cells treated with the empty liposomes were characterized by a 40% increase in this mRNA expression (Fig. 5C). After the 24-h treatment, the $A549^{EGFR+}$ cells treated with AgNPs showed by 33% lower expression of the *CLTC* gene than the control, and a similar effect was observed in the $A549^{EGFR-}$ cells (Fig. 5D). In turn, in the EGF-LipoAgNPs-treated cells, the expression of the *CLTC* gene was increased by 395% in the $A549^{EGFR+}$ cells, compared to the control. After transfection with EGFR siRNA, the expression of this mRNA was decreased by 16%, compared to the control (Fig. 5D). The expression of the *CLTC* gene was increased by 221%, compared to the control in the cells transfected with Random siRNA, in contrast to the

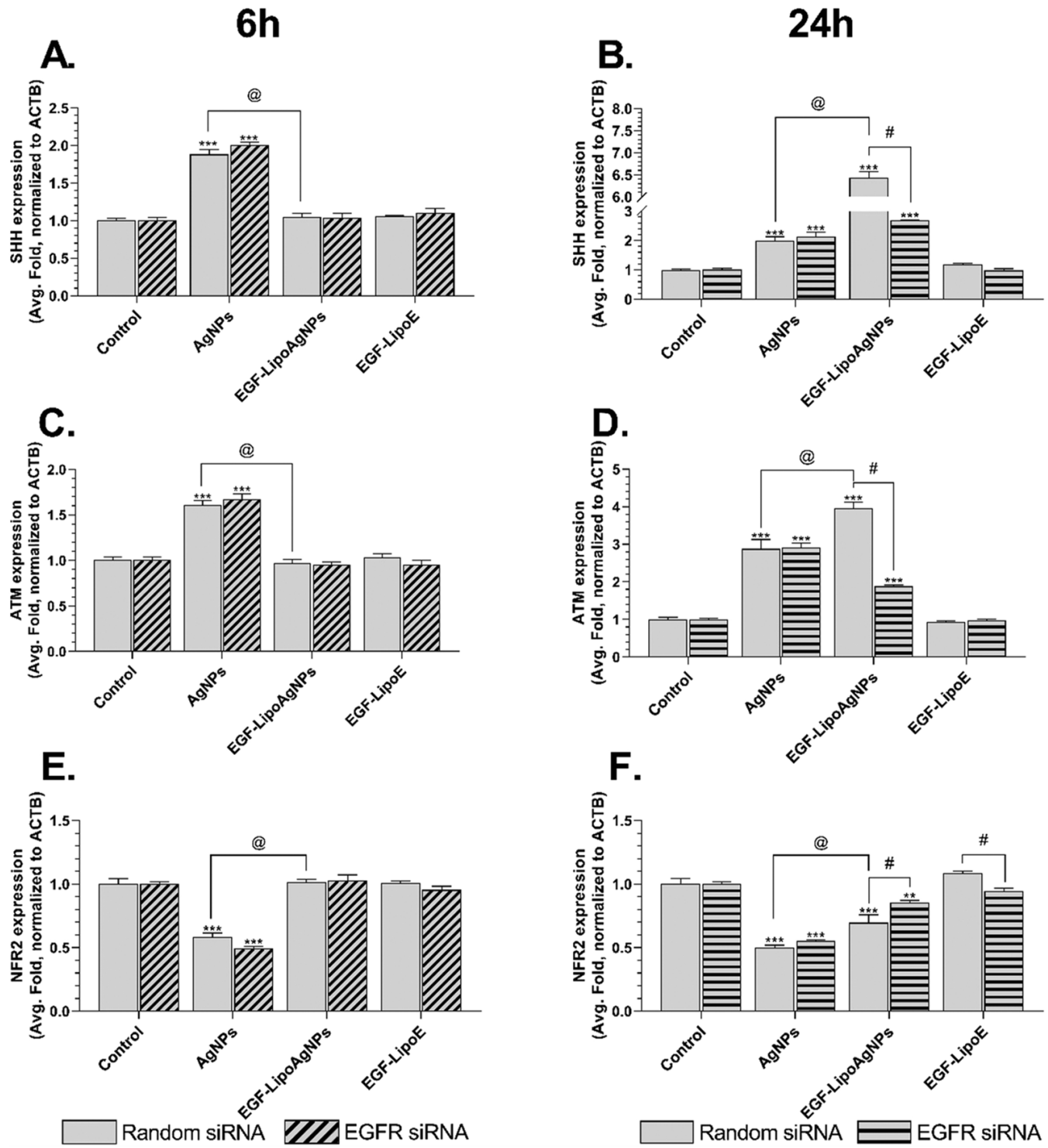

Fig. 4. Expression of *SHH* (A-B), *ATM* (C-D), and *NRF2* (E-F) in the SCC-15 cells transfected with Random siRNA and EGFR siRNA after the 6-h (A, C, E) and 24-h (B, D, F) treatment with AgNPs, EGF-LipoAgNPs, and EGF-LipoE. The means ± SD (error bars) with ** and *** are statistically different from the respective control at $p < 0.01$ and $p < 0.001$, respectively (one-way ANOVA, Tukey's test). # and @ mean statistically significant differences ($p < 0.05$) between certain groups (*t*-test).

EGFR siRNA-transfected cells, which were characterized by a 27% decrease in this mRNA expression, compared to the control (Fig. 5D).

After 6-h, the expression of the *AP2M1* gene in the $EGFR^+$ and $EGFR^-$ SCC-15 cells was decreased by 20% and 12%, respectively, after the AgNPs treatment, compared to the control (Fig. 6A). In contrast, the $SCC\text{-}15^{EGFR+}$ cells were characterized by a 95% increase in the *AP2M1* gene expression (compared to the control) after the treatment with EGF-LipoAgNPs, while the $EGFR^-$ cells showed a 20% decrease in this mRNA expression, compared to the control (Fig. 6A). A similar effect was noted in the EGF-LipoE-treated cells, which were characterized by a 68% increase and a 24% decrease in the *AP2M1* gene expression, in the $EGFR^+$ and $EGFR^-$ cells, respectively, compared to the control (Fig. 6A). After the 24-h treatment with AgNPs, the expression of the *AP2M1* gene was decreased by 42% and 46% in the $EGFR^+$ and $EGFR^-$ cells, respectively, compared to the control (Fig. 6B). In contrast, the expression of this mRNA was increased by 158%, compared to the control, in the $EGFR^+$

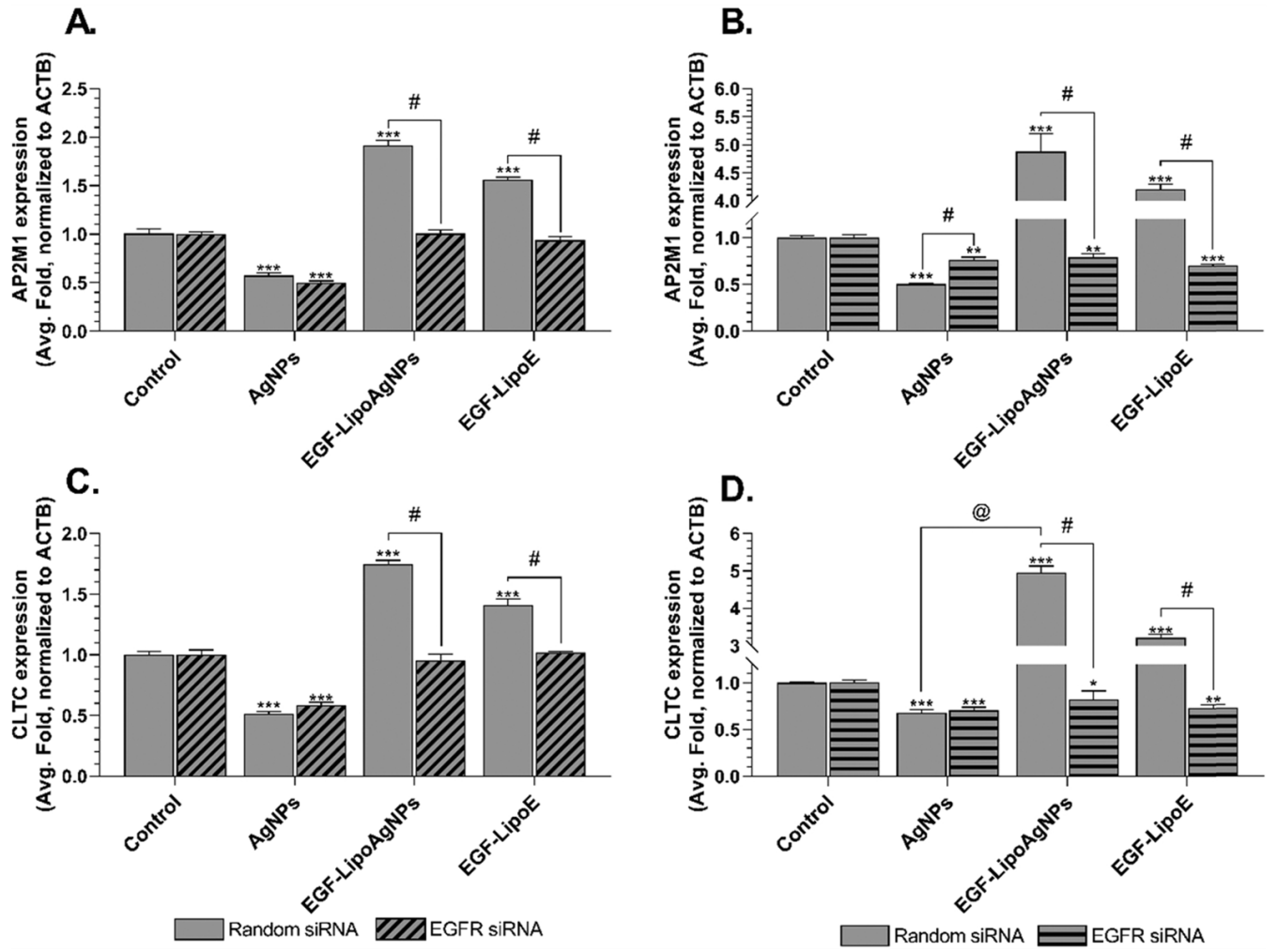

Fig. 5. Expression of *AP2M1* (A-B) and *CLTC* (C-D) in the A549 cells transfected with Random siRNA and EGFR siRNA after the 6-h (A, C) and 24-h (B, D) treatment with AgNPs, EGF-LipoAgNPs, and EGF-LipoE. The means ± SD (error bars) with * , ** , and *** are statistically different from the respective control at $p < 0.05$, $p < 0.01$, and $p < 0.001$, respectively (one-way ANOVA, Tukey's test). # and @ mean statistically significant differences ($p < 0.05$) between certain groups (*t*-test).

cells treated with EGF-LipoAgNPs, while the cells with EGFR siRNA were characterized by a 38% decrease in the expression of this gene (Fig. 6B). The treatment with EGF-LipoAgNPs caused a 106% increase in the *AP2M1* expression in the $EGFR^+$ cells and a 31% decrease in this parameter after transfection (Fig. 6B).

The expression of the *CLTC* gene after the 6-h treatment with AgNPs was decreased by 46% and 37% in the SCC-15^{EGFR+} and SCC-15^{EGFR-} cells, respectively, compared to the control (Fig. 6C). In contrast, the EGFR+ cells treated with EGF-LipoAgNPs and EGF-LipoE exhibited a 127% and 105% increase in this parameter, respectively, compared to control (Fig. 6C). The cells transfected with EGFR siRNA and treated with EGF-LipoAgNPs and EGF-LipoE showed a 12% and 30% decrease in this mRNA expression, respectively (Fig. 6C). After the 24-h treatment, the $EGFR^+$ and $EGFR^-$ cells treated with AgNPs were characterized by a 35% and 30% decrease in the *CLTC* gene expression, respectively, compared to the control (Fig. 6D). EGF-LipoAgNPs caused a 417% increase in this gene expression in the $EGFR^+$ cells, compared to the control, while the $EGFR^-$ cells showed an 18% decrease in the expression of this gene, compared to the control (Fig. 6D). EGF-LipoAgNPs exerted a similar effect in this time interval and caused a 322% increase in the *AP2M1* gene expression in the $EGFR^+$ cells, compared to the control, and a 19% decrease in this parameter after transfection, compared to the control (Fig. 6D).

3.5. Expression of genes related to caveolin-dependent endocytosis

The expression of the *CAV1* gene after the 6-h treatment with AgNPs caused a significant 159% and 165% increase in the expression of this mRNA in the A549^{EGFR+} and A549$^-$ cells, respectively, compared to the control (Fig. 7A). No changes were detected in the cells exposed to the tested liposomes in this time interval. After the 24-h treatment with AgNPs, the increase in the *CAV1* gene expression reached 155% and 158% in the cells transfected with Random siRNA and EGFR siRNA, respectively, compared to the control (Fig. 7B). EGF-LipoAgNPs and EGF-LipoE did not induce any changes in the expression of this mRNA (Fig. 7B).

The expression of the *SH3GLB1* gene in the A549 cells treated with AgNPs for 6 h increased by 48% and 45% in the $EGFR^+$ and $EGFR^-$ cells, respectively, compared to the control (Fig. 7C). EGF-LipoAgNPs caused a 26% increase in the gene expression in the $EGFR^-$ cells, while the $EGFR^-$ cells showed an 18% decrease in this parameter, compared to the control (Fig. 7C). In turn, the A549^{EGFR-} and A549^{EGFR-} cells were characterized by a 23% increase and a 21% decrease in the *SH3GLB1* gene expression, respectively, compared to the control (Fig. 7C). After the 24-h treatment with AgNPs, the $EGFR^+$ and $EGFR^-$ cells were characterized by a 30% and 28% decrease in the *SH3GLB1* gene expression, respectively, compared to the control (Fig. 7D). In turn, EGF-LipoAgNPs caused a 28% increase and a 15% decrease in this mRNA expression, respectively, compared to the control (Fig. 7D). The EGF-LipoE-treated cells were

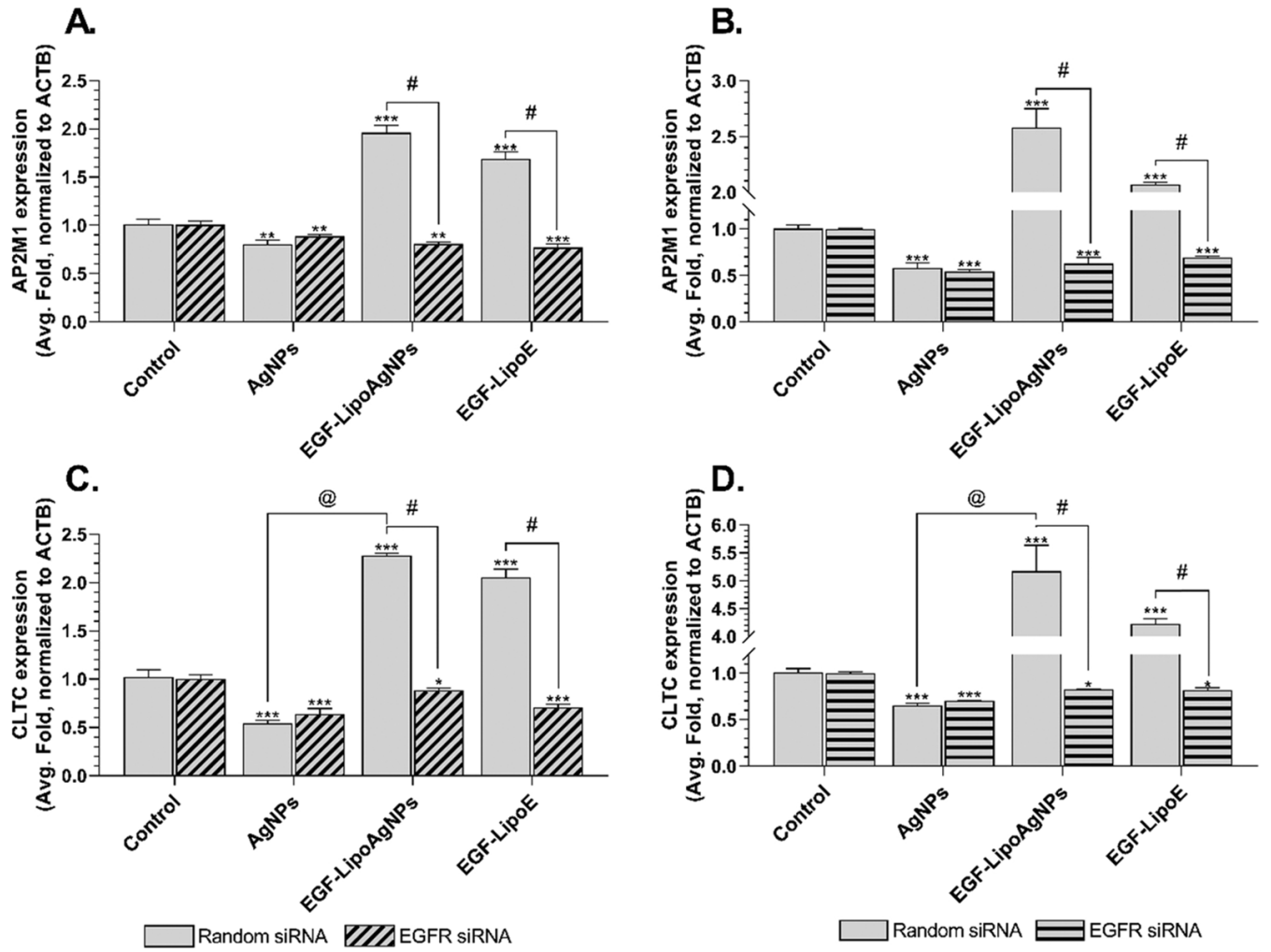

Fig. 6. Expression of *AP2M1* (A-B) and *CLTC* (C-D) in the SCC-15 cells transfected with Random siRNA and EGFR siRNA after the 6-h (A, C) and 24 h (B, D) treatment with AgNPs, EGF-LipoAgNPs, and EGF-LipoE. The means ± SD (error bars) with * , ** , and *** are statistically different from the respective control at $p < 0.05$, $p < 0.01$, and $p < 0.001$, respectively (one-way ANOVA, Tukey's test). # and @ mean statistically significant differences ($p < 0.05$) between certain groups (*t*-test).

characterized by a 17% increase in this mRNA expression, in the $EGFR^+$ cells (compared to control) and a 20% decrease in this parameter in the $EGFR^-$ cells (compared to control) (Fig. 7D).

The *CAV1* gene expression after the 6-h treatment with AgNPs was increased by 141% and 154% in the SCC-15^{EGFR+} and SCC-15^{EGFR-} cells, respectively, compared to the control (Fig. 8A). In turn, no changes were noticed in the treatment with the liposomes in this time interval (Fig. 8A). After the 24-h treatment with AgNPs, the expression of the *CAV1* gene was increased by 215% and 217% in the $EGFR^+$ and $EGFR^-$ cells, respectively, compared to the control (Fig. 8B).

The expression of the *SH3GLB1* gene in the SCC-15^{EGFR+} and SCC-15^{EGFR-} cells after 6 h was increased by 106% and 99%, respectively, compared to the control (Fig. 8C). In turn, EGF-LipoAgNPs and EGF-LipoE increased the mRNA expression in the $EGFR^+$ cells by 16% and 21%, respectively, compared to control (Fig. 8C). This effect was not observed in the $EGFR^-$ cells (Fig. 8C). After the 24-h treatment with AgNPs, a 32% and 30% decrease in the *SH3GLB1* gene expression was observed in the $EGFR^+$ and $EGFR^-$ cells, respectively, compared to the control (Fig. 8D). In turn, a 41% and 26% increase in the expression of this gene was observed in the EGF-LipoAgNPs-treated $EGFR^+$ cells and the EGF-LipoE-treated $EGFR^+$ cells, compared to the control (Fig. 8D).

4. Discussion

It has been reported that AgNPs are able to induce redox imbalance in the cell, resulting in apoptosis induction [20,21]. This prooxidative and proapoptotic effect occur both in normal and in cancer cells [22–24]. Therefore, the use of such nanostructures as a potential cure in anticancer therapy is limited. To date, few approaches have been taken to target the toxicity of AgNPs towards cancer cells. Montalvo-Quiros et al. synthesized nanosilica carriers with an attached protein-AgNP complex on their surface, which were able to increase the toxicity of this NPs in human hepatocarcinoma cells (HepG2) [25]. In turn, Kumar Thapa et al. proved that AgNPs entrapped inside the graphene oxide structure conjugated with methotrexate (folate receptor ligand) were characterized by higher uptake and toxicity in folate-positive human breast cancer cells (MCF-7) than in folate-negative cells [26]. The recent decade has also shown increased interest in encapsulation of metal nanoparticles inside liposomes such as L-α-phosphatidylcholine /cholesterol-based liposomes or DPPC-based liposomes [27,28]. However, the knowledge of the ligand-dependent targeting of AgNPs entrapped in liposomes toward EGFR is still insufficient. Our previous work showed that enclosure of AgNPs inside the liposome labeled with the EGF protein allows targeting the toxicity of the AgNP surface toward EGFR-overexpressing cancer cells, which was proved by the lactate dehydrogenase (LDH) release assay and KI67 protein expression [17]. Our

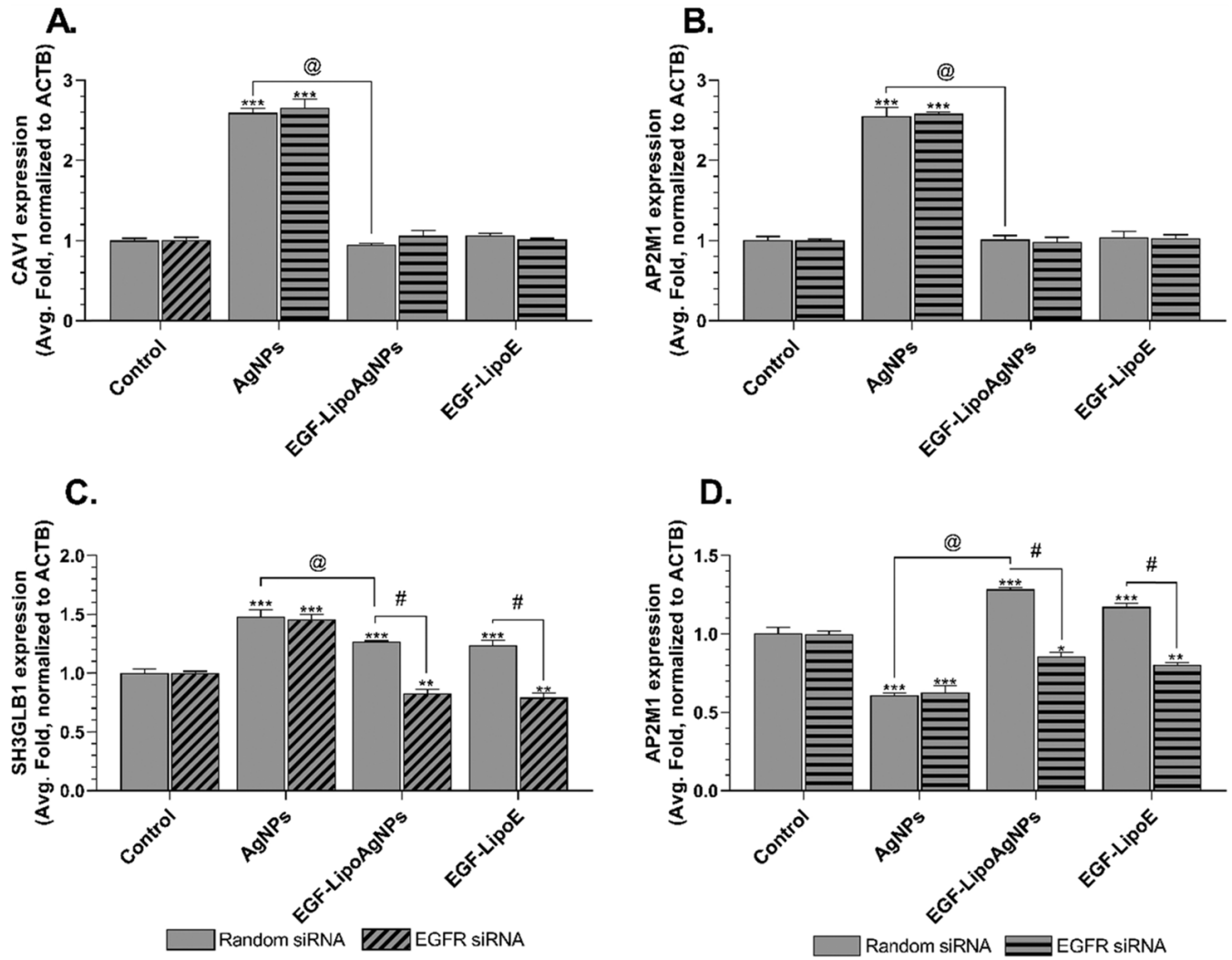

Fig. 7. Expression of *CAV1* (A-B) and *SH3GLB1* (C-D) in the A549 cells transfected with Random siRNA and EGFR siRNA after the 6-h (A, C) and 24 h (B, D) treatment with AgNPs, EGF-LipoAgNPs, and EGF-LipoE. The means ± SD (error bars) with * , ** , and *** are statistically different from the respective control at $p < 0.05$, $p < 0.01$, and $p < 0.001$, respectively (one-way ANOVA, Tukey's test). # and @ mean statistically significant differences ($p < 0.05$) between certain groups (*t*-test).

present results showed higher uptake of EGF-LipoAgNPs in the $EGFR^+$ lung and tongue cancer cells, which was proved by confocal microscopy. Moreover, the EGFR-negative cells were characterized by few times weaker fluorescence of the EGF-LipoAgNPs present inside the cells. These results also showed indirectly the EGFR-dependent internalization of the tested liposomes in the EGFR-overexpressing cancer cells. This conclusion covers the results of the previous work, in which the indirect engagement of EGFR was shown by pretreatment of the cells with pure EGF and subsequent exposure to the tested liposomes [17].

As described by Zhang et al., the sonic hedgehog (*SHH*) gene encodes a protein engaged in the regulation of oxidative stress and antiapoptotic cell response [29]. As described many times, AgNPs are a strong prooxidative factor in the cell, showing the ability to induce oxidative stress and increase the activity of antioxidant enzymes, such as superoxide dismutase and catalase [30]. Both these proteins are activated by the presence of ROS in the cell; moreover, as described by Chen et al., SHH can be activated through ROS stimulation [31]. In turn, our previous work showed that EGF-LipoAgNPs induced ROS more efficiently than AgNPs in A549 and SCC-15 cells, while pretreated cells did not show such an effect [17]. Our previous findings and the results obtained in this work show that the tested liposomes were able to increase the *SHH* gene expression in the A549 and SCC-15 EGFR-positive cells after 24 h of treatment, while this effect was not observed in the $EGFR^-$ cells. Furthermore, the mRNA expression was not increased after the 6-h treatment, which mainly proves the increased prooxidative features of the AgNPs entrapped in the obtained liposomes and the delayed uptake of EGF-LipoAgNPs in comparison with native AgNPs.

In turn, Liu et al. have shown that the ataxia-telangiectasia mutated kinase (*ATM*) gene is strictly related to the antioxidant defense system and engaged in the DNA fragmentation response in the cell, preventing apoptosis [32]. As described by Lim et al., AgNPs are able to increase the *ATM* gene expression by 2.2-fold of the control, proving the engagement of these NPs in DNA damage [33]. Our results showed a similar increase in the *ATM* gene expression just after the 6-h treatment of AgNPs, which was also increased after 24 h in the tested cell lines. Additionally, we have proved that AgNPs delivered into the cell by the EGF-LipoAgNPs carrier increase the mRNA expression of the gene only after 24 h. Moreover, this effect was not observed in the EGFR siRNA-treated cells, which proves the engagement of this receptor in the uptake and induction of oxidative stress in both tested cell lines. Interestingly, higher *ATM* expression was observed in the SCC-15 cells than in the A549 cells, which is probably correlated with the higher *EGFR* expression and is convergent with the results of the EGFR status presented by Rusnak et al. [34]. The above-mentioned results also showed slower release and

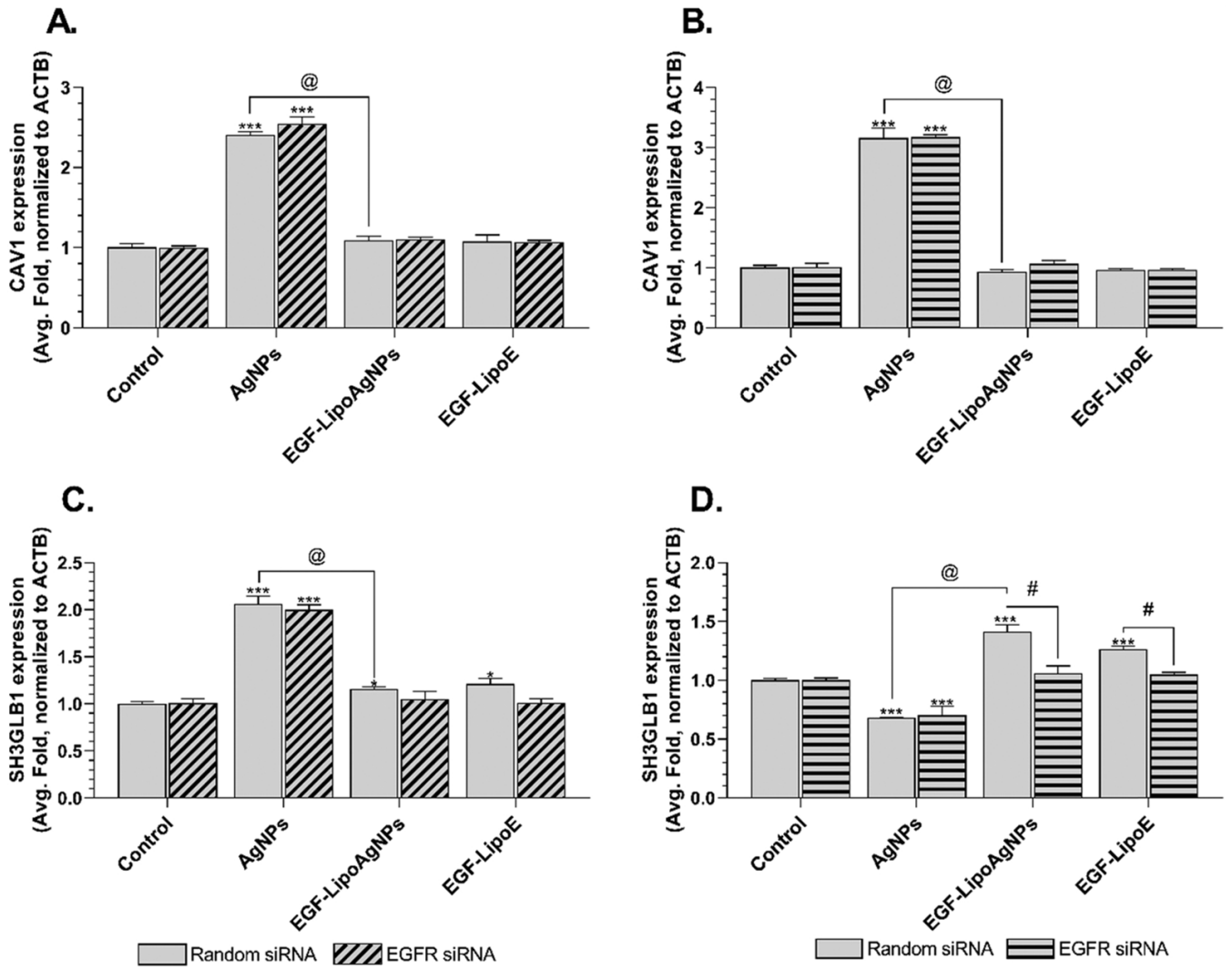

Fig. 8. Expression of *CAV1* (A-B) and *SH3GLB1* (C-D) in the SCC-15 cells transfected with Random siRNA and EGFR siRNA after the 6-h (A, C) and 24 h (B, D) treatment with AgNPs, EGF-LipoAgNPs, and EGF-LipoE. The means ± SD (error bars) with * , ** , and *** are statistically different from the respective control at $p < 0.05$, $p < 0.01$, and $p < 0.001$, respectively (one-way ANOVA, Tukey's test). # and @ mean statistically significant differences ($p < 0.05$) between certain groups (*t*-test).

delayed action of AgNPs delivered as EGF-LipoAgNPs liposomes than native AgNPs, which were able to affect the *ATM* expression just after the 6-h treatment.

On the other hand, the Nuclear Factor Erythroid 2-Like 2 (*NFE2L2* or *NFR2*) gene encodes a protein which is a transcription factor affecting the expression of genes responsible for oxidative stress (antioxidant response element) and inflammation prevention in mammalian cells [35]. Kasai et al. [37] proved that *NRF2* gene activation is strict depend on ROS level in the cell, which was also confirmed by Mao et al. [36]. Furthermore, Yamadori et al. revealed that the *NFR2* gene expression was also regulated by EGFR in non-small cell lung cancer cells [38]. In contrast, Sun et al. showed that AgNPs can directly interrupt the *NRF2*-dependent antioxidant mechanism in vascular endothelial cells, resulting in redox imbalance [39]. Our results showed a similar tendency, namely a decrease in the *NRF2* gene expression in both $EGFR^+$ and $EGFR^-$ cells after 6 h and 24 h of treatment with AgNPs. Additionally, after 24 h, EGF-LipoAgNPs were able to decrease the mRNA expression, which indicated that the release of AgNPs from liposomes was probably slower and correlated with EGFR, as evidenced by the weaker *NRF2* expression in the $EGFR^-$ cells. Our previous work also showed increased antioxidant enzyme activity after the exposure to EGF-LipoAgNPs than in AgNPs-treated cells, which also proves that these NPs delivered in the obtained carrier induce oxidative stress more efficiently than AgNPs through the EGFR-dependent uptake.

As described above, the confocal microscopy analysis showed that EGF-LipoAgNPs were uptaken via the EGFR-dependent pathway [17]. However, as described by Andar et al. and Ichikawa et al., depending on their size, liposomes can be uptaken through a clathrin-dependent or clathrin-independent pathway [10,11]. Moreover, Kang et al. showed that all the three neutral, anionic, and cationic liposomes are uptaken via endocytosis not pinocytosis [8]. Among others, the Clathrin Heavy Chain (*CLTC*) gene is the main indicator of the clathrin-mediated endocytosis due to its major role in the formation of clathrin-coated intracellular vehicles [40]. However, as described by Blixt and Royle (2011), the adaptor protein complex 2 (*AP2M1*) gene encodes a protein playing a crucial role in the regulation of clathrin-mediated endocytosis via its high affinity to the cell membrane and in the recruitment of clathrin chains for formation of pits and vehicles [40]. Our results showed that, in contrast to the AgNPs-treated cells, EGF-LipoAgNPs increased the *CLTC* gene expression both after 6 h and 24 h of treatment in the $A549^{EGFR+}$ and $SCC\text{-}15^{EGFR-}$ cells. In contrast, the EGFR siRNA-treated cells exhibited no changes or decrease in this mRNA expression, indicating the major role of EGFR in the uptake of such complexes. Moreover, this proved the clathrin-dependent pathways of

endocytosis. Interestingly, the expression of the *CLTC* gene was increased just after 6 h, while the *ATM*, *SHH*, and *NRF2* gene expression was not changed, which shows that EGF-LipoAgNPs are uptaken during the first 6 h of treatment. However, the release of entrapped AgNPs takes longer, thus the impact of released AgNPs on the *ATM, SHH*, and *NRF2* genes is detectable only after 24 h. Moreover, no increase in the expression of these genes was recorded in the EGF-LipoE-treated cells. It is worth noticing that, after the transfection with the EGFR siRNA, the *CLTC* gene expression decreased, especially after 24 h. In turn, Huang et al. showed the decrease in the CLTC protein expression caused inhibition of the EGFR internalization by the cell [41]. Similarly, Delos Santos et al. proved the engagement of this receptor in the formation of clathrin-coated pits, showing the selective regulation of clathrin-dependent endocytosis by EGFR [42]. As described above, the *AP2M1* gene, encoding the AP-2 protein, plays a major role in the regulation of clathrin-mediated endocytosis. As shown by the results, the *AP-2* gene expression was increased in the EGF-LipoAgNPs and EGF-LipoE liposomes after both 6 h and 24 h of treatment in the $EGFR^+$ cells. This effect was not observed after the transfection, where this mRNA expression was decreased, indicating the engagement of the AP-2-dependent pathway in such liposomes uptaken by the A549 and SCC-15 cells.

As described by de Almeida, the *CAV1* gene, encoding the caveolin 1 protein, is one of the crucial factors in caveolin-mediated endocytosis, allowing creation of vehicles and internalization [43]. Our results showed an increase in this mRNA expression in the AgNPs-treated $EGFR^+$ and $EGFR^-$ cells. The tested liposomes did not affect the *CAV1* gene expression. Moreover, the endophilin protein, encoded by the *SH3GLB1* gene, is engaged in caveolin-dependent uptake and clathrin-mediated endocytosis [44]. Our results showed an increase in the expression of this gene in all the compound-treated cells. However, after 24 h of treatment with AgNPs, the cells exhibited a decrease in the *CAV1* gene expression. In the case of the liposome-treated cells, the increase in this mRNA expression was observed in the $EGFR^+$ cells. This suggests that AgNPs used in this study were uptaken via the caveolin-mediated pathway. Similar conclusions were formulated by Wu et al., who showed that the mode or the uptake differs depending on the size of NPs, although the engagement of caveolin was prevalent in mouse melanoma B-16 cells *in vitro* [45]. As reported by Miethling-Graff et al. (2014), AgNPs were able to upregulate caveolin-dependent genes, such as *SH3GLB1* [46]. Taking the above into account, it can be assumed that the synthesized liposomal vehicles for AgNPs delivery are uptaken by A549 and SCC-15 cells based on the clathrin-mediated endocytosis pathway with engagement of the AP-2 complex but also with some role of the endophilin-A2 isoform 1 (*SH3GLB1*). Moreover, it can be concluded that, since there was no effect of the empty liposomes on the expression of the *SHH, ATM* and *NRF2* genes, the prooxidative and toxic effect was caused by AgNPs delivered by the EGF-Lipo carriers more effectively than native AgNPs.

5. Conclusions

This study is the first to show that AgNPs entrapped in liposomes labeled with EGF (EGF-LipoAgNPs) are uptaken via an EGFR-dependent pathway, which was proved with the use of the EGFR siRNA knock-out method showing increased amounts of the liposomes in the cytoplasm in the $EGFR^+$ cells in comparison to the $EGFR^-$ cells. Our experiments also show that AgNPs delivered in the EGF-LipoAgNPs carriers caused a higher prooxidative and toxic effect (reflected by the expression of the *ATM* and *SHH* genes) than native AgNPs. The investigations also revealed that the obtained liposomes were uptaken via clathrin-mediated endocytosis with engagement of the AP-2 complex and SH3GLB1. Summarizing, the liposomal encapsulation and targeting AgNPs toward EGFR with the use of EGF may be an efficient way to increase the toxicity effect of such NPs. This issue needs to be further studied to evaluate every aspect of such an approach as a potential anticancer treatment also *in-vivo* experiments.

Funding source

This work was supported by statuary funds from the University of Information Technology and Management in Rzeszow, Poland (DS: 503–07–01–27 and DS: 503–07–01–31).

CRediT authorship contribution statement

Bartosz Skóra - Conceptualization; Data curation; Formal analysis; Funding acquisition; Investigation; Methodology; Visualization; Roles/Writing - original draft; Writing - review & editing.Konrad A. Szychowski – Supervision; Roles/Writing - original draft; Writing - review & editing.

Declaration of Competing Interest

The authors declare that they have no known competing financial interests or personal relationships that could have appeared to influence the work reported in this paper.

Data Availability

Data will be made available on request.

References

[1] I. Vhora, N. Khatri, J. Desai, H.P. Thakkar, Caprylate-conjugated cisplatin for the development of novel liposomal formulation, AAPS PharmSciTech (2014), https://doi.org/10.1208/s12249-014-0106-y.
[2] R. Sabaté, R. Barnadas-Rodríguez, J. Callejas-Fernández, R. Hidalgo-Álvarez, J. Estelrich, Preparation and characterization of extruded magnetoliposomes, Int. J. Pharm. (2008), https://doi.org/10.1016/j.ijpharm.2007.06.047.
[3] B. Skóra, K.A. Szychowski, J. Gmiński, A concise review of metallic nanoparticles encapsulation methods and their potential use in anticancer therapy and medicine, Eur, J. Pharm. Biopharm. 154C (2020) 153–165, https://doi.org/10.1016/j.ejpb.2020.07.002.
[4] M. Daeihamed, S. Dadashzadeh, A. Haeri, M. Akhlaghi, Potential of liposomes for enhancement of oral drug absorption, Curr. Drug Deliv. 13 (2016), https://doi.org/10.2174/1567201813666160115125756.
[5] J.J. Rennick, A.P.R. Johnston, R.G. Parton, Key principles and methods for studying the endocytosis of biological and nanoparticle therapeutics, Nat. Nanotechnol. 16 (2021), https://doi.org/10.1038/s41565-021-00858-8.
[6] G. Sahay, D.Y. Alakhova, A.V. Kabanov, Endocytosis of nanomedicines, J. Control. Release. 145 (2010), https://doi.org/10.1016/j.jconrel.2010.01.036.
[7] K. Cui, Y. Dong, B. Wang, D.B. Cowan, S.-L. Chan, J. Shyy, H. Chen, Endocytic adaptors in cardiovascular disease, Front. Cell Dev. Biol. 8 (2020), https://doi.org/10.3389/fcell.2020.624159.
[8] J.H. Kang, W.Y. Jang, Y.T. Ko, The effect of surface charges on the cellular uptake of liposomes investigated by live cell imaging, Pharm. Res. 34 (2017), https://doi.org/10.1007/s11095-017-2097-3.
[9] M. Takikawa, M. Fujisawa, K. Yoshino, S. Takeoka, Intracellular distribution of lipids and encapsulated model drugs from cationic liposomes with different uptake pathways, Int. J. Nanomed. Volume 15 (2020), https://doi.org/10.2147/IJN.S267638.
[10] S. Ichikawa, N. Shimokawa, M. Takagi, Y. Kitayama, T. Takeuchi, Size-dependent uptake of electrically neutral amphipathic polymeric nanoparticles by cell-sized liposomes and an insight into their internalization mechanism in living cells, Chem. Commun. 54 (2018) 4557–4560, https://doi.org/10.1039/C8CC00977E.
[11] A.U. Andar, R.R. Hood, W.N. Vreeland, D.L. Devoe, P.W. Swaan, Microfluidic preparation of liposomes to determine particle size influence on cellular uptake mechanisms, Pharm. Res. (2014), https://doi.org/10.1007/s11095-013-1171-8.
[12] A. Alshehri, A. Grabowska, S. Stolnik, Pathways of cellular internalisation of liposomes delivered siRNA and effects on siRNA engagement with target mRNA and silencing in cancer cells, Sci. Rep. 8 (2018), https://doi.org/10.1038/s41598-018-22166-3.
[13] S. Kim, D.Y. Ryu, Silver nanoparticle-induced oxidative stress, genotoxicity and apoptosis in cultured cells and animal tissues, J. Appl. Toxicol. (2013), https://doi.org/10.1002/jat.2792.
[14] A. Yusuf, A. Casey, Evaluation of silver nanoparticle encapsulation in DPPC-based liposome by different methods for enhanced cytotoxicity, Int. J. Polym. Mater. Polym. Biomater. (2019), https://doi.org/10.1080/00914037.2019.1626390.
[15] B.E. Wildt, A. Celedon, E.I. Maurer, B.J. Casey, A.M. Nagy, S.M. Hussain, P. L. Goering, Intracellular accumulation and dissolution of silver nanoparticles in L-929 fibroblast cells using live cell time-lapse microscopy, Nanotoxicology 10 (2016), https://doi.org/10.3109/17435390.2015.1113321.

[16] B. Şahin, E. Demir, A. Aygün, H. Gündüz, F. Şen, Investigation of the effect of pomegranate extract and monodisperse silver nanoparticle combination on MCF-7 cell line, J. Biotechnol. 260 (2017), https://doi.org/10.1016/j.jbiotec.2017.09.012.
[17] B. Skóra, T. Piechowiak, K.A. Szychowski, Epidermal Growth Factor-labeled liposomes as a way to target the toxicity of silver nanoparticles into EGFR-overexpressing cancer cells in vitro, Toxicol. Appl. Pharmacol. 443 (2022), 116009, https://doi.org/10.1016/j.taap.2022.116009.
[18] K.A. Szychowski, A. Wnuk, J. Rzemieniec, M. Kajta, T. Leszczyńska, A. K. Wójtowicz, Triclosan-evoked neurotoxicity involves NMDAR subunits with the specific role of GluN2A in caspase-3-dependent apoptosis, Mol. Neurobiol. 56 (2019) 1–12, https://doi.org/10.1007/s12035-018-1083-z.
[19] K.A. Szychowski, B. Skóra, M. Mańdziuk, Tris (2,3-Dibromopropyl) isocyanurate (TDBP-TAZTO or TBC) shows different toxicity depending on the degree of differentiation of the human neuroblastoma (SH-SY5Y) cell line, Neurotox. Res. 39 (2021), https://doi.org/10.1007/s12640-021-00399-x.
[20] M. Bin-Jumah, M. AL-Abdan, G. Albasher, S. Alarifi, Effects of green silver nanoparticles on apoptosis and oxidative stress in normal and cancerous human hepatic cells in vitro, Int. J. Nanomed. Volume 15 (2020) 1537–1548, https://doi.org/10.2147/IJN.S239861.
[21] J. Tang, X. Lu, B. Chen, E. Cai, W. Liu, J. Jiang, F. Chen, X. Shan, H. Zhang, Mechanisms of silver nanoparticles-induced cytotoxicity and apoptosis in rat tracheal epithelial cells, J. Toxicol. Sci. 44 (2019) 155–165, https://doi.org/10.2131/jts.44.155.
[22] P. Sanpui, A. Chattopadhyay, S.S. Ghosh, Induction of apoptosis in cancer cells at low silver nanoparticle concentrations using chitosan nanocarrier, ACS Appl. Mater. Interfaces. (2011), https://doi.org/10.1021/am100840c.
[23] M. Bin-Jumah, M. AL-Abdan, G. Albasher, S. Alarifi, Effects of green silver nanoparticles on apoptosis and oxidative stress in normal and cancerous human hepatic cells in vitro, Int. J. Nanomed. Volume 15 (2020), https://doi.org/10.2147/IJN.S239861.
[24] S. Kim, D.-Y. Ryu, Silver nanoparticle-induced oxidative stress, genotoxicity and apoptosis in cultured cells and animal tissues, J. Appl. Toxicol. 33 (2013), https://doi.org/10.1002/jat.2792.
[25] S. Montalvo-Quiros, G. Aragoneses-Cazorla, L. Garcia-Alcalde, M. Vallet-Regí, B. González, J.L. Luque-Garcia, Cancer cell targeting and therapeutic delivery of silver nanoparticles by mesoporous silica nanocarriers: insights into the action mechanisms using quantitative proteomics, Nanoscale 11 (2019), https://doi.org/10.1039/C8NR07667G.
[26] R.K. Thapa, J.H. Kim, J.-H. Jeong, B.S. Shin, H.-G. Choi, C.S. Yong, J.O. Kim, Silver nanoparticle-embedded graphene oxide-methotrexate for targeted cancer treatment, Colloids Surfaces B Biointerfaces 153 (2017), https://doi.org/10.1016/j.colsurfb.2017.02.012.
[27] B. Skóra, T. Piechowiak, K.A. Szychowski, J. Gmiński, Entrapment of silver nanoparticles in L-α-phosphatidylcholine/cholesterol-based liposomes mitigates the oxidative stress in human keratinocyte (HaCaT) cells, Eur. J. Pharm. Biopharm. 166 (2021), https://doi.org/10.1016/j.ejpb.2021.06.006.
[28] A. Yusuf, A. Brophy, B. Gorey, A. Casey, Liposomal encapsulation of silver nanoparticles enhances cytotoxicity and causes induction of reactive oxygen species-independent apoptosis, J. Appl. Toxicol. 38 (2018), https://doi.org/10.1002/jat.3566.
[29] R. Zhang, Z. Qiao, H. Liu, J. Ma, Sonic hedgehog signaling regulates hypoxia/reoxygenation-induced H9C2 myocardial cell apoptosis, Exp. Ther. Med. (2018), https://doi.org/10.3892/etm.2018.6678.
[30] J. Blanco, S. Tomás-Hernández, T. García, M. Mulero, M. Gómez, J.L. Domingo, D. J. Sánchez, Oral exposure to silver nanoparticles increases oxidative stress markers in the liver of male rats and deregulates the insulin signalling pathway and p53 and cleaved caspase 3 protein expression, Food Chem. Toxicol. 115 (2018), https://doi.org/10.1016/j.fct.2018.03.039.
[31] K.-Y. Chen, C.-H. Chiu, L.-C. Wang, Anti-apoptotic effects of Sonic hedgehog signalling through oxidative stress reduction in astrocytes co-cultured with excretory-secretory products of larval Angiostrongylus cantonensis, Sci. Rep. 7 (2017), https://doi.org/10.1038/srep41574.
[32] N. Liu, G. Stoica, M. Yan, V.L. Scofield, W. Qiang, W.S. Lynn, P.K.Y. Wong, ATM deficiency induces oxidative stress and endoplasmic reticulum stress in astrocytes, Lab. Investig. 85 (2005), https://doi.org/10.1038/labinvest.3700354.
[33] H.K. Lim, P.V. Asharani, M.P. Hande, Enhanced genotoxicity of silver nanoparticles in DNA repair deficient mammalian cells, Front. Genet. 3 (2012), https://doi.org/10.3389/fgene.2012.00104.
[34] D.W. Rusnak, K.J. Alligood, R.J. Mullin, G.M. Spehar, C. Arenas-Elliott, A.-M. Martin, Y. Degenhardt, S.K. Rudolph, T.F. Haws Jr, B.L. Hudson-Curtis, T. M. Gilmer, Assessment of epidermal growth factor receptor (EGFR, ErbB1) and HER2 (ErbB2) protein expression levels and response to lapatinib (Tykerb, GW572016) in an expanded panel of human normal and tumour cell lines, Cell Prolif 40 (2007), https://doi.org/10.1111/j.1365-2184.2007.00455.x.
[35] K.T. Bogen, Low-dose dose–response for in vitro Nrf2-ARE activation in human HepG2 cells, Dose-Response 15 (2017), https://doi.org/10.1177/1559325817699696.
[36] B.-H. Mao, Z.-Y. Chen, Y.-J. Wang, S.-J. Yan, Silver nanoparticles have lethal and sublethal adverse effects on development and longevity by inducing ROS-mediated stress responses, Sci. Rep. 8 (2018), https://doi.org/10.1038/s41598-018-20728-z.
[37] S. Kasai, S. Shimizu, Y. Tatara, J. Mimura, K. Itoh, Regulation of Nrf2 by mitochondrial reactive oxygen species in physiology and pathology, Biomolecules 10 (2020), https://doi.org/10.3390/biom10020320.
[38] T. Yamadori, Y. Ishii, S. Homma, Y. Morishima, K. Kurishima, K. Itoh, M. Yamamoto, Y. Minami, M. Noguchi, N. Hizawa, Molecular mechanisms for the regulation of Nrf2-mediated cell proliferation in non-small-cell lung cancers, Oncogene 31 (2012), https://doi.org/10.1038/onc.2011.628.
[39] X. Sun, Y. Yang, J. Shi, C. Wang, Z. Yu, H. Zhang, NOX4- and Nrf2-mediated oxidative stress induced by silver nanoparticles in vascular endothelial cells, J. Appl. Toxicol. 37 (2017), https://doi.org/10.1002/jat.3511.
[40] M.K.E. Blixt, S.J. Royle, Clathrin heavy chain gene fusions expressed in human cancers: analysis of cellular functions, Traffic. 12 (2011), https://doi.org/10.1111/j.1600-0854.2011.01183.x.
[41] F. Huang, A. Khvorova, W. Marshall, A. Sorkin, Analysis of clathrin-mediated endocytosis of epidermal growth factor receptor by RNA interference, J. Biol. Chem. 279 (2004) 16657–16661, https://doi.org/10.1074/jbc.C400046200.
[42] R.C. Delos Santos, S. Bautista, S. Lucarelli, L.N. Bone, R.M. Dayam, J. Abousawan, R.J. Botelho, C.N. Antonescu, Selective regulation of clathrin-mediated epidermal growth factor receptor signaling and endocytosis by phospholipase C and calcium, Mol. Biol. Cell. 28 (2017) 2802–2818, https://doi.org/10.1091/mbc.e16-12-0871.
[43] C.J.G. de Almeida, Caveolin-1 and Caveolin-2 can be antagonistic partners in inflammation and beyond, Front. Immunol. 8 (2017), https://doi.org/10.3389/fimmu.2017.01530.
[44] A. Casamento, E. Boucrot, Molecular mechanism of fast endophilin-mediated endocytosis, Biochem. J. 477 (2020) 2327–2345, https://doi.org/10.1042/BCJ20190342.
[45] M. Wu, H. Guo, L. Liu, Y. Liu, L. Xie, Size-dependent cellular uptake and localization profiles of silver nanoparticles, Int. J. Nanomed. Volume 14 (2019) 4247–4259, https://doi.org/10.2147/IJN.S201107.
[46] R. Miethling-Graff, R. Rumpker, M. Richter, T. Verano-Braga, F. Kjeldsen, J. Brewer, J. Hoyland, H.-G. Rubahn, H. Erdmann, Exposure to silver nanoparticles induces size- and dose-dependent oxidative stress and cytotoxicity in human colon carcinoma cells, Toxicol. Vitr. 28 (2014) 1280–1289, https://doi.org/10.1016/j.tiv.2014.06.005.

4. Podsumowanie i wnioski

4.1. Wprowadzenie i uzasadnienie wyboru tematu

Nanocząstki srebra (ang. *silver nanoparticles*, AgNPs) są strukturami, których jeden z wymiarów zawiera się w zakresie 1 – 100 nm (1). Nanorozmiary determinują ich unikatowe właściwości fizykochemiczne, manifestowane m.in. przez zwiększający się stosunek powierzchni do średnicy w miarę zmniejszania wielkości nanocząstki (2). Wpływają również bezpośrednio na pro-oksydacyjny charakter AgNPs w układach biologicznych (3,4). Wielokrotnie wykazano silne działanie antybakteryjne AgNPs w stosunku do szczepów pochodzenia środowiskowego, a także ich zdolność do degradacji biofilmu bakterii patogennych (5,6). Wpływ AgNPs na komórki ssacze został również dobrze poznany i opisany w literaturze, zarówno w warunkach *in vitro* oraz *in vivo* - w modelach zwierzęcych (7,8). Mechanizm działania cytotoksycznego AgNPs jest ściśle związany z ich właściwościami pro-oksydacyjnymi, wynikającymi bezpośrednio z ich właściwości utleniających (donory elektronów) (9). W następstwie czego, dochodzi do szeregu reakcji wewnątrzkomórkowych, których końcowym efektem jest produkcja znacznych ilości reaktywnych form tlenu (ang. *reactive oxygen species*, ROS) (10). Obserwowany jest również wtórny efekt działania AgNPs w komórce tj. oksydacyjne zniszczenie składników błon biologicznych, powodujących lizę komórki (11). Zjawisko to zaobserwowano m.in. w komórkach śródbłonka naczyń krwionośnych (ang. *human umbilical vein endothelial cells*, HUVECs) oraz pierwotnych ludzkich fibroblastach *in vitro* (12,13). Potencjał AgNPs do indukcji wewnątrzkomórkowego stresu oksydacyjnego jest związany również ze zdolnością tych nanostruktur do bezpośredniego oddziaływania z określonymi enzymami cytoplazmatycznymi oraz mitochondrialnymi. Konsekwencją czego jest uwalnianie jonów srebra (Ag^+), powodujących zaburzenie równowagi redoks w komórce, ostateczne prowadząc do jej śmierci na drodze apoptotycznej, rzadziej nekrotycznej (14,15). Zaobserwowano bezpośredni wpływ AgNPs na depolaryzację błony mitochondrialnej, uwolnienie cząsteczki cytochromu c, a w następstwie indukcję apoptozy z zaangażowaniem aktywności kaspazy-9 (16). Wspomniane zjawisko zostało opisane już dla stężeń ppm (ang. *parts per milion*) m.in. przez Banerjee i in. – dla komórek nowotworu piersi (MCF-7 i MDA-MB-231) - 156 ppm oraz Zielińską i in. – w komórkach nowotworu trzustki (PANC-1) - 50 ppm (17,18). Działające cytotoksycznie, stosunkowo niskie stężenia AgNPs w komórkach zmienionych nowotworowo uzasadniają potencjalne zastosowanie tych nanostruktur jako czynników

leczniczych w terapii przeciwnowotworowej. Dodatkowo, udowodniono zdolność AgNPs do przezwyciężania fenotypu oporności wielolekowej (ang. *multidrug ressistence*, MDR) w komórkach nowotworowych. Zjawisko to jest związane ze zdolnością AgNPs do hamowania działania kompleksu transporterów ABC (ang. *ATP-binding cassette transporter*), a w konsekwencji powodując zmniejszenie proliferacji oraz indukcję apoptozy w komórkach nowotworowych (19,20). Jednak, ze względu na właściwości pro-oksydacyjne i cytotoksyczne AgNPs w komórkach prawidłowych, jak i zmienionych nowotworowo (brak specyficzności działania), możliwość wykorzystania AgNPs, jako potencjalnego czynnika leczniczego w terapii przeciwnowotworowej jest ograniczone.

W ostatnich dziesięcioleciach opracowano metody enkapsulacji/pułapkowania (ang. *encapsulation*) pozwalające na dostarczanie leków, substancji aktywnych oraz nanocząstek (ang. *nanoparticles,* NPs) metalicznych w sposób kontrolowany i bezpieczny dla komórek zdrowych (21). Wyróżnić można trzy główne typy enkapsulacji, znajdujących zastosowanie dla metalicznych NPs (przedstawione w pracy przeglądowej Skóra i in.) (21). Spośród nich - najczęściej badaną w kontekście wykorzystania w medycynie jest enkapsulacja liposomalna (ang. *liposomal encapsulation*) (21,22). Podejście zakładające całkowite umieszczenie NPs wewnątrz liposomu pozwala na ograniczenie bezpośredniego kontaktu komórek niecelowanych z danym czynnikiem leczniczym (23). Enkapsulacja liposomalna metalicznych NPs stanowi obecnie nowe podejście w poszukiwaniu zastosowania tego typu nanostruktur w medycynie. Ze względu na swoje wysokie właściwości cytotoksyczne oraz efektywne działanie w komórkach MDR, enkapsulacja AgNPs pozwala - przede wszystkim - na ograniczenie kontaktu reaktywnej powierzchni AgNPs z komórkami zdrowymi, niebędącymi celem terapii (21). Jednak, zamknięcie AgNPs wewnątrz liposomu nie pozwala na ukierunkowanie właściwości cytoksycznych, zwiększa natomiast możliwości modyfikacji powierzchni tych nanostruktur (24). Koniecznym staje się zatem rozszerzenie procedury enkapsulacji o etap koniugacji powierzchni liposomu z ligandem – zapewniającym dostarczenie kompleksu liposom-nanocząsteczka do komórek zmienionych nowotworowo z zaangażowaniem określonego receptora (21,25).

Receptor nabłonkowego czynnika wzrostu (ang. *epidermal growth factor receptor,* EGFR) występuje w wielu typach komórek ssaków (26). Nadekspresja tego receptora jest cechą charakterystyczną dla komórek nowotworów głowy i szyi, nerek, czy nie drobnokomórkowego raka płuc (ang. *non-small cell lung cancer,* NSCLC) (27,28). Jednym z ligandów receptora EGFR jest nabłonkowy czynnik wzrostu (ang. e*pidermal growth factor,*

EGF), dla którego udowodniono zdolność do indukcji endocytozy receptora EGFR oraz jego degradację na drodze zależnej od lizosomu (29,30). Sugeruje to użyteczność receptora EGFR w badaniach nad ukierunkowaniem toksyczności AgNPs do komórek nowotworowych. Wykazano bowiem wysoką skuteczność dostarczania oksaliplatyny do komórek nowotworu jelita grubego (HCT 116 oraz RKO) *in vitro* za pomocą receptora EGFR, a także cząsteczki siRNA – jako czynnika leczniczego w nowotworze jajnika (HEY A8) (31,32). Jednak, do tej pory nie podjęto próby ukierunkowania działania AgNPs do komórek nowotworowych za pomocą receptora EGFR. Co więcej, brak jest danych literaturowych dotyczących wykorzystania enkapsulacji liposomalnej oraz koniugacji z białkiem EGF, jako platformy pozwalającej na dostarczenie AgNPs bezpośrednio do komórek zmienionych nowotworowo. Opisany problem badawczy jest kluczowy, biorąc pod uwagę rosnącą ilość przypadków nowotworów z fenotypem MDR. Istotny w tej kwestii jest również brak możliwości przystosowania się komórki nowotworowej do działania AgNPs po pobraniu. Wynika to z ich metalicznego charakteru oraz utrudnionej egzocytozy, co jest bezpośrednio związane z niewielkimi rozmiarami tych nanostruktur.

Dlatego, celem głównym rozprawy doktorskiej było opracowanie selektywnego sposobu ukierunkowania toksyczności AgNPs za pomocą enkapsulacji liposomalnej oraz czynnika EGF do komórek nowotworowych z nadekspresją receptora EGFR w warunkach *in vitro*.

Cele szczegółowe rozprawy doktorskiej obejmowały:

- Opracowanie sposobu syntezy AgNPs zamkniętych wewnątrz liposomu oraz znakowanie ich powierzchni za pomocą EGF wraz z charakterystyką fizykochemiczną uzyskanej platformy dostarczania AgNPs.

- Ocenę skuteczności ukierunkowanej indukcji efektu toksycznego wytworzonych liposomów w modelach komórkowych, charakteryzujących się różną ekspresją receptora EGFR *in vitro*.

- Określenie molekularnego mechanizmu pobierania oraz toksyczności wytworzonych liposomów w komórkach nowotworowych z nadekspresją receptora EGFR *in vitro*.

4.2. Omówienie publikacji stanowiących cykl

Publikacja 1: B. Skóra, K. A. Szychowski, J. Gmiński, *A concise review of metallic nanoparticles encapsulation methods and their potential use in anticancer therapy and medicine*, European Journal of Pharmaceutics and Biopharmaceutics, 2020; 154, 153-165.

Ze względu na – opisane powyżej – niespecyficzne działanie metalicznych NPs – ich zastosowanie, jako czynników potencjalnie leczniczych jest ograniczone (21,33). Pomimo tego, wykazują one obiecujące właściwości biologiczne – pożądane z punktu widzenia terapii przeciwnowotworowej, jak choćby zdolność do indukcji stresu oksydacyjnego, czy uszkadzania DNA (34,35). Z tego względu w ostatnich latach obserwowany jest wzrost zainteresowania metodami enkapsulacji metalicznych NPs (36,37). Zastosowanie poszczególnych typów enkapsulacji jest ściśle związane z przyszła aplikacją tych nanostruktur. Wynika to bezpośrednio z właściwości fizykochemicznych uzyskanych kompleksów takich jak: wielkość, stabilność, możliwość sterylizacji, czy efektywność pokrycia powierzchni NPs (21). Poszczególne metody enkapsulacji charakteryzują się różnym stopnie złożoności syntezy, wynikających z zastosowanych substratów, cząsteczek kierunkujących, czy pochodzenia pierwiastkowego metalicznych NPs (38). Wiedza dotyczącą potencjalnego wykorzystania metod enkapsulacji tych nanostruktur w medycynie jest ciągle poszerzana, natomiast ich klasyfikacja nie została dotychczas przeprowadzona.

Celem pierwszej publikacji była analiza danych literaturowych dotyczących obecnie dostępnych metod enkapsulacji metalicznych NPs oraz ich wykorzystania jako platform specyficznego dostarczania tego typu nanostruktur do komórek nowotworowych z pominięciem komórek zdrowych.

Pierwszym etapem pracy była ocena wykorzystania enkapsulacji z wykorzystaniem liposomów. Tego typu podejście zakłada wykorzystanie właściwości amfifilowych fosfolipidów, które ze względu na budowę chemiczną (występowanie części hydrofilowej i części hydrofobowej), są zdolne do tworzenia dwuwarstwy w środowisku wodnym. Zasadniczo, najczęściej wykorzystywanym substratem podczas syntezy są pochodne choliny np. 1,2-dimirystylo-sn-glicero-3-fosfocholina (ang. *1,2-dimyristoyl-sn-glycero-3-phosphocholine,* DMPC), czy 1,2-dipalmitylo-sn-glicero-3-fosfocholina (ang. *1,2-dipalmitoilo-sn-glicero-3-fosfocholine,* DPPC). Sterole – najczęściej cholesterol – stabilizują

dwuwarstwę fosfolipidową, natomiast dodatkowe składniki np. glikol polietylenowy (ang. *polyethylene glycol*, PEG) wykorzystywane są w trakcie syntezy jako cząsteczki mające na celu zmniejszenie immunogenności wytworzonych kompleksów. Przeprowadzona analiza dostępnych danych literaturowych pozwala stwierdzić, że obecnie wyróżnia się trzy główne podtypy enkapsulacji liposomalnej. Spośród nich najczęściej wykorzystywaną jest całkowita enkapsulacja liposomalna (ang. *total liposomal encapsulation*), która pozwala na zamknięcie wszystkich metalicznych NPs wewnątrz (*lumen*) liposomu. Podejście to pozwala na całkowite wyeliminowanie kontaktu powierzchni NPs ze środowiskiem, stąd powszechność badania tego typu liposomów w kontekście prób ukierunkowania działania toksycznych rodzajów metalicznych NPs. Kolejny podtyp enkapsulacji liposomalnej zakłada zamknięcie metalicznych NPs pomiędzy warstwami dwuwarstwy fosfolipidowej – enkapsulacja dwuwarstwowa (ang. *bilayer entrapping*), która znalazła zastosowanie przede wszystkim dla magnetycznych NPs (ang. *magnetic nanoparticles*). Umieszczenie tego typu NPs pomiędzy warstwami liposomu jest wykorzystywane do ukierunkowania migracji liposomu w organizmie za pomocą pola elektromagnetycznego. Struktury takie nazywane są również magnetoliposomami, przykładem których są liposomy zawierające tlenek żelaza (II) diżelaza (III) (Fe_3O_4). Częstym podejściem jest również łączenie metod enkapsulacji całkowitej oraz dwuwarstwowej. Efektem czego jest kompleks liposomalny, w którego świetle (*lumen*) znajduje się lek, kierunkowany za pomocą pola elektromagnetycznego. Jednak, wykazano zdolność magnetycznych NPs do destabilizacji dwuwarstwy fosfolipidowej wskutek oddziaływań z wiązaniami pomiędzy poszczególnymi kwasami tłuszczowymi liposomu, co wymusza konieczność dalszej optymalizacji procesu syntezy. Kolejnym podejście stosowanym w pułapkowaniu nanocząstek metalicznych jest enkapsulacja z wykorzystaniem dendrymerów (ang. *dendrimer encapsulated nanoparticles*, DENs). Dendrymery są organicznymi polimerami o uorganizowanej, symetrycznej strukturze, w której naturalnie występują puste przestrzenia, wykorzystywane do umieszczania w nich leków, katalizatorów oraz metalicznych NPs. Synteza kompleksów typu DENs przebiega najczęściej z wykorzystaniem dendrymerów poliamidoaminowych (ang. *poly(amidoamine) dendrimers,* PAMAM) ze względu na dobrze poznaną strukturę przestrzenną tych polimerów. DENs jest szczególnie wykorzystywana w chemii ze względu na brak ścisłego pokrycia powierzchni nanocząstki przez polimery, a co za tym idzie - dostęp substratów reakcji do powierzchni NPs. Z tego względu zastosowanie enkapsulacji dendrymalnej w redukcji kontaktu nanocząstki metalicznej z komórkami niecelowanymi jest ograniczone. Zasadniczo, na

podstawie dostępnych danych literaturowych wyróżnić można trzy podtypy enkapsulacji z wykorzystaniem dendrymerów. Pierwszym z nich jest enkapsulacja rdzeniowa (ang. *metalic core DENs*, MN DENs), charakteryzująca się występowaniem metalicznej NP w centrum kompleksu, do której powierzchni dołączane są kolejne polimery, tworzące strukturę przestrzenną. Do tej pory badania właściwości biologicznych takich kompleksów przeprowadzono wyłącznie dla nanocząstek złota (ang. *gold nanoparticles*, AuNPs), jako potencjalnej platformy o zastosowaniu w fototerapii przeciwnowotworowej. Kolejnym podtypem DENs jest osadzenie nanocząstek metalicznych w przestrzeniach miedzypolimerowych – „pomiędzy gałęziami dendymerów" (ang. *branch-embedded DENs*, BE DENs). Ten typ enkapsulacji jest najczęściej rozwijanym obecnie oraz wykorzystywanym w badaniach biologicznych i medycznych z jednoczesnym wykorzystaniem koniugacji zewnętrznych wiązań dendrymeru z określonym ligandem. Udowodniono, że AuNPs w formie BE DENs oraz koniugowane z cząsteczką kwasu foliowego pozwoliły na dużo wyższą akumulacje AuNPs w komórkach nowotworu skóry (KB) w warunkach *in vitro*. Podobne wyniki uzyskano w przypadku badań na modelach nowotworu jajnika (SK-OV-2), nerki (SK-RC-2), jąder (NCCIT) czy pęcherza (MES-SA) *in vitro*. Trzecim podejściem w enkapsulacji nanocząstek metalicznych jest ich pułapkowanie za pomocą białek (ang. *protein encapsulation*). W związku z wieloetapowym procesem syntezy oraz jego kosztochłonnością stanowi najrzadziej wykorzystywane sposób w enkapsulacji metalicznych NPs. Nie mniej istotna jest również ilość zmiennych wpływających bezpośrednio na efektywność syntezy – m.in. wielkość, kształt oraz pochodzenie pierwiastkowe NPs, co bezpośrednio wiąże się z różnym stopniem powinowactwa powierzchni NPs oraz białka. Dwie główne strategie obserwowane w enkapsulacji metalicznych NPs za pomocą białek to wykorzystanie NPs jako leku (ang. *nanoparticles as a drug*) oraz użycie metalicznej NPs jako nośnika (ang. *nanoparticles as a vector*). W pierwszym podejściu warstwa białkowa ma na celu ograniczenie kontaktu powierzchni nanocząstki z komórkami niecelowanymi. Dodatkowo, stosuje się również dołączenie do powierzchni białka cząsteczek sygnałowych – kierunkujących. Powyższy sposób zastosowano w przypadku AuNPs opłaszczonych za pomocą albuminy, dla których udowodniono zwiększoną toksyczność w komórkach nowotworu wątroby (HepG2) oraz szyjki macicy (HeLa) w warunkach *in vitro*. Podejście zakładające wykorzystanie NPs jako nośnika polega przede wszystkim na dołączeniu do jej powierzchni cząsteczek sygnałowych oraz białek o właściwościach katalitycznych (enzymów) w celu ułatwienia ich pobierania przez komórki. W taki sposób dostarczono

cząsteczki insuliny (połączonej z AuNPs) do krwiobiegu szczura z wyindukowaną cukrzycą, u którego doszło do istotnego zmniejszenia poziomu glikemii w porównaniu do konwencjonalnie podanej insuliny.

Przeprowadzona w powyższej publikacji analiza dostępnych danych literaturowych - po raz pierwszy- umożliwiła sklasyfikowanie dostępnych metod enkapsulacji metalicznych NPs. Przedstawiona w publikacji dyskusja zalet oraz wad poszczególnych typów enkapsulacji w medycynie, wykazała konieczność optymalizacji poszczególnych metod otrzymywania ww. kompleksów, co jest związane m.in. z ich niewystarczającą stabilnością lub brakiem dostatecznie istotnego efektu biologicznego. Dodatkowo, powyższa analiza dotychczas opublikowanych badań wskazuje, że najwyższą użyteczność w ograniczaniu kontaktu powierzchni metalicznych NPs w układach biologicznych cechuje się enkapsulacja całkowita z wykorzystaniem liposomów. Jak wskazano, podejście to umożliwia również bezpośrednią modyfikację powierzchni kompleksu liposom-NPs za pomocą specyficznych cząsteczek kierunkujących (np. ligandów określonych receptorów). Dlatego metodę enkapsulacji całkowitej z użyciem liposomów wykorzystano w przeprowadzonych badaniach dotyczących ukierunkowania toksyczności AgNPs do komórek nowotworowych.

Publikacja 2: B. Skóra, T. Piechowiak, K. A. Szychowski, *Epidermal Growth Factor-labeled liposomes as a way to target the toxicity of silver nanoparticles into EGFR-overexpressing cancer cells in vitro*, Toxicology and Applied Pharmacology 2022; 443, 116009.

Powszechnie przyjmuje się, że wskutek zachwiania równowagi redoks oraz produkcji dużych ilości ROS, AgNPs wykazują zdolność do indukcji stresu oksydacyjnego w komórce (39). Udowodniono również zdolność jonów Ag^+ - uwalnianych z powierzchni AgNPs – do łączenia się z ujemnie naładowanymi resztami fosforanowymi w łańcuchu DNA, a w efekcie powstawanie masowych pęknięć w jego strukturze indukujących apoptozę, jako efekt niewydajnego mechanizmu naprawy DNA (40,41). Ponadto, wykazano, że AgNPs są w stanie negatywnie oddziaływać na funkcjonowanie poszczególnych organelli, m.in. poprzez bezpośrednie, mechaniczne zniszczenie błony mitochondrialnej, a także hamować działanie cytochromów wchodzących w skład łańcucha oddechowego (42,43). Wielokrotnie potwierdzono również, że w miarę zmniejszania średnicy AgNPs dochodzi do wzrostu ich właściwości cytotoksycznych (44). Podstawą działania AgNPs jest zatem oddziaływanie mechaniczne z poszczególnymi strukturami komórkowymi, jak również ich działanie

utleniające. Jednak, nieswoista aktywność biologiczna AgNPs, skutkuje efektem cytotoksycznym w komórkach prawidłowych oraz zmienionych nowotworowo (45,46). Konieczne jest zatem ukierunkowanie działania tego typu nanostruktur do komórek nowotworowych z pominięciem komórek zdrowych. Powszechnie wiadomo, że nadeskpresja receptora EGFR występuje w wielu typach nowotworowych i stanowi cel terapii przeciwnowotworowej m.in. za pomocą przeciwciał monoklonalnych (ang. *monoclonal antibodies*, mAb) skierowanych przeciwko domenie zewnątrzkomórkowej tego receptora (47,48). Wykorzystanie receptora EGFR w kierunkowanym dostarczaniu substancji aktywnej jest zasadne, zwłaszcza w kontekście internalizacji ww. receptora za pomocą endocytozy klatryno-zależnej, jednak do tej pory niewykorzystane w przypadku AgNPs (49,50).

Celem drugiej publikacji było opracowanie sposobu pozwalającego na dostarczenie AgNPs do komórek nowotworowych z nadekspresją receptora EGFR za pomocą enkapsulacji liposomalnej oraz EGF *in vitro*. Jako model badawczy wykorzystano ludzkie linie komórkowe o różnym poziomie ekspresji receptora EGFR – fibroblasty prawidłowe (BJ); komórki nowotworu NSCLC (A549) oraz komórki nowotworu płaskonabłonkowego języka (SCC-15), reprezentujące odpowiednio komórki o standardowej ekspresji tego receptora, 3-krotnej oraz 15-krotnej nadekspresji receptora EGFR.

Pierwszym etapem pracy było opracowanie sposobu syntezy AgNPs enkapsulowanych wewnątrz liposomu oraz znakowanie jego powierzchni z użyciem cząsteczki EGF (EGF-LipoAgNPs). W trakcie prac zsyntetyzowano trzy typy kompleksów liposom-NPs, były to odpowiednio: EGF- LipoAgNPs (opisany powyżej); EGF-LipoE (liposomy niezawierające AgNPs) oraz Fluo-EGF-LipoAgNPs (kompleksy analogiczne do EGF-LipoAgNPs z wbudowanym fluorochromem – wykorzystane w mikroskopii konfokalnej). Charakterystyka fizykochemiczna wytworzonych kompleksów wykazała w roztworach obecność liposomów o średnicy mieszczącej się w przedziale 107,9 – 116,8 nm, potwierdzając powtarzalność opracowanej metody. Co więcej, przeprowadzona analiza mikroskopowa (ang. *transmission electron microscope*, TEM) oraz pomiary dynamicznego rozpraszania światła (ang. *dynamic light scattering*, DLS) nie wykazały w badanych roztworach obecności struktur o średnicy mniejszej niż 70 nm. Wskazuje to na brak natywnych („wolnych") AgNPs oraz udowadnia wysoką efektywność opracowanej procedury enkapsulacji AgNPs. Wynik ten został potwierdzony za pomocą skanu w zakresie światła widzialnego i ultrafioletowego (ang. *ultraviolet–visible spectroscopy*, UV-VIS). Dodatkowo, pomiar stabilności roztworów – wyrażony jako wartość ζ-potencjału – zawierał się w zakresie

-30 mV – +30 mV, co udowadnia stabilność wytworzonych roztworów liposomów i ich równomierną dyspersję. Kolejnym etapem pracy była ocena działania cytotoksycznego oraz swoistego wytworzonych liposomów w trzech typach komórek, reprezentujących różny poziom ekspresji receptora EGFR - BJ, A549 oraz SCC-15. W układzie eksperymentalnym wykorzystano trzy typy nanostruktur: natywne (niemodyfikowane) AgNPs – kontrola pozytywna; EGF-LipoAgNPs – badany kompleks oraz EGF-LipoE – kontrola negatywna eksperymentu. Przeprowadzone badania wykazały, że EGF-LipoAgNPs są toksyczne w komórkach A549 oraz SCC-15 po 24 i 48 godz. Efekt ten był opóźniony w stosunku do natywnych AgNPs – które wykazywały toksyczność już po 6 godzinach ekspozycji. Podobną zależność zaobserwowano w przypadku wewnątrzkomórkowej produkcji ROS, dla którego istotnie wyższy wzrost (w porównaniu do natywnych AgNPs) obserwowano w komórkach nowotworowych. Wysycenie receptora EGFR za pomocą białka EGF spowodowało redukcję lub całkowite zniesienie opisanego efektu. Dodatkowo, przeprowadzone analizy wykazały, że w komórkach traktowanych EGF- LipoAgNPs dochodziło do wzrostu aktywności kaspazy-9, co świadczy o indukcji apoptozy z zaangażowaniem ścieżki mitochondrialnej. Ta z kolei jest ściśle związana z zaburzeniem równowagi redoks w komórce lub zmianą potencjału błony mitochondrialnej. Co więcej, efekt ten zależał od typu badanych komórek z różną ekspresja EGFR, skutkując wyższą aktywnością kaspazy-9 w komórkach SCC-15, natomiast niższą w komórkach A549. Powyższe wskazuje na zdolność EGF-LipoAgNPs do indukcji apoptozy, postrzeganej jako bezpieczny sposobu usuwania komórek nowotworowych z organizmu, niepowodujący rozwoju zapalenia. Dodatkowo, analizy określonych białek tj. aktywności enzymów antyoksydacyjnych, takich jak katalaza (ang. *catalase,* CAT), dysmutaza ponadtlenkowa (ang. *superoxide dismutase*, SOD) oraz redukcja ilości białka KI67, a także korelujących z nimi genów (*CAT, SOD, KI67, TP53*) wykazały wyższą odpowiedź po traktowaniu komórek nowotworowych za pomocą EGF-LipoAgNPs – w porównaniu do natywnych AgNPs. Odwrotną zależność zaobserwowano w komórkach zdrowych (BJ), dla których AgNPs wykazywały istotnie wyższy efekt toksyczny w porównaniu do EGF-LipoAgNPs. Zaobserwowano również istotnie różny poziom pobierania wytworzonych liposomów w poszczególnych typach modeli komórkowych.

Przeprowadzone doświadczenia wykazały, że wytworzona platforma swoistego dostarczania AgNPs do komórek nowotworowych jest skuteczna w warunkach *in vitro*. Mechanizm działania EGF-LipoAgNPs jest związany z zaburzeniem homeostazy *redox* zachodzącym w komórce po internalizacji AgNPs. Wytworzone kompleksy liposom-NPs

charakteryzują się opóźnionym działaniem w stosunku do natywnych AgNPs, związanym z uwalnianiem większej ilości Ag^+ w komórce, skutkując indukcją apoptozy w sposób zintensyfikowany. Udowodnione działanie ochronne w komórkach zdrowych oraz zwiększona toksyczność kompleksów w komórkach nowotworowych – w porównaniu do natywnych AgNPs – pozwala na sformułowanie wniosku o swoistości działania EGF-LipoAgNPs.

Publikacja 3: B. Skóra, K.A. Szychowski, *Molecular mechanism of the uptake and toxicity of EGF-LipoAgNPs in EGFR-overexpressing cancer cells*, Biomedicine and Pharmacotherapy, 2022; 150, 113085.

Receptor EGFR jest zaliczany do rodziny białek onkogennych, w których mutacje są bezpośrednio związane z indukcją karcynogenezy (51). Jedną z charakterystycznych cech komórek nowotworowych związanych z ww. receptorem jest jego nadeskpresja (52). Wynika to z auto- i parakrynnej regulacji wzrostu tkanek nowotworowych, stanowiącego przystosowanie tych komórek, co skutkuje ciągłą stymulacją proliferacji (53,54). Receptor EGFR jest internalizowany przez komórkę na drodze klatrynozależnej, natomiast w zależności od rodzaju liganda tego receptora dochodzi do jego degradacji lub recyrkulacji do błony komórkowej (55,56). Czynnik wzrostowy EGF posiada wysokie powinowactwo do receptora EGFR oraz udowodnione działania pro-degradacyjne dla EGFR (56). Jest to szczególnie ważne w przypadku kierunkowania działania AgNPs. Degradacja EGFR na drodze klatryno-zależnej z zaangażowaniem lizosomu, a przez to zapewnienie niskiego pH środowiska – znacząco zwiększa ilość uwalnianych jonów srebrowych z powierzchni AgNPs (57).

Celem trzeciej publikacji było określenie mechanizmu pobierania oraz toksyczności wytworzonych kompleksów liposomowych (EGF-LipoAgNPs) w komórkach nowotworowych z nadeskpresją receptora EGFR. Jako model badawczy wykorzystano dwie ludzkie linie komórkowe – A549 oraz SCC-15. W celu określenia zaangażowania receptora EGFR w pobieranie wytworzonych liposomów zmniejszono ekspresję genu kodującego receptor EGFR z użyciem transfekcji przejściowej, wykorzystując cząsteczkę siRNA (ang. *small interfering RNA*), uzyskując komórki EGFR-negatywne ($A549^{EGFR-}$, $SCC\text{-}15^{EGFR-}$). Jako kontrolę eksperymentu wykorzystano komórki poddane działaniu siRNA o losowej

sekwencji – nie powodującej wyciszenie żadnego genu, uzyskując komórki EGFR-pozytywne ($A549^{EGFR+}$, $SCC\text{-}15^{EGFR+}$).

Pierwszym etapem pracy było określenie ilości pobieranych EGF-LipoAgNPs (znakowanych difluoresceiną; Fluo-EGF-LipoAgNPs) z użyciem fluorescencyjnej mikroskopii konfokalnej. Przeprowadzona analiza mikroskopowa ww. liposomów wskazała, że komórki $A549^{EGFR-}$ oraz $SCC\text{-}15^{EGFR-}$ charakteryzowały się istotnie mniejszym pobieraniem kompleksów liposomowych w porównaniu do komórek $A549^{EGFR+}$ oraz $SCC\text{-}15^{EGFR+}$. Potwierdza to wyniki uzyskane w poprzedniej pracy i wskazuje na zaangażowanie receptora EGFR w internalizację wytworzonych liposomów, a tym samym – w odwołaniu do wyników toksyczności - potwierdza ich specyficzność działania. Dodatkowo, dalsze analizy na poziomie mRNA wykazały wzrost ekspresji genów niezbędnych do prawidłowego przebiegu endocytozy klatryno-zależnej tj. genu *CLTC* (ang. *clathrin heavy chain*) oraz genu *AP2M1* (ang. *adaptor-related protein complex 2 mu 1 subunit*) w komórkach $A549^{EGFR+}$ oraz $SCC\text{-}15^{EGFR+}$ po podaniu EGF-LipoAgNPs. Opisanego efektu nie zaobserwowano w komórkach $A549^{EGFR-}$ oraz $SCC\text{-}15^{EGFR-}$. Uzyskane wyniki są zbieżne z danymi literaturowymi sugerującymi, korelację pomiędzy wielkością nanostruktury a typem endocytozy biorącym udział w ich internalizacji. Co więcej, wszystkie typy komórek ($A549^{EGFR-}$, $A549^{EGFR+}$, $SCC\text{-}15^{EGFR-}$ oraz $SCC\text{-}15^{EGFR+}$) poddane działaniu natywnych AgNPs charakteryzowały się zwiększoną ekspresją genów związanych z endocytozą kaweolino-zależną tj. genu *CAV1* (ang. *caveolin 1*) oraz genu *SH3GLB1* (ang. *SH3 domain containing GRB2 like endophilin B1*), co świadczy o pobieraniu AgNPs za pomocą tego typu endocytozy. Potwierdza to również powszechnie obowiązującą teorię o braku specyficzności w internalizacji oraz działaniu tego typu nanostruktur w komórkach ssaczych. Istotna jest również zwiększona ekspresja genu *ATM* (ang. *ataxia telangiectasia mutated serine/threonine kinase*) – wewnątrzkomórkowego markeru uszkodzeń DNA - w komórkach $A549^{EGFR+}$ i $SCC\text{-}15^{EGFR+}$ poddanych działaniu EGF-LipoAgNPs w porównaniu do komórek EGFR-negatywnych, udowadniając genotoksyczność wytworzonych liposomów. Opisanego powyżej wpływu nie zaobserwowano dla EGF-LipoE, co potwierdza, że wywoływany efekt jest bezpośrednim skutkiem obecności AgNPs w komórce – a nie samej platformy dostarczającej nanocząstki.

Przedstawione wyniki udowadniają, że wytworzone kompleksy (EGF-LipoAgNPs) są pobierane przez komórki nowotworowe na drodze receptoro- i klatryno-zależnej oraz, że ich działanie toksyczne jest związane z właściwościami utleniającymi tego typu nanostruktur tj.

indukcję uszkodzeń DNA oraz zaburzenie równowagi redoks w komórce, skutkujących indukcją apoptozy.

W powyższych publikacjach po raz pierwszy wykazano, że ukierunkowanie toksyczności AgNPs jest możliwe z wykorzystaniem receptora EGFR oraz całkowitej enkapsulacji liposomalnej. Opracowany sposób syntezy kompleksów EGF-LipoAgNPs pozwala na uzyskanie homogennych - pod względem wielkości nanostruktur - roztworów. Dodatkowo, wykazano wysoką efektywność procedury enkapsulacji, skutkującą brakiem natywnych AgNPs w roztworach oraz ich prawidłową dyspersję i stabilność. Otrzymane wyniki badań po raz pierwszy udowodniły, że wytworzone kompleksy EGF-LipoAgNPs są w stanie zmniejszać toksyczność tych nanostruktur w komórkach prawidłowych, z jednoczesnym zwiększeniem ich efektu cytotoksycznego w komórkach nowotworowych – charakteryzujących się nadekspresją receptora EGFR w warunkach *in vitro*. Udowodniono również, że internalizacja EGF-LipoAgNPs odbywa się za pomocą wspomnianego receptora na drodze klatryno-zależnej. Tym samym, opracowane rozwiązanie daje podstawę do dalszego badania EGF-LipoAgNPs, jako nośnika eliminującego nieswoistą aktywność AgNPs, przy jednoczesnym zwiększenie toksyczności testowanych nanostruktur w komórkach nowotworowych z nadeskpresją receptora EGFR.

4.3. Wnioski

- Opracowany sposób syntezy liposomów EGF-LipoAgNPs jest wydajny, skuteczny oraz charakteryzuje się powtarzalnością uzyskanych wyników, pozwalając na uzyskanie homogennych i stabilnych roztworów kompleksów liposomalnych.

- System celowania toksyczności AgNPs jest skuteczny w warunkach *in vitro* i powoduje zwiększenie tego efektu w komórkach nowotworowych oraz jego zmniejszenie w komórkach zdrowych.

- Cytotoksyczny i antyproliferacyjny efekt wywoływany przez wytworzone liposomy jest związany z zaburzeniem równowagi *redox* w komórce, a w konsekwencji indukcję apoptozy związanej ze ścieżką mitochondrialną tego procesu.

- Efekt toksyczny EGF-LipoAgNPs jest zależny od poziomu receptora EGFR i wzrasta wraz ze zwiększonym występowaniem tego receptora w badanych typach komórek nowotworowych.

- Internalizacja wytworzonych liposomów odbywa się na drodze receptorowej z zaangażowaniem EGFR oraz endocytozy klatryno-zależnej, powodując opóźnienie w czasie działania AgNPs wraz ze zwiększeniem ich efektu cytotoksycznego.

5. Bibliografia

1. Al-Ahmady Z, Lozano N, Mei KC, Al-Jamal WT, Kostarelos K. Engineering thermosensitive liposome-nanoparticle hybrids loaded with doxorubicin for heat-triggered drug release. International Journal of Pharmaceutics 2016; 514: 133-141.
2. Jamkhande PG, Ghule NW, Bamer AH, Kalaskar MG. Metal nanoparticles synthesis: An overview on methods of preparation, advantages and disadvantages, and applications. Journal of Drug Delivery Science and Technology 2019; 53, 101174.
3. Mittapally S, Taranum R, Parveen S. Metal ions as antibacterial agents. Journal of Drug Delivery and Therapeutics 2018; 8: 411-419.
4. Dąbrowska-Bouta B, Sulkowski G, Strużyński W, Strużyńska L. Prolonged Exposure to Silver Nanoparticles Results in Oxidative Stress in Cerebral Myelin. Neurotoxicity Research 2019; 35: 495–504.
5. Bhandi S, Mehta D, Mashyakhy M, Chohan H, Testarelli L, Thomas J, Dhillon H, Raj AT, Balaji TM, Varadarajan S, Patil S. Antimicrobial Efficacy of Silver Nanoparticles as Root Canal Irrigant's: A Systematic Review. Journal of Clinical Medicine 2021; 10: 1152.
6. Kalantari K, Mostafavi E, Afifi AM, Izadiyan Z, Jahangirian H, Rafiee-Moghaddam R, Webster TJ. Wound dressings functionalized with silver nanoparticles: promises and pitfalls. Nanoscale 2020; 12: 2268–2291.
7. Cho Y-M, Mizuta Y, Akagi J, Toyoda T, Sone M, Ogawa K. Size-dependent acute toxicity of silver nanoparticles in mice. Journal of Toxicologic Pathology 2018; 31: 73–80.
8. Kobos L, Alqahtani S, Xia L, Coltellino V, Kishman R, McIlrath D, Perez-Torres C. Comparison of silver nanoparticle-induced inflammatory responses between healthy and metabolic syndrome mouse models. Journal of Toxicology and Environmental Health, Part A 2020; 83: 249–68.
9. Zhang W, Xiao B, Fang T. Chemical transformation of silver nanoparticles in aquatic environments: Mechanism, morphology and toxicity. Chemosphere 2018; 191: 324–34.
10. Flores-López LZ, Espinoza-Gómez H, Somanathan R. Silver nanoparticles: Electron transfer, reactive oxygen species, oxidative stress, beneficial and toxicological effects. Mini review. Journal of Applied Toxicology 2019; 39: 16–26.
11. Shi J, Sun X, Lin Y, Zou X, Li Z, Liao Y, Miaomiao D, Hongwu Z. Endothelial cell

injury and dysfunction induced by silver nanoparticles through oxidative stress via IKK/NF-κB pathways. Biomaterials 2014; 35: 6657–66.

12. Reidy B, Haase A, Luch A, Dawson KA, Lynch I. Mechanisms of silver nanoparticle release, transformation and toxicity: A critical review of current knowledge and recommendations for future studies and applications. Materials 2013; 6: 2295–350.
13. Sun X, Shi J, Zou X, Wang C, Yang Y, Zhang H. Silver nanoparticles interact with the cell membrane and increase endothelial permeability by promoting VE-cadherin internalization. Journal of Hazardous Materials 2016; 317: 570–578.
14. Govindaraju K, Krishnamoorthy K, Alsagaby SA, Singaravelu G, Premanathan M. Green synthesis of silver nanoparticles for selective toxicity towards cancer cells. IET Nanobiotechnology 2015; 9: 325–330.
15. Simard JC, Durocher I, Girard D. Silver nanoparticles induce irremediable endoplasmic reticulum stress leading to unfolded protein response dependent apoptosis in breast cancer cells. Apoptosis 2016; 21: 1279–1290.
16. Sanpui P, Chattopadhyay A, Ghosh SS. Induction of apoptosis in cancer cells at low silver nanoparticle concentrations using chitosan nanocarrier. ACS Applied Materials and Interfaces 2011; 3: 218–228.
17. Banerjee PP, Bandyopadhyay A, Harsha SN, Policegoudra RS, Bhattacharya S, Karak N, et al. Mentha arvensis (Linn.)-mediated green silver nanoparticles trigger caspase 9-dependent cell death in MCF7 and MDA-MB-231 cells. Breast Cancer: Targets and Therapy 2017; 9: 265–78.
18. Zielinska E, Zauszkiewicz-Pawlak A, Wojcik M, Inkielewicz-Stepniak I. Silver nanoparticles of different sizes induce a mixed type of programmed cell death in human pancreatic ductal adenocarcinoma. Oncotarget 2018; 9: 4675–4697.
19. Kovács D, Szoke K, Igaz N, Spengler G, Molnár J, Tóth T, et al. Silver nanoparticles modulate ABC transporter activity and enhance chemotherapy in multidrug resistant cancer. Nanomedicine: Nanotechnology, Biology, and Medicine 2016; 12: 601–610.
20. Krzyzanowski D, Kruszewski M, Grzelak A. Differential Action of Silver Nanoparticles on ABCB1 (MDR1) and ABCC1 (MRP1) Activity in Mammalian Cell Lines. Materials 2021; 14: 3383.
21. Skóra B, Szychowski KA, Gmiński J. A concise review of metallic nanoparticles encapsulation methods and their potential use in anticancer therapy and medicine. European Journal of Pharmaceutics and Biopharmaceutics 2020; 154: 153–65.

22. Subramani T, Ganapathyswamy H. An overview of liposomal nano-encapsulation techniques and its applications in food and nutraceutical. Journal of Food Science and Technology 2020; 57: 3545–3555.
23. Yusuf A, Casey A. Evaluation of silver nanoparticle encapsulation in DPPC-based liposome by different methods for enhanced cytotoxicity. International Journal of Polymeric Materials and Polymeric Biomaterials 2019; 69: 2585-2594.
24. Skóra B, Piechowiak T, Szychowski KA, Gmiński J. Entrapment of silver nanoparticles in L-α-phosphatidylcholine/cholesterol-based liposomes mitigates the oxidative stress in human keratinocyte (HaCaT) cells. European Journal of Pharmaceutics and Biopharmaceutics 2021; 166: 163–74.
25. Liu Y, Castro Bravo KM, Liu J. Targeted liposomal drug delivery: a nanoscience and biophysical perspective. Nanoscale Horizons 2021; 6: 78–94.
26. Sigismund S, Avanzato D, Lanzetti L. Emerging functions of the EGFR in cancer. Molecular Oncology 2018; 12: 3-20.
27. Hirsch FR, Varella-Garcia M, Cappuzzo F. Predictive value of EGFR and HER2 overexpression in advanced non-small-cell lung cancer. Oncogene 2009; 28: 32-37.
28. Lin G, Sun XJ, Han QB, Wang Z, Xu YP, Gu JL, Wu W, Zhang GU, Hu JL, Sun WY, Mao WM. Epidermal growth factor receptor protein overexpression and gene amplification are associated with aggressive biological behaviors of esophageal squamous cell carcinoma. Oncology Letters 2015; 10: 901–906.
29. Kumar A, Petri ET, Halmos B, Boggon TJ. Structure and Clinical Relevance of the Epidermal Growth Factor Receptor in Human Cancer. Journal of Clinical Oncology 2008; 26: 1742–1751.
30. Salova A V., Belyaeva TN, Leontieva EA, Kornilova ES. EGF receptor lysosomal degradation is delayed in the cells stimulated with EGF-Quantum dot bioconjugate but earlier key events of endocytic degradative pathway are similar to that of native EGF. Oncotarget 2017; 8: 44335–44350.
31. Cao P, Xia Y, He W, Zhang T, Hong L, Zheng P, et al. Enhancement of oxaliplatin-induced colon cancer cell apoptosis by alantolactone, a natural product inducer of ROS. International Journal of Biological Sciences 2019; 15: 1676–1684.
32. Mangala LS, Han HD, Lopez-Berestein G, Sood AK. Liposomal siRNA for ovarian cancer. Methods in Molecular Biology 2009; 555: 29–42.
33. Skóra B, Piechowiak T, Szychowski KA. Epidermal Growth Factor-labeled liposomes

as a way to target the toxicity of silver nanoparticles into EGFR-overexpressing cancer cells in vitro. Toxicology and Applied Pharmacology 2022; 443: 116009.

34. McShan D, Ray PC, Yu H. Molecular toxicity mechanism of nanosilver. Journal of Food and Drug Analysis 2014; 22: 116-127.
35. Perde-Schrepler M, Florea A, Brie I, Virag P, Fischer-Fodor E, Vâlcan A, Gurzău E, Lisencu C, Maniu A. Size-Dependent Cytotoxicity and Genotoxicity of Silver Nanoparticles in Cochlear Cells *In Vitro*. Journal of Nanomaterials 2019; 2019: 6090259.
36. Gherasim O, Puiu RA, Bîrcă AC, Burdușel A-C, Grumezescu AM. An Updated Review on Silver Nanoparticles in Biomedicine. Nanomaterials 2020; 10: 2318.
37. Xu L, Wang YY, Huang J, Chen CY, Wang ZX, Xie H. Silver nanoparticles: Synthesis, medical applications and biosafety. Theranostics 2020; 10: 8996–9031.
38. Gao A, Hu X, Saeed M, Chen B, Li Y, Yu H. Overview of recent advances in liposomal nanoparticle-based cancer immunotherapy. Acta Pharmacologica Sinica 2019; 40: 1129– 1137.
39. Mukherjee SG, O'Claonadh N, Casey A, Chambers G. Comparative in vitro cytotoxicity study of silver nanoparticle on two mammalian cell lines. Toxicology in Vitro 2012; 26: 238–251.
40. Gopinath P, Gogoi SK, Sanpui P, Paul A, Chattopadhyay A, Ghosh SS. Signaling gene cascade in silver nanoparticle induced apoptosis. Colloids and Surfaces B: Biointerfaces 2010; 77: 240–245.
41. Ullah I, Khalil AT, Ali M, Iqbal J, Ali W, Alarifi S, Shinwari ZK. Green-Synthesized Silver Nanoparticles Induced Apoptotic Cell Death in MCF-7 Breast Cancer Cells by Generating Reactive Oxygen Species and Activating Caspase 3 and 9 Enzyme Activities. Oxidative Medicine and Cellular Longevity 2020; 2020: 1–14.
42. Liu P, Guan R, Ye X, Jiang J, Liu M, Huang G, Chen X. Toxicity of nano- and micro-sized silver particles in human hepatocyte cell line L02. In: Journal of Physics: Conference Series 2011; 390: 012036.
43. Bin-Jumah M, AL-Abdan M, Albasher G, Alarifi S. Effects of Green Silver Nanoparticles on Apoptosis and Oxidative Stress in Normal and Cancerous Human Hepatic Cells in vitro. International Journal of Nanomedicine 2020; 15: 1537–1548.
44. Jeong Y, Lim DW, Choi J. Assessment of Size-Dependent Antimicrobial and Cytotoxic Properties of Silver Nanoparticles. Advances in Materials Science and

Engineering 2014; 2014: 1–6.

45. Galandáková A, Franková J, Ambrožová N, Habartová K, Pivodová V, Zálešák B, Šafářová K, Smékalová M, Ulrichová J. Effects of silver nanoparticles on human dermal fibroblasts and epidermal keratinocytes. Human & Experimental Toxicology 2016; 35: 946-957.
46. Zhang X-FF, Shen W, Gurunathan S. Silver Nanoparticle-Mediated Cellular Responses in Various Cell Lines: An in Vitro Model. Int J Mol Sci 2016; 17: 1603.
47. Martinelli E, De Palma R, Orditura M, De Vita F, Ciardiello F. Anti-epidermal growth factor receptor monoclonal antibodies in cancer therapy. Clinical and Experimental Immunology 2009; 158: 1–9.
48. Heinemann V, Stintzing S, Kirchner T, Boeck S, Jung A. Clinical relevance of EGFR- and KRAS-status in colorectal cancer patients treated with monoclonal antibodies directed against the EGFR. Cancer Treatment Reviews 2009; 35: 262–271.
49. Kim B, Park YS, Sung JS, Lee JW, Lee SB, Kim YH. Clathrin- mediated EGFR endocytosis as a potential therapeutic strategy for overcoming primary resistance of EGFR TKI in wild- type EGFR non- small cell lung cancer. Cancer Medicine 2021; 10: 372–385.
50. Delos Santos RC, Bautista S, Lucarelli S, Bone LN, Dayam RM, Abousawan J, Botelho RJ, Antonescu CN. Selective regulation of clathrin-mediated epidermal growth factor receptor signaling and endocytosis by phospholipase C and calcium. Molecular Biology of the Cell 2017; 28: 2802–2818.
51. Uribe ML, Marrocco I, Yarden Y. EGFR in Cancer: Signaling Mechanisms, Drugs, and Acquired Resistance. Cancers 2021; 13: 2748.
52. Ayati A, Moghimi S, Salarinejad S, Safavi M, Pouramiri B, Foroumadi A. A review on progression of epidermal growth factor receptor (EGFR) inhibitors as an efficient approach in cancer targeted therapy. Bioorganic Chemistry 2020; 99: 103811.
53. Nickerson NK, Mill CP, Wu H-J, Riese DJ, Foley J. Autocrine-Derived Epidermal Growth Factor Receptor Ligands Contribute to Recruitment of Tumor-Associated Macrophage and Growth of Basal Breast Cancer Cells In Vivo. Oncology Research Featuring Preclinical and Clinical Cancer Therapeutics 2013; 20: 303–317.
54. Wee P, Wang Z. Epidermal Growth Factor Receptor Cell Proliferation Signaling Pathways. Cancers 2017; 9: 52.
55. Chi S, Cao H, Wang Y, McNiven MA. Recycling of the Epidermal Growth Factor

Receptor Is Mediated by a Novel Form of the Clathrin Adaptor Protein Eps15. Journal of Biological Chemistry 2011; 286: 35196–35208.

56. Tomas A, Futter CE, Eden ER. EGF receptor trafficking: Consequences for signaling and cancer. Trends in Cell Biology 2014; 24: 26-34.

57. Miyayama T, Matsuoka M. Involvement of lysosomal dysfunction in silver nanoparticle-induced cellular damage in A549 human lung alveolar epithelial cells. Journal of Occupational Medicine and Toxicology 2016; 11: 1.

6. Streszczenie w języku polskim

Nanocząstki srebra (AgNPs) wykazują silne działanie cytotoksyczne. Jednak, ze względu na brak swoistości działania, wykorzystanie AgNPs w terapii przeciwnowotworowej jest ograniczone. Enkapsulacja liposomalna nanocząstek metalicznych zyskuje na znaczeniu i jest metodą pozwalającą na ograniczenie kontaktu nanocząstek z otoczeniem. Ułatwia ona znacząco modyfikację powierzchni nanocząstek metalicznych oraz zwiększa ich toksyczność. Nadeskpresja receptor nabłonkowego czynnika wzrostu (EGFR) występuje w wielu typach nowotworów m.in. niedrobnokomórkowym raku płuc, czy nowotworach głowy i szyi. Receptor ten jest internalizowany przez komórkę na drodze klatryno-zależnej z zaangażowaniem lizosomu. Jednym z lepiej poznanych ligandów ww. receptora jest nabłonkowy czynnik wzrostu (EGF), o wysokim powinowactwie i zdolnością do indukcji degradacji receptora EGFR. Jednak, brak jest danych literaturowych dotyczących próby ukierunkowania działania toksycznego AgNPs do komórek nowotworowych z wykorzystaniem receptora EGFR.

Dlatego celem niniejszej rozprawy doktorskiej była ocena wykorzystania enkapsulacji liposomalnej oraz czynnika EGF w ukierunkowaniu toksyczności AgNPs do komórek nowotworowych z nadekspresją receptora EGFR z jednoczesnym zmniejszeniem efektu toksycznego tych nanostruktur w komórkach zdrowych w warunkach *in vitro*.

W pierwszym etapie badań wykorzystano trzy ludzkie linie komórkowe tj. fibroblasty (BJ), komórki raka niedrobnokomórkowego płuc (A549) oraz komórki nowotworu płaskonabłonkowego języka (SCC-15), reprezentujące odpowiednio komórki o prawidłowej ekspresji EGFR, 3-krotnej oraz 15-krotnej nadekspresji tego receptora. W kolejnych etapach badań wykorzystano komórki ze zmniejszoną ekspresją genu EGFR za pomocą cząsteczki siRNA, uzyskując komórki EGFR-negatywne ($A549^{EGFR-}$ i $SCC\text{-}15^{EGFR-}$) oraz komórki EGFR-pozytywne ($A549^{EGFR+}$ oraz $SCC\text{-}15^{EGFR+}$) – za pomocą cząsteczki siRNA o losowej sekwencji.

Opracowany sposób syntezy AgNPs zamkniętych w liposomach i znakowanych EGF (EGF-LipoAgNPs) pozwolił na uzyskanie nanostruktur o średnicy 107,9 nm oraz 116,8 nm, odpowiednio dla EGF-LipoAgNPs oraz liposomów nie zawierających AgNPs (EGF-LipoE). Obserwacja mikroskopowa wytworzonych kompleksów nie ujawniła natywnych nanocząstek w roztworze, co zostało potwierdzone skanem w zakresie światła ultrafioletowego i widzialnego. Wartość ζ-potencjału wytworzonych roztworów mieściła się w przedziale -

30 mV - +30 mV dla wszystkich roztworów. Wyniki badań w modelach komórkowych *in vitro* wykazały, że EGF-LipoAgNPs wykazywały toksyczność po 24 i 48 godzinach. Efekt ten był istotnie wyższy w komórkach A549 i SCC-15 w porównaniu do komórek BJ. Analogiczne wyniki uzyskano dla pomiaru poziomu wewnątrzkomórkowych reaktywnych form tlenu (ROS). Dodatkowo, wytworzone liposomy charakteryzowały się wyższym efektem toksycznym w stosunku do natywnych (niemodyfikowanych) AgNPs w komórkach nowotworowych. EGF-LipoAgNPs indukowały wzrost aktywności kaspazy-9 oraz kaspazy-3 po 24 i 48 godz. od podania. Zmiany na poziomie białka m.in. aktywność katalazy, dysmutazy ponadtlenkowej oraz białka KI67 potwierdziły właściwości toksyczne i antyproliferacyjne wytworzonych liposomów, których podstawą była indukcja stresu oksydacyjnego. Wyniki potwierdzono także za pomocą analiza ekspresji genów (*CAT, SOD, KI67, TP53*). EGF-LipoE nie wykazywały istotnego efektu dla badanych parametrów w komórkach BJ, A549 oraz SCC-15. Uzyskane wyniki badań udowodniły istotnie mniejsze pobieranie EGF-LipoAgNPs w komórkach $A549^{EGFR-}$ i $SCC\text{-}15^{EGFR-}$ w porównaniu do komórek $A549^{EGFR+}$ oraz $SCC\text{-}15^{EGFR+}$. Analiza poziomu mRNA udowodniła zdolność wytworzonych liposomów do indukcji wzrostu ekspresji genów związanych z przebiegiem procesu endocytozy klatryno-zależnej w komórkach EGFR- pozytywnych. Efektu takiego nie zaobserwowano w komórkach EGFR-negatywnych lub był on istotnie niższy. Podobną zależność zaobserwowano w przypadku analizy poziomu mRNA dla genów związanych z uszkodzeniem DNA oraz stresem oksydacyjnym (*ATM, NRFL2*).

Podsumowując, opracowany sposób dostarczania AgNPs do komórek nowotworowych z nadeskpresją receptora EGFR jest skuteczny w warunkach *in vitro* i pozwala na zwiększenie efektu toksycznego badanych AgNPs w komórkach nowotworowych, przy jednoczesnym zmniejszeniu efektu negatywnego w komórkach zdrowych. Wywoływany efekt toksyczny był związany z indukcją stresu oksydacyjnego w komórkach nowotworowych oraz indukcją apoptozy z zaangażowaniem drogi mitochondrialnej tego procesu. Dodatkowo, uzyskane wyniki badań udowadniają pobieranie wytworzonych liposomów na drodze klatryno-zależnej z zaangażowaniem receptora EGFR.

7. Streszczenie w języku angielskim

Silver nanoparticles (AgNPs) are characterized by strong cytotoxic properties. However, due to the lack of specificity of action, the use of AgNPs in anticancer therapy is limited. Liposomal encapsulation of metallic nanoparticles is gaining in an importance and is a method that allows to limit the contact of nanoparticles with the environment. It significantly facilitates the modification of the surface of metallic nanoparticles and increases their toxicity. Epidermal growth factor receptor (EGFR) is overexpressed in many types of cancers, including non-small cell lung cancers as well as head and neck cancers. This receptor is internalized by the cell *via* a clathrin-dependent pathway with involvement of the lysosomes. One of the well- known ligands of the above-mentioned receptor is epidermal growth factor (EGF), with high affinity and ability to induce degradation of the EGFR receptor. However, there is no literature data on an approach to direct the toxic effect of AgNPs to cancer cells using the EGFR.

Therefore, the aim of this doctoral dissertation is to evaluate the use of liposomal encapsulation and EGF in targeting of the toxicity of AgNPs to cancer cells overexpressing the EGFR, while reducing the toxic effect of these nanostructures in healthy cells *in vitro*.

In the first stage of the research, three human cell lines were used, i.e. fibroblasts (BJ), non-small cell lung cancer cells (A549) and squamous tongue cell carcinoma cells of the (SCC- 15), representing cells with the normal expression of the EGFR receptor as well as 3-fold and 15-fold overexpression of this receptor, respectively. In the next stages of the research, cells with silenced expression of the EGFR gene were used obtained by using of the siRNA, resulting in the EGFR-negative cells ($A549^{EGFR-}$ and $SCC\text{-}15^{EGFR-}$) and EGFR-positive cells ($A549^{EGFR+}$ and $SCC\text{-}15^{EGFR+}$) - using a siRNA molecule with a random sequence.

The developed method of synthesis of AgNPs encapsulated in liposomes and labeled with EGF (EGF-LipoAgNPs) allowed to obtain nanostructures with a diameter of 107.9 nm and 116.8 nm, respectively for EGF-LipoAgNPs and liposomes without AgNPs (EGF-LipoE). Microscopic observation of the formed complexes did not reveal free nanoparticles in the solution, which was confirmed by a scan in the ultraviolet and visible light range. The value of the ζ-potential of the prepared solutions was in the range between -30 mV - +30 mV. The results of the cell model-based *in vitro* studies have revealed that EGF-LipoAgNPs showed toxicity after 24 and 48 hours. This effect was significantly higher in A549 and SCC-

15 cells, compared to BJ cells. Similar results were obtained in the level of intracellular reactive oxygen species (ROS). In addition, the synthetized liposomes were characterized by a higher toxic effect compared to native (unmodified) AgNPs in cancer cells. EGF-LipoAgNPs induced an increase in the activity of caspase-9 and caspase-3 after 24 and 48 hours of treatment. The changes at the protein level, e.g. the activity of catalase, superoxide dismutase and KI67 protein confirmed the toxic and antiproliferative properties of the produced liposomes, which were based on the induction of oxidative stress. The results were also confirmed by gene expression analysis (*CAT, SOD, KI67, SHH, TP53*). EGF-LipoE showed no significant effect on the tested parameters in BJ, A549 and SCC-15 cells. The obtained results showed significantly lower uptake of EGF-LipoAgNPs in $A549^{EGFR-}$ and $SCC\text{-}15^{EGFR-}$ cells compared to $A549^{EGFR+}$ and $SCC\text{-}15^{EGFR+}$ cells. Analysis of the mRNA level has proved the ability of the synthetized liposomes to induce an increase in the expression of genes related to the course of the process of clathrin-dependent endocytosis in EGFR-positive cells. Such an effect was not observed in EGFR-negative cells or was significantly lower. A similar relationship was observed in the analysis of mRNA levels for genes related to DNA damage and oxidative stress (*ATM, NRFL2*).

Summarizing, the developed method of delivering AgNPs to cancer cells, overexpressing the EGFR receptor is effective *in vitro* and allows to increase the toxic effect of the tested AgNPs in cancer cells, while reducing the negative effect in healthy cells. The toxic effect was associated with the induction of oxidative stress in cancer cells and the induction of apoptosis with the involvement of the mitochondrial pathway of this process. In addition, the obtained results of the research prove the uptake of the produced liposomes in the clathrin- dependent way with the involvement of the EGFR receptor.

8. Opinia Komisji Bioetycznej

Prace eksperymentalne prowadzono na dostępnych komercyjnie liniach komórkowych – ludzkich fibroblastach (BJ), komórkach raka niedrobnokomórkowego płuc (A549) oraz komórkach nowotworu płaskonabłonkowego języka (SCC-15). Doświadczenia na tego typu modelu *in vitro* nie wymagają zgody Komisji Bioetycznej, a także Komisji ds. Doświadczeń na Zwierzętach.

Załącznik nr 3 do Regulaminu

9. Oświadczenia współautorów publikacji

Kielce, dnia 23.05.2022r.

Imię i nazwisko współautora pracy: Bartosz Skóra

Rada Naukowa Instytutu
Nauk Medycznych
Uniwersytetu Jana Kochanowskiego
w Kielcach

Oświadczenie o współautorstwie

Niniejszym oświadczam, że w pracy Skóra B., Szychowski K.A., Gmiński J., *A concise review of metallic nanoparticles encapsulation methods and their potential use in anticancer therapy and medicine*, European Journal of Pharmaceutics and Biopharmaceutics, 2020:154, p. 153-165 mój udział wynosił 80% i polegał na stworzeniu koncepcji pracy, wykonaniu analizy i krytycznej oceny dostępnych danych literaturowych, wykonaniu rycin zamieszczonych w publikacji oraz przygotowaniu tekstu manuskryptu. Ponadto oświadczam, że jestem autorem korespondencyjnym pracy.

Bartosz Skóra
podpis

Załącznik nr 3 do Regulaminu

Kielce, dnia 23.05.2022r.

Imię i nazwisko współautora pracy: Konrad Szychowski

Rada Naukowa Instytutu
Nauk Medycznych
Uniwersytetu Jana Kochanowskiego
w Kielcach

Oświadczenie o współautorstwie

Niniejszym oświadczam, że w pracy Skóra B., Szychowski K.A., Gmiński J., *A concise review of metallic nanoparticles encapsulation methods and their potential use in anticancer therapy and medicine*, European Journal of Pharmaceutics and Biopharmaceutics, 2020:154, p. 153-165 mój udział wynosił 15% i polegał na nadzorze merytorycznym oraz przygotowywaniu tekstu manuskryptu.

Jednocześnie wyrażam zgodę na wykorzystanie w/w publikacji w postępowaniu doktorskim p. mgra Bartosza Skóry.

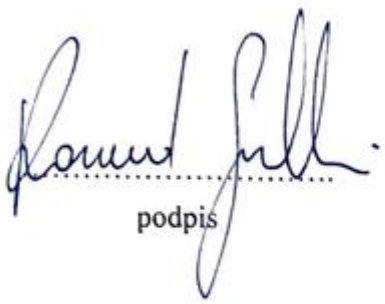

podpis

Kielce, 23.05.2022r.

OŚWIADCZENIE

My – niżej podpisani – zgodnie oświadczamy, że z przyczyn niezależnych od nas nie jest możliwe uzyskanie oświadczenia o współautorstwie w publikacji B. Skóra, K. A. Szychowski, J. Gmiński, *A concise review of metallic nanoparticles encapsulation methods and their potential use in anticancer therapy and medicine*, European Journal of Pharmaceutics and Biopharmaceutics, 2020:154, 153-165. od p. Jana Gmińskiego.

Wkład współautora w powstanie ww. pracy polegał na nadzorze merytorycznym i wynosił 5%.

Promotor

Kandydat

Załącznik nr 3 do Regulaminu

Kielce, dnia 23.05.2022r.

Imię i nazwisko współautora pracy: Bartosz Skóra

Rada Naukowa Instytutu
Nauk Medycznych
Uniwersytetu Jana Kochanowskiego
w Kielcach

Oświadczenie o współautorstwie

Niniejszym oświadczam, że w pracy B. Skóra, T. Piechowiak, K.A. Szychowski, *Epidermal Growth Factor-labeled liposomes as a way to target the toxicity of silver nanoparticles into EGFR-overexpressing cancer cells in vitro*, Toxicology and Applied Pharmacology 2022:443, 116009 mój udział wynosił 70% i polegał na opracowaniu koncepcji pracy, przeprowadzeniu syntezy liposomów, wykonaniu analiz biochemicznych, molekularnych, mikroskopowych, opracowaniu statystycznemu uzyskanych wyników, przygotowaniu rycin, opisu materiałów, metod oraz wyników, przeprowadzeniu dyskusji otrzymanych wyników oraz sformułowaniu wniosków. Ponadto oświadczam, że jestem autorem korespondencyjnym pracy.

Bartosz Skóra
podpis

Załącznik nr 3 do Regulaminu

Kielce, dnia 23.05.2022r.

Imię i nazwisko współautora pracy: Tomasz Piechowiak

Rada Naukowa Instytutu
Nauk Medycznych
Uniwersytetu Jana Kochanowskiego
w Kielcach

Oświadczenie o współautorstwie

Niniejszym oświadczam, że w pracy B. Skóra, T. Piechowiak, K.A. Szychowski, *Epidermal Growth Factor-labeled liposomes as a way to target the toxicity of silver nanoparticles into EGFR-overexpressing cancer cells in vitro*, Toxicology and Applied Pharmacology 2022:443, 116009 mój udział wynosił 20% i polegał na przeprowadzeniu syntezy liposomów, przeprowadzeniu części analiz fizykochemicznych oraz przygotowywaniu tekstu manuskryptu.

Jednocześnie wyrażam zgodę na wykorzystanie w/w publikacji w postępowaniu doktorskim p. mgra Bartosza Skóry.

Tomasz Piechowiak

podpis

Załącznik nr 3 do Regulaminu

Kielce, dnia 23.05.2022r.

Imię i nazwisko współautora pracy: Konrad Szychowski

Rada Naukowa Instytutu
Nauk Medycznych
Uniwersytetu Jana Kochanowskiego
w Kielcach

Oświadczenie o współautorstwie

Niniejszym oświadczam, że w pracy B. Skóra, T. Piechowiak, K.A. Szychowski, *Epidermal Growth Factor-labeled liposomes as a way to target the toxicity of silver nanoparticles into EGFR-overexpressing cancer cells in vitro*, Toxicology and Applied Pharmacology 2022:443, 116009 mój udział wynosił 10% i polegał na przygotowaniu tekstu manuskryptu oraz nadzorze merytorycznym prowadzonych prac badawczych.

Jednocześnie wyrażam zgodę na wykorzystanie w/w publikacji w postępowaniu doktorskim p. mgra Bartosza Skóry.

.....
podpis

Załącznik nr 3 do Regulaminu

Kielce, dnia 23.05.2022r.

Imię i nazwisko współautora pracy: Bartosz Skóra

Rada Naukowa Instytutu
Nauk Medycznych
Uniwersytetu Jana Kochanowskiego
w Kielcach

Oświadczenie o współautorstwie

Niniejszym oświadczam, że w pracy B. Skóra, K. A. Szychowski, *Molecular mechanism of the uptake and toxicity of EGF-LipoAgNPs in EGFR-overexpressing cancer cells*, Biomedicine and Pharmacotherapy 2022:150, 113085 mój udział wynosił 90% i polegał na stworzeniu koncepcji pracy, przeprowadzeniu syntezy liposomów fluorescencyjnych, wykonaniu transfekcji za pomocą metody siRNA, przeprowadzeniu analiz molekularnych oraz mikroskopowych, opracowaniu statystycznemu uzyskanych wyników, przygotowaniu rycin oraz tekstu manuskryptu w zakresie: opisu materiałów i metod, opisu wyników, przeprowadzeniu dyskusji uzyskanych wyników oraz formułowaniu wniosków. Ponadto oświadczam, że jestem autorem korespondencyjnym pracy.

Bartosz Skóra
podpis

Załącznik nr 3 do Regulaminu

Kielce, dnia 23.05.2022r.

Imię i nazwisko współautora pracy: Konrad Szychowski

Rada Naukowa Instytutu
Nauk Medycznych
Uniwersytetu Jana Kochanowskiego
w Kielcach

Oświadczenie o współautorstwie

Niniejszym oświadczam, że w pracy B. Skóra, K. A. Szychowski, *Molecular mechanism of the uptake and toxicity of EGF-LipoAgNPs in EGFR-overexpressing cancer cells*, Biomedicine and Pharmacotherapy 2022:150, 113085 mój udział wynosił 10% i polegał na nadzorze merytorycznym prowadzonych prac oraz przygotowaniu tekstu manuskryptu.

Jednocześnie wyrażam zgodę na wykorzystanie w/w publikacji w postępowaniu doktorskim p. mgra Bartosza Skóry

.....
podpis

10. Całościowy dorobek naukowy kandydata

Ilość wszystkich publikacji: 26

Całkowita ilość cytacji (bez autocytowań): 148

Indeks H: 7

Sumaryczna wartość wskaźnika IF: 126,186

Sumaryczna ilość punktów MEiN: 2580 pkt.

10.1. Wykształcenie

1. **2019 – tytuł zawodowy magistra biotechnologii w specjalności biotechnologia molekularna**, Wydział Biotechnologii Uniwersytetu Rzeszowskiego, promotor pracy magisterskiej: dr hab. Małgorzata Kus-Liśkiewicz, prof. UR.
2. **2018 – tytuł zawodowy inżyniera biotechnologii w specjalności biotechnologia analityczna**, Wydział Biotechnologii Uniwersytetu Rzeszowskiego, promotor pracy inżynierskiej: dr hab. Małgorzata Kus-Liśkiewicz, prof. UR.

10.2. Publikacje niewchodzące w skład cyklu

1. **B. Skóra**, P. Matuszewska, M. Masicz, K. Sikora, M. Słomczewska, P. Sołtysek, K. A. Szychowski, *Crosstalk between the aryl hydrocarbon receptor (AhR) and the peroxisome proliferator-activated receptor gamma (PPARγ) as a key factor in the metabolism of silver nanoparticles in neuroblastoma (SH-SY5Y) cells in vitro*, Toxicology and Applied Pharmacology 2022; 458, 116339.

(IF=4,460; $MEiN_{n.\ med.=}$140 pkt.)

2. T. Piechowiak, **B. Skóra**, M. Balawejder, *Ozonation process causes changes in PARP-1 expression and the metabolism of NADPH in strawberry fruit during storage*, Journal of Biotechnology, Journal of Biotechnology 2022; 357, 84-91.

(IF=3,595; $MEiN_{n.\ med.}$=70 pkt.)

3. M. Bar, **B. Skóra**, A. Tabęcka-Łonczyńska, S. Holota, D. Khyluk, O. Roman, R. Lesyk, K. A. Szychowski, *New 4-thiazolidinone-based molecules Les-2769 and Les-3266 as possible PPARγ modulators*, Bioorganic Chemistry 2022; 128, 106075.

(IF=5,307; MEiN$_{n.\ med.=}$100 pkt.)

4. K. A. Szychowski, **B. Skóra**, A. Tabęcka-Łonczyńska, *Calcium channel antagonists interfere with the mechanism of action of elastin-derived peptide VGVAPG in mouse cortical astrocytes in vitro*, Neurochemistry International 2022; 159, 105405.

(IF=4,297; MEiN$_{n.\ med.}$=100 pkt.)

5. K. A. Szychowski, **B. Skóra**, A. Wójtowicz, *Involvement of sirtuins (Sirt1 and Sirt3) and aryl hydrocarbon receptors (AhR) in the effects of triclosan (TCS) on production of neurosteroids in primary mouse cortical neurons cultures*, Pesticide Biochemistry and Physiology 2022; 184, 105131.

(IF=4,966; MEiN$_{n.\ med.}$=100 pkt.)

6. K. A. Szychowski, **B. Skóra**, T. Pomianek, *Effect of the elastin-derived peptides (VGVAPG and VVGPGA) on breast (MCF-7) and lung (A549) cancer cell lines in vitro*, Biomedicine and Pharmacotherapy 2022; 151, 113149.

(IF=7,419; MEiN$_{n.\ med.}$=100 pkt.)

7. K.A. Szychowski, **B. Skóra**, M. Bar, T. Piechowiak, *Triclosan (TCS) affects the level of DNA methylation in the human oral squamous cell carcinoma (SCC-15) cell line in a nontoxic concentration*, Biomedicine & Pharmacotherapy 2022; 149, 112815.

(IF=7,419; MEiN$_{n.\ med.}$=100 pkt.)

8. **B. Skóra**, A. Lewińśka, A. Kryshchyshyn-Dylevych, D. Kaminskyy, R. Lesyk, K. A. Szychowski, *Evaluation of anticancer and antibacterial activity of four 4-thiazolidinone-based derivatives*, Molecules 2022; 27, 894.

(IF = 4,927; MEiN$_{n.\ med.}$=140 pkt.)

9. K. A. Szychowski, **B. Skóra**, *Review of the relationship between reactive oxygen species (ROS) and elastin-derived peptides (EDPs)*, Applied Sciences 2021; 11, 8732.

(IF= 2,838; MEiN$_{n.\ farm.}$=70 pkt.)

10. K. A. Szychowski, **B. Skóra**, A. Wójtowicz, *Elastin-Derived Peptides in the Central Nervous System: Friend or Foe*, Cellular and Molecular Neurobiology 2021; 42: 2473–2487.

(IF= 4,231; $MEiN_{n.\ med.}$ =100 pkt.)

11. K.A. Szychowski, **B. Skóra**, M. Mańdziuk, *Tris (2,3-dibromopropyl) isocyanurate (TDBP-TAZTO or TBC) shows different toxicity depending on the degree of differentiation of the human neuroblastoma (SH-SY5Y) cell line*, Neurotoxicity Research 2021; 39, 1575–1588.

(IF = 3,978; $MEiN_{n.\ med.}$ = 70 pkt.)

12. T. Piechowiak, **B. Skóra**, P. Sowa, *Changes in the activity of flavanone 3β-hydroxylase in blueberry fruit during storage in ozone-enriched atmosphere*, Journal of the Science of Food and Agriculture 2021; 102, 1300-1304.

(IF= 4,125; $MEiN_{n.\ med.}$ =100 pkt.)

13. B. Skóra, U. Krajewska, A. Nowak, A. Dziedzic, A. Barylyak, M. Kus-Liśkiewicz, *Noncytotoxic silver nanoparticles as a new antimicrobial strategy*, Scientific Reports 2021; 11, 13451.

(IF= 4,996; $MEiN_{n.\ med.}$ =140 pkt.)

14. B. Skóra, T. Piechowiak, K. A. Szychowski, J. Gmiński, *Entrapment of silver nanoparticles in L-α-phosphatidylcholine/cholesterol-based liposomes mitigates the oxidative stress in human keratinocyte (HaCaT) cells*, European Journal of Pharmaceutics and Biopharmaceutics 2021; 166, 164-173.

(IF = 5,589; $MEiN_{n.\ med.}$ = 100 pkt.)

15. K.A. Szychowski, **B. Skóra**, A. Kryshchyshyn-Dylevych, D. Kaminskyy, J. Tobiasz, R. Lesyk, J. Gmiński, *4-thiazolidinone-based derivatives do not affect differentiation of mouse embryo fibroblasts (3T3-L1 cell line) into adipocytes*, Chemico-Biological Interactions 2021; 345, 109538.

(IF = 5,168; $MEiN_{n.\ biol.}$ = 100 pkt.)

16. T. Piechowiak, **B. Skóra**, K. Grzelak-Błaszczyk, M. Sójka, *Extraction of antioxidant compounds from blueberry fruit waste and evaluation of their in vitro biological activity in human keratinocytes (HaCaT)*, Food Analytical Methods 2021; 14, 2317–2327.

(IF = 3,498; $MEiN_{n.\ med.}$ =70 pkt.)

17. K. A. Szychowski, **B. Skóra**, A. Kryshchyshyn-Dylevych, D. Kaminskyy, D. Hylyuk, R. Lesyk, *4-thiazolidinone-based derivatives rosiglitazone and pioglitazone affect the expression of antioxidant enzymes in different human cell lines*, Biomedicine & Pharmacotherapy 2021; 139, 111684.

(IF= 7,419; $MEiN_{n.\ med.}$ = 100 pkt.)

18. K. A. Szychowski, **B. Skóra**, A. K. Wójtowicz, *Triclosan affects the expression of nitric oxide synthases (NOSs), peroxisome proliferator-activated receptor gamma (PPARγ), and nuclear factor kappa-light-chain-enhancer of activated B cells (NF-κB) in mouse neocortical neurons in vitro*, Toxicology in Vitro 2021; 73, 105143.

(IF=3,685; $MEiN_{n.\ med.}$ =100 pkt.)

19. K. A. Szychowski, **B. Skóra**, A. Kryshchyshyn-Dylevych, D. Kaminskyy, K. Rybczyńska-Tkaczyk, R. Lesyk, J. Gmiński, *Induction of Cyp450 enzymes by 4-thiazolidinone-based derivatives in 3T3-L1 cells in vitro*, Naunyn-Schmiedeberg's Archives of Pharmacology 2020; 394, 293-302.

(IF=3,000; $MEiN_{n.\ med.}$ =70 pkt.)

20. K. A. Szychowski **B. Skóra**, T. Pomianek, J. Gmiński, *Inonotus obliquus - from folk medicine to clinical use*, Journal of Traditional and Complementary Medicine 2020; 11, 293-302.

(IF=4,420; $MEiN_{n.\ med.}$ =100 pkt.)

21. K. A. Szychowski, **B. Skóra**, J. Tobiasz, J. Gmiński, *Elastin-derived peptide VGVAPG decreases differentiation of mouse embryo fibroblast (3T3-L1) cells into adipocytes*, Adipocyte 2020; 6, 234-245.

(IF= 4,534; $MEiN_{n.\ med.}$ =70 pkt.)

22. T. Piechowiak, **B. Skóra**, M. Balawejder, *Ozone treatment induces changes in antioxidative defense system in blueberry fruit during storage*, Food and Bioprocess Technology 2020; 13, 1240–1245.

(IF = 4,465; $MEiN_{n.\ med.}$ = 100 pkt.)

23. I. B. Tahar, P. Fickers, A. Dziedzic, D. Płoch, **B. Skóra**, M. Kus-Liśkiewicz, *Green pyomelanin-mediated synthesis of gold nanoparticles: modelling and design, physico-chemical and biological characteristics*, Microbial Cell Factories 2019; 18, 210.

(IF = 4,400; $MEiN_{n.\ med.}$ = 100 pkt.)

Przedstawione wartości wskaźnika Impact Factor (IF) odpowiadają dacie opublikowania lub bazują na najnowszym, dostępnym wskaźniku IF dla danego czasopisma.

10.3. Konferencje naukowe

1. **B. Skóra**, K. A. Szychowski, *Impact of elastin derived peptides on neurosteroids production in cells in vitro*, poster, 12th Neuronus Neuroscience Forum – Kraków, 15–17.10.2022r.

2. **B. Skóra**, K. A. Szychowski, *Enkapsulacja liposomonalna nanocząstek srebra i jej wpływ na stres oksydacyjny w ludzkich keratynocytach in vitro (HaCaT)*, poster, V Ogólnopolska Konferencja Naukowa Nanotechnologia wobec oczekiwań XXI w. - Lublin, 22.05.2021r.

3. P. Matuszewska, M. Nowak, **B. Skóra,** *Rola analogów adenozyny w leczeniu SARS-CoV-2*, wystąpienie, I Ogólnopolska Konferencja Kopernikańska, COVID-19 wyzwania we współczesnej nauce - Toruń, 14-15.05.2021r.

4. M. Szczepanik, A. Lichtarska, N. Stelmach, **B. Skóra**, *Metabolity jadalnych alg jako potencjalne źródło nowych substancji przeciwwirusowych wspomagających leczenie SARS-CoV-2*, wystąpienie, I Ogólnopolska Konferencja Kopernikańska, COVID-19 wyzwania we współczesnej nauce - Toruń, 14-15.05.2021r.

5. **B. Skóra**, J. Szetela, M. Kus-Liśkiewicz, *Biochemiczna i molekularna analiza nowych izolatów drożdżowych*, poster, Wkraczając w Świat Nauki - Wrocław, 20-21.09.2018.

10.4. Udział w projektach naukowych

1. **marzec 2021 – grudzień 2021** – kierownik projektu, *Określenie mechanizmu endocytozy i toksyczności nanocząstek srebra pułapkowanych w liposomach znakowanych EGF dla linii nowotworowych z nadekspresją receptora EGFR*, finansowane ze środków działalności statutowej Wyższej Szkoły Informatyki i Zarządzania, Katedra Biotechnologii i Biologii Komórki, Wyższa Szkoła Informatyki i Zarządzania z siedzibą w Rzeszowie.

2. **kwiecień 2022 – kwiecień 2023** – opiekun i wnioskodawca projektu, *Ocena wykorzystania nanocząstek srebra w terapii przeciwko komórkom nowotworowym mózgu in vitro*, kwota finansowania: 69 995,00 zł, program Studenckie Koła Naukowe Tworzą Innowacje Nabór III, Ministerstwo Edukacji i Nauki.

3. **luty 2021 – lipiec 2021** – wykonawca w projekcie, *Pozyskanie substancji bioaktywnych z Inonotus obliquus w formie możliwej do zastosowania we wzbogacaniu żywności*, Podkarpackie Centrum Innowacji Nabór III, Kierownik: dr hab. n. med. Konrad Szychowski, prof. WSIiZ, Katedra Biotechnologii i Biologii Komórki, Kolegium Medyczne, Wyższa Szkoła Informatyki i Zarządzania z siedzibą w Rzeszowie.

4. **luty 2021 – lipiec 2021** – wykonawca w projekcie, *Rola metabolizmu energetycznego mitochondriów w kształtowaniu jakości owoców jagodowych przechowywanych w atmosferze ozonu*, kierownik: dr inż. Tomasz Piechowiak, Zakład Chemii i Toksykologii Żywności, Uniwersytet Rzeszowski, Narodowe Centrum Nauki, OPUS 18 2019/35/B/NZ9/01552.

5. **luty 2021 – lipiec 2021** – wykonawca w projekcie, *Peptyd elastynopochodny VGVAPG jako transporter leków cytostatycznych do komórek nowotworowych*, Podkarpackie Centrum Innowacji Nabór II, kierownik: dr hab. n. med. Konrad Szychowski, prof. WSIiZ, Zakład Biotechnologii i Biologii Komórki, Wyższa Szkoła Informatyki i Zarządzania w Rzeszowie.

10.5. Zgłoszenia patentowe

Współautor zgłoszenia patentowego o nr P.441769 autorstwa K. A. Szychowski, T. Pomianek, **B. Skóra**, U. Binduga pt. *Sposób ekstrakcji substancji aktywnych z błyskoporka podkorowego*, data zgłoszenia do Urzędu Patentowego RP: 19.07.2022r.

10.6. Działalność popularyzująca naukę

1. **2022 –** wywiad dotyczący możliwości wykorzystania nanocząstek srebra w terapii przeciwnowotworowej i wyzwań z tym związanych, Polskie Radio Rzeszów.
2. **2021 – obecnie –** opiekun i pomysłodawca między kierunkowego, studenckiego Koła Naukowego Biotechnologii Medycznej „HELISA".
3. **2021 –** współautor artykułu popularnonaukowego, K. A. Szychowski, B. Skóra, *Wpływ produktów rozpadu elastyny na komórki układu nerwowego*, Wszechświat 2021, t. 122, nr 10-12.
4. **2020 –** autor artykułu popularnonaukowego *Pułapki dla insuliny – szansą w leczeniu cukrzycy*, Blog Naukowy Wyższej Szkoły Informatyki i Zarządzania z siedzibą w Rzeszowie.